
The Regulation of Spinal Neurogenesis by PTP γ

Hamid Hashemi

A thesis submitted in partial fulfilment of the requirements of
University College London
for the award of the degree Doctor of Philosophy

Neural Development Unit, Institute of Child Health
& Great Ormond Street Hospital for Children



Declaration

‘I, Hamid Hashemi confirm that the work presented in this thesis is my own. Where information has been derived from other sources, I confirm that this has been indicated in this thesis.’

HAMID HASHEMI Electronic Copy

Abstract

RPTPs have striking patterns of expression within the neural tube; raising interesting questions as to their role in the development of this structure. PTP γ expression is initially observed in the first born neurons and this expression domain progressively expands to the lateral motor columns and intermediate zone of differentiating neurons. Short hairpin encoding RNAi constructs were generated against PTP γ , which effectively knocked down this gene *in vitro* and *in ovo*. Analysis of silenced embryos through neuronal markers presented a range of phenotypes. The most striking was a dorsoventral truncation of the neural tube arising from a loss of LIM-HD expressing cells not observed among controls. During the onset of neurogenesis, a loss of Lim1/2/3, Islet1/2, and Mnr2/Hb9 positive cells was observed. At later stages, Islet1/2 cells showed no such sustained effect essentially recovering. A further heterotopic phenotype was observed with mislocated neurons located ectopically in the ventricular lumen, that were Islet1/2 and Nkx2.2 positive but never Lim1/2/3. The targeted regions showed a significant decrease in apoptosis suggesting newly born neurons were dying before reaching their pool specific domains. A reduction in the proliferative capacity in the ependymal zone demonstrated by Histone3 activity. Over expression of PTP γ showed a similar reduction in LIM-HD expression however no overall change in S-Phase was observed yet cells at M Phase were reduced with no apoptosis detected through Caspase3 activity. The data suggests PTP γ silencing may result in a failure of Lim1/2/3 cells to reach their final destinations and acquire LIM-HD identities, implicating this gene in the development of inter and motor neuron populations. Preliminary RNAi experiments against PTP σ show a reduction in LIM-HD fated cells and a triggering of the apoptosis programme along with a reduction in number of mitotically active cells. This is consistent with a potential role for PTPs during neurogenesis and the birth of the first neuronal populations in the neural tube.

Table of Contents

ABSTRACT	I
TABLE OF CONTENTS.....	II
TABLE OF FIGURES	III
CHAPTER 1: INTRODUCTION.....	1
1.1 NEURAL INDUCTION AND DEVELOPMENT OF NEURAL PROGENITORS	1
1.1.1 <i>Neural Inducers and their genetic interactions.....</i>	3
1.1.2 <i>The development of progenitor cells and Notch signalling.....</i>	5
1.1.3 <i>Downstream of the Notch pathway in vertebrates.....</i>	10
1.2 CONTROL OF CELL MOVEMENTS IN THE EARLY NEURAL TUBE.....	13
1.2.1 <i>Interkinetic Nuclear Migration.....</i>	16
1.2.2 <i>Radial glia and laminins.....</i>	17
1.3 NEUROGENESIS AND THE CELL CYCLE.....	18
1.3.1 <i>Cyclins as key components of the cell cycle.....</i>	19
1.3.2 <i>Control of cell cycle & Wnt signalling.....</i>	20
1.3.3 <i>Cadherins-catenin functions in the neural tube.....</i>	25
1.4 GENERATING THE ANTERIOR-POSTERIOR PATTERN OF THE NEURAL TUBE	27
1.4.1 <i>Retinoic acid and rostrocaudal polarity.....</i>	28
1.4.2 <i>FGF Signalling and anteroposterior patterning.....</i>	28
1.5 ESTABLISHING DORSOVENTRAL POLARITY OF THE NEURAL TUBE.....	30
1.5.1 <i>Shh and neural tube patterning.....</i>	30
1.5.2 <i>Dorsal fate determined by BMPs.....</i>	33
1.5.3 <i>Wnt pathway and dorsoventral patterning.....</i>	34
1.6 CONTROLLING NEURONAL FATE - THE β HLH GENES.....	35
1.6.1 <i>Generation of progenitor pools.....</i>	38
1.6.2 <i>Shh signal transduction and the Gli genes.....</i>	45
1.6.3 <i>Downstream of Shh action.....</i>	48
1.7 LIM HOMEODOMAIN PROTEINS.....	49
1.7.1 <i>Motor neuron specification.....</i>	51
1.7.2 <i>Pool specific identities & columnar fates.....</i>	56
1.7.3 <i>Pax Genes.....</i>	60
1.8 SEGMENTAL IDENTITY OF MOTOR NEURONS AND HOX GENES	63
1.9 PROTEIN TYROSINE PHOSPHATASES.....	66
1.9.1 <i>Functional studies of RPTPs.....</i>	68
1.9.1.1 <i>PTP action in motor neurons.....</i>	68
1.9.1.2 <i>PTP function in the visual system.....</i>	73
1.9.1.3 <i>Roles of PTPs in synaptogenesis.....</i>	75
1.9.1.4 <i>Interactions of RPTPs with cadherins and catenins.....</i>	77
1.9.1.5 <i>RPTP ligands and their functions.....</i>	79
1.9.1.6 <i>RPTPs and neural tube development.....</i>	82
1.9.1.7 <i>PTP!.....</i>	88
1.9.1.8 <i>PTP.....</i>	90
1.10 RNA INTERFERENCE.....	92
1.10 EXPERIMENTAL AIMS.....	98
CHAPTER 2: METHODS & MATERIALS.....	100
2.1 DNA PREPARATION.....	100
2.1.1 <i>Bacterial Cultures.....</i>	100
2.1.2 <i>DNA Extraction.....</i>	100
2.1.3 <i>DNA Filtration.....</i>	101
2.1.4 <i>DNA Elution.....</i>	101
2.1.5 <i>DNA Purification.....</i>	101
2.2 MICRO PREPARATION.....	102
2.2.1 <i>Colony selection and pre-treatment.....</i>	102
2.2.2 <i>Agarose gel preparation.....</i>	102

2.2.3	<i>Agarose gel electrophoresis</i>	103
2.3	THE GENERATION OF SILENCING CONSTRUCTS.....	103
2.3.1	<i>Designing and preparing the plasmids</i>	103
2.3.2	<i>Annealing the PTPσ oligonucleotides</i>	104
2.3.3	<i>Ligation of templates</i>	104
2.3.4	<i>Culturing the clones</i>	105
2.3.5	<i>Sequencing the constructs</i>	105
2.4	CELL CULTURE STUDIES.....	106
2.4.1	<i>Creating a working stock</i>	106
2.4.2	<i>Expanding the cells</i>	106
2.4.3	<i>Cell Transfections</i>	107
2.4.4	<i>Protein Extraction</i>	107
2.4.5	<i>Luciferase Assays</i>	108
2.5	PROTEIN DETECTION.....	109
2.5.1	<i>Cell Lysis</i>	109
2.5.2	<i>Protein Reduction</i>	109
2.5.3	<i>SDS-PAGE Electrophoresis</i>	110
2.5.4	<i>Gel Transfer</i>	110
2.5.5	<i>Immunoblotting</i>	110
2.5.6	<i>Protein Detection</i>	111
2.6	IN OVO ELECTROPORATION.....	111
2.6.1	<i>Microinjection</i>	111
2.6.2	<i>Electroporation</i>	112
2.6.3	<i>Embryo Dissection and Storage</i>	112
2.6.4	<i>Cryoprotection and frozen sections</i>	112
2.7	CELL DEATH AND PROLIFERATION.....	113
2.7.1	<i>Apoptosis</i>	113
2.7.2	<i>Proliferation</i>	115
2.8	IMMUNOHISTOCHEMISTRY.....	117
2.9	HISTOLOGICAL STAINING.....	120
2.10	NON-RADIOACTIVE IN SITU HYBRIDISATION WITH DIGOXYGENIN (DIG) LABELLED PROBES.....	120
2.10.1	<i>DNA Linearisation</i>	120
2.10.2	<i>Probe Synthesis</i>	121
2.10.3	<i>Hybridization</i>	122
2.10.4	<i>Antibody Treatment</i>	122
2.10.5	<i>Signal Detection</i>	122
2.11	QUANTIFICATION OF CELL NUMBERS FROM SPINAL CORD SECTIONS.....	123
CHAPTER 3: TESTING SHRNA KNOCKDOWN OF PTPS IN CULTURE.		124
3.1	RNA INTERFERENCE IN THE CHICK.....	124
3.2	DESIGNING THE RNAI CONSTRUCTS.....	125
3.2.1	<i>Designing the target sequences</i>	125
3.2.2	<i>The optimum parameters</i>	130
3.2.3	<i>Building the PTPσ silencing vectors</i>	130
3.3	IN VITRO ASSAYS.....	133
3.3.1	<i>PTPγ</i>	133
3.3.2	<i>Setting the control experiments</i>	133
3.3.3	<i>Quantifying the level of mRNA knock down</i>	134
3.3.4	<i>PTPσ</i>	137
3.3.5	<i>PTPγ over-expression vectors</i>	137
3.3.6	<i>Conclusions of in vitro assays</i>	140
CHAPTER 4: DEFINING THE PTPγ AND NEURONAL EXPRESSION DOMAINS.		143
4.1	INTRODUCTION.....	143
4.2	AXONOGENESIS.....	144
4.3	LIM-HD EXPRESSION PROFILES OF DIFFERENTIATING NEURONS.....	147
4.3.1	<i>Islet1/2</i>	147
4.3.2	<i>Lim 1/2</i>	150
4.3.3	<i>Lim3</i>	153
4.4	MNX-HD AND NKX-HD TRANSCRIPTION FACTOR PROFILES OF NASCENT MOTOR NEURONS.....	153

4.5 THE EXPRESSION OF PTP γ IN THE CHICK SPINAL CORD	157
4.6 SIGNALLING NEUROGENESIS.....	163
4.7 PTP γ IN THE CONTEXT OF CELLULAR DIFFERENTIATION.....	167
CHAPTER 5: PTPγ LOSS-OF-FUNCTION.....	172
5.1 INTRODUCTION.....	172
5.1.1 Silencing RPTP's in ovo.....	172
5.1.2 Taking a closer look at PTP γ	173
5.1.3 Experimental Aims.....	174
5.2 ESTABLISHING THE RNAi SYSTEM IN OVO.....	175
5.2.1 Electroporation efficiency.....	175
5.2.2 Embryo Viability and Controls.....	175
5.3 PTP γ SILENCING INDUCES A RANGE OF ECTOPIC PHENOTYPES AT E5 & E7.....	178
5.3.1 Classification of phenotypes.....	178
5.3.2 Silencing PTP γ and resulting gross phenotypes in ovo.....	183
5.3.3 Explaining the phenotypes.....	186
5.4 QUANTITATIVE ANALYSIS OF NEURONAL POOLS.....	198
5.4.1 Effects on Islet1/2 positive neuronal populations.....	198
5.4.2 Effects on Lim 1/2 positive neuronal populations.....	198
5.4.3 Summary.....	201
5.5 STUDYING PTP LOSS-OF-FUNCTION AT EARLIER EMBRYONIC TIME POINTS.....	204
5.5.1 HH18.....	204
5.5.2 HH20.....	204
5.5.3 HH22.....	211
5.6 PTP γ SILENCING INDUCES A REDUCTION IN THE PROLIFERATIVE CAPACITY OF LIM-HD EXPRESSING PROGENITORS.....	220
5.7 PTP γ SILENCING INDUCES APOPTOSIS AT HH20 AND HH22.....	220
5.8 SUMMARY.....	228
CHAPTER 6: PTPγ GAIN-OF-FUNCTION.....	233
6.1 INTRODUCTION.....	233
6.2 PTP γ OVER EXPRESSION CAUSES A BROAD REDUCTION IN THE NUMBER OF LIM-HD EXPRESSING NEURONS ALONG THE ENTIRE DV ASPECT OF THE SPINAL CORD.....	233
6.3 THE REDUCTION IN LIM-HD CELL EXPRESSION PERSISTS TO HH 22.....	238
6.3.1 LIM-HD cell counts.....	238
6.3.2 Further patterns at HH22 in IRES-PTP γ treated embryos.....	243
6.4 PTP γ GAIN-OF-FUNCTION DOES NOT LEAD TO APOPTOSIS.....	248
6.5 MEASURING THE MITOTIC ACTIVITY AT HH22.....	251
6.6 PTP γ OVER-EXPRESSION DOES NOT AFFECT THE RATE OF S-PHASE.....	251
6.7 DISCUSSION.....	259
CHAPTER 7: SILENCING PTPσ.....	260
7.1 INTRODUCTION.....	260
7.1.1 PTP σ expression and RNAi.....	261
7.1.2 Aims.....	261
7.2 PTP σ LOSS-OF-FUNCTION CONSTRUCTS AND IN OVO ELECTROPORATION.....	262
7.3 PTP σ SILENCING HAS A GENERAL EFFECT ON LIM-HD EXPRESSING CELLS.....	262
7.4 PTP σ LOSS-OF-FUNCTION TRIGGERS APOPTOSIS OF LIM HD FATED PROGENITOR MOTOR NEURONS IN THE SPINAL CORD.....	265
7.5 PTP σ GAIN-OF-FUNCTION INDUCES A REDUCTION IN THE NUMBER OF MITOTICALLY ACTIVE RADIAL GLIA.....	268
7.6 DISCUSSION.....	271
CHAPTER 8: DISCUSSION.....	273
8.1 PTP γ LOSS-OF-FUNCTION FUNCTION DISRUPTS NEUROGENESIS IN THE CHICK.....	276
8.2 PTP γ FUNCTION AND LIM HD TRANSCRIPTION FACTORS.....	277
8.3 VENTRICULAR ZONE ACTIVITY AND NEURONAL DIFFERENTIATION.....	279
8.4 PTP γ GAIN-OF-FUNCTION.....	282
8.5 KNOCKING DOWN PTP σ	283

8.6	THE ROLE OF PTPs DURING THE DEVELOPMENT OF THE NEURAL TUBE.....	284
8.7	CADHERINS, ADHESION AND MIGRATION.....	285
8.8	PTP γ , β -CATENIN AND WNT PROLIFERATION CONTROL.....	288
8.9	PTP γ AND NEURAL TUBE PATTERNING.....	293
8.10	FUTURE STUDIES.....	295
	REFERENCES.....	297
	APPENDIX A: NEURONAL COUNTS.....	323
	APPENDIX B: PUBLICATION.....	330

Table of Figures

FIGURE 1.1	SCHEME OF NOTCH SIGNALLING	9
FIGURE 1.2	SUMMARY OF MIGRATORY PATTERNS IN THE CHICK SPINAL CORD	15
FIGURE 1.3	SCHEME OF WNT SIGNALLING AND CADHERIN-CATENIN COMPLEX	23
FIGURE 1.4	SCHEME FOR SPINAL CORD DEVELOPMENT IN THE CHICK	32
FIGURE 1.5	SCHEME OF GENE PATHWAYS REGULATING NEUROGENESIS	37
FIGURE 1.6	SCHEME OF PROGENITOR AND NEURONAL PATTERNING	42
FIGURE 1.7	SCHEME OF COLUMNAR ORGANISATION OF THE SPINAL CORD	54
FIGURE 1.8	THE RPTP FAMILY	70
FIGURE 1.9	EXPRESSION OF RPTPS IN THE CHICK NEURAL TUBE	84
FIGURE 1.10	SCHEME OF RPTP EXPRESSION IN THE SPINAL CORD	86
FIGURE 1.11	MODEL OF RNAI	96
FIGURE 3.1	TABLE OF DNA TARGET SEQUENCES FOR PTP σ	127
FIGURE 3.2	RNAI PLASMIDS AND HAIRPIN OLIGONUCLEOTIDES, PSILENCER 1.0	129
FIGURE 3.3	RNAI PLASMIDS AND HAIRPIN OLIGONUCLEOTIDES, PSILENCER 2.0	132
FIGURE 3.4	PTP γ PROTEIN EXPRESSION FOLLOWING LOSS-OF-FUNCTION	136
FIGURE 3.5	PTP σ PROTEIN EXPRESSION FOLLOWING LOSS-OF-FUNCTION	139
FIGURE 3.6	PTP γ PROTEIN EXPRESSION FOLLOWING GAIN-OF-FUNCTION	139
FIGURE 3.7	RPTP EXPRESSION VECTOR MAPS USED IN LOF & GOF STUDIES	142
FIGURE 4.1	EXPRESSION OF NEURAL MARKERS IN WT HH18 CHICK BRACHIAL SPINAL CORD	146
FIGURE 4.2	EXPRESSION OF NEURAL MARKERS IN WT HH20 CHICK BRACHIAL SPINAL CORD	149
FIGURE 4.3	EXPRESSION OF NEURONAL MARKERS IN WT HH22 CHICK BRACHIAL SPINAL CORD ..	152
FIGURE 4.4	EXPRESSION OF NEURONAL MARKERS IN WT HH26 CHICK BRACHIAL SPINAL CORD ..	155
FIGURE 4.5	EXPRESSION OF PTP γ AND NEUOM IN WT CHICK BRACHIAL SPINAL CORD SECTIONS FROM HH16-23	160
FIGURE 4.6	EXPRESSION OF PTP γ IN WT CHICK BRACHIAL SPINAL CORD SECTIONS AT HIGH MAGNIFICATION AT HH20 & HH22	162
FIGURE 4.7	EXPRESSION OF PTP γ AND NEUOM IN WT CHICK BRACHIAL SPINAL CORD SECTIONS FROM HH26	166
FIGURE 4.8	EXPRESSION OF PTP γ AND NEURONAL MARKERS IN WT CHICK BRACHIAL SPINAL CORD SECTIONS AT HH20 AND HH22	170
FIGURE 5.1	MICROINJECTION & ELECTROPORATION AT HH10	177
FIGURE 5.2	CONTROL HAIRPIN TREATED EMBRYOS AT E5 AND E7	180
FIGURE 5.3	SCHEMATIC REPRESENTATION OF THE PHENOTYPES OBSERVED AMONGST PTP γ LOSS-OF- FUNCTION EMBRYOS	185
FIGURE 5.4	EXPRESSION OF NEURONAL MARKERS IN PTP γ LOF E5 CHICK BRACHIAL SPINAL CORD	185
FIGURE 5.5	EXPRESSION OF HISTOLOGICAL & NEURONAL MARKERS IN PTP γ LOF E7 CHICK BRACHIAL SPINAL CORD	188
FIGURE 5.6	EXPRESSION OF NEURONAL MARKERS PTP γ LOF E7 CONTROL CHICK BRACHIAL SPINAL CORD	190
FIGURE 5.7	EXPRESSION OF NEURONAL MARKERS IN PTP γ LOF E5 CHICK BRACHIAL SPINAL CORD	192
FIGURE 5.8	EXPRESSION OF Mnr2 PTP γ LOF E5 CHICK BRACHIAL SPINAL CORD	195
FIGURE 5.9	EXPRESSION OF NEURONAL MARKERS IN PTP γ LOF E5 CHICK BRACHIAL SPINAL CORD	197
FIGURE 5.10	SCREENSHOT OF THE OPENLAB SOFTWARE AND METHOD OF COUNTING CELLS	200
FIGURE 5.11	CHARTS OF ISLET1/2 AND LIM1/2 NEURONAL COUNTS AT E5	203
FIGURE 5.12	EXPRESSION PATTERNS IN PTP γ LOF HH18 CHICK BRACHIAL SPINAL	208
FIGURE 5.13	CHART OF LIM-HD POSITIVE CELL NUMBERS IN PTP γ LOF HH18 EMBRYOS	210
FIGURE 5.14	EXPRESSION PATTERNS IN PTP γ LOF HH20 CHICK BRACHIAL SPINAL	213
FIGURE 5.15	CHART OF LIM-HD POSITIVE CELL NUMBERS IN PTP γ LOF HH20 EMBRYOS	215

FIGURE 5.16	EXPRESSION PATTERNS IN PTP γ LOF HH22 CHICK BRACHIAL SPINAL	217
FIGURE 5.17	CHART OF LIM-HD POSITIVE CELL NUMBERS IN PTP γ LOF HH22 EMBRYOS.....	219
FIGURE 5.18	IMMUNOCYTOCHEMICAL CELL DEATH AND PROLIFERATION MARKERS IN PTP γ LOF HH20 CHICK BRACHIAL SPINAL CORD	222
FIGURE 5.19	IMMUNOCYTOCHEMICAL CELL DEATH AND PROLIFERATION MARKERS IN PTP γ LOF HH22 CHICK BRACHIAL SPINAL CORD	224
FIGURE 5.20	CHART OF PROLIFERATING CELL NUMBERS PTP γ LOF EMBRYOS AT HH20	226
FIGURE 5.21	SCHEMATIC REPRESENTATION OF PROLIFERATING CELLS IN PTP γ LOF EMBRYOS AT HH20	226
FIGURE 5.22	CHART OF CELL NUMBERS UNDERGOING APOPTOSIS IN PTP γ LOF EMBRYOS AT HH20 & HH22	230
FIGURE 5.23	SCHEMATIC REPRESENTATION OF APOPTOTIC CELLS IN PTP γ LOF AT HH20 & HH22	232
FIGURE 6.1	EXPRESSION PATTERNS IN PTP γ GOF CONTROL HH22 CHICK BRACHIAL SPINAL CORD	237
FIGURE 6.2	EXPRESSION PATTERNS IN PTP γ GOF HH20 CHICK BRACHIAL SPINAL CORD.	240
FIGURE 6.3	EXPRESSION PATTERNS IN PTP γ GOF HH22 CHICK BRACHIAL SPINAL CORD	242
FIGURE 6.4	CHART OF LIM-HD EXPRESSING CELL NUMBERS IN PTP γ GOF HH22 EMBRYOS	245
FIGURE 6.5	EXPRESSION PATTERNS IN PTP γ GOF HH22 CHICK BRACHIAL SPINAL CORD.....	247
FIGURE 6.6	CHART OF CELLS UNDERGOING APOPTOSIS IN PTP γ GOF HH22 EMBRYOS	250
FIGURE 6.7	CHART OF CELLS UNDERGOING MITOSIS IN PTP γ GOF HH22 EMBRYOS	253
FIGURE 6.8	BRdU LABELLING IN PTP γ GOF HH18 CHICK BRACHIAL SPINAL CORD.....	256
FIGURE 6.9	SCREENSHOT OF THE OPENLAB SOFTWARE AND METHOD OF COUNTING THE PROLIFERATING CELLS	256
FIGURE 6.10	CHARTS OF BRdU POSITIVE PROLIFERATIVE CELL NUMBERS IN PTP γ GOF HH18 EMBRYOS.....	258
FIGURE 7.1	EXPRESSION PATTERNS IN PTP σ LOF HH18 CHICK BRACHIAL SPINAL CORD	264
FIGURE 7.2.	CHART OF LIM-HD EXPRESSING CELL NUMBERS IN PTP σ LOF HH18 EMBRYOS	267
FIGURE 7.3	CHART OF CELLS UNDERGOING APOPTOSIS IN PTP σ LOF HH18 EMBRYOS.....	270
FIGURE 7.4	CHART OF CELLS UNDERGOING MITOSIS IN PTP σ LOF HH18 EMBRYOS.....	270
FIGURE 8.1	MODEL OF POSSIBLE PTP γ INTERACTION WITH CATENIN-CADHERIN COMPLEX.....	292

Chapter 1: Introduction

Within the early embryo, as the ball of multipotent cells called the blastula takes form during gastrulation, cell to cell interactions between the ectodermal cap and the underlying mesoderm give rise to all of the bodies cells. As gastrulation proceeds, a carefully choreographed movement of cells within the embryo's three germ layers establishes the beginnings of a body axis that leads to the formation of the nervous system. In the following sections, the development of the neural tube will be discussed as well as the transcription factors involved in this process. This will be followed by an introduction into the genes involved in neuronal differentiation and finally the impact of Receptor Protein Tyrosine Phosphatases (PTPs) on neuronal populations during and following neurogenesis will be discussed. Following this, the aims of the thesis will be addressed within the context of the spinal cord to better understand the role of PTPs within the spinal cord region during neurogenesis.

1.1 Neural Induction and development of neural progenitors.

The nervous system of animals has its origins within a distinct region of the dorsal ectoderm, where interactions between these ectodermal cells, the mesendoderm and 'organiser centres' confer a neural fate of cells within this region through neural induction. These ectodermal cells are in fact neural by default where the presence of neural inducing factors block an overriding inhibitory signal through activin receptors that initially presides over the ectoderm. This maintains an epidermal fate within the ectodermal cells (Spemann, 1938; Waddington, 1933; Hemmati-Brivanlou & Melton, 1994).

Once neural induction is initiated, the neural ectodermal cells thicken to form the neural plate with a conferred anteroposterior identity along a neuroaxis, providing an anterior end that gives rise to the brain and the posterior end that culminates in the spinal cord. As this process of neurulation proceeds, the neural plate rapidly elongates and cell interactions convert a predominantly cuboidal morphology of epithelial cells into a pseudo-stratified arrangement. Through signals from cells residing outside of the neural plate, along the notochord in higher vertebrates, the neural plate bends at its midline through apical narrowing and basal widening of the cells along the presumptive floor plate, creating a hinge where the neural plate folds upwards. The neural folds elevate further through convergence-extension movements within the neural plate and overlying ectoderm (Schoenwolf et al, 1988; Catala et al, 1996).

Along the prospective spinal cord region running the anteroposterior length of the neural plate, the notochord and floor plate are intimately associated. Further bends occur in the neural folds as secondary hinge points form dorsally along its mediolateral aspect on both sides. This has the effect of encapsulating the neural plate whereby the edges of the neural fold at the margins of the neural plate fuse along the dorsal midline, forming the roof plate and creating the distinctive enclosed keyhole appearance of the neural tube under the overlying epidermis. At this point the shape of the neural tube changes further through cell movements as the neural tube readies itself for neurogenesis and cell proliferation (Schoenwolf & Alvarez, 1992; Smith & Schoenwolf, 1997; Nurse, 2000).

1.1.1 Neural Inducers and their genetic interactions.

Classical studies in *Xenopus* led to the discovery of factors driving the induction of neural genes within dorsal lip tissues. These were Noggin, Chordin and Follistatin and were all found to be sufficient in driving neural fate of tissues in ectopic locations. These studies led to the realisation that activin signals inhibit ectodermal cells from developing a neural fate. Induction of neuronal development therefore occurs through inhibition of the activin-like TGF- β family signals through signals emanating from the organiser centres, such as Follistatin, supporting the 'neural default' state of early ectodermal tissues. (Lamb et al, 1993; Smith et al, 1993; De Robertis & Sasai, 1996; Hemmati-Brivanlou & Melton, 1994).

Early experiments in *Drosophila* found a homologue to *Xenopus* Chordin called the Short gastrulating gene (Sog). Sog loss of function experiments revealed an expansion of epidermal fate within tissues along with a reduction in neurogenic regions, and further ectopic expression of Sog resulted in the formation of ectopic neural tissue (De Robertis & Sasai, 1996). Sog was found to interact with the Decapentaplegic (Dpp) gene that is a TGF- β related protein similar to Bone Morphogenic Protein (BMP) in vertebrates. The BMP receptor consist of Type I and Type II subunits, whereby the Type II subunit acts as a Kinase phosphorylating serine/threonine amino acids on the Type I subunit. This results in further phosphorylation of R-SMADs, which once phosphorylated, form complexes with co-SMADs that enter the nucleus; activating the transcription of target genes via BMP response elements in target gene promoter regions.

BMPs are expressed dorsally in the neural tube acting in this domain, furthermore Sog and Dpp antagonise each other's action and display opposing phenotypes with Dpp mutants showing an expansion of neurogenic regions at the expense of epidermis. Classical studies in *Xenopus* have shown a conservation of neural induction function demonstrated in earlier *Drosophila* studies whereby recombinant BMP4 expression suppressed chordin/noggin/folloistatin induced neural induction in animal caps. This implicates the antagonisation of BMP signals as the driver of neural induction and furthermore, expression of a truncated activin receptor blocked the endogenous BMP4 signals (Wilson & Hemmati-Brivalou, 1995; Piccolo et al, 1996; McMahon et al, 1998).

Neural induction in the chick embryo occurs prior to gastrulation and members of the Fibroblast Growth factor family (FGF) of genes have been implicated as potent neural inducers. Blocking of this FGF signal by inhibitors, namely SU5402 was shown to prevent the initiation of early phase neural induction (Streit et al, 2000). Further studies in the ascidian embryo showed that Chordin and Follistatin were by themselves not sufficient to drive neural induction and that FGF signals were critical here as in the chick embryo (Bertrand et al, 2003; Delaune et al, 2005). Downstream components of the BMP pathway, SMADs were further shown to be inhibited through phosphorylation resulting from FGF signalling (Pera et al, 2003).

Looking at more detail at the convergence of BMP and FGF pathways reveals two transcription factors as key mediators of neural Induction. *Zic1* and *Zic3* are expressed in the region of the ectoderm fated to become the neural plate and are both required for the formation of the neural plate, and are induced by Noggin. When FGF signals are

inhibited, *Zic3* expression is lost, however *Zic1* expression remains unaffected, thus inhibition of BMP and activation of FGF signalling act in concert during the specification of the neural plate (Marchal et al, 2009).

On the other hand, ectodermal BMP signals result in the activation of intracellular proteins that bring about the repression of *Zic1*, giving rise to epidermal tissue. Within the neural tube, once BMP signals are inhibited, the SMAD pathway is activated and *Zic1* expression ensues. This, coupled with FGF signals, results in the activation of *Zic3*, together with *Zic1* directing a neural fate through activation of downstream neural progenitor genes such as *Sox2*. Dominant negative *Sox2* over expression resulted in a blockade of neural induction (Sasai, 2001).

1.1.2 The development of progenitor cells and Notch signalling.

Following the definition of the neurogenic regions by BMP/Dpp, the action of proneural genes are required for the correct formation of neural progenitor cells from the epidermis. The *drosophila* *achaete/scute* and the *atonal* genes encode β HLH transcription factors that bind specific E-box sequences in promoter regions of target genes thereby activating their transcription. Expression of *Achaete/scute* genes and consequent neuroblast formation is regulated by lateral inhibition through the Notch receptor and Delta ligand signalling. Notch is a transmembrane protein with cysteine rich EGF repeats that binds to its ligands Delta and Serrate. In *drosophila*, Notch signalling serves to regulate neuroblast formation with a low level of expression in neuroblasts and high levels of expression in epidermal cells. Notch loss of function results in more neurons differentiating in neurogenic regions, a similar phenotype to

Delta loss of function mutants (Pierfelice et al, 2011). Notch signalling enables an individual cell to maintain achaete-scute expression, and suppresses its own expression in neighbouring cells (Kopan & Ilagan, 2009).

The production of the correct number and type of neurons is in part regulated by Notch activity, whereby during cell division a progenitor cell can give rise to either two progenitors or two neuronal cells, via symmetrical division, or a neuron and a progenitor through asymmetrical division. Studies in the brain reveal Notch signalling is required to maintain progenitor cells during neurogenesis whereby cells undergoing differentiation express Notch ligands, in turn activating notch signalling in neighbouring progenitor cells. This prevents their differentiation through lateral inhibition temporarily since the notch signal is then extinguished, resetting the potential of progenitors. (Gotz & Huttner, 2005; Louvi & Artavanis-Tsakonas, 2006).

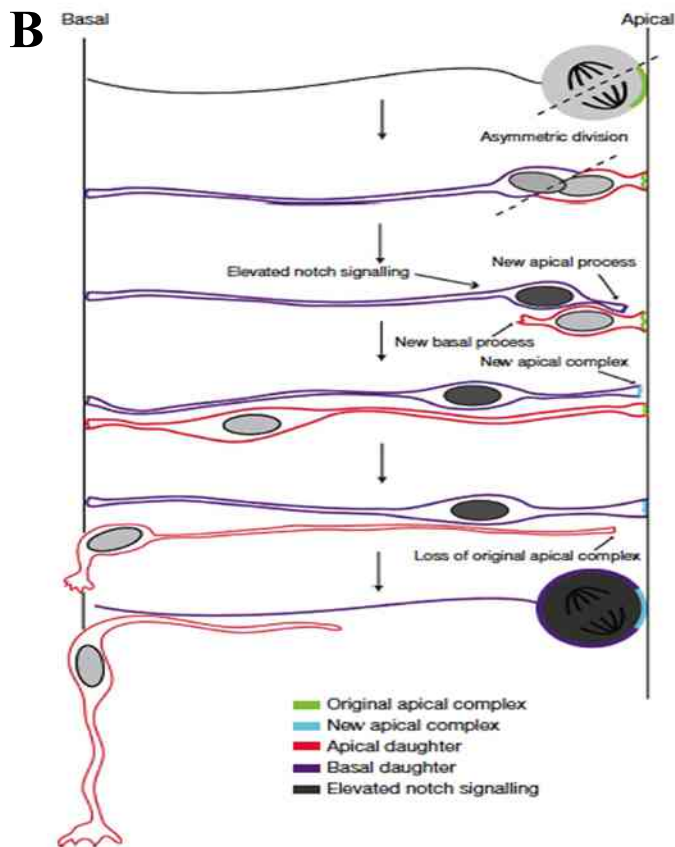
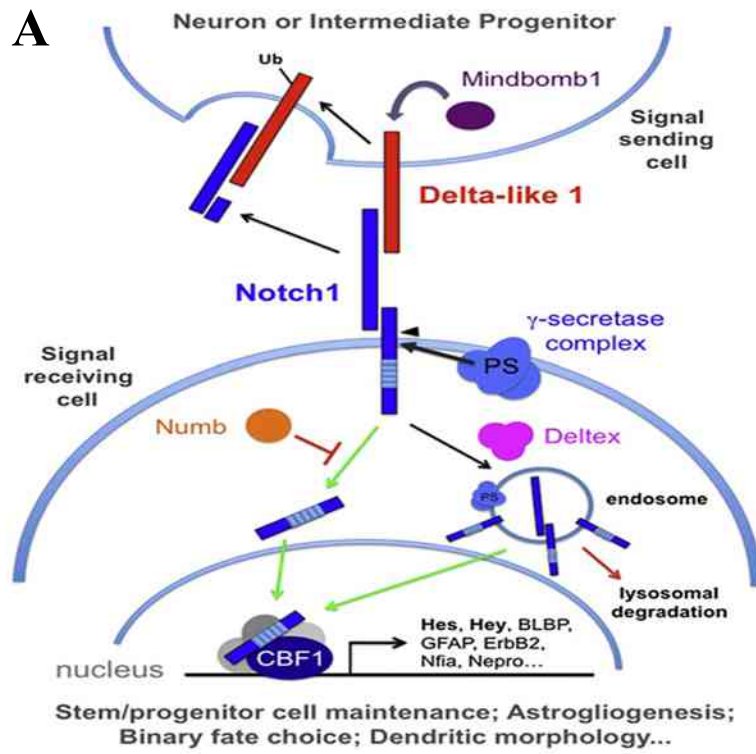
Previous studies have shown that Notch1, a homologue of the *Drosophila* Notch gene is concentrated basally in the dividing progenitor cells. The Notch1 protein is inherited asymmetrically in horizontal divisions whereas vertical cleavages distribute Notch1 equally to the two daughter cells. Notch1 may then provide an instructive role within progenitor cells determining whether cell fates are the same or different (Chenn & McConnell, 1995; Donovan & Dyer 2005). These studies arguing for a role for asymmetric Notch in progenitor cells have been superseded by other studies contesting these findings (Fortini, 2009; Pierfelice et al, 2011).

The current mechanism of Notch signalling involves the binding of Delta to Notch resulting in the proteolytic cleavage of the intracellular Notch domain by γ -secretase, a

protease. The cleaved Notch fragment brings about nuclear transcriptional activation complex with Suppressor of Hairless (SuH) and Mastermind (MAM) proteins enabling the expression of downstream targets namely the β HHLH Enhancer of Split genes. These genes repress *Asc* expression and blocks further neural differentiation along with down regulating delta expression (Pierfelice et al, 2011) (Figure 1.1 A). Initially all *achaete-scute* expressing cells have equal levels of Notch and Delta activity. When a cell expresses more *achaete-scute*, it activates the Delta promoter to produce more Delta protein that then activates Notch on neighbouring cells. This resulting in more Notch fragments binding to SuH that further joins Enhancer of Split in a transcriptional complex. This complex binds the N-box regulatory region in *achaete* gene to suppress its transcription thereby downregulating delta and forming a single neuroblast (Castro et al, 2005).

Further studies have indicated that the onset of notch activity is a random event that governs progenitor fate, with Notch signalling occurring both before and after mitosis (Wilcock et al, 2007; Vilas-Boas et al, 2011). However this has been ruled out in more recent studies observing cells during normal neurogenesis where the establishment of apical polarity is crucial to this process (Das & Storey, 2012) (Figure 1.1 B). In this study, dividing cells with non-perpendicular cleavage planes are able to generate daughter cells through asymmetrically inheriting the apical Par protein complex. Par3 specifically promotes the stem cell state of progenitors through Notch signalling. This complex is associated with dynein proteins and microtubule networks that contact the mitotic spindle (Zhong et al, 2008). This results in the basal daughter cell rapidly regrowing an apical process, re-establishing apical polarity. Loss of apical protein complex may serve to release the cells from the surface of the lumen.

Figure 1.1 (A) Scheme of Notch signalling between two adjacent cells. Arrowhead denotes the site of S2 ligand dependent processing. Grey arrow denotes site of S3 cleavage by γ -secretase as well as CBF1 mediated transcription of target genes in the nucleus. Ub – ubiquitin; PS – Presenilin. Taken from Pierfelice et al, 2011. (B) Cell movements during neurogenesis in the chick neural tube. Asymmetric divisions generate daughter cells inheriting apical (red) or basal (blue) cell poles. Upon division, apical daughters inherit the original apical complex (green) and the basal daughter inherits the basal process. The basal daughter makes new apical complex proteins (light blue) and extends a new apical process and elevates Notch signalling (grey). The apical daughter generates a new basal process, whilst down regulating apical proteins, evident as it commences apical process withdrawal during neuronal differentiation. The notch activated basal daughter cell that retains apico-basal polarity then goes on to divide again. Taken from Das & Storey, 2012.



In the neural tube as in the cortex, cells that inherit the apical component during division more often than not exit the cell cycle and become neurons. Therefore the basal daughter remains the progenitor daughter cell, and continues to function as a progenitor cell with inheritance of basal process a requirement for the maintenance of the neural stem cell state (Alexandre et al, 2010; Das & Storey, 2012). The model presented was that Notch signalling is differentially activated after apical-basal division indicating that mitotic spindle orientation influences Notch signalling. Increased levels of Notch in basal daughter cells reiterates their progenitor profile and indicates that asymmetric division results in a 'cell intrinsic' difference in ability of sibling cells or neighbouring cells to respond to Notch. Moreover basal daughter express Par3 and have active notch signalling while apical daughters, inherit Par3 but have no active Notch signals. The apical daughter then down regulates Par3 driving as differentiation proceeds (Das & Storey, 2012).

1.1.3 Downstream of the Notch pathway in vertebrates.

There are 4 Notch receptors in mammals, Notch1-4 that are activated by the Delta-like ligands Dll1, Dll3 and Dll4 and Jagged proteins, Jag1 and Jag2 on adjacent cells (Reviewed in Pierfelice et al, 2011). Delta and Serrate/Jagged proteins are further notch ligands that are expressed in complimentary domains within the ventricular zone (Myat et al, 1996). As described above, activation of the Notch receptor results in the intracellular Notch domain (NICD) being cleaved by Presenilin proteases Psen1/2 of the γ -secretase complex. This NICD travels to the nucleus where it associates with CBF1 and mastermind-like (Maml) that then transcriptionally activate target genes. These Notch target genes include the Hes family, Hes1 and Hes5, and Hey genes that

encode inhibitory β HHLH proteins that bring about the repression of proneural β HHLH genes such as *Ascl1* and *Neurogenin1/2*, two genes that promote neural differentiation. Therefore cells activated by Notch are inhibited from developing into differentiated neurons and reside in a stem cell state. Further targets of Notch signalling may be *cyclinD1*, *p21*, *ErbB2* and *GFAP* to name a few although the mechanisms behind these remain unclear (Figure 1.1 A).

Notch1 loss of function mice reveal a faster rate of differentiation of ventral spinal neurons with lower levels of *Hes1* and *Hes5* expression and higher levels of *Mash1* and *Neurogenin1* and *Neurogenin2* expression. There was also a reduction among multiple progenitor subtypes with marked increases in V0, V1 and especially *Lim3/Chx10* positive V2 interneurons accompanied by a decrease in *Lim3/Islet1* positive motor neurons. This suggests Notch1 down regulation generates interneurons at the expense of motor neurons (Yang et al 2006). This compensatory effect is accompanied by a fusion of the ventral central spinal cord canal emanating from the floor plate perhaps through the loss of progenitor cells closest to the ventricles. Furthermore premature development of post mitotic neurons occurs that interconnect laterally, with *Chx10* positive V2 neurons and *Sim1* positive V3 neurons located more medially fusing together at the midline. Looking more closely, Notch 1 in the ventral spinal cord may serve to restrict the size of *Lim3* positive progenitors through its action in progenitors. Within *Lim3* population may then favour motor neuron development, yet the mechanism is unclear and may involve LIM-NLI tetramer complexes (Yang et al 2006).

The notch pathway genes and proneural transcription factors are expressed in progenitors and differentiating neurons (Bertrand et al, 2002). The proneural genes Mash1, Neurogenin and Olig1/2 maintain progenitor cells by activating Dll1-3, which further activates notch receptors on dividing progenitor cells (Kageyama et al, 2008). The downstream expression of Hes1/Hes5 genes maintain cells as progenitors. Blocking the Notch receptor function results in premature neural differentiation (Nelson et al, 2007). Over expressing Notch blocks the differentiation of progenitors to neurons, whereby they either stall or become glia. The progenitor pool is maintained if the cells express Dll, neurogenin and Hes1 equally. However, if a daughter cells has more neurogenin expression, this in turn stimulates the expression of Dll, activating Notch in the sister progenitor cell, which lowers its Dll expression. The daughter cell with higher neurogenin levels then terminates as a neuron. Therefore a change in the balance of Ngn or Hes1 levels in the Notch pathway results in an amplification of the surplus signal through feedback between the cells. Hes1 represses its own transcription resulting in a feedback loop that oscillates the level of Hes1 protein in each progenitor cell (Shimojo et al, 2008).

The Hes1 oscillation results in counter oscillations of Ngn, and Dll gene activity in each cell whereby two neighbouring progenitor cells in contact cycle in opposite phases to each other. A second oscillation occurs during the progenitor expansion phase at Mitosis where Hes1 levels are high at S-phase but low entering M phase and G1 phase at the ventricular surface. Notch thus demethylates STAT3 binding site of the GFAP promoter enabling CNTF to activate this region (Namihira et al, 2009). Notch further induces NFIA, a glial promoting transcription factor during late astrocyte generation, repressing neurogenesis through Hes5 (Daneen et al, 2006).

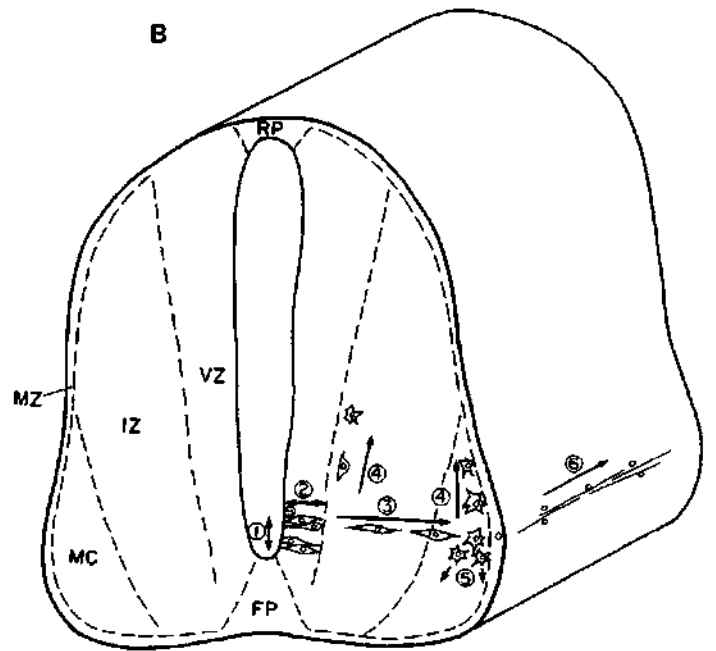
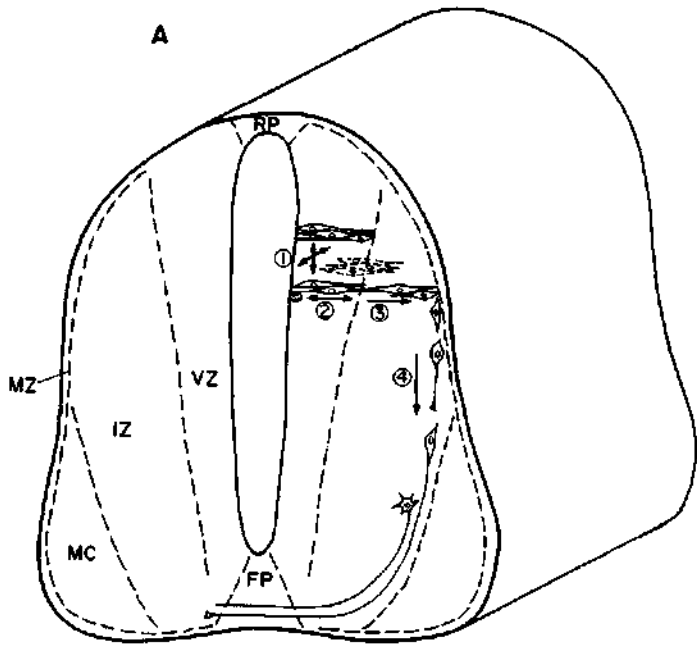
1.2 Control of cell movements in the early neural tube.

Cell movements within the neural tube are critical to the final location of neuronal subtypes, as demonstrated by studies on the distribution of motor neurons innervating the chick limb muscles and consequent columnar functional grouping of neurons (Landmesser, 1978; Landmesser, 2001; Hollyday & Hamburger, 1977; Hollyday, 1980). Post mitotic daughter cells arising from ventricular zone neural progenitors, initially inhabit the midline ventricular zone either side of the lumen along distinct domains, and then migrate laterally and subsequently dorsoventrally along the neural tube (Leber & Sanes, 1995). The different combinations of transcription factors maintain regional properties and functionality during the migration of neuronal populations (Briscoe et al, 2000).

Retroviral recombinant labelling of cells has shown a lateral displacement of cells within the ventricular zone, which becomes increasingly restricted into clonal groups, whilst initial migration is predominantly radial. Here radial stacking of progenitors in the ventricular zone and their migration occurs in spoke-like routes. Circumferential migration of neurons along axons and short distance dispersal of differentiating neurons, along with late migration of glia along white matter tracts also occurs (Leber & Sanes, 1995; Cepko et al, 1995) (Figure 1.2).

Neuroepithelial radial glial cells are the first precursor cell types to develop in the spinal cord prior to the onset of neurogenesis. These cells are bipolar in morphology with both ventricular anchorage through apical adherens junctions with the lumen, and an elongated process with a conical pial end foot.

Figure 1.2 A Summary of the migratory patterns in dorsal (A) and ventral (B) chick spinal cord. (1) Cell mixing in the VZ (2) Radial Stacking in the VZ (3) Radial migration into the IZ (4) Tangential migration (5) Dispersal of differentiated cells (6) Longitudinal migration of glia. FP-Floor Plate, IZ-Intermediate Zone, MC-Motor Column, MZ-Marginal Zone, RP-Roof Plate, VZ-Ventricular Zone. Taken from Leber & Sanes 1995.



The radial glial cell bodies lie predominantly in the ventricular zone and their bipolar morphology distinguishes them from the neuroepithelial cells within the cord (Rakic, 1972; DeFelipe et al, 1988; Anthony et al, 2004). These radial glia ultimately give rise to all the different neuronal subtypes within the neural tube and a large majority develop into astrocytes at later stages of development. Post-mitotic pioneer neurons migrate along the radial glial fibre scaffold towards the pial surface and their fated pools (McDermott et al, 2005).

1.2.1 Interkinetic Nuclear Migration.

The nuclei of radial glial cells shuttle back and forth along the width of the ventricular zone as they undergo cell division. Once the daughter cells exit the cell cycle, they migrate radially and differentiate. Studies in the vertebrate retina and chick hindbrain have revealed that Interkinetic Nuclear Migration (INM) may have an impact on the fate of the daughter cells during cell division (Fujita, 1964; Fujita 2003; Guthrie et al, 1991). Interkinetic nuclear migration as demonstrated in fish therefore drives nuclei to be exposed to proliferative versus differentiation signals (Frade, 2002; Gotz & Huttner, 2005; Del Bene et al, 2008). During this nuclear migration, the nucleus shuttles through the cytoplasm during the cell cycle whereby M phase of mitosis, and consequent G phases occurs at the basal surface, respectively, and S phase where DNA synthesis occurs basally during asymmetric cell divisions (Jacobson, 1985).

Studies of radial glia in the mammalian cerebral cortex have identified two distinct progenitor cell behaviours following cell division at the onset of neurogenesis. Firstly, a vertical symmetrical cleavage occurs whereby both daughter cells maintain contact

with the ventricular surface, which may serve to replenish the progenitor pool as radial glia. Secondly, horizontal asymmetrical cleavage occurs where one daughter cell re-enters the cell cycle, and the other migrates radially as a post mitotic neuron undergoing differentiation.

1.2.2 Radial glia and Laminins

Asymmetrical cell divisions thus produce one progenitor cell and one neuron thereby replenishing the progenitor pool and producing differentiating neurons. Daughter cells that maintain both basal and apical adhesive junctions remain in the progenitor pool as radial glia (Chenn et al, 1998; Konno et al, 2008). The mechanisms behind how radial glia interact at adhesive junctions with the extracellular matrix of the spinal cord is only recently being elucidated. Studies in the Medaka fish have suggested that Laminin signalling through the downstream Focal Adhesion Kinase (FAK) is required for planar cell division and interkinetic migration. This is possibly through an interaction between FAK and the dynein machinery, which is required for migration and movement (Tsuda et al, 2010).

Laminins form key subunits of basement membranes structurally and also serve within signalling complexes with Integrins (Yurchenco et al, 2004). In higher vertebrates during neurogenesis, laminin function was shown to be necessary for the correct positioning of cortical basement membranes. Loss of laminin function resulted in ectopic neuronal protrusions, yet laminin mutants are predominantly embryonic lethal (Halfter et al, 2002; Miner et al 2004). These early processes set the scene for neurogenesis in the neural tube and a complex patterning programme consequently ensues giving rise to neuronal populations at distinct locations in the spinal cord.

1.3 Neurogenesis and the cell cycle.

During early growth of the neural tube, progenitor cells produce a large number of radial glial cells that are initially bipolar in morphology with one process attached to the central canal at the ventricular surface and the other connected to the outer, basal cell surface of the neural tube. The nuclei of these cells shuttle back and forth during the cell cycle, through Interkinetic Nuclear Migration. The nuclei move to the inner ventricular surface just prior to mitosis and divide into two daughter cells. The nuclei then move away during S-Phase (Norden et al, 2009).

Astrocytes and oligodendrocytes also arise from the same cells that give rise to motor neurons highlighting the multipotency of the early ventricular zone progenitor cells, where neurons are generated first and then glial population follow (Leber et al, 1990; Tosney et al, 1995; Wilcock et al, 2007). Thus, multipotent progenitors in the neural tube can give rise to several lineages producing neurons, astrocytes and oligodendrocyte progenitors. However this multipotency gets restricted over time so that progenitors become committed to producing either neurons or glia and thus the potential of progenitor cells ultimately becomes restricted over time to unipotency.

It is thought that phosphorylation signals are also required for the establishment of cell polarity, position and regulation of these precursor and daughter cells during neurogenesis. Phosphorylation through the action of a typical protein kinase C (Baye & Link, 2007), regulates cell polarity and influences the decision of progenitors to maintain stem-like properties or commit to a post-mitotic state.

1.3.1 Cyclins as key components of the cell cycle.

As development progresses, the number of new cells generated by progenitors decreases and the cells take longer to progress through the cell cycle. Cyclins are key components of cell cycle regulation and their expression coincides with the various stages on the cell cycle temporally. The cyclins associate with cyclin-dependent kinases (CDKs) resulting in their activation and consequent phosphorylation of key cell cycle proteins. Pairs of cyclins/cdk complexes regulate the different stages of the cell cycles and serve as start/stop cues. The progression through M Phase is controlled by Cyclin B and Cdk2 whilst the transition of G1 phase to S Phase is governed by Cyclin D and Cdk4 or Cdk6. Here Cyclin D causes cells to enter S phase by phosphorylation of Retinoblastoma protein (Rb), a tumour suppressor gene. Rb releases E2F that drives the transcription of target genes. Cdk inhibitors such as p27kip and p21 inhibit the cell cycle during mitosis in progenitor cells, causing exit of the cell cycle and differentiation of neurons and glia (Calegari et al, 2005).

Ultimately FGF and EGF signals also play a role in the progression of G1 to S phase controlling cyclin D1 expression, with the Wnt pathway crucial for progenitor cell proliferation. Progenitor cells express receptors for specific mitogens and respond to their signals accordingly. EGF and FGF stimulate cell division by driving the expression of Cyclin D during S-phase. TGF-beta acts as stop signal for proliferating cells, through cell surface signalling and up regulation of p27kip. Further mechanisms act in concert to regulate cell cycle progression and generate the correct numbers of differentiated cells. Furthermore a shift occurs from a symmetric expansion phase of progenitor cell division to an asymmetric phase of cell division during neurogenesis.

As the cell cycle progression lengthens, progenitors gradually switch from producing further progenitor cells to producing differentiated neurons (Calegari et al, 2005).

1.3.2 Control of cell cycle & Wnt signalling

The overall regulation of cell cycle progression, cell proliferation and generation of neurons from neural tube progenitors are mediated in part by the Wnt family of secreted signalling proteins, related to the *Drosophila* Wingless gene, whose ligands bind to various Frizzled receptors on the cell surface and propagate a downstream signal (Nusse, 2001; Willert et al, 2003; Ohnuma & Harris; 2003). The Wnt pathway has been implicated in cell proliferation and adhesion, through various co-factors and structural adaptor proteins including dishevelled, β -catenin, and competitive cadherin dependent sequestration of β -catenin. These molecules transduce the signal from Wnt proteins, ultimately leading to β -catenin stabilisation and nuclear signalling. (Cadigan & Nusse, 1997; Jamora & Fuchs, 2002).

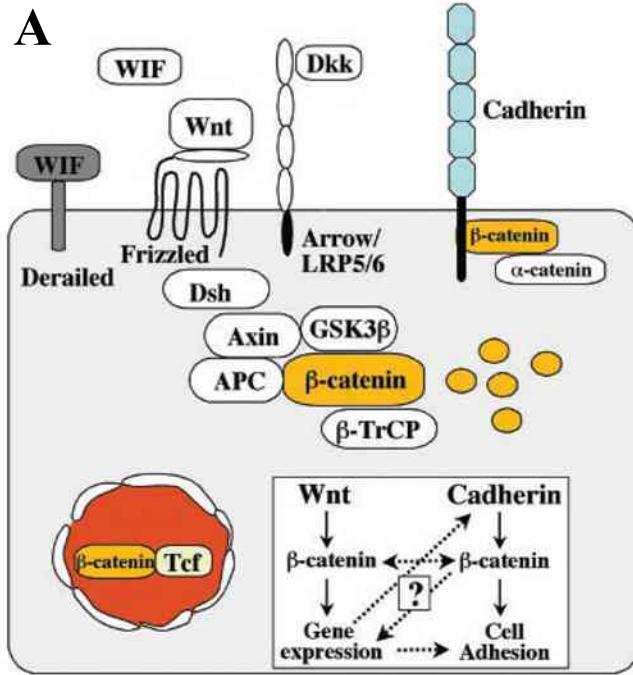
Knockout studies of members of the Wnt family (Wilson et al, 2001), Wnt1, namely in mice show a deletion of the midbrain. Wnt3a loss of function reveals loss of the hippocampus. Double Wnt1/Wnt3a loss of function mice exhibit defects of the midbrain, hindbrain, and spinal ganglia indicating semi-redundant roles of these two genes in controlling the growth of the spinal cord as opposed to specification of regional fates (McMahon & Bradley, 1990; Ikeya et al, 1997). The ectopic expression of Wnt1 also results in a larger neural tube without affecting the patterning of precursor cells (Dickinson et al, 1994).

Wnt1 and Wnt3a have been shown to act as mitogens by promoting proliferation and inhibiting the differentiation of progenitor populations of neurons. This is thought to occur via a gradient of Wnt activity, high dorsally, lower ventrally across the ventricular zone, initiated by Wnt genes expression in the dorsal midline of the spinal cord. Here the Wnt activity may affect the rate of proliferation and differentiation of precursor cells, while the dorsal TGF β and ventral Shh gradients would be involved in the patterning of distinct precursor identity (Megason & McMahon, 2002).

McMahon and colleagues investigated the action of Wnt in the chick spinal cord and found that ectopic expression of Wnt1 resulted in a reduction of the number of differentiating neurons and increased rate of progenitor cell proliferation. Such mitogenic growth was greater at ventral regions with bulging of the ventricular zone. Furthermore this mitogenic effect was not observed amongst progenitors in the dorsal most region of the neural tube, yet elicits the greatest effect on the ventral most progenitor domains. The overall rate of proliferation in the neural tube following ectopic Wnt1 expression increased by 50% predominantly in the ventral region of the spinal cord through increasing the number of S-Phase cells and shortening the G1/G2 phases of the cell cycle. This in turn reduced the differentiation of interneurons and motor neurons by over 50% without affecting the rate of apoptosis, demonstrating of role for Wnt1 in cell cycle progression and exit (Megason & McMahon, 2002).

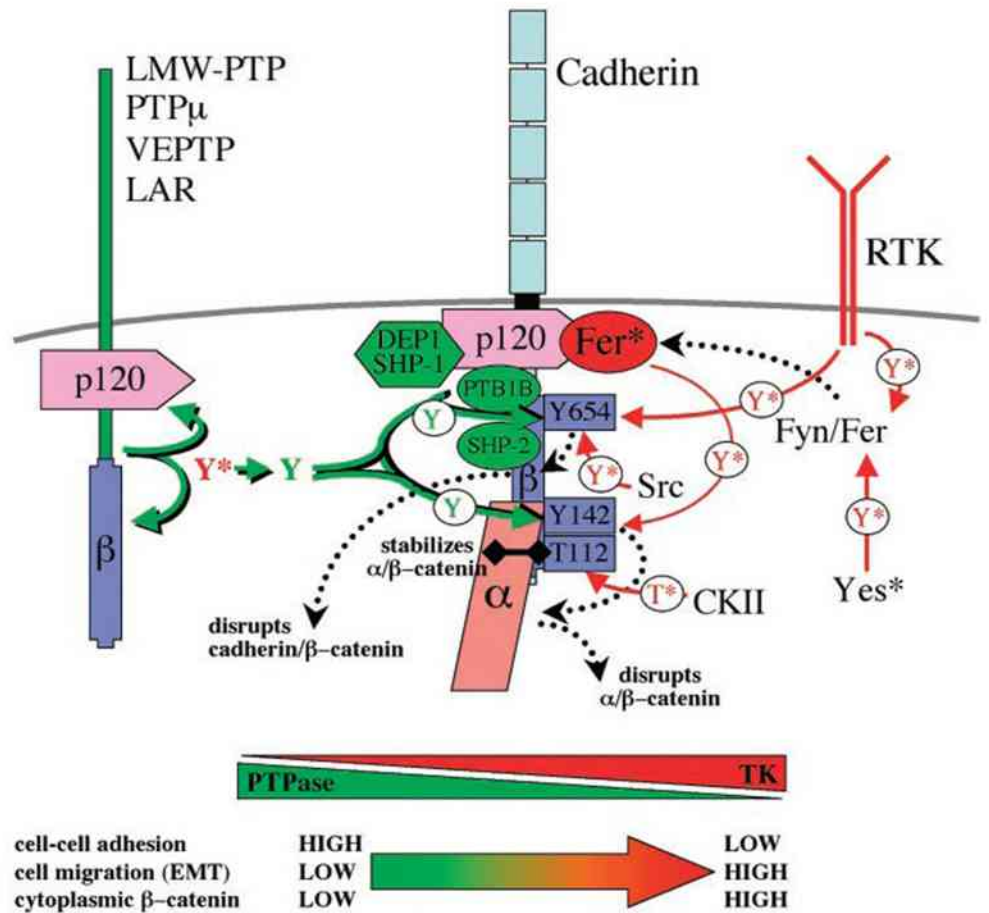
The transduction of Wnt signals is mediated by a number of factors, bringing about its action through the classical 'canonical' pathway where β -catenin is recruited and stabilised and initiates the binding of the TCF/Lef family of transcription factors that transcriptionally activate Wnt target genes (Nelson and Nusse, 2004) (Figure 1.3 A).

Figure 1.3 (A) Scheme of β -catenin in Wnt signalling and the cadherin complex. β -Catenin exists as a cadherin-bound form that regulates adhesion. This occurs in a complex with axin, APC, and GSK-3 β , where it is phosphorylated and targeted for degradation by β -TrCP; or in the nucleus with TCF/LEF transcription factors. Wnt signalling, proceeding through Frizzled, activates Dishevelled (Dsh), which results in uncoupling β -catenin from the degradation pathway and its entry into the nucleus, where it interacts with TCF/LEF to control transcription. Wnt protein can also interact with the Derailed receptor to control axon path finding. The Wnt pathway is also subject to extensive regulation and feedback control by extracellular factors that bind Wnt i.e. Wnt inhibitory factor (WIF) and Frizzled-related protein (FRP) or the coreceptor LRP (Dickkopf). Taken from Nelson & Nusse, 2004). (B) Regulation of the cadherin-catenin complex by the balance of tyrosine kinase and phosphatase activities. Cadherin binds p120 and β -catenin, which in turn binds α -catenin. The integrity of this complex is negatively regulated by phosphorylation of β -catenin by receptor tyrosine kinases (RTKs) and cytoplasmic tyrosine kinases (Fer, Fyn, Yes, and Src), which phosphorylate (red arrows) specific tyrosine residues in β -catenin (Y654, Y142), which leads to dissociation of the cadherin-catenin complex. Integrity of the cadherin-catenin complex is positively regulated by β -catenin phosphorylation by casein kinase II, and dephosphorylation by protein tyrosine phosphatases that bind p120 and β -catenin (green arrows). Changes in the phosphorylation state of β -catenin (bottom) affect cell-cell adhesion, cell migration, and the level of signalling β -catenin.



B

- Y* phospho-tyrosine
- Y tyrosine
- T* phospho-threonine
- \rightarrow kinase activity
- \leftarrow phosphatase activity
- \rightarrow change in binding
- Fyn } cytoplasmic tyrosine kinase (TK)
- Fer }
- Src }
- Yes }
- RTK receptor tyrosine kinase
- LMW-PTP } transmembrane protein tyrosine phosphatase (PTP)
- PTP μ }
- VEPTP }
- LAR }
- DEP1 } cytoplasmic protein tyrosine phosphatase (PTP)
- SHP-1 }
- PTB1B }
- α α -catenin
- β β -catenin
- p120 p120^{cas}



Megason and colleagues found that transfection of a dominant active form of β -catenin also resulted in an overgrowth phenotype similar to Wnt1 yet more pronounced, suggesting other factors may be involved downstream of Wnt and upstream of β -catenin. The ectopic expression of Wnt1 or dominant active β -catenin was sufficient to reduce the differentiation of progenitors along the entire dorsoventral axis, blocking their differentiation without inducing apoptosis.

Furthermore, ectopic dominant negative β -catenin expression resulted in an expansion of all progenitor domains evident by Pax6, Pax7 and Nkx2.2 yet precursor boundaries and domains were correctly patterned. Of the TCF/Lef family, TCF3 and TCF4 are expressed in neuronal precursor cells, ectopic expression of dominant negative TCF4 that is unable to interact with β -catenin acts as a repressor of wnt pathway target genes and caused the cell autonomous blocking of the cell cycle prior to S-Phase without differentiation and therefore remaining stalled (Megason & McMahon, 2002).

In the chick neural tube, only Wnt1 and Wnt3a demonstrate mitogenic activity and are expressed in dorsal midline cells, however Wnt3, Wnt4, Wnt7a, Wnt7b showed no such mitogenic properties and did not have any effect on the proliferation of precursor cells. Wnts elicit their responses through transcriptional targets to bring about regulation of the cell cycle. A key target is cyclin D1 (Nurse, 2000; Megason & McMahon, 2002). Cyclin D1 is expressed in the neural tube in a high dorsal to ventral gradient in mitotically active neural precursors, regulating the G1 exit of the cell cycle. In the early neural tube cyclin D1 expression is evident along the ventricular zone, however this expression gradient becomes restricted dorsally. Furthermore, dominant active β -catenin upregulates G1 phase cyclin D1 and cyclin D2 but not G2/Mphase

cyclins, cyclin A1 or cyclin B3 within precursor cells indicating the transcriptional regulation of cyclinD1 by Wnt signals to be a direct action.

Ectopic expression of Wnt1 and Wnt3a also resulted in cyclinD1 up regulation, yet only in intermediate to ventral regions of the spinal cord as ventral cells have a stronger response to mitogenic wnt activity. Also, high levels of dominant negative TCF4 down regulated cyclin D1 expression. The ectopic expression of dominant negative cyclin D1 resulted in the formation of abortive complexes with G1 cyclin dependent kinases CDK4 and CDK6, causing a reduction in the expansion of progenitor populations without blocking the cell cycle, or abnormal expansion of progenitors. Dorsal midline wnts in the neural tube therefore serve to act as mitogens spatially and temporally (early progenitor expansion, later increased differentiation) on precursor populations, increasing their proliferative rate and decreasing the rate of proliferation through a gradient of activity from high dorsal to low ventral across the ventricular zone (Megason & McMahon, 2002).

1.3.3 Cadherin-catenin functions in the neural tube

The control of cell-cell adhesion is also important for neural tube growth and patterning. This is in part regulated by cadherins and catenin signalling. Cadherin signalling ultimately establishes adhesive contacts and to mobilise cells through the neural tube. Cadherin-based cell-cells contacts involve homodimerisation and consequent association with the cytoskeleton via actin clustering (Adams & Nelson, 1998). Tyrosine phosphorylation of β -catenin in the Cadherin/Catenin complex plays an important role in its regulation (Anastasiadis & Reynolds, 2000) (Figure 1.3 B).

Interestingly, the binding of α -catenin to actin at the cytoplasmic end of the Cadherin receptor, through a β -catenin complex, involving p120 that binds with microtubules is also regulated by phosphorylation. For our purposes we will focus on the type I Cadherins that include E-Cadherin and N-Cadherin and the Type II Cadherins that include MN-Cadherin (Shapiro & Colman, 1998).

Serine/Threonine phosphorylation of β -catenin results in stabilization of the Cadherin complex, however tyrosine phosphorylation of β -catenin directly disrupts this complex making more β -catenin available to the cytoplasm (Roura et al, 1999). Furthermore, a few PTPs bind to p120 and reverse the phosphorylation of tyrosine, which stabilizes the cadherin complex and establishes adhesive contacts (Lilien et al, 2002; Nelson & Nusse, 2004) (Figure 1.3 B).

Cadherins have also been shown to define and segregate pools of motor neurons during neurogenesis. The combined profiles of type II Cadherins that have been shown to define functional motor pools within the chick neural tube, namely the differential expression of individual members of the Cadherin family such as MN-Cadherin in the segregation of neuronal subsets within the motor columns and further segregation of neurons within each subdivision (Price et al, 2002). The Cadherins are also critically implicated in maintaining adhesive contacts between cells in the epithelium, with intracellular links to the actin filament cytoskeleton (Harstock & Nelson, 2007; Halbleib et al, 2006). As previously described, adherens junctions are located at the apical surface of the neuroepithelium and have many functions, namely cell adhesion, signalling, cytoskeletal regulation and transcriptional control. These junctions facilitate

the migration and dispersal of precursor and post mitotic cells and earlier transitional states of the epithelial cells (Yamada et al, 2005; Ferreri & Vincent, 2008)

The birth of the first neurons during neurogenesis forms a critical milestone in the development of the spinal cord. Complex gene interactions generate distinct populations of neuronal subtypes through a combination of signalling factors whilst guidance molecules guide newly born cells to their resting places in the spinal cord. Here, cells project axons to their targets and begin building the complicated array of connections within the central nervous system. From a mere cluster of blastula cells giving rise to the a pseudo stratified epithelium, the neural tube folds and holds together our wiring, connecting our peripheral motor and sensory circuits ultimately to our brain (Jessell, 2000). What triggers the birth and temporal-spatial distribution of spinal neurons within the neural tube and what cues guide this development, arranging the distinct functional cohorts into refined patterns?

1.4 Generating the anterior-posterior pattern of the neural tube

The Hox family genes were first discovered in drosophila. The Anteroposterior axis was initially established through the distribution of Bicoid anteriorly and nanos posteriorly, establishing a framework for further segmentation of the embryo (Driever & Nusslein-Volhard, 1998). Hox function has been conserved from flies to vertebrates, however the mechanisms of patterning vary.

1.4.1 Retinoic acid and rostrocaudal polarity

A major regulator of Hox gene expression has been identified as Retinoic Acid (RA), which permeates the cell membrane and binds a cytoplasmic retinoic acid receptor complex that moves to the nucleus to regulate the expression of target genes via 'Retinoic Acid Response Elements' (RARE). RA expression proceeds through a gradient with anterior regions of the embryo possessing a ten fold greater concentration compared to posterior regions. Embryos treated with RA fail to develop heads and display an inhibition of anterior Hox gene expression (Durstion et al, 1989).

RA is able to induce Hox gene expression in embryonic stem cells with increasing concentrations of RA, resulting in the expression of more posterior Hox genes (Simeone et al, 1991). The source of RA is the overlying paraxial mesoderm which enzymatically synthesises RA that consequently diffuses into the neural tube in order to activate the correct expression of the Hox genes. In vertebrates, the neural inducers through the organiser centres produce, as described previously, Chordin/Noggin/Follistatin that transforms the neural tube to provide anterior brain characteristics, whilst caudal transforming features are brought about through the action of RA, Wnts, Hox and FGFs in synergy with BMP signalling (Nordstrom et al, 2006).

1.4.2 FGF signalling and anteroposterior patterning.

Along the rostrocaudal aspect of the neural tube, the Fibroblast growth factor genes (FGFs) and Retinoic Acid and expression profiles of the Hox transcription factors determine the pattern of neural progenitor cells and position along the length of the

spinal cord (Bel-Vialar et al, 2002; Dasen et al, 2003, Sockanathan et al, 2003). Many Hox genes ultimately work with other factors to determine motor neuron pool identity with a very ordered and restricted expression profile (Jungbluth et al, 1999; Briscoe & Wilkinson, 2004; Dasen et al, 2005).

Progenitor cell culture experiments show that adding FGF drives their differentiation to neurons whilst those cultured with EGF, CNTF or BMP produced astrocytes. Progenitor cells cultured with PDGF produced oligodendrocytes (Ravin et al, 2008; Bonni et al, 1997; Raff et al, 1988). CNTF receptor activation causes phosphorylation of STAT3 that in its active form enters the nucleus and binds to specific sites in the promoter regions of GFAP and S100 genes. This direct transcriptional control is reinforced by BMP, where early progenitor cells remain unresponsive to CNTF and therefore few glia are produced at these stages. The DNA in promoter regions of GFAP is methylated in early progenitors blocking the binding of STAT3 and activation of GFAP function (Fan et al, 2005).

The anteroposterior gradient of Wnt/ β -catenin and further co-inhibition of Wnt/BMPs leads to the induction of anterior CNS characteristics. Mediators in the inhibition of the Wnt pathway include Cerberus, FrzB receptor that competes for Wnt thereby blocking its signal propagation and Dickkopf, which are all expressed in the organiser region (Kiecker & Niehrs, 2001). The FGF family of growth factors act in a dose dependent manner similar to the action of RA during neural induction. High FGF expression induces posteriorising genes of the Hox family such as FGF8 in the chick (Liu et al, 2001; Maden et al, 2006).

1.5 Establishing dorsoventral polarity of the neural tube.

Dorsoventral polarity within the spinal cord occurs through a sequence of cell movements and formation of the ventral floor plate and dorsal roof plate. The sulcus limitans forms as a fissure along the length of the spinal cord dorsoventrally. Signals emanating from the notocord and other neural and non-neural tissues further develops and refines this axis.

1.5.1 Shh and neural tube patterning

A large number of transcription factors determine the DV patterning of the spinal cord during development (Tanabe & Jessell, 1996; Lumsden & Krumlauf, 1996; Goodman, 1996). An initial pattern is established by Sonic Hedgehog (Shh) and Bone Morphogenic Protein (BMP) (Roelink et al, 1994; Roelink et al, 1995; McMahon et al, 1998). Along the dorsoventral aspect of the cord, the Shh gradient expression extends from the notochord and floor plate, decreasing dorsally resulting in progenitor cells generated in the ventricular zone of the neural tube, whilst BMP's operate dorsally and in competition (Poh et al, 2002; Liem et al, 1995).

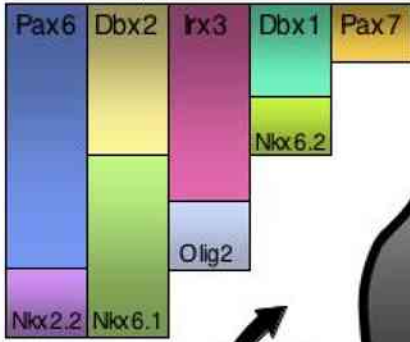
Pax7, Olig 2 and Nkx2.2 are main players in this process and are expressed in well defined domains with Pax7 responding to lower levels of SHH, while Nkx2.2 to the highest levels of SHH ventrally. Shh loss of function embryos for example reveal a block in the development of all ventral cell types in the spinal cord, including motor neurons (Chiang et al, 1996). The Gli genes are implicated as transducers of the Shh signal and these are described in more detail in section 1.6. (Figure 1.4 A & B).

Figure 1.4 (A) A scheme for spinal cord development in the chick. On the left is a diagram of the cross-regulatory interactions between Class I & II genes, which establish the cell fate domains at the corresponding levels of interacting pairs, where boundaries represent cross-repressive pairs. They act either side of the midline of the spinal cord to set up the progenitor domains p0 to p3 in the spinal cord scheme at the centre of the diagram against a decreasing Shh gradient from the ventral to the dorsal aspect of the spinal cord. These then gives rise to their corresponding cell fate domains V0 to V3, which by E5 express various differentiation factors, also listed in the table on the right against their cell fate domains. VZ-Ventricular zone. Adapted from Jessell, 2000. (B) Molecular pathway for motor neuron development where Nkx6.1 unconstrained by Irx3 and Nkx2.2 is sufficient to induce MNR2 expression, which then induces downstream transcription factors Lim3, Isl1/2 and HB9. MNR2 also auto-activates its own expression consolidating progenitors toward a motor neuron fate. After Jessell, 2000.

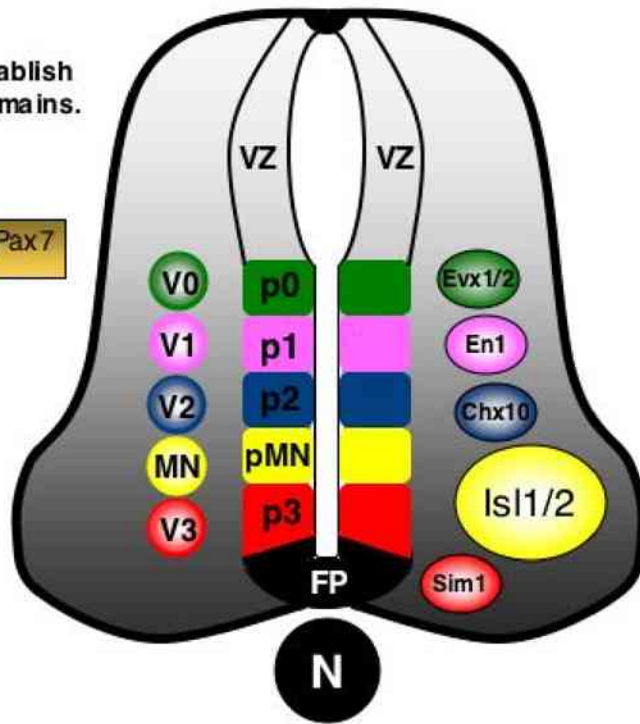
A

Progenitor factors that establish corresponding cell fate domains.

Class I - Repression



Class II - Induction

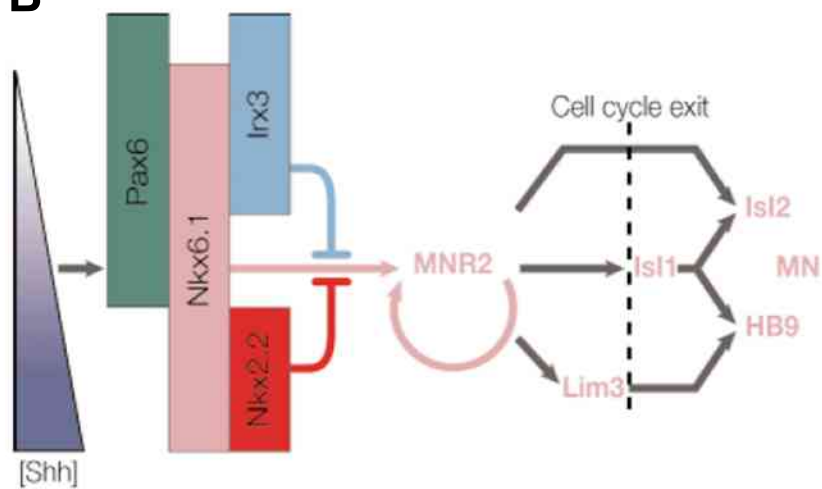


↑ DORSAL
↓ VENTRAL

V0	Evx1/2
V1	En1
V2b V2a	Chx10 Gata2/3
MN	Isl1/2, Lim3 Mnr2, Hb9
V3	Sim1

Differentiation factors.

B



1.5.2 Dorsal fate determination by BMPs

The progressive restriction of neuronal fate within the spinal cord as development proceeds derives from many factors acting in concert to maintain the regional identity of neuronal progenitors through overlapping and restricted gene expression profiles. Members of the TGF β family namely the Bone Morphogenic Protein (BMP) genes act dorsally, originating from the roof plate in a graded manner within the neural tube alongside the ventral Shh signals. BMP loss of function mice (GDF-7) display a loss of the dorsal-most neural precursor cells in the neural tube (Lee et al, 1998).

Further experiments have demonstrated a role for BMPs whose expression from the roof plate promotes, regulates and defines the expression domains of the Pax genes. The Pax 3/6/7 genes are expressed in a dose-dependent manner prior to cell differentiation within the dorsal and intermediate regions of the neural tube, promoting cell differentiation and β HLH gene expression. BMPs then serve to activate various homeobox transcription factors that further define progenitor pools within the neural tube and alongside Wnt signals (Timmer et al, 2002; Lee et al, 2000; Zhuang & Stockanathan, 2006).

Studies in the chick have shown that BMPs and Wnts function within separate pathways, with BMPs acting as morphogens during neural patterning whilst Wnts may act as mitogens during neural tube growth. BMPs may also regulate Wnt and homeobox genes during a later phase of spinal cord specification and progenitor pool refinement (Chesnutt et al, 2004; Wine-Lee et al, 2004).

1.5.3 Wnt pathway and dorsoventral patterning.

Wnts are secreted molecules that bind the Frizzled receptor, a membrane bound protein with seven transmembrane domains. A further component of the frizzled receptor is called LRP that presents as a single transmembrane strand. In the absence of binding of Wnt protein to Frizzled, β -catenin binds to a complex and causes the ubiquitination and ultimate degradation of β -catenin (Cadigan & Nusse, 1997; Polakis, 2002). During the binding of Wnt to its receptor, a further protein, called dishevelled (Dsh) is activated, blocking the degradation of β -catenin and allowing its accumulation in the cell. This β -catenin then translocates into the nucleus forming a transcriptional activator complex with TCF/Lef, initiating the transcription of target genes (Reviewed in Nelson & Nusse, 2004).

Furthermore, Wnt signals are thought to result in the accumulation of β -catenin in the cytoplasm, translocation into the nucleus and interaction with the transcription factor T cell Factor/Lymphoid Enhancer Factor (TCF/LEF) that regulates gene expression. In the absence of Wnt signals, phosphorylation of β -catenin by CKI and Glycogen Synthase 3 β (GSK3 β) results in its degradation. Activation of Wnt leads to inhibition of GSK-3 β and accumulation of cytoplasmic β -catenin thus providing a level of β -catenin regulation within the cell (Polakis et al, 2002). Wnt signals therefore not only affect proliferation but also affect Shh induced patterning to a certain degree (Briscoe & Novitch, 2008; Muroyama et al, 2002; Robertson et al, 2004).

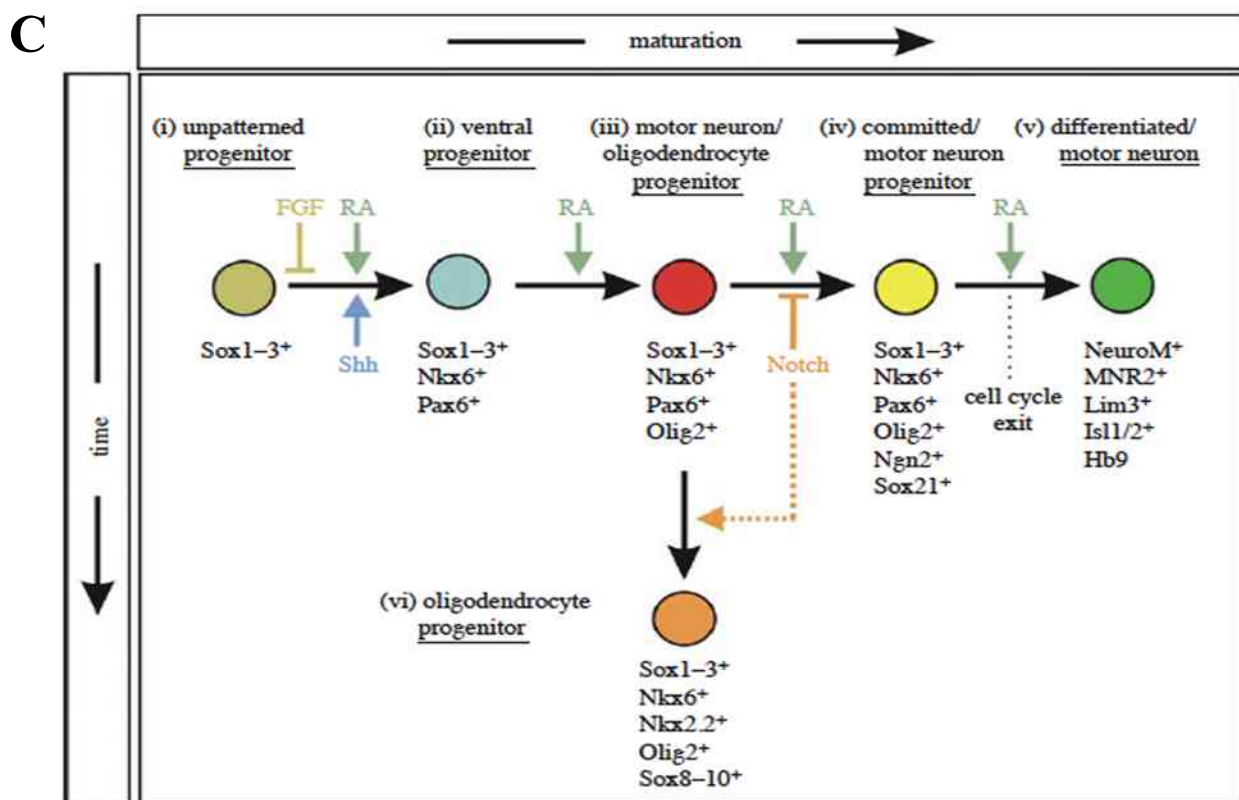
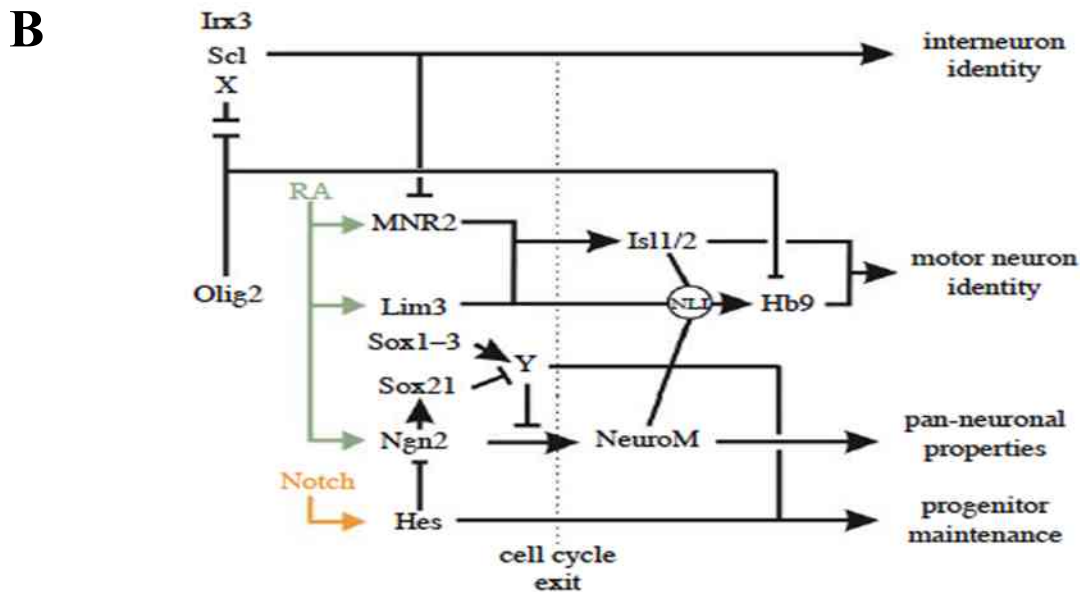
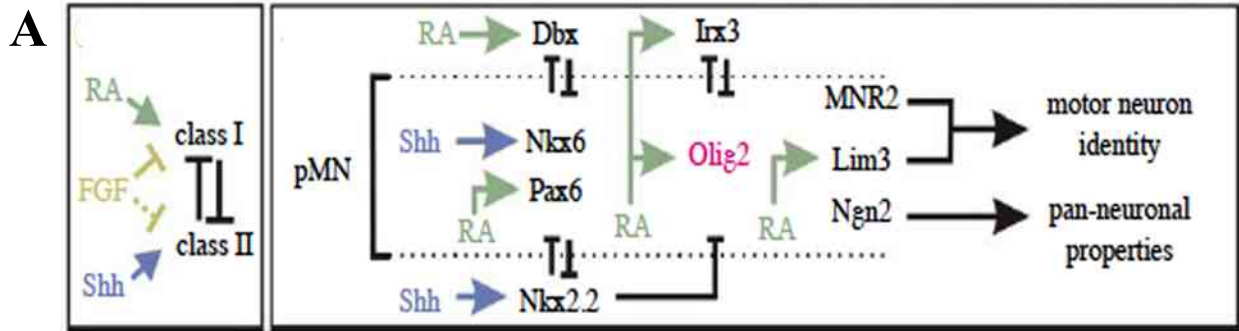
This sequence of events determines the expression of other transcription factors that establish the patterning of neural progenitor cells. Post mitotic daughter cells arising

from neural progenitor cells within the ventricular zone consequently follow a radial and tangential migration to end up in their transcription factor-specific domains creating diverse neural circuits (Briscoe & Novitch, 2008). Classical studies in the rat spinal cord reveal a ventral to dorsal sequence of neuronal production in the neural tube, whereby spinal motor neurons are the first to be generated followed closely by interneurons and finally dorsal horn neuronal populations (Altman & Bayer, 1985; Jessell, 2000).

1.6 Controlling neuronal fate – the β HLH genes.

A complex array of signalling processes orchestrate the assembly, birth and migration of neurons within the neural tube. The dorsoventral pattern of neurons in the cord is largely established by signals coming from Shh ventrally and BMP dorsally (Jessell, 2000). How are ventral Shh signals interpreted by progenitor cells? These occur through the action of Class I and Class II homeodomain transcription factors, whose distinct boundaries of expression are defined by cross-repressive interactions between the two pairs of genes. Motor neurons arise from the pMN domain that expresses Nkx6.1 and Pax6, which repress the determination of other neuronal cell types in this domain. Nkx2.2, Irx3 and Dbx2 repress motor neuron differentiation in non-pMN domains (Lee et al, 2004; Muhr et al, 2001). This results in Olig2 expression at the pMN domain driving motor neuron differentiation and expression of neuronal transcription factors Isl1/2, MNR2, Hb9 and Lim3. MNR2 then self regulates its expression, directing the cell toward a motor neuron fate. Gain of function studies of class I and class II transcription factors revealed they act repressively through the Groucho family of co-repressors (Muhr et al, 2001) (Figure 1.5 A-C).

Figure 1.5 (A) *Scheme of gene pathways regulating neurogenesis*. Shh and RA initiate the expression of Nkx6.1, Nkx6.2 (Nkx6) and Pax6 in ventral spinal cord progenitors. The repressor activities of Nkx6 and Pax6 prevent the expression of inhibitors of MN formation, such as Dbx1, Dbx2 (Dbx) and Nkx2.2, and permit ligand-bound retinoid receptors to activate Olig2 expression (red). Within MN progenitors, Olig2 directs MN differentiation by repressing Irx3 and other unidentified target genes that regulate the expression of the MN-specific transcription factors, MNR2, Lim3, Isl1, Isl2 and Hb9, and the pan-neuronal transcription factors, Ngn2 and NeuroM/Math3. The repressor activity of Olig2 works in conjunction with the activator function of ligand bound retinoid receptors. (B) *Transcription factor network controlling motor neuron differentiation*. Olig2 promotes motor neuron development through repression of Irx3, Scl and unidentified targets (X). RA signaling lead to the expression of transcription factors downstream of Olig2, including MNR2, Lim3 and Ngn2. Ngn2 is negatively regulated by Hes that act downstream of the Notch signaling pathway. The activator properties of Sox1–3 appear to induce the expression of unknown inhibitors of Ngn2 function (Y). Through blocking Ngn2 expression, Notch signaling, Hes genes and Sox1–3 maintain progenitors in an undifferentiated state. The release of Ngn2 leads to the up regulation of NeuroM and the exit of progenitors from the cell cycle. NeuroM then forms a transcriptional activator complex with Lim3 and Isl1/2, mediated by NLI, that activates Hb9. (C) *Scheme of cellular expression profiles during neurogenesis*. Progressive changes in progenitor cells during motor neuron development from (i) unpatterned progenitors to (ii) ventral progenitors, (iii) MN/Oligodendrocyte progenitors, (iv) committed MN progenitors and (v) differentiated MN state. A-C taken from Briscoe & Novitch, 2008.



For motor neurons to arise, the combined expression of Nkx2.2, Nkx6.1 and Irx3 at the pMN domain is required (Briscoe et al, 2000). Nkx2.2 and Irx3 define the ventral and dorsal limits of motor neuron production while Nkx6.1 then induces Olig2 and MNR2 expression (Novitsch et al, 2001, Tanabe et al, 1998). Mnr2 was in fact sufficient to generate ectopic neurons in the neural tube without any effect or feedback onto the Class I and Class II transcription factors (Tanabe et al, 1998).

Oligodendrocytes arise from older multipotent precursors that had already generated motor neurons from the pMN domain in the ventral spinal cord, through FGF signalling (Pringle et al, 2003). The two transcription factors Olig1 and Olig2 are expressed in this pMN domain. Olig1/2 loss of function reveals a failure of oligodendrocytes and motor neurons to develop, whilst over expression induced ectopic oligodendrocyte development. During motor neuron development, the proneural factor Neurog2 is expressed in the same domain as Olig2 and is involved in the production of motor neurons initially (Kessaris et al, 2001; Zhou et al, 2001). As development progresses, the progenitor cells switch off Neurog2 expression and instead express Nkx2.2. This represses motor neuron production whilst Olig1/2 expression is maintained in these cells, and this Oligodendrocyte production ensues. A single progenitor cell therefore is able to produce phases of motor neurons and then glial cells.

1.6.1 Generation of Progenitor pools

Along the spinal cord, before axonogenesis, neurons acquire transcription factor-specific columnar identities that strongly relate to their ultimate fate and function.

They can be grouped into subsets according to their expression profiles of transcription factors that determine their positional identity in the spinal cord (Jessell, 2000).

Motor neuron generation in the ventral neural tube is dependent upon a graded Shh signal from the floor plate and notochord (Chiang et al, 1996), which specifies the identity of motor neuron progenitors along the ventricular zone of the spinal cord (Ericson et al, 1996). This in turn regulates the expression of homeodomain and β HLH transcription factors in the 2 major groups: Class I, repressed by Shh, and Class II, activated by Shh. These genes work in complementary pairs whereby Class I and Class II transcription factors cross-repress each other at the boundary of their expression, defining distinct expression profiles of these genes within these progenitor domains. This then sets up progenitor domains dorsoventrally with distinct boundaries along the ventricular zone (Jessell, 2000; Briscoe & Ericson, 2001) (Figure 1.4 A).

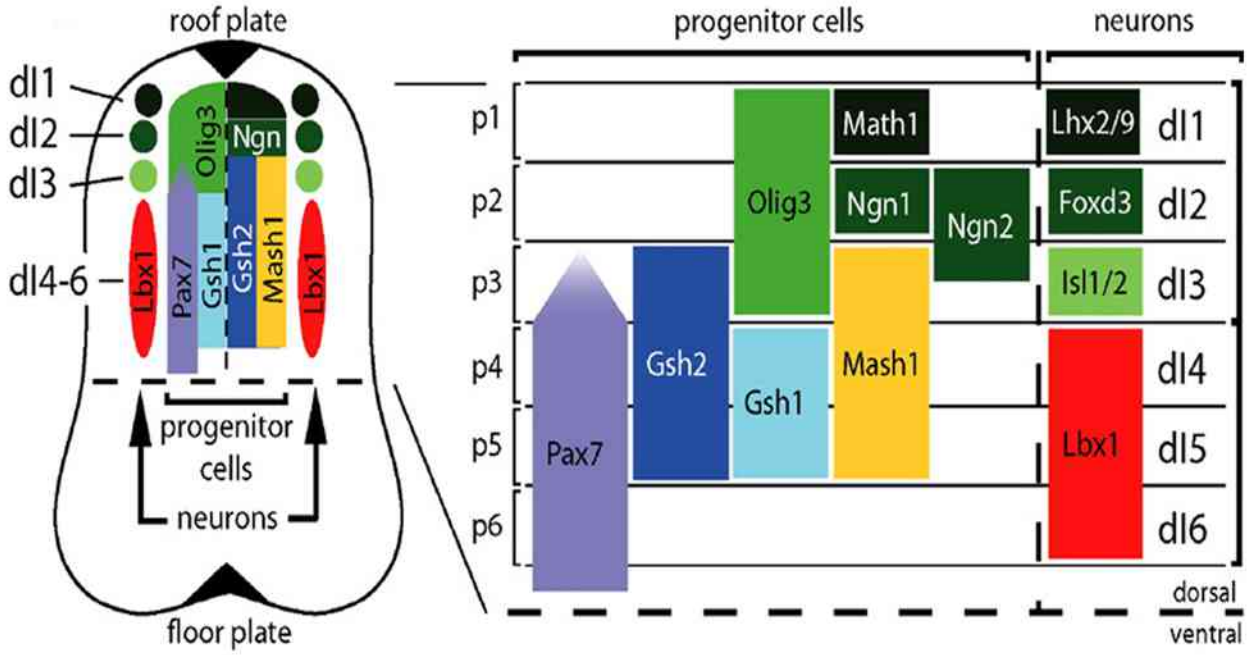
Early studies on the specification of progenitor identity and neural cell fate in the ventral neural tube reveal that the combinatorial expression of Nkx6.1, Nkx2.2 and Irx3 is responsible for the identity of 3 neuronal subtypes here (Briscoe et al, 2000). In vitro studies reveal 5 classes of ventral neurons are generated in response to varying concentrations of Shh activity and therefore corresponds to their positional identities within the neural tube and Shh dose required for their specification (Ericson et al, 1997). Downstream of the Shh signal various homeodomain genes elicit the effects of the Shh dose in driving the differentiation of progenitor cells that are expressed within these progenitor cell domains, namely the Pax3/6/7, Nkx2.2 and Dbx1/2 genes regulating neuronal subtype identity (Briscoe et al, 2000). Progenitor cells expressing Nkx6.1 and Irx3 are regulated by a specific SHH dose and located within a distinct

domain in the ventral neural tube. Moreover, 5 class I homeodomain proteins are repressed by Shh, namely Pax7, Irx3, Pax6, and Dbx1/2 and two class II homeodomain proteins are induced by Shh namely Nkx6.1 and Nkx2.2. The initial pattern of Class II protein expression ultimately becomes independent of Shh signalling by HH10-15. At the ventral limits of these class I expression domains and dorsal limits of class 2 expression domains sharp progenitor boundaries are defined. These cross repressive interactions are responsible for dividing the ventral tube into 5 distinct progenitor domains, V0, V1, V2, pMN and p3 in a dorsal to ventral progression (Briscoe et al 2000) as well as 6 dorsal progenitor domains (Muller et al, 2002) (Figure 1.6 A–D).

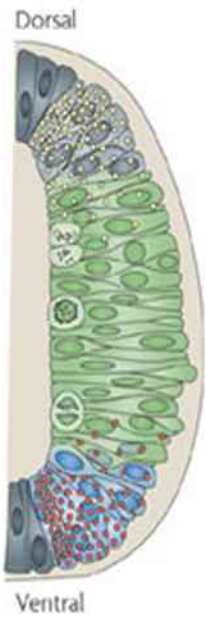
Misexpression of individual homeodomain proteins in a mosaic fashion by electroporation or retroviral transduction within the chick neural tube revealed an interesting effect on the progenitor boundaries. When considering the boundary at the pMN/p3 domain, delineated by Pax6 and Nkx2.2, misexpression of Pax6 ventral to its normal expression generate a cluster of ectopic Pax6 cells evident in the p3 domain, which lacked Nkx2.2 expression. The expression of Nkx2.2 in the p3 domain however was maintained by the other p3 domain cells that did not express ectopic Pax6, demonstrating a cell autonomous role for Pax6 here. The other homeodomain proteins were not affected by the misexpression of Pax6. Misexpression of Nkx2.2 dorsal to the p3 domain, its region of expression, the progenitor cells expressing ectopic Nkx2.2 did not express Pax6. Pax6 expression was however maintained in cells neighbouring the ectopic Nkx2.2 cells indicating a further cell-autonomous, selective function of Nkx2.2, as other homeodomain proteins remained unaffected by Nkx2.2 misexpression.

Figure 1.6 (A) *Scheme of dorsal progenitor cell patterning*. There are six progenitor cell subpopulations, p1–p6, in the medial spinal cord, with specific bHLH expression profiles. The six progenitor domains generate dorsal interneurons, dI1–dI6. These neurons are located laterally of the progenitors and are defined by their expression of homeodomain transcription factors. Taken from Zechner et al, 2007. (B) & (C) *Scheme of mouse spinal progenitor patterning and specification*. At E9 in the mouse (B), a gradient of Sonic hedgehog (red) ventrally and BMP/GDF7 (yellow) dorsally provide instructive positional signals to dividing progenitors in the ventricular zone. This leads to the restricted activation of patterning factors in discrete dorsoventral domains, which are represented by Nkx6.1 (ventral), Pax6 (intermediate) and Pax3 and Pax7 (dorsal). At E11 in the mouse (C), eleven early classes of post mitotic neuron are present in the embryonic spinal cord. dI1–dI5 neurons that are derived from dorsal progenitors (grey) primarily contribute to sensory spinal pathways, while dI6, MN and V0–V3 neurons from ventral progenitors (yellow) are elements of the locomotor circuitry. Some of the post mitotic transcription factors that mark each of the eleven early generic populations are indicated. Taken from Goulding, 2007. (D) *Specification of neuronal subtype identity in the mouse/chick spinal cord*. Right: neurons (circles) in the developing spinal cord can be uniquely identified by their transcription factor profiles. The different types of interneuron and motor neuron shown here derive from corresponding dorsoventral progenitor domains in the ventricular layer (Dp1 to Vp3), although their final location might alter due to cell migration. Left: neuronal identity is acquired when cells are still in the ventricular layer, in specific progenitor domains (vertical bars). Taken from del Corral & Storey, 2001.

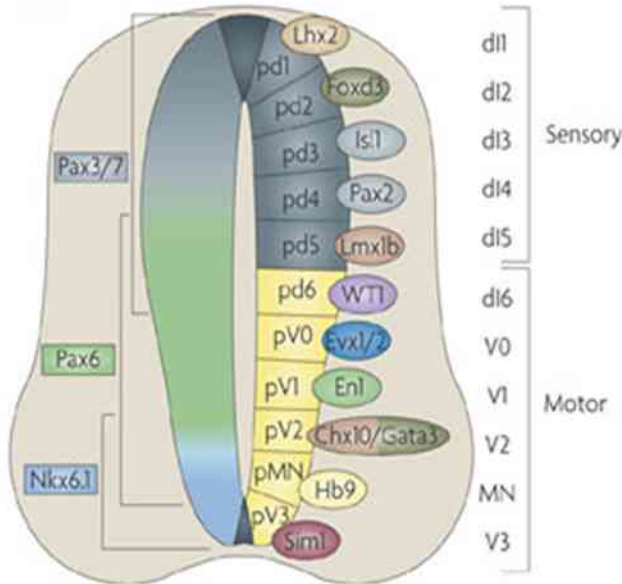
A



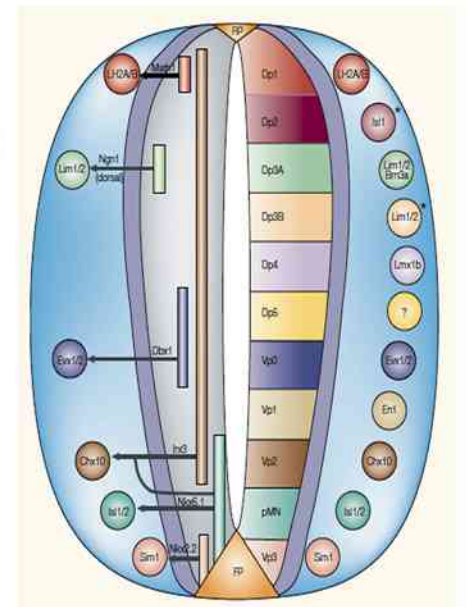
B



C



D



- Nkx6.1
- Pax6
- Pax3/7
- Sonic hedgehog
- BMP4,6,7, GDF-7

Nkx2.9 expression transiently overlaps with that of Nkx2.2 in the p3 domain and misexpression of Nkx2.9 resulted in ectopic Nkx2.9 cells that lacked Pax6 activity. The repression of Pax6 was shown to be independent of Nkx2.2 in this instance suggesting the ventral boundary of the pMN domain may be influenced by Nkx2.9 as well.

Observing the interactions at the p1/p2 boundary, between Dbx2 and Nkx6.1, misexpression of Dbx2 ventral to the p1 domain similarly showed the ectopic Dbx2 positive cells lacking Nkx6.1 expression whilst neighbouring cells maintained this expression without affecting Pax6 or Pax7 expression. Misexpression of Nkx6.1 resulted in the down regulation of Dbx2 in ectopic Nkx6.1 cells whilst Dbx2 expression was maintained in neighbouring cells. This further suggested a selective, cell autonomous role for Dbx2 and Nkx6.1 in this domain.

Looking at further progenitor relationships, the p0 domain gives rise to Evx1/2 positive neurons, whilst the p1 domain gives rise to V1 En1 positive neurons. The p3 domain gives rise to Sim1 positive V3 neurons and p2 domain gives rise to Chx10 positive V2 neurons. The pMN domain exclusively gives rise to HB9 positive motor neurons (Saha et al, 1997). The division of V2 neurons and motor neuron progenitors initiates the onset of Lim3 expression, with later motor neuron progenitors expressing MNR2. Lim3 was shown to be expressed in the p2 and pMN domains whilst MNR2 was expressed exclusively in the pMN domain (Reviewed in Price & Briscoe, 2004; Tanabe et al, 1998; Sharma et al, 1998; Briscoe et al, 2000).

When considering the three ventral most progenitor domains, misexpression of Nkx6.1 in the absence of high level Irx3 expression (that begins after neural tube closure at p2/pMN domain) at early stages revealed an ectopic pattern of MNR2 and Lim3 positive cells in dorsal positions to p2 domain in both progenitor cells and post mitotic neurons. Ectopic Islet1/2 and HB9 positive cells were also found on the lateral margins of the neural tube, possibly induced by the ectopic MNR2 expression driven by Nkx6.1. Furthermore, ectopic Chx10 V2 neurons were also observed in the p0 and p1 domains. Thus Nkx6.1 in the absence of Irx3 was sufficient to generate motor neurons in ectopic locations. Where Nkx6.1 was misexpressed in regions with persistent Irx3 activity, this resulted in ectopic Chx10 V2 neurons in the p0 and p1 domains as well as Lim3 positive cells within the dorsal most ventral progenitor domains.

Ectopic expression of Nkx6.1 within the p0 and p1 domain also resulted in the ectopic expression of En1 V1 and Evx1/2 V0 neurons but not motor neuron markers. This suggests Irx3 counters the ability of Nkx6.1 to drive motor neuron fate, and that conversely Nkx6.1 and Irx3 together drive the generation of V2 neurons. Misexpression of Irx3 in regions ventral to the p2 domain resulted in Irx3 positive cells in ectopic locations that did not express MNR2, Islet1/2 or HB9, with V2 Chx10 expressing neurons generated at more ventral positions often within the pMN domain. The Lim3 expression profile remained unaltered by Irx3 misexpression. Thus the domain at which Nkx6.1 is able to generate motor neurons is limited by Irx3 expression dorsal to the p2/pMN progenitor boundary domain.

Further misexpression of Nkx2.2 in more dorsal regions to the p3 domain resulted in a repression of MNR2, Lim3, Islet1/2 and HB9 in such cells ectopically expressing

Nkx2.2, ultimately allowing a sharpening of the p3/pMN domain. The misexpression of Nkx2.2 further resulted in the generation of V3 Sim1 positive neurons in the Nkx6.1 domain and throughout the dorsal neural tube independently of Nkx6.1, suggesting an element of functional redundancy of Nkx2.2 and Nkx6.1 or they may have overlapping roles (Briscoe et al, 2000).

1.6.2 Shh signal transduction and the Gli genes

The zinc finger proteins of the Gli family, homologue of the *Drosophila* Cubitus Interruptus transcription factor (Ci) are thought to transcriptionally mediate the Shh signal in the neural tube and drive the dorsoventral patterning of this structure in vertebrates. Three Gli genes are implicated in this process namely Gli1, Gli2 and Gli3. Gli proteins are thought to integrate the various patterning signals during neurogenesis (Reviewed in Jacob & Briscoe, 2003). The Gli genes function as transcriptional activators in a graded manner and are expressed in the mouse in the ventral neural tube. Their expression is ultimately dependent upon Shh signals, with Gli2 taking a lead in the initial transduction of the Shh signal (Ruiz I Altaba, 1997; Dai et al, 1999; Wang et al, 2000; Bai et al, 2002). Individual Gli gene mutants show minor developmental defect yet ventral cell types fail to differentiate when all Gli signals are blocked. Gli signalling has also been implicated in the Wnt pathway and specifically GSK3 interaction (Mullor et al 2001) and also in BMP signalling whereby Smads associate physically with processed Gli proteins (Liu et al, 1998) whereby BMPs may regulate the post transcriptional control of Gli activity in concert with Shh derived signals.

Further studies revealed a gradient of Gli activity mediates the graded Shh signal (Stamatakis et al, 2005). Gli2 and Gli3 but not Gli1 act dually as transcriptional repressors and activators, through proteolytic processing. Mouse knockout studies of Gli1 reveal normal patterns of spinal cord development whilst Gli2 knockout mice display abnormal ventral neural tube patterning. Gli3 loss of function mice reveal a dorsal expansion of the intermediate zone within the spinal cord. In mice with complete loss of all 3 genes, the ventral patterning of the spinal cord was abnormal with a loss of ventral cells and segregation defects throughout (Matisse et al, 1998; Park et al, 2000; Persson et al, 2002; Bai et al, 2004).

Stamatakis and colleagues further generated activated Gli3 constructs that produce different levels of Gli activity to test if a Gli gradient of transcriptional activity was sufficient to mediate the graded Shh signal. Three dominant negative Gli3 variants Gli3^{Ahigh} delivering stronger activation than the second, Gli3^{Amed} by two to three fold, and similarly the third, Gli3^{Alow} offering the lowest levels of activated by two or three fold were electroporated in ovo. The group found that Gli3^{Ahigh} led to cells expressing floor plate and V3 neuronal markers in ectopic positions in a cell autonomous manner. Furthermore not all the cells expressing Gli3^{Ahigh} co expressed either Nkx2.2 or FoxA2, markers of the ventral most neural tube cells. Ectopic expression of Gli3^{Amed} and Gli3^{Alow} however was not sufficient to induce FoxA2 or Nkx2.2. Gli3^{Amed} expression reduced levels of Pax6 and both Gli3^{Amed} and Gli3^{Alow} sometimes resulted in ectopic cells close to the roof plate that were FoxA2 positive. Thus lower doses of Gli3 seem to have activator functions in this domain and that higher doses of Gli3 were sufficient to induce cells with ventral characteristics and markers in the intermediate zone of the neural tube.

The group further observed the action of the Gli3 constructs on the pMN and p2 regions where ectopic expression of Gli3^{Ahigh} in cells dorsal to p2 caused a cell autonomous ectopic expression of Olig2, MNR2/HB9, and Nkx6.1 whilst at the same time bringing about repression of Pax7 and Irx3. Within the pMN and p2 regions however this high dose of Gli3 results in down regulation of Olig2 and MNR2/HB9, with cells here acquiring a more ventral identity. With Gli3^{Amed}, pMN and p2 markers Olig2, Chx10 and Nkx6.1 were observed in the intermediate zone and Pax7 repression amongst ectopic cells. The study suggested that lower doses of Gli3 were sufficient to induce V2 and MNs but not the ventral most cell fates. When the Gli3^{Alow} construct was transfected, within the intermediate zone, low levels of ectopic Nkx6.1 expression was observed but not Olig2 or any motor neuron markers yet V2 neuronal markers were observed. However the low levels of Gli3 were sufficient to induce ectopic V1, V0 and dl6 fates with cells expressing Dbx2 and Cad7, while repressing Msx1 and Pax7 in these ectopic cells. This repression was sufficient to drive V1 and V0 neuronal fates in more dorsal positions and therefore the lower Gli3^A doses were sufficient to induce intermediate neural tube characteristics (Stamatakis et al, 2005).

Furthermore, to test whether ongoing Shh signalling was required for Gli3 action, coelectroporation of the higher dose constructs along with a Shh inhibitor. This on its own results in repression of ventral progenitor cell identities and ventral expansion of dorsal markers. Coelectroporation did not affect Gli3 activity and embryos displayed induction of FoxA2, Nkx2.2, Olig2 and Pax7 repression. This suggests that Gli3^A effects are cell autonomous and not due to increased floor plate Shh or ectopic

induction of Shh, and further that an ongoing Shh signal is not required for Gli3 activity, which is sufficient at the correct doses to drive the Shh dependent ventral patterning of the neural tube (Stamatakis et al, 2005).

1.6.3 Downstream of Shh action.

Thus an initial external Shh signal is interpreted by the Gli genes that transduce the signal, converting the Shh gradient into an intracellular signal that can initiate a response in individual cells which then ultimately serve to regulate gene expression and control the identity of neurons during neurogenesis (Reviewed in Dessaud et al, 2008). Once secreted, Shh itself undergoes post-translational modifications namely auto-catalytical cleavage and cholesterol modification at the C terminal, whilst being palmitoylated at the N terminus forming a molecule with a high molecular weight (Chen et al, 2004). The active Shh requires the transmembrane protein Dispatched1 for its function whereby Disp1 loss of function eliminates the active high molecular weight Shh and severely disrupts ventral neural tube patterning. Further extracellular proteins modulate the Shh signal, whereby proteins bind extracellular Shh with the aim of restricting its diffusion or affecting its degradation.

One such example are Heparan Sulphate Proteoglycans (HSPGs) that bind high molecular weight Shh at conserved sites (Rubin et al, 2002). Further, Shh binds to transmembrane proteins that transduce the Shh signal, ultimately affecting the differentiation of such cells in the ventral neural tube. For instance Shh action causes the transcriptional up regulation of Ptch1, a Shh receptor and Hhip1 that encodes an EGF-repeat membrane protein, whereby their expression then brings about inhibition

of Shh cell autonomously either through sequestration of the ligand or degradation of Shh and this helps modulate the Shh signal through a negative feedback loop and ligand dependent antagonism (Jeong & McMahon, 2005).

Intracellularly, the transmembrane protein smoothed (Smo) is activated by extracellular Shh through a graded manner mimicking the Shh gradient and initiating a signalling cascade offering temporal adaption and positional regulation (Chen et al, 2002; Dessaud et al, 2007; Chamberlain et al, 2008). Initially cells are highly sensitive to Shh, and low levels of Shh are able to induce the Gli genes however as development progresses, cells start to become desensitized to Shh and much higher levels of Shh are required to generate high levels of Gli expression whereby different amounts of Shh illicit an intracellular response at different time point where the duration of the signal is proportional to the Shh concentration. A negative feedback loop then comes into play by inhibitors such as Ptch1 that ultimately serve to desensitise cells to Shh. Furthermore these mechanisms then regulate the patterning of the ventral neural tube through the action on the β HHLH and homeobox genes. The intracellular mechanisms behind Shh signalling are the subject of much ongoing investigations.

1.7 LIM homeodomain proteins

Interneuronal and motor neuron populations are initially derived from progenitor cells expressing Nkx2.2 or Pax6, whereby Nkx2.2 has a primary role in interpreting a Shh signal and the determination of neuronal pattern, whilst Pax6 serves to provide indirect control of this pattern (Briscoe et al, 1999). Motor neuron progenitors are located within the pMN domain that also gives rise to oligodendrocytes. Oligodendrocyte

development is also dependant upon a Shh signal. Following the production of somatic motor neurons in the ventral neuroepithelium, oligodendrocytes arise from progenitors within the ventral most Nkx2.2 expressing domain, and not within the Pax6 territory. Shh is sufficient for their induction but not required for their maintenance (Soula et al, 2001).

Olig2 is a proneural gene expressed in the pMN domain, a region of motor neuron and oligodendrocyte progenitors and is essential for their development, where it determines two different cell fates. Olig2 activates Ngn2 in the pMN domain, activating motor neuron production; consequently, Ngn2 down regulation initiates Nkx2.2 up regulation that then acts alongside Olig2 to produce oligodendrocytes (Marquardt and Pfaff, 2001). More recently phosphorylation of Neurogenin2 was shown to regulate motor neuron development (Ma et al, 2008).

The β HHLH genes have traditionally acted through the notch signalling pathway, yet studies have implicated their interaction with the evolutionary conserved LIM-HD transcription factors and various other regulators in the specification of motor neuron subsets (Bertrand et al, 2002). LIM-HD transcription factors initiate their expression in early post-mitotic motor neurons, an event that is closely linked to cell cycle exit, and the commitment to a neuronal fate. Cell fate acquisition is synchronised with cell cycle exit, and the β HHLH genes are involved in the specification of different neuronal and glial subgroups.

1.7.1 Motor neuron specification

Motor neurons acquire their columnar identities once they have left the cell cycle. 5 main columnar subgroups exist based on their expression of various transcription factors namely of the LIM-HD family (Fig 1.7). Two of these subgroups are located in the MMC at thoracic levels with its lateral branch projecting to somatic targets whilst a medial branch projects to axial muscles (Tsuchida et al, 1994). Another subgroup exists called the Column of Ternii at thoracic levels and contains preganglionic autonomic motor neurons, which project to sympathetic targets. Two other subgroups exist located within the lateral motor columns at limb levels with a medial subset projecting to ventrally derived somatic targets and a lateral subset whose neurons innervate dorsally derived limb muscles (Tosney et al, 1995).

Dorsoventrally Shh acts to regulate Pax gene patterns in the ependymal layer to produce different classes of precursors. The ventral-most group of cells become motor neurons and express Islet1, which is required for the differentiation of all motor neurons initially. Early born motor neurons at the limb levels innervate ventral muscles and continue to express Islet1 but not Lim-1. In contrast, later born neurons migrate through these early cells settling laterally and innervating dorsal muscles, where these cells now turn off Islet-1 and switch on Lim-1 (Tsuchida et al, 1994).

Islet1 & Islet2 are some of the first genes switched on in motor neurons after they leave the cell cycle (Pfaff et al, 1996). Cross-regulatory interactions between the β HDLH genes establish the pMN domain where motor neurons arise, through the interaction of Nkx6.1, Nkx2.2 and Irx3 (Islet 1/2 are also expressed dorsally as well),

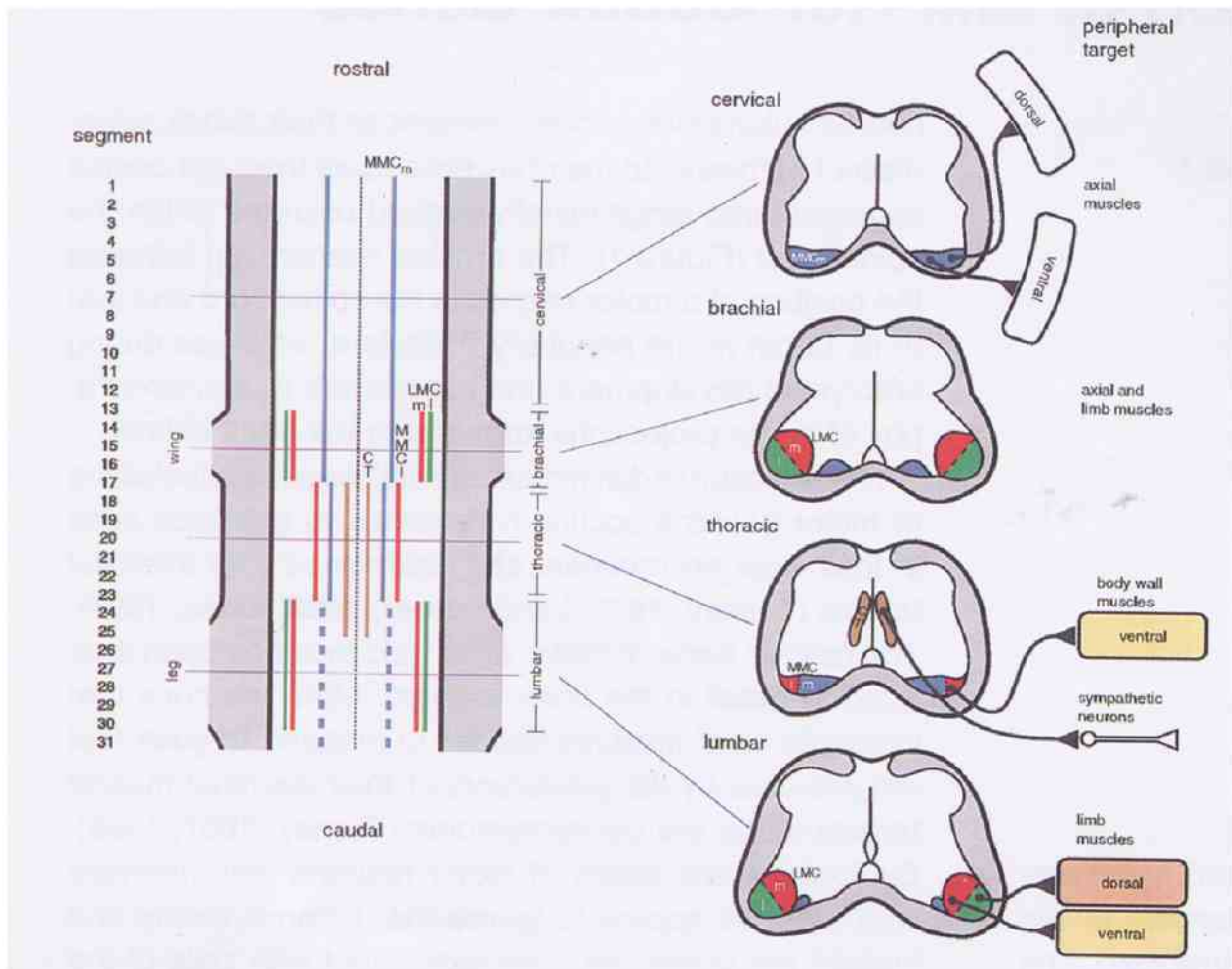
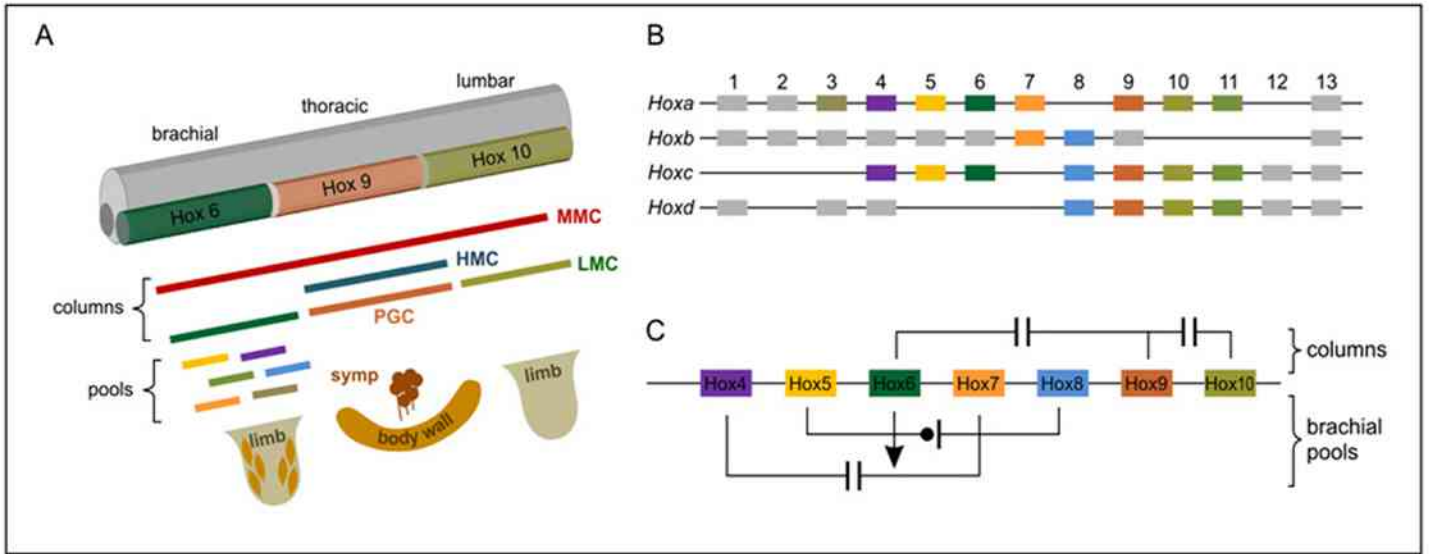
resulting in the expression of downstream genes namely Mnr2 and Lim3 (Tanabe et al, 1998; Thaler et al, 1999; Sharma et al, 2000; Jessell, 2000) (Figure 1.5).

Mnr2 is expressed by post mitotic motor neurons and helps to establish their identity, but in the chick its expression is initially restricted to the pMN domain (Tanabe et al, 1998). Mnr2 and its related protein Hb9 (Saha et al, 1997), are expressed by motor neurons and belong to the Mnx class of homeobox transcription factors with a role in the determination of motor neuron fate.

In Hb9/Mnr2 loss of function studies in mice, HB9 was found to be required for the consolidation of motor neuron identity and the correct emergence of motor neuron subtype identity along with the subsequent projection of motor axons. In this study the ectopic expression of Mnr2 in the chick lead to motor neuron differentiation and repression of V2 interneuronal character, whilst in the mouse, the generated motor neurons acquire characteristics of V2 interneurons once again (Arber et al, 1999). More recent studies have further implicated Notch1 signalling in V2 interneuronal and motor neuron generation, where Notch1 knockout mice exhibit lower numbers of motor neurons generated from the ventricular zone and higher numbers of V2 interneurons to compensate (Yang et al, 2006).

Mnr2 is initially normally expressed in the Medial Motor Column (MMC), Lateral Motor Column (LMC) and Column of Ternii (CT) neurons but only persists in the MMC. Mnr2 is required for the formation of CT neurons whereby Mnr2 & Hb9 act to suppress the generation of these neurons induced by Lim3. It acts as a transcriptional repressor during the acquisition of motor neuron fate (William et al, 2003).

Figure 1.7 (TOP) *Organization of Hox proteins, motor columns and pools*. MMC: median motor column; HMC: hypaxial motor column (formerly lateral MMC); PGC: preganglionic motor column; LMC: lateral motor column. Symp: sympathetic chain ganglion neurons. (B) 21 Hox proteins assign spinal MN identity. (C) Hox interactions specifying MN identity. Taken from Dasen et al, 2008. (BOTTOM) *Columnar identities at different levels within the spinal cord*. Taken from Tuschida et al, 1994. The diagram on the right represents the rostrocaudal location of motor columns in the chick neural tube, with schematic sections through the cord at different levels showing the columnar expression of transcription factors: [Blue – Isl1/2 & Lim3; Red – Isl1/2; Green – Isl2 & Lim1; Orange – Isl1] and the location of their peripheral targets to the right. LMC-Lateral Motor Column, m-medial branch, l-lateral branch; MMC-Medial Motor Column, m-medial branch, l-lateral branch; CT-Column of Ternii.



A study of the LIM-HD protein Hb9 has suggested a derepression model of gene regulation and cell fate specification in the neural tube, whereby ‘enhancer’ sequences can also target gene expression to a single neuronal subtype (Lee et al, 2004). This paper suggests 3 strategies that contribute to Hb9 regulation temporally and spatially in post-mitotic neurons. First, activator proteins in the neural tube interact with the Hb9 promoter and stimulate its transcription. Second, the non-specific functions of these activators is constrained by repressor proteins such as Nkx2.2 in non motor neuronal cell sub-types and finally Hb9 expression is activated and maintained by an enhancer region within the Hb9 regulatory region which contains ‘cis’ elements for ‘positive’ factors such as Islet1, Ngn2, NeuroM & NeuroD. Synchronization of neurogenesis and motor neuron specification then occurs via β HLH and homeodomain transcription factors (Lee & Pfaff, 2003). Repressor proteins might also function in interneuronal populations such as those determined by Chx10, En1 and Evx1/2, which interact with the Gro/TLE class of co-repressors and this method of transcriptional depression can also operate within progenitor and post mitotic cells (Lee & Pfaff, 2003).

Motor neurons have pool-specific identities during their initial outgrowth indicating that they must have cell surface differences, allowing their later axons to fasciculate with like axons. Furthermore these motor neurons recognize path finding guidance cues, enabling their axons to move around the neural tube (Landmesser, 2001). Motor neuron growth cones respond to guidance cues within targets and along the way, providing a differential detection and response both to inhibitory and attractive guidance cues, which are contact mediated or chemical as observed through fate

mapping studies using Dil labelling of progenitor cells (Tessier-lavigne & Goodman, 1996; Erskine et al, 1998).

1.7.2 Pool specific neuronal identities & columnar fates.

The LIM-Homeodomain family of transcription factors play a pivotal role in the development of spinal cord tissues, and are predominantly expressed in interneurons and motor neurons along the length of the neural tube (Tsuchida et al, 1994). In this study the LIM homeobox genes *Islet-1*, *Islet-2*, *Lim-1* and *Lim-3* were cloned in the chick and found to define subclasses of motor neurons that subsequently segregated into columns within the neural tube. Previous studies in the *Xenopus* embryo have isolated variants of the *Lim* genes namely *Xlim1* and *Xlim3* (Taira et al, 1992; Taira et al, 1993). The purpose of the study was to identify the LIM genes that distinguish the different subclasses of neurons based on their dorsoventral and anteroposterior position within the neural tube. Combinatorial expression of the LIM genes was shown to define subclasses of neurons, which arrange neatly into columns yet this LIM-HD expression did not confer rostrocaudal identity or the delineation of individual motor pools. These genes were shown to be expressed post mitotically before these neurons arrange themselves into columns and further axonal pathways. During neurogenesis for example, motor neurons express *Islet-1* once they leave the cell cycle suggesting this LIM homeobox gene is involved in the differentiation of these neurons.

Tsuchida and colleagues found that LIM homeobox genes are expressed by motor neurons prior to axonogenesis and columnar segregation, suggesting these genes may confer the topographical identities of motor neurons and their targets (Tsuchida et al,

1994). Antibodies raised against chick Islet-1 were found to label motor neurons that ultimately innervate somatic (skeletal) & visceral (sympathetic) motor neuron targets. The mRNA distribution of Islet-1 was found to overlap with the immunohistological pattern. However from HH23 onwards not all Islet-1 immunoreactive cells expressed Islet-1 mRNA suggesting a related gene encoding a protein is also recognised by Islet-1 antibodies. The expression of Islet-2 was found to overlap with Islet-1 distribution within all somatic motor neurons in the ventral spinal cord suggesting the Islet-1 antibody also recognizes Islet-2. The group's results showed that Islet-2 expression was restricted to motor neurons whilst Islet-1 was also expressed dorsally by a subset of developing interneurons. Two further homeobox genes, Lim1 and Lim3 were later shown to be expressed by motor neurons as well, however expression of Lim-1 was also seen in interneuronal populations within the neural tube and Lim-3 expression also in a subset of cells dorsal to the motor neuron populations. Lim-2 and Lmx-1 expression was not seen in motor neurons but other distinct groups of neuronal cells.

Based on these expression profiles, the chick spinal cord was divided into 5 columnar subsets. This pattern was apparent by HH35 with neurons migrate away from the ventricular zone laterally. These columns are the Median Motor Column (MMC) with a medial division MMCm projecting to axial muscles of the vertebrate column and a lateral division MMCl projecting to body wall muscles. The Lateral Motor Column (LMC) subdivides into a medial division LMCm with motor neurons contained here projecting to limb muscles of the ventral muscle mass and a lateral division LMCl projecting axons to limb muscles of the dorsal muscle mass. The fifth set, the column of terti (CT) contains visceral motor neurons projecting to sympathetic targets.

The combinatorial expression of the LIM homeobox genes was shown to overlap with this columnar organisation of the spinal chord at various rostrocaudal levels by stage HH35. At this stage within the MMC extending rostrocaudally, where the lateral subdivision is restricted to thoracic levels, MMCm motor neurons co express Islet1, Islet2 and Lim3. MMCl motor neurons co express Islets 1 & 2 but not Lim3. Lim1 was not expressed by any MMC motor neurons. Within the LMC, restricted to the brachial and lumbar regions of the neural tube, Islet2 is expressed throughout, but not Lim3 at any level. Islet 1 expression was restricted to LMCm motor neurons. Lim 1 expression was restricted to LMCl neurons also co expressing Islet2. Within the column of tennii, extending to thoracic and rostral lumbar segments of the spinal cord, ventral neuronal populations express Islet1 but not Islet2, Lim1 or Lim3. Dorsal neuronal populations within the CT however did not express any of the Islet or Lim genes. Looking to understand what drives this columnar pattern by stage HH35, the onset of LIM homeobox gene expression was investigated at earlier stages.

Within the MMCm, Islet1, Islet2 and Lim3 expression were first seen at HH14-15 with a sharp increase in cells expressing these LIM factors by HH 1718. Within the cervical spinal cord, by HH18 Islet-1 positive cells were observed that did not express Islet2 and in particular these cells were located close to the ventricular zone. Furthermore, Lim3 cells were detected at the very lateral border of the neural tube. As neurons migrate laterally away from the ventricular zone, earlier born neurons will be located in more lateral locations, therefore the data suggested Islet1 is the first LIM homeobox expressing gene to be switched on followed by Islet2 and then Lim3 (Tsuchida et al, 1994).

Within the LMC, at lumbar levels where only MMCm neurons are present in the absence of MMCl and CT neurons, LMCm neurons were found to be born at HH18-19 whilst LMCl neurons were generated at HH20-21 with earlier born neurons therefore taking up positions within the LMCm column. At HH17, cells of LMCm showed Islet1 expression preceding that of Islet2, yet by HH18 both Islet1 and Islet2 were expressed in the LMCm, but not Lim1. In the LMCl at HH21 when only a few Lim1 positive cells are located in the ventral spinal cord, these cells co express Islet1. By HH23, numbers of Lim1 cells increased sharply, and now these cells began to co express Islet2 but not Islet1, suggesting the latter is switched off. Further mRNA in situ studies of these LIM genes revealed that LMCl neurons express Islet1 before Lim1 or Islet2, and that the transient Islet1 expression in these cells is followed by the lateral migration of cells and Lim1 & Islet 2 expression by HH24 and well before the formation of axonal trajectories by LMC neurons. Furthermore, neurons that co express Lim1 and Islet2 in the LMC migrate through the LMCm that were previously generated to reach their final positions within the LMCl. This also suggests that the LIM gene expression profile of these neurons is determined prior to lateral migration of cells and columnar organisation (Tsuchida et al, 1994).

Spinal motor neuron development is also crucially dependent upon Retinoid signalling. LMC neurons express RALDH2, an enzyme capable of synthesising retinoic acid, converting inactive retinoid precursors to into retinoids that then carry out their effects in a non-cell-autonomous manner in order to bulk up motor neuron populations and bring about the LMCl expression profile. RALDH2 expression begins during the early phase of motor neuron development at brachial levels of the spinal cord specifically, that then distinguishes LMC neurons from other visceral or somatic neuronal

populations and leads to the differentiation of Islet2 positive, Lim1 positive LMCI neurons. Explant analysis at thoracic levels revealed that RA was sufficient to induce Islet2/Lim1 positive neurons phenotypes (Sockanathan & Jessell, 1998).

When considering interneuronal cell populations that do not express RALDH2 normally, brachial explants with or without RA resulted in many Chx10 positive V2 cells yet none co expressed Lim1. However at HH14, dorsal neural tube explants grown alone contained D2 Islet1 positive neurons but Lim1 expression failed to be induced by Retinoic acid, therefore the ability of retinoid signalling to induce Lim1 is a selective feature amongst motor neurons. Ultimately motor neurons then lose the ability to respond to retinoid signalling once a LMCI phenotype is generated (Sockanathan & Jessell, 1998).

1.7.3 Pax Genes

Further studies in the early chick embryo reveal that Pax 2 is expressed by numerous interneuronal populations within the neural tube, suggesting this gene alone is not responsible for conferring regional identities of inter neuronal subsets. Pax2 is mainly expressed in dorsal subsets of post mitotic interneurons from Stage HH15-17 onwards with two distinct populations, a dorsal and ventral group with this expression extending from HH18 to HH24. From HH25 onwards, Pax2 expression was observed in the ventral and dorsal horns, displaying a similar pattern of expression in both the chick and the mouse. At HH20 all Pax2-positive cells were found to express Lim1/2. Some cells expressing only Lim1/2 and not Pax2 were observed dorsally, which may include commissural neurons, and in more intermediate zones. Pax2-positive cells did

not however co-express *Islet1*, demonstrating *Pax2* is not expressed by motor neurons or dorsal interneurons (Burrill et al, 1997).

Pax2 was shown to be expressed in new post mitotic neurons as they migrate into the mantle zone following neuronal differentiation and it is thought to function to determine cell fate. Within HH19 chick spinal cords, *Pax2*-positive cell domains were shown to overlap with *Evx1* transcripts in a subset of ventral *Pax2* cells, yet only half of the *Evx1* cells expressed *Pax2*. However, nearly all *En1* positive cells expressed *Pax2*, highlighting a distinct subset of *pax2* expressing cells that project ipsilaterally in the ventral neural tube. Furthermore the group found that *En1* and *Evx1* neurons did not overlap (Burrill et al, 1997).

Pax7, an early patterning gene is expressed in the neuroepithelium, while *Pax6* is expressed more widely in the dorsal basal plate and ventral alar plates, where it displays stronger levels of expression and weaker levels in the dorsal spinal cord region. *Pax2* expression dorsally is found on the border of the dorsal expression domain of *Pax6* and adjacent to *Pax7* expression. The more ventrolateral *Pax2* expression is adjacent to the domain of *Pax6* precursors whereby the dorsal boundary of *Pax6* expression demarcates the boundary between the two populations of *Pax2* cells with *En1*-expressing cells evident adjacent to the ventral-most *Pax6*-positive precursor cells, suggesting *Pax6*-positive cells give rise to *En1*-positive neurons. Thus the combinatorial expression of *PAX2*, *EN1* and *EVX1* proteins may confer neuronal subtype identity in the neural tube in a similar manner to the combinatorial action of Lim homeobox genes during motor neuron development, with *Pax2* being required for interneuronal determination and *En1* and *Evx1* controlling terminal interneuronal post

mitotic function following on from the earlier actions of patterning genes such as Pax6 (Burrill et al, 1997).

Further studies highlighting the role of Shh in motor and interneuronal development reveal that an initial phase of Shh mediated repression of Pax3 and Pax7 leads to the formation of a subset of ventral progenitor cells in the neural tube. A later second phase of Shh activity then leads to the development of motor neurons and ventral interneurons (Ericson et al, 1996; Ericson et al 1997). Shh signalling was found to be necessary for the generation and induction of V1 and V2 subsets of ventral interneurons and also for motor neuron development in a dose dependent manner relative to the position of the cells within the spinal cord. Considering the downstream effects of Shh, the homeobox genes Nkx2.2 and Pax6 (Goulding et al, 1993) were analysed with mutations in the Pax6 gene leading to defects in eye and forebrain development amongst Small Eye (*Sey*) mouse mutants. Thus Nkx2.2 and Pax6 were found to be involved in Shh orchestrated control of neuronal patterning and identity.

Within the spinal cord, Pax6 expression in the ventral half shows a low ventral to high dorsal gradient of expression, however Nkx2.2 positive cells are restricted to just above the floor plate that do not express Pax6. Repression of Pax6 allows the generation of a second wave of ventral progenitor cell development that express Nkx2.2, driving the differentiation of progenitor cells and change in motor neuron fate. Ultimately the lack of Pax6 function amongst *Sey* mutants within more dorsal ventral progenitors of the spinal cord results in the loss of specific ventral interneuronal populations. However among these mutants, loss of Pax6 more dorsally in the ventral

spinal cord does not result in a ventral transformation of identity amongst progenitors causing the elimination of V1 interneurons altogether.

The loss of Pax6 more ventrally however does cause a dorsal to ventral transformation of identity among progenitors, initially at spinal cord levels C1 to R7, albeit without changing motor neuron number but changing their identity from somatic neurons to visceral neurons. At cervical levels C4 to C3, progenitor cells are driven from motor neuron fate towards a ventral cell fate transforming the identity of these cells. Thus the consequences of Pax6 expression on motor neurons ultimately depends on their position along the rostrocaudal spinal cord (Ericson et al, 1996; Ericson et al 1997).

Nkx2.2 is normally expressed above the floor plate and ventral to the Pax6 domain. Analysis of Nkx2.2 mutants reveals that the expression of Pax6 remained unaltered. Pax6 and Nkx2.2 were shown to have a reciprocal repressive relationship whereby ectopic expression of Nkx2.2 results in repression of Pax6, but with no effect on Pax7 expression. Within Nkx2.2 mouse mutants the Pax6 expression domain remains unaltered and does not expand ventrally. However Nkx2.9 here was shown to be expressed transiently within the Nkx2.2 domain, suggesting a degree of functional redundancy between the Nkx family of genes (Briscoe et al, 1999; Briscoe & Ericson 1999).

1.8 Segmental identity of motor neurons and Hox genes.

The rostrocaudal, segmental identity of motor neurons is irreversibly specified by embryonic day 2 (E2) in the chick, where signals from the paraxial mesoderm cause

the limb regions of the spinal cord to become distinctly different. The Hox genes play an important early role in the specification of the rostrocaudal patterning of neuronal populations within the neural tube. Motor neurons also arise along distinct dorsoventral domains along the spinal cord acquiring columnar characteristics. Such imposition of columnar fate was shown to be influenced by the Hoxc cluster of genes following transposition of the neural tube soon as it closes. Signals emanating from the paraxial mesoderm were shown to affect the fate of spinal motor neurons and their arrangement (Ensini et al, 1998) (Figure 1.7).

Post mitotic motor neurons express a subset of Hox genes namely of the Hoxc cluster, and differential Hoxc expression with profiles of lumbar, thoracic and brachial MNs was shown to be induced in vitro through a dose dependent FGF stimulus (Liu et al, 2001; Bel-Vialar et al, 2002). More specifically looking at LMC and CT neurons at brachial and thoracic levels respectively, that express Hoxc5/6/8/9, Dasen and colleagues found that brachial motor neurons expressed Hoxc6 whilst thoracic motor neurons expressed Hoxc9 with cells expressing both Hox genes located at the border of the thoracic and brachial regions. Hoxc5 and Hoxc8 expression followed a similar pattern with co expressing cells located at the mid brachial region. Thus rostral brachial LMC neurons co expressed Hoxc5 and Hoxc6 whilst caudal brachial LMC neurons co expressed Hoxc6 and Hoxc8.

Within rostral thoracic levels, motor neurons initially expressed both Hoxc8 and Hoxc9 coincident with the temporal and spatial organisation of the columns. Ectopic expression of FGF8 in brachial and thoracic regions revealed down regulation of Hoxc6 expression and initiation of Hoxc9 expression at brachial regions suggesting

FGF over expression results in a brachial to thoracic transition of Hoxc profiles. Brachial expression of FGF8 reduced the Islet1/2 positive motor neuron pool by 30% (Stockanathan & Jessell, 1998; Dasen et al 2003).

At brachial regions however following Fgf8 expression, motor neurons failed to express RALDH2 a marker of LMC neurons, with a loss of Islet2 and Lim1 expression, suggesting increased FGF8 signalling here suppressed LMC differentiation similar to Hoxc6 suppression. Furthermore, raised levels of FGF8 signalling in brachial regions resulted in a shift from Hoxc6 to Hoxc9 expression and LMC to CT (thoracic) character respectively as a direct action of FGF8 cell-autonomously (Dasen et al, 2003).

The group further examined if the switch in fate from LMC to CT neurons imposed by FGF8 could be mimicked by ectopic expression of Hoxc proteins. In the brachial region, Hoxc9 expression inhibited Hoxc6 in motor neurons cell-autonomously reducing the number of Islet1/2 positive and Lim1 positive LMC1 neurons, furthermore these Hoxc9/Islet1/2 positive motor neurons also expressed BMP5 and were in dorsomedial positions similar to the arrangement of CT neurons.

Thus Hoxc9 was found to mimic the action of FGF8 and repress Hoxc9 and LMC character whilst driving CT character (Dasen et al 2003). However, expression of Hoxc6 at rostral thoracic regions did not suppress Hoxc8 and further mis-expression of Hoxc8 at rostral brachial levels did not suppress Hoxc6 or RALDH2. Furthermore, misexpression of Hoxc8 at rostral brachial levels suppressed Hoxc5 action suggesting the expression domains of Hoxc5 and Hoxc8 arise as a result of a cross-repressive

relationship. Looking at the expression of Hoxc genes at HH15 in neural progenitors, demonstrated that brachial progenitors lacked Hoxc9 and Hoxc6 expression whilst thoracic progenitors lacked Hoxc6 but expressed Hoxc9. The influence of FGF8 misexpression in progenitor cells at brachial levels showed that Hoxc9 was induced without Hoxc6, mimicking a thoracic shift in progenitor profiles.

Furthermore to assess if motor neuron columnar identity could be changed through direct expression of Hoxc protein in post mitotic brachial motor neurons, the expression of Hoxc9 suppressed Hoxc6 and stopped the differentiation of LMCI neurons. Conversely, Hoxc6 was able to block CT differentiation at thoracic levels through repression of complimentary Hox pairs. Thus the Hoxc cluster in the neural tube appears to specify columnar identity through mutual pairs of cross-repressive interactions, thereby inducing column specific markers of differentiated motor neurons. Furthermore, the interaction of Hox5 and Hox8 during motor pool specification is asymmetric with activator roles here. Furthermore, the repressive, independent interaction of Hox4 and Hoxa7 during intersegmental motor pool diversification is required for correct patterning of this motor pool, but not an absolute requirement. The Hox genes are therefore essential in refining and determining the pattern of motor neurons in their distinct pools (Dasen et al, 2003; Dasen et al, 2005).

1.9 Protein Tyrosine Phosphatases.

Many of these transcriptional processes that define cell-cell adhesion events, cell proliferation and neurogenesis involve the phosphorylation and dephosphorylation of key amino acid residues within receptors and their effectors. Ultimately the product of

these processes is a well-organised, functionally-led pattern of transcription factor-specific neuronal groups. Some of the signalling pathways and cellular behaviours seen during this early period of neural tube development are governed by key protein tyrosine phosphorylation events. Such phosphorylation results in conformational changes of target proteins, allowing interactions with other molecules. However, not all interactions are dependent upon a conformational change. Simply the presence of a phosphate is sufficient to trigger binding or “docking” to other effectors. These phosphorylation events must be co-regulated by receptor and non-receptor tyrosine kinases (PTKs), such as FGFR and src kinases, and the large, complementary family of Protein Tyrosine Phosphatases (PTPs). However, very little is known about the role of PTPs in spinal cord development. In the following section the literature on RPTPs will be introduced, as well as how these receptors might function within the early neural tube.

The classical, tyrosine-specific PTP families fall into 2 categories: receptor-like PTP's (RPTP's), which are plasma membrane bound, and the cytoplasmic non-receptor PTP's (Stoker, 2001; Tonks & Neel, 2001; Johnson & Van Vector, 2003; Alonso, 2004; Stoker, 2005; Tonks, 2006; Hendriks et al, 2012). There are 21 mammalian RPTP's, grouped into eight main subtypes based on their extra cellular domain structures (Figure 1.4).

Their intracellular catalytic domains are highly conserved. They have been shown to be involved particularly in the regulation of neuronal development and axonal guidance (Ensslen-Craig & Brady-Kalnay, 2004; Alonso, 2004). These molecules

often have extracellular domains similar to cell adhesion molecules, implicating their role in axonogenesis and path finding.

Differences in these extracellular domains suggest they have specific ligands and studies have led to the emergence of both heterophilic and homophilic ligands for these molecules. One such example is PTP σ , which has been shown to bind the heparan sulphate proteoglycans agrin and collagen XVIII (Aricescu et al, 2002) and Nucleolin (Alete et al, 2006).

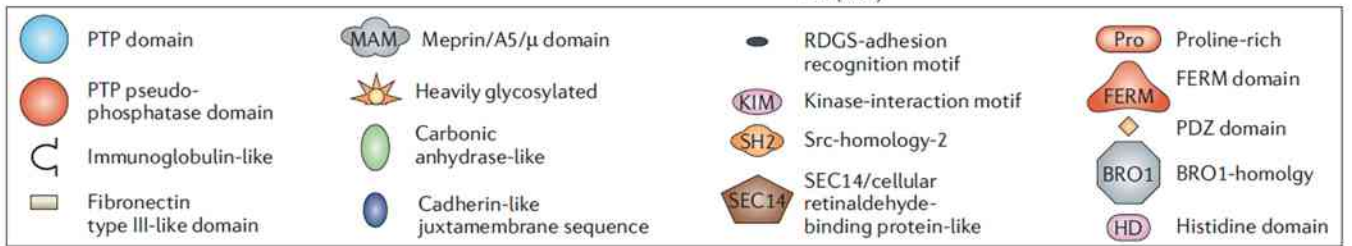
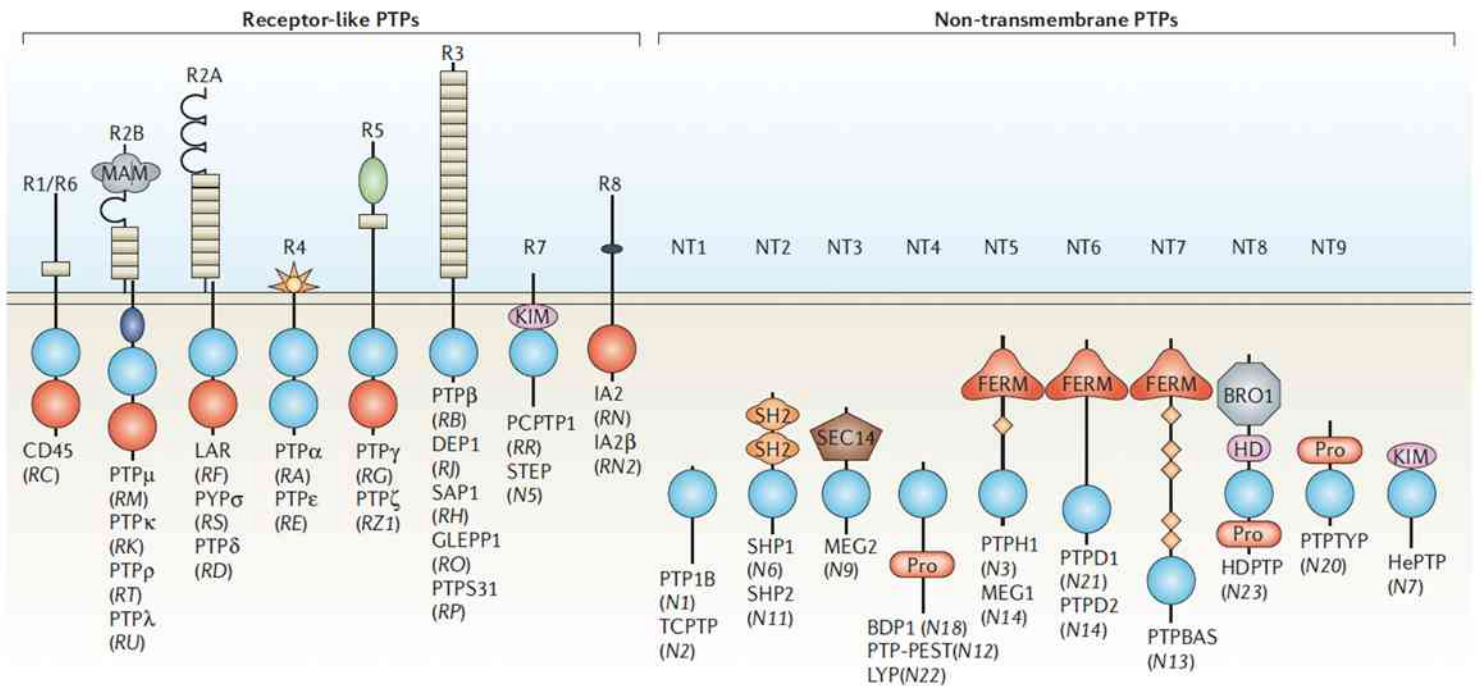
1.9.1 Functional studies of RPTPs

Loss of function data have demonstrated a role for RPTP's in promoting axon target recognition in the motor nerve system and developing visual system, recognising guidance cues and later participating in synapse formation. This was first demonstrated in the *Drosophila* visual system.

1.9.1.1 PTP action in motor axons

Early studies of PTP function in *Drosophila* looked at the role of these molecules in axonogenesis and more specifically motor axon guidance. These studies arose as a result of the homology of RPTP's extracellular domains to neuronal adhesion molecules such as N-CAM, implicating their potential role in cell surface signalling via tyrosine phosphorylation.

Figure 1.8 The RPTP family. The classical protein tyrosine phosphatases (PTPs) can be categorized as receptor-like (R) or non-transmembrane (NT) proteins. Use of alternative promoters (PTP ϵ) or alternative splicing (PTPRO) leads to the production of transmembrane and cytoplasmic forms of some PTPs from a single gene. 8 RPTP subgroups exist. For RPTPs with two intracellular PTP domains, the membrane-proximal D1 domain is catalytically active. In group R4, the D2 domain of PTP α also displays a low residual activity. For the remaining RPTPs, including PTP ϵ , the D2 domain maintains a PTP fold but lacks activity and is known as a pseudophosphatase domain. In each case, the PTPs have been designated by a name that is commonly used in the literature. Where this differs from the gene symbol, the latter is included in parentheses for clarification. In each case, the various subdivisions are based upon sequence similarity (After Tonks, 2006).



As several RPTPs are specifically expressed on axons, Desai and colleagues demonstrated their role in growth cone guidance and axonogenesis. They demonstrated that DPTP69D and DPTP99A were important for the correct guidance of certain motor axons (Desai et al 1996). Mutations in the DPTP69D and DPTP99A genes revealed that DPTP69D mutations resulted in an ectopically guided SNb nerve and in a limited number of cases the SNa nerve also displayed defects. DPTP99A single mutations did not reveal any abnormal phenotypes. Double mutations however in these two genes resulted in abnormal development of all SNb and SNa nerves, highlighting functional redundancy amongst the drosophila PTPs during development. Furthermore this and other studies in up to four drosophila RPTP's have clearly demonstrated redundancy amongst these proteins (Desai et al, 1996; Krueger et al, 1996; Desai et al, 1997; Sun et al, 2001).

The range of phenotypes observed amongst double mutants, namely the bypassing, stalling and detour of the SNb nerve, showed similarity with those of the adhesion molecule fasciclin II (drosophila homologue of N-CAM) over expression on motor axons, which also affects SNa nerves. Thus the group postulated that RPTPs could oppose fasciclin II-directed adhesion and therefore regulate repulsive ligands by decreasing tyrosine kinase signalling and allow growth cones to defasciculate from axonal bundles (Desai et al, 1996).

In a further study Desai and colleagues observed drosophila motor axon patterns amongst DPTP69D, DPTP99A and DLAR mutants and showed a hierarchical control of RPTPs in the regulation of growth cone guidance along a single pathway, with these RPTPs acting both in competition and cooperatively (Desai et al 1997). Mutants of

DPTP69D, DPTP99A and DLAR (Krueger et al, 1996), show defects in the specific trajectory of the ISN, SNb and SNd motor axons whilst SN root branches namely SNa and SNc nerves remain normal. Furthermore the study revealed that in mutants, the bypass phenotype of SNb axons show their outgrowth is not stalled by loss of RPTP function. The combinatorial effect of RPTPs is also required for correct axonal trajectories of the ISN root motor axons either acting cooperatively at certain choice points or in opposition for instance at SNb choice points (Desai et al, 1997).

In a screen of candidate signalling partners through dose dependent genetic interactions within growth cone choice points in drosophila RPTPs, Wills and co-workers found that DLAR function during the guidance of ISNb axons has an antagonistic relationship with *Drosophila Abl*, a tyrosine kinase (Wills et al, 1999). Loss of function *Abl* mutants suppress DLAR axon guidance phenotypes in double DLAR loss of function mutants, whilst *Abl* gain of function was found to mimic the DLAR mutant guidance defects in retinal axons described in the literature. In vitro studies revealed a directing binding of *Abl* to the DLAR cytoplasmic domain resulting in its phosphorylation, highlighting the role of DLAR in such axons to be dependent upon a tyrosine kinase domain to transduce the signal. The *Abl* substrate Enabled (*Ena*) also bound to the DLAR cytoplasmic domain in vitro, demonstrating DLAR, *Abl* and *Ena* may function as a 'phosphorylation dependent' switch to guide growth cones through signals at the cell surface that are transmitted to the actin cytoskeleton (Wills et al, 1999).

The regulation of axon guidance across the midline of the drosophila embryo by RPTPs has shed light on further mediators of axon guidance cues. The group isolated a

fourth member of the DPTP family, DPTP10D and demonstrated that loss of function of this PTP did not show any abnormal phenotype. Double mutants however of DPTP10D and DPTP69D revealed defects in the guidance of the segmental (SN) nerve along with a re-routing of a subset of longitudinal axons across the midline. The guidance of axons at the midline is regulated by attractive cues from Netrins and repulsive cues from Slits, with Robo acting as a slit receptor, whilst the Commissureless protein down regulates Robo activity permitting axons to cross the midline. The group suggested that a midline repulsive signal required from Robo, was not being transduced by DPTP10D and DPTP69D. The group further conducted quadruple mutants of all 4 DPTPs and found that most longitudinal pathways of axons were converted to commissures suggesting that the tyrosine phosphorylation may regulate the response of growth cones to midline cues as positive regulators of Robo signalling (Sun et al 2000; Sun et al 2001).

1.9.1.2 PTP function in the visual system.

There have been further studies of RPTP function in *Drosophila*, this time in the visual system. Here photoreceptor axons showed a requirement for PTP69D during projection to the brain (Reviewed in Stoker, 2001). Photoreceptors in *Drosophila* occur as ommatidial clusters of eight neurons R1-R8, whereby pioneer R8 axons (and later R7 axons) terminates in the medulla, whilst R1-R6 axons fasciculate with R8 until they normally reach their terminus in the more proximal lamina. PTP69D was shown to be required for the retinal axons R1-R6 to terminate correctly in the lamina cell autonomously, where mutant retinal axons overshot the lamina and terminated in the medulla (Garrity et al, 1999). The group proposed that these retinal axons required

PTP69D to detect extracellular signals leading to growth cone motility via phosphorylation of specific substrates. This signal is translated to a 'stop' cue for the growth cone via dephosphorylation of a substrate, without which the R1-R6 axons terminate ectopically in the medulla of the optic lobe, remaining there in the adult suggesting the defect is permanent. Similarly in the drosophila visual system, RPTP DLAR mutants fail to synapse with their correct laminal targets (Garrity et al, 1999; Clandinin et al, 2001; Maurel-Zaffran et al, 2001).

Further studies in the drosophila eye utilizing a mosaic model also demonstrated the role of DPTP69D in the guidance of photoreceptor axons. Moreover DPTP69D loss of function mutants showed mistargeting of R7 axons along with an overshooting of R1-R6 axons beyond their normal targets. These defects were hypothesised to occur as a result of a loss of permissive signal within retinal axons in response to a defasciculation cue (reducing adhesion at choice points) as R1-R6 fasciculate with the R8 pioneer axon beyond the normal target (Newsome et al, 2000).

Recent studies on LAR in the drosophila visual system have demonstrated that the correct targeting of R7 neurons requires 3 elements of the FNIII LAR domain as opposed to the Ig domains. Since the Ig domains bind known ligands Sdc and Dlp, these data may indicate the role of further unknown ligands for FNIII regions. In contrast to the neuromuscular junction development, R7 axon path finding does not require catalytic phosphatase domain activity. The group also tested a mutation in the wedge region of LAR, which prevents its intracellular dimerization and maintains phosphatase activity and therefore the ability to promote Neuromuscular junction formation. This mutation, however, displays defects in R7 axon path finding, even if

the catalytic site is further mutated, suggesting dual functions for this phosphatase domain, not restricted simply to its catalytic activity (Hofmeyer & Treisman, 2009).

In vertebrates, RPTPs have various roles during neural development, as demonstrated by loss of function studies. PTP σ antibody perturbation (Ledig et al, 1999), or the expression of a catalytically inactive mutant form of the protein (Johnson et al, 2001), has resulted in defects of RGC outgrowth when cultured on retinal basement membranes. Experiments perturbing the interaction of PTP σ through the ectopic expression of a secreted form of the protein ectodomain (PTP σ -VSV) in the chick produced axon guidance defects to tectal targets where additionally, the tectal basement membrane was shown to bind PTP σ -VSV (Rashid-Doubell et al, 2002). These data indicate that PTP σ plays a role in retinal axon targeting. Furthermore, Ephrin receptors are activated by the autophosphorylation of tyrosine residues upon the binding of their ligands, the ephrins where protein tyrosine phosphatase receptor type O (Ptpro) dephosphorylates EphA and EphB receptors as substrates at a phosphotyrosine residue required for the activation of the Eph receptor (Shintani et al, 2006).

1.9.3 Roles of PTPs in synaptogenesis.

The LAR receptor family of tyrosine phosphatases has been widely studied in many invertebrate and vertebrate developmental systems (Reviewed in Chagnon et al, 2004). A study of DLAR in the drosophila larval neuromuscular junction showed that it was required for the correct formation of neuromuscular synaptic junctions along with its associated intracellular protein Dliprin- α . Yeast trap assays showed a binding of

Liprin- α to DLAR, furthermore both loss of function mutants revealed similar neuromuscular phenotypes. Kaufmann suggests liprin- α may act downstream of DLAR, although liprin- α itself is not known to be phosphorylated. Instead it may recruit synaptic scaffold proteins as it is associated with them, or Liprin- α may serve to guide the DLAR receptors to their target sites (Kaufmann et al, 2002). These functions may be evolutionarily conserved in mammals since homologues of these proteins are found to be expressed in mammalian synapses (Kaufmann et al, 2002; Wyszynski et al 2002).

Roles for RPTPs have also been described during synaptogenesis through cell-cell signalling with key interactions with Cadherins and β -catenin which are both tyrosine phosphorylated, with LAR specifically implicated in synaptic adhesion and development (Dunah et al, 2005; Reviewed in Brigidi & Bamji, 2001). Further functions for PTPs have been described for the regulation of presynaptic vesicle clustering where the cadherin/p120-catenin complex binds to the cytoplasmic protein kinase Fer which results in the uptake of SHP2 that dephosphorylates β -catenin (Lee et al, 2008; Reviewed in Hendriks et al, 2012).

Further interactions have been described between LAR and PTP σ and the adhesion molecule netrin-G ligand 3 (NGL-3) during presynaptic differentiation and the promotion of synaptic differentiation (Woo et al, 2009; Kwon et al, 2010). Furthermore, PTP σ on axons and its HSPG ligands bind differentially to Trk proteins, through complexes with TrkA and TrkC, but not TrkB where the transmembrane domain of PTP σ and TrkA were sufficient to drive the interaction of these two proteins. PTP σ is able to dephosphorylate Trk A, B and

C suppressing their phosphorylation in the presence of neurotrophins. The Trk proteins are receptor protein tyrosine kinases (RTKs) and are activated by neurotrophins that act as signaling centers for adaptor proteins and bring about transphosphorylation (Faux et al, 2007). More recently TrkC was shown to bind the ectodomain of PTP σ during synaptic differentiation and pre and postsynaptic functions in the cerebral cortex. This study found that PTP σ presynaptically triggers and TrkC post synoptically mediates clustering of postsynaptic molecules in dendrites, demonstrating a bidirectional function for these two proteins during synaptic organization (Takahashi et al, 2011).

1.9.4 Interactions of RPTPs with cadherins and catenins

As seen above, RPTPs can have significant influences over cadherin/catenin function. Experiments in *Xenopus* with PTP δ and PTP μ , expressed along a dorsoventral gradient in the retina, show these molecules contribute to retinotectal development (Wang & Bixby, 1999; Sun et al 2000; Johnson & Holt, 2000). PTP μ has been shown to act selectively as both an inhibitory and permissive guidance cue within the visual system (Ensslen-Craig & Brady-Kalnay, 2005). Moreover, PTP μ has been shown to be required selectively for E-cadherin and N-cadherin dependent neurite outgrowth, with PKC function required for E-cadherin but not N-cadherin (Oblander et al, 2007; Oblander & Brady-Kalnay, 2010).

Other phosphotyrosine signalling processes and adhesive cell-cell interactions have also been shown to involve cadherins and catenins and so likely involve regulation by

PTPs (Larsen et al 2003; Burridge et al 2006; Salle et al, 2006; McLachlan & Yap, 2007). PTPs have been shown to play an important role in the regulation of cell-cell contacts at adherens and tight junctions whereby protein tyrosine inhibition can induce the release of cell-cell contacts (Chen et al 2007). Several further RPTPs have been implicated in the regulation of β -catenin and its dephosphorylation. For example LAR over expression resulted in an inhibition of cell migration. Furthermore, when PTP β/ζ , is bound to its ligand pleiotrophin this results in an increase in β -catenin tyrosine phosphorylation (Muller et al, 1999; Meng et al, 2000). Previous studies have also implicated PTP κ interaction with β -catenin, with PTP κ directly dephosphorylating β -Catenin. PTP μ has been shown to affect Cadherin and bring about its dephosphorylation where its absence results in an increased state of Cadherin phosphorylation or its affinity for p120 (Fuchs et al, 1996; Cheng et al, 1997; Brady-Kalnay et al, 1998; Zondag et al, 2000). PTP μ and cadherins also have a very precise trans interactions that creates a “spacer” complex at cell-cell interfaces (Coles et al, 2011).

In the chick embryo, PTP λ has been shown to regulate the shape of the mid-hindbrain boundary (MHB) region (Badde & Schulte, 2008). Here this gene is expressed in a tight ring in the location of repressed Wnt1 activity. Furthermore RPTP λ was shown to bind to β -Catenin and participate in the canonical Wnt pathway. Upon over expression of RPTP λ , the activity of a β -Catenin responsive promoter was suppressed, resulting in reduced progenitor cell proliferation (Badde & Schulte, 2008). This indicates that RPTPs may be involved in the key regulatory processes that underlie cell proliferation and neurogenesis through the Wnt/ β -Catenin pathway and multiple RPTPs may in fact share this role.

1.9.5 RPTP ligands and their functions

The various isoforms of PTP σ have been implicated in neuronal development and its expression is localised on axonal growth cones (Stoker 1994; Stoker et al, 1995). Furthermore, its expression has been described amongst spinal motor neurons in the mouse (Schaapveld et al, 1998). PTP σ has also been shown to promote axon outgrowth and growth cone guidance and morphology (Ledig et al, 1999; Rashid-Doubell et al, 2002). Extracellular heterotypic ligands for PTP σ have been described in the chick, where it has been shown to bind Heparan Sulphate Proteoglycans (HSPGs) in the retinotectal system, developing muscle and nucleolin (Haj et al, 1999; Aricesu et al 2002, Sajani-Perez, 2003, Alete et al, 2006).

Nucleolin on developing skeletal muscle has been identified as a potential ligand and binding partner for PTP σ . It is also expressed in retinal basement membranes. Nucleolin was found to bind PTP σ ectodomains *in vitro* and shares a complimentary expression pattern in developing muscle with PTP σ . Furthermore nucleolin is expressed on developing myotube surfaces and furthermore lectoferrin, a binding partner of nucleolin, blocks the binding of PTP σ ectodomains with muscle and retinal targets. This suggests nucleolin provides a target binding site for PTP σ on motor axons within muscles and the same may be true for the binding sites of PTP σ in retinal basement membranes, possibly through a surface receptor complex (Alete et al, 2006).

This finding that associates PTP σ intimately with HSPGs within the extra cellular matrix has turned out to be an important one. A reduction in PTP σ expression has led to faster regrowth of nerves (McLean et al, 2002), whereas in mice lacking functional

LAR, a structurally similar PTP family member to PTP σ , have shown decreased nerve repair capacities (Van der Zee et al, 2003). The role of HSPGs here is proving to be of increasing interest.

Heparan Sulphate Proteoglycans were shown to bind PTP σ with high affinity in the basal lamina. HSPGs are found in retinal basement membranes and glial end feet. Here the HSPGs Agrin and collagen XVIII were found to bind PTP σ through the heparan sulphate chains and first Ig-like domain of PTP σ in vitro (Aricescu et al, 2002). Furthermore site directed mutagenesis of the heparan binding site in the Ig domain blocked this binding affinity (Aricescu et al, 2002). Agrin, collagen XVIII and PTP σ have similar patterns of expression in the chick retinal system. All this demonstrates a heterotypic ligand for PTP σ , bridging the link between axonal/growth cone PTP σ expression and signalling and extracellular matrix interactors.

Of the ligands described for RPTPs (Reviewed in Mohebiany et al, 2012) members of the contactin family of IgCAMs, CNTN3, 4, 5 and 6 have been shown to bind PTPRG and PTPRZ in vitro. CNTN1 shows a high binding affinity to PTPRZ whilst PTPRG could potentially bind CNTN3 and CNTN4 in vivo as these genes are expressed in the same regions of the olfactory bulb in mice as PTPRG. Furthermore, PTPRG and PTPRZ are expressed in layer V of the cerebral cortex, and hippocampal pyramidal CA1 neurons. (Bouyain & Watkins, 2008). PTPRG loss of function mice and CNTN6 loss of function mice reveal similar phenotypes displaying impaired motor function and coordination. CNTN5 expression domain matches that of PTPRG within the cochlear nuclei post embryonic stages and nuclei of the vestibulocochlear nerve during

embryonic stages indicating these genes may serve a common function in the domain in addition to their binding affinities in vitro (Bouyain & Watkins, 2008).

Recent studies have indicated a proteoglycan specific molecular switch for the clustering of PTP σ during neurite extension. Here, this clustering results in a broadly uneven spread of phosphatase activity at the cell surface, with regions of depleted phosphatase activity enhancing the phosphorylated state for proteins, allowing neurite extension. Thus factors promoting PTP σ oligomerization may promote regeneration through proteoglycan binding. Both Heparan and Chondroitin sulphate proteoglycans are involved in cell signalling and it turns out that both serve as ligands for PTP σ . Importantly, CSPGs are able to inhibit nerve regeneration via PTP σ . PTP σ was found to act bimodally during sensory neuron extension. It inhibited axon elongation when contacting CSPGs, but promoted elongation when contacting HSPGs. Through detailed crystallography of these proteoglycans, Heparan Sulphate was shown to induce PTP σ ectodomain oligomerisation, this was inhibited by Chondroitin Sulphate. This demonstrates the proteoglycans can bring about opposing effects on neuronal outgrowth through competition during the control of oligomerization of PTP σ (Coles et al, 2011).

Further studies have highlighted the formation of a complex between CNTN1 and soluble PTPRZ in culture that activates a signalling pathway crucial to the proliferation of oligodendrocyte precursor cells (OPCs) regulated by phosphacan that may serve as a promyelinating factor. This is supported by the impaired myelinating capacity of PTPRZ loss of function mice and PTPRZ up regulation in myelin sheath lesion repair in oligodendrocytes. Thus the modulation of OPC proliferation occurs through PTPRZ

binding via CNTN1 at the surface of these precursor cells as phosphacan actively inhibits proliferation of these cells (Lamprianou et al 2011).

1.9.6 RPTPs and neural tube development

RPTPs thus could participate in a wide array of developmental processes within the spinal cord beyond their roles in axon guidance, potentially including neurogenesis cell movement and later on synaptogenesis. In relation to this, RPTP proteins were indeed shown to be expressed strongly within the neural tube at early stages of development (Chilton & Stoker 2000). Within the early spinal cord and during neurogenesis, members of the RPTP family display a striking pattern of expression and it can be proposed that such receptors may have novel roles in the specification, differentiation or migration of neuronal precursors from their radial cell progenitors. (Chilton & Stoker, 2000; Gustafson & Mason, 2000; Ivanova et al, 2004) (Figure 1.9) (Figure 1.10).

The expression profiles of members of the RPTP family at E4 and E6 in the chick brachial spinal cord may suggest a role for these genes during early spinal cord development. PTP σ is a group IIa RPTP formerly known as CRYP α in the chick, and it has two main isoform, CRYP α 1 and CRYP α 2, products of alternative splicing of mRNA and differing by their number of fibronectin domains (Figure 1.9) (Figure 1.10). In the developing neural tube, the short isoform 1 is expressed in the ventricular zone with strongest expression with the LMC and MMC, whilst the long isoform 2 is expressed selectively within the ventricular and subventricular zones, with expression in a few scattered cells within the dorsal and ventral horns.

Figure 1.9 Expression of RPTPs in transverse sections of E6 chick brachial spinal cord. Immunocytochemical staining of (A) Islet1, (B) Lim1/2, and (C) Lim3 protein expression. DIG-labelled mRNA in situ hybridization to (D, H) RPTP γ in the intermediate zone, above the floor plate (arrow, H) at thoracic levels (D) and in the dorsomedial LMC at brachial levels (H); (E) CRYP α (PTP σ) in the ventricular zone, LMC and MMC (arrow); (F) RPTP α in the LMC and ventral midline; (G) CRYP2 in LMC; (I) CRYP α 2 (PTP σ) in the ventricular zone; (J) RPTP δ in the dorsal neural tube and between the MMC and floor plate (arrow); (K) RPTP ψ in the lateral neural tube and floor plate (arrow); (L) RPTP μ in the vasculature. After Chilton & Stoker, 2000.

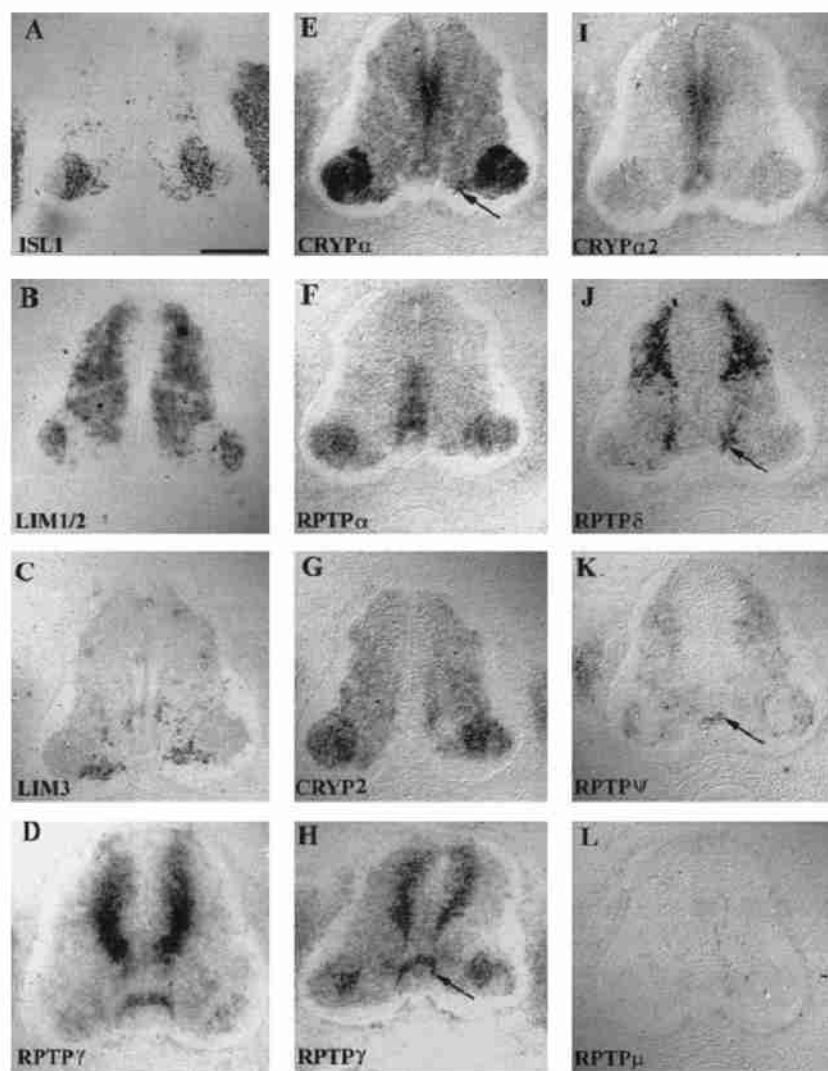
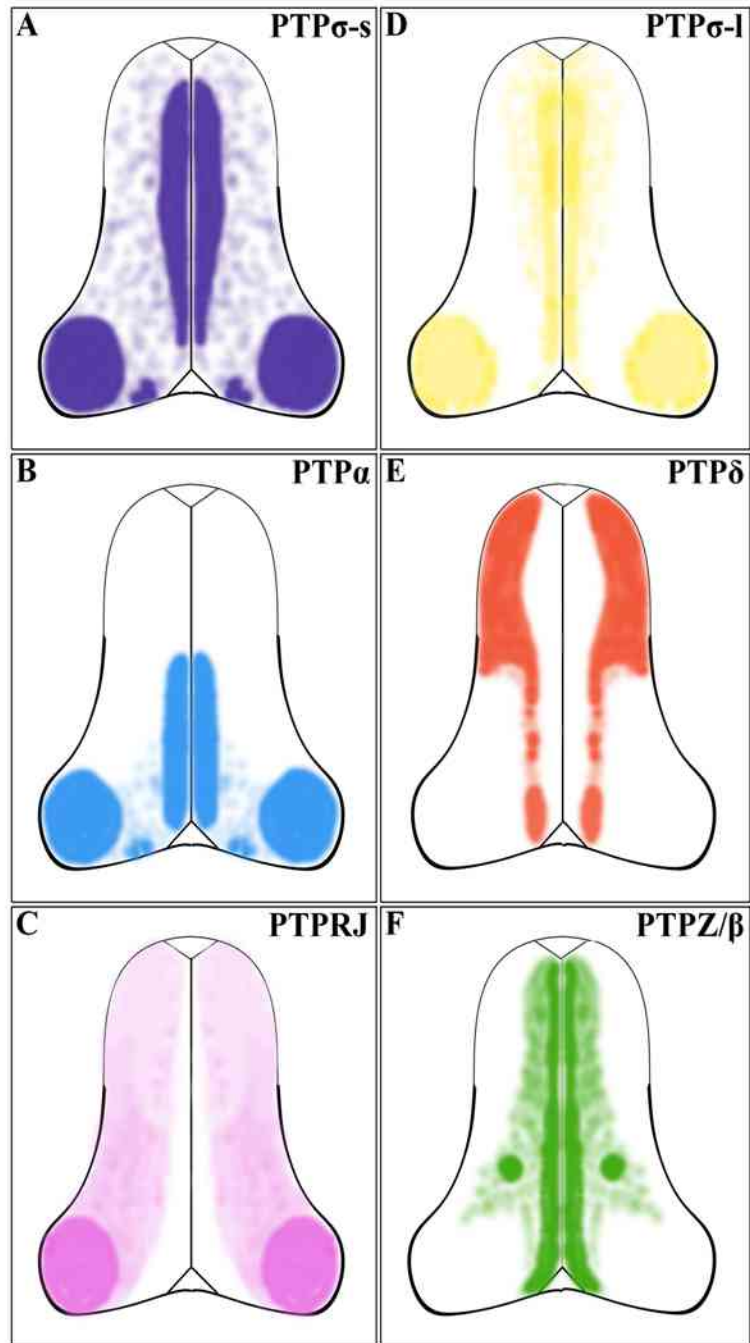


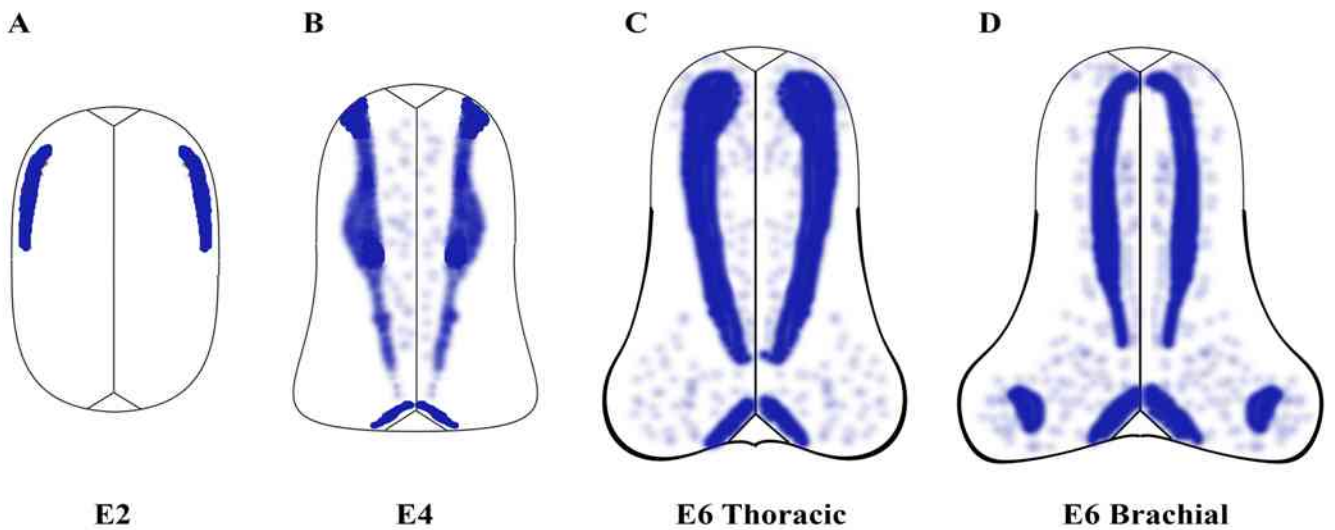
Figure 1.10 (TOP) *Scheme of expression of RPTPs in transverse sections of E6 chick brachial spinal cord.* Schematic DIG-labelled mRNA in situ hybridization to (A) PTP σ short isoform in the LMC and ventricular zone; (B) PTP α in the LMC and ventral midline; (C) PTPRJ in the LMC and faint expression in lateral regions; (D) PTP σ long isoform albeit a weaker expression to the short isoform in the ventricular zone and LMC; (E) RPTP δ in the dorsal neural tube and between the MMC and floor plate; (F) PTPZ/ β in the ventricular zone. Adapted from Chilton & Stoker, 2000.

(BOTTOM) *Scheme of PTP γ expression in the chick neural tube from E2-E6.* Schematic DIG-labelled mRNA in situ hybridization to RPTP γ at (A) E2, in the dorsal region of the spinal cord laterally in brachial sections; (B) E4 in the intermediate zone and above the floor plate in brachial regions; (C) E6, in the intermediate zone, above the floor plate at thoracic levels; (D) E6, in the dorsomedial LMC at brachial levels and intermediate zone as well as expression above the floor plate. Adapted from Chilton & Stoker, 2000; Ivanova et al, 2003; Gustafson & Mason, 2000.

RPTP family expression patterns



PTP γ expression pattern in the chick spinal cord



A group 3 RPTP, PTPRO, formerly known as CRYP2, displays an expression profile restricted ventrally within the LMC and absent from the Lim3-positive MMC (Chilton & Stoker, 2000). In this paper, further RPTP patterns are described where RPTP α expression is observed ventrally within the ventral midline, surrounding the floor plate and LMC where it may have further unknown developmental roles.

PTP δ , a member of group IIA RPTPs and LAR family member (Sommer et al, 1997), also reveals a striking expression pattern at E6 in the chick brachial spinal cord, with strong dorsal expression that overlaps with Lim1/2 cells. A population of ventromedial cells also express PTP δ in between the MMC and floor plate. This may suggest a role in the development of interneuronal populations rather than motor neurons. A group IIB member, PTP λ , known as PTP ψ and PTPru (Alonso et al, 2004), displays a weak expression profile at the same ventral time point described for PTP δ within the lateral neural tube with a slight, albeit very weak resemblance of PTP δ expression, suggesting these genes may cooperate functionally within the more dorsal aspect of the neural tube. PTP μ is also a member of the group 2B family, however at E6 its expression is generally absent from the spinal cord and is only expressed in the capillaries of the spinal cord (Brady Kalnay et al, 1995; Stoker & Chilton, 2000).

At thoracic levels at E4, PTP γ expression is evident as a strong stripe dorsoventrally along the intermediate zone, overlapping the pattern of Lim1/2 interneurons within the dorsal and intermediate aspects of the neural tube. A line of expression above the later floor plate, the site of oligodendrocyte birth is also seen as an inverted smile by E6. At brachial levels, the expression patterns of PTP γ at thoracic levels also extend to the dorsomedial LMC at stage E6, implicating a role for this gene during motor neuron

development (Chilton & Stoker, 2000; Gustafson & Mason, 2000) (Figure 1.5) (Figure 1.6). The family of RPTPs is thus widely expressed, in a variety of developmentally regulated patterns in the early neural tube. This thesis focuses on two RPTPs with particularly interesting expression, PTPs and PTP γ . These will now be described in some further detail.

1.9.7 PTP γ

The functions of RPTPs are still poorly understood during neural development, particularly in the development of the spinal cord. In situ data reveal striking patterns of expression in the spinal cord suggesting that they may play a role in the development of these tissues (Chilton & Stoker, 2000.) In particular PTP γ displayed an interesting pattern of expression within the spinal cord, which correlates closely with the expression of proneural genes described earlier. This has led to the initiation of a study into the actions of this gene during spinal cord development.

Chick PTP γ was first isolated and described in 1996 (Xiong et al, 1996,) and displays approximately 88% sequence homology to its human counterpart. It contains a fibronectin type III repeat along with a carbonic anhydrase domain and is highly glycosylated. Intracellularly it has two tandem catalytic domains typical of the receptor like PTPs. The protein exists as both transmembrane and secreted isoforms (Shintani et al, 1997). PTP γ expression in the chick is predominantly seen in the nervous system from gastrulation onwards, with low level expression in the primitive streak and the first formed somites.

Within the avian neural tube PTP γ is first detected in the elevated neural folds of the presumptive forebrain and during neurogenesis of the spinal cord, it is initially expressed in the dorsal interneuron domain that consequently gives rise to neurons and interneurons at around E2. (Gustafson and Mason, 2000).

PTP γ expression then expands along the dorsoventral aspect of the spinal cord in two lateral stripes within the intermediate zone that partially overlaps with Lim1/2 expression, and just above the floor plate in an inverted smile by HH24 (Gustafson and Mason, 2000; Chilton & Stoker, 2000). At brachial levels strong expression is also detected within the lateral motor columns. These data suggest that PTP γ may have a significant role during early neuronal development in the chick neural tube.

PTP γ has been studied in experiments with Rat PC12 cells, where in cells transfected with PTP γ , NGF-induced neurite outgrowth was inhibited. This did not occur when these cells were transfected with the closely related RPTP PTP ζ , suggesting a specific inhibitory effect of this protein on neurite outgrowth (Shintani et al, 2001). Further cell culture studies have also shown PTP γ to inhibit anchorage-dependent growth of breast cancer cells, suggesting that this phosphatase may have an important role during cell proliferation and regulation of tumorigenesis (Liu et al, 2004). Furthermore PTP γ has been shown to regulate hematopoietic differentiation in culture (Sorio et al, 1997).

In the mouse, PTP γ has been shown to be expressed in the brain among cortical layers II and IV consisting of pyramidal neurons, suggesting this gene may play a role here in neuronal development maintenance of cortical function (Lamprianou et al, 2006). It is also expressed in sensory neurons. Genetic knock down of the gene however showed

that it was not apparently necessary for gross normal development, although these mice have subtle behavioural defects (Lamprianou et al, 2006). Further expression was observed in the sensory cells of the retina, ear and tongue suggesting there may be a level of functional redundancy amongst phosphatases when considering that the PTP γ mutants appeared normal in such organs (Lamprianou et al, 2006). It is also worthy to note that in the mouse PTP γ is expressed very weakly in the spinal cord, in contrast to the chick.

1.9.8 PTP σ

PTP σ has a dynamic expression pattern in the spinal cord with a strong expression pattern in two stripes intimately related to the ventricular layer and site of mitotic cells within the spinal cord, and in the lateral motor columns at E4 (Chilton & Stoker, 2000.) A more diffuse expression is seen elsewhere in the cord. This expression persists in the ventricular layer to E6 in both the long and short isoforms studied and expression of a shorter isoform becomes restricted to the lateral motor column (Chilton & Stoker, 2000). These data suggest that PTP σ may be involved in early neurogenesis and axonogenesis.

The knock out of PTP σ expression in the mouse has demonstrated a requirement for this gene in the proliferation and adhesiveness of various cell types (Elchebly et al, 1999). Analysis of these mice highlighted defects in pituitary gland development, a reduced brain size and retarded growth patterns (Elchebly et al, 1999; Wallace et al, 1999). Further studies have shown that PTP σ is required for normal cytoarchitectural development in the CNS and late onset expression of GAP-43 in the mouse (Meathrel

et al 2002). PTP σ knockout mice have also indicated a role for this molecule in axonal guidance and regeneration (Uetani et al, 2006; Shen et al, 2009; Fry et al, 2010).

A study using dsRNAi in ovo to knock down the expression of PTP σ , PTP δ and PTPRO from HH18 in the lumbar spinal cord has shown defects in the dorsal anterior iliotibialis nerve in all three gene knockdown experiments despite apparently normal development of the limbs (Stepanek et al, 2005). Combined RNAi targeting of two or all three of these PTPs showed less severe phenotypes than the silencing of PTPRO alone implying a dose dependant function of PTPs during axonal outgrowth or an incomplete penetrance of the 3 genes studied (Stepanek et al, 2005).

The roles of LAR, PTP σ and PTP δ during motor neuron axon targeting were studied further amongst single and double mutants in mice. Although the single PTP δ and PTP σ mutants were viable, the double PTP σ / δ knockout mice displayed severe muscle dysgenesis and a severe loss of motor neurons in the spinal cord. Within these embryos, spinal cord development is initially normal yet after the generation of motor neurons is when motor neuron death occurs possibly due to a lack of target contact. This study also showed functional redundancy of these two genes during motor neuron development (Uetani et al, 2006).

Further studies have indicated that PTP σ $-/-$ stem cells have altered functions and considering the ventricular expression profile of PTP σ it is probably involved at some level in neurogenesis (Kirkham et al, 2006).

In this study, PTP σ was implicated in neuroendocrine and neuronal development, whereby sub ventricular zone neural stem cell cultures of PTP σ knockout mice and sibling controls showed that neurospheres from the knockout mice developed heterogeneous characteristics showing similar morphological characteristics to the age matched siblings. However, although PTP σ expression decreases as development progresses, it remains high with the continued renewal and passage of the neurospheres. Progenitor cells and differentiated neurons, astrocytes and oligodendrocytes all expressed PTP σ . No differences were observed in developing neurospheres or glia from PTP σ knockout mice, the neuronal migration patterns and neurites were affected in vitro. In particular, neurons migrated farther from the neurosphere centers and the neurite outgrowth exceeded the length of the neuronal processes from age matched sibling controls. The study implicated a specific role for PTP σ in the neuronal lineage through inhibitory influences on neurite outgrowth, and showed a role for PTPs in neuronal progenitor cell differentiation. (Kirkham et al, 2006).

1.10 RNA interference

These studies on PTP σ and PTP γ have together have raised questions into the role and function of these two genes in the chick, looking specifically at their potential roles in spinal cord growth and neurogenesis. In order to potentially perturb the function of these two genes in ovo, I adopted an experimental approach utilizing RNAi in this thesis and this will now be described.

RNA interference (RNAi) is a post-transcriptional method of gene silencing first discovered in *C.elegans* where double stranded RNA (dsRNA) resulted in sequence-specific gene silencing (Fire et al, 1998). Sense and antisense RNA were able to direct interference and this system was developed as an approach to inhibit gene expression. The dsRNAs were shown to be a more potent silencing trigger following studies in plant pigmentation, where RNA viruses were used to generate dsRNA molecules (Bernstein et al, 2001). The dsRNA operate at the post-transcriptional level, resulting in the targeted loss of mRNA through its degradation, or translational blockage. However, additional mechanisms exist where the dsRNA can target promoter sequences resulting in transcriptional repression (Mette et al, 2000).

Studies in *Drosophila* have shed light into the cellular mechanisms driving RNAi. Hairpin RNA precursors or dsRNA are processed cytoplasmically by a Dicer nuclease complex, an evolutionary conserved dimeric enzyme complex which cleaves these sequences into 21-25 nucleotide RNA sequences termed small interfering RNAs (siRNAs) (Zamore et al 2000). There are no intermediate cleavage products of dsRNA, and these siRNAs are double stranded duplexes with 2 nucleotide 3' overhangs and 5' phosphate termini. The siRNAs are then recruited into an RNA-induced silencing complex (RISC) (Hammond et al 2000).

The conserved Argonaute family of genes are important for the assembly of the silencing complex and contain PAZ domains also found in dicer proteins (Hammond et al, 2001). Upon activation of the RISC complex by ATP, the complex is remodelled into an effector nuclease complex causing the siRNA to unwind, guiding it to its target mRNA. Single stranded siRNAs are more effective at finding their targets. Silencing is

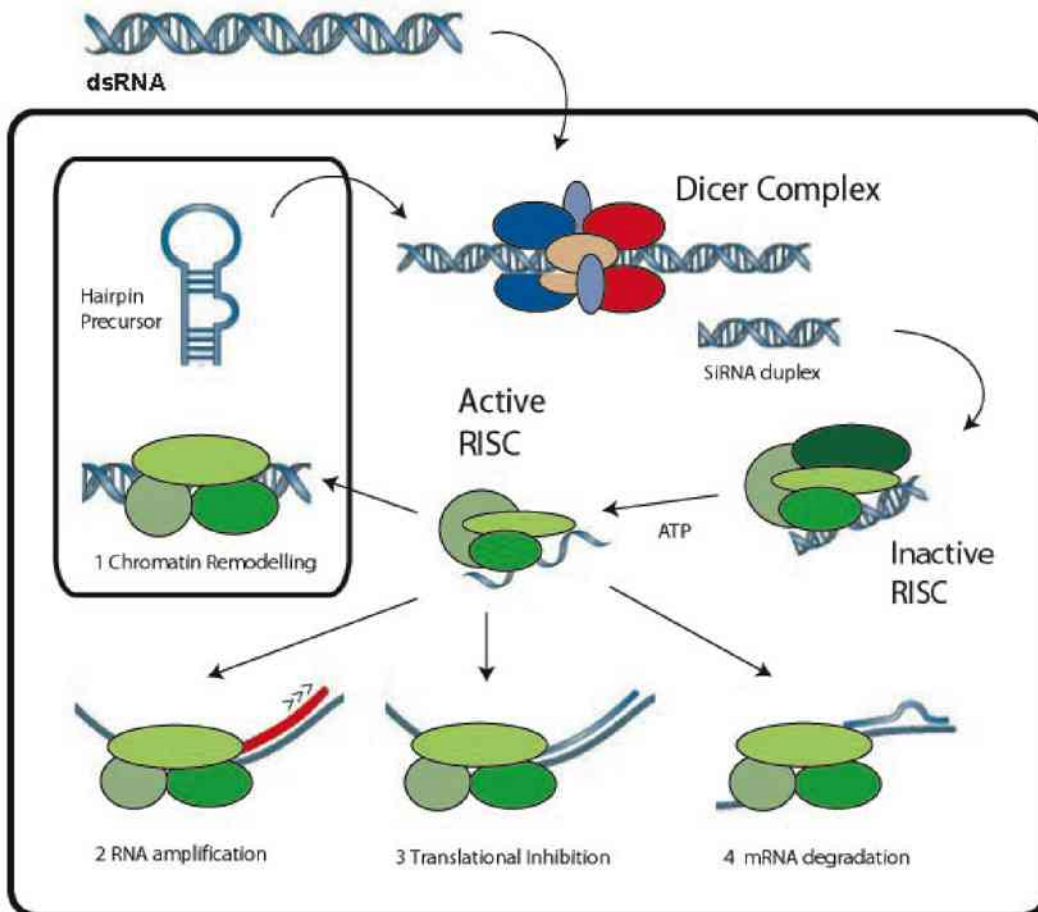
triggered through the nuclease complex targeting homologous mRNAs for degradation or by inhibiting mRNA translation. The effector complex may cause RNA amplification or drive chromatin remodelling in the nucleus (Figure 1.11).

RNAi can be triggered by small amounts of dsRNA (Bernstein et al, 2001). This model suggests a mechanism for cell-autonomous amplification of the silencing signal but not on its transmission. SiRNAs must have perfect complementarity to their mRNA target except for the overhangs. However, naturally occurring siRNAs such as those involved in viral host defence mechanisms e.g. *lin-4* and *let-7*, are termed micro RNAs (miRNA) and do not show perfect complementarity to their targets, driving translational inhibition rather than degradation of the target mRNA (Ambros et al 2004; Silva et al, 2002).

RNAi presents a powerful tool for analysing gene function. However siRNAs have transient effects and mammals may lack the mechanisms that amplify its signal as in *C.elegans*. Stabilisation can instead be made to occur through a hairpin loop of the inverted repeated sequence. Small hairpin RNAs (ShRNA) can be expressed in vivo from polIII promoters to induce stable expression, however non-specific off-target effects can occur as with the induction of the RNA-dependant protein kinase (PKR) pathway (Ohkawa et al, 2000; Sui et al, 2002; Brummelkemp et al, 2002).

Off target RNAi effects can be avoided if sequences are ~21bp (El-Bashir et al, 2001.) Novel phenotypes can therefore only be accepted and corroborated if the generation of a cell phenotype occurs with at least 2 different siRNAs targeting different sites on the same mRNA molecule.

Figure 1.11 Model of RNAi. Adapted from Hannon, 2000. Nuclear Hairpin or extra cellular dsRNA precursors are cleaved by the dicer complex into siRNA duplexes. These are recruited into the RNA-induced silencing complex (RISC) which upon activation by ATP causes unwinding of the siRNA duplex which guides the single stranded RNA to its target for either: 1 nuclear chromatin remodelling; 2 RNA amplification; 3 Translational inhibition or 4 mRNA degradation.



This then largely rules out off-target effects. At the time our experiments were instigated, another common, negative control was usually obtained using an shRNA with no homology to any other gene in the genome.

Gene silencing in chick embryos using a vector-based shRNA system was described in 2003, allowing spatially and temporally restricted gene silencing via an shRNA using the pSilencer commercial vector in ovo (Katahira & Nakamura, 2003). The chick also serves as a good model due to ease of embryo accessibility and manipulation, allowing in ovo gene transfer by electroporation. Through combining RNAi with electroporation in ovo, a powerful model system was therefore established for screening gene function (Pekarik et al, 2003). This system has since successfully been used during neurogenesis to analyse the function of *Transitin* during stem cell division and localisation of *Numb* in mitotic neuroepithelial cells (Wakamatsu et al, 2007).

A further study has demonstrated a functional knock-down of the neuropilin-1 receptor in ovo by siRNAs derived from hairpin structures driven by a mouse U6 promoter, whereby the embryos displayed nervous system defects associated with the functions of the Neuropilin receptor (*Nrp-1*) for semaphorins. The DRG defects presented, implicated *Sema3A* and its receptor on neurons, with misprojections of DRG axons and defects in the guidance of primary sensory afferents to their synaptic targets.

This study demonstrated an effective use of shRNAs to effectively knock down the targeted gene and was published after the start of my research (Bron et al, 2004). Later studies have also demonstrated the use of RNAi to study the effect of serine/threonine phosphatases, where interference of the Protein Phosphatase-1 (PP1) gene, through

small interfering RNA molecules, was shown to enhance the phosphorylation state of Pax-6 both in culture and in vivo thereby showing the modulation of Pax-6 by PP1 (Yan et al, 2007).

RNAi has been used in the chick using dsRNA molecules directed against PTP δ , PTP σ , LAR and PTPRO in the developing nervous system (Stepanek et al, 2005). Furthermore, shRNA molecules directed against PTP λ in the chick mid-hindbrain barrier have shown evidence for PTP λ in the regulation of the Wnt-1 expression domain (Badde & Schulte, 2008). The RNAi technology has also moved to the mouse whereby Cre-LoxP systems and U6 promoters have been used to deliver RNAi through shRNA in a tissue specific manner (Shukla et al, 2007; Seibler et al 2007).

Further applications of siRNA specifically in the chick are discussed in chapter 3. Based on the literature studied at the time our study was started (2003), RNAi in the chick was considered a good and novel method of potentially analysing gene function of the RPTP's during neurogenesis within the neural tube.

1.11 Experimental Aims.

In the following study, the RNAi approach was taken to knock down PTP γ and, in a more limited study PTP σ , in the chick spinal cord prior to and during the onset of neurogenesis. To complement this, PTP γ gain of function experiments were also conducted to test the effects of over expression of this gene within the neural tube.

Given the known functions of RPTPs during neural development and the expression patterns of PTP γ and PTP σ in the developing spinal cord, we hypothesised that these two RPTPs could be integrally involved in regulating either early neural tube growth, neurogenesis, or early neuronal migration, or a combination of these. At the start of this project, no vertebrate RPTPs had been functionally tested for such roles in the neural tube.

The aims of the experiment were therefore to determine through the use of RNAi, the potential functions of PTP γ and PTP σ during the development of different neuronal populations within the spinal cord. In particular, we wanted to address if these RPTPs could be specifically involved in either the proliferation, survival, differentiation or migration of neuronal precursors and progenitors. We wanted to determine the function of these two genes more specifically during early neurogenesis and motor neuron patterning and whether RPTPs may be involved in these early processes.

The specific aims of the project were to:

- Establish an shRNA system for use *in ovo*, in order to suppress the mRNA expression of RPTPs in the early neural tube.
- Define the potential developmental function of PTP γ in the early neural tube, using shRNA knockdown.
- Define the potential developmental function of PTP γ in the early neural tube, using cDNA over expression *in ovo*.
- Establish similar findings with the PTP σ gene in the neural tube.

Chapter 2: Methods & Materials

2.1 DNA preparation.

This procedure was used to obtain sterile quantities of DNA plasmids for transfection in culture or microinjection in vivo. DNA extraction kits were used throughout that are described further below.

2.1.1 Bacterial Cultures.

Bacteria (Competent DH5 α cells, Sigma) were transformed with the required DNA plasmid by heat shock at 42°C for 45 seconds and were then incubated overnight in 200ml sterile Luria Broth (LB, Sigma) solution at 37°C whilst vigorously shaking. The bacterial cells were then centrifuged at 6000g for 20 minutes at 4°C, and the supernatant discarded. The pellet that remained was processed using the Qiagen HiSpeed Plasmid Maxi Prep Kit.

2.1.2 DNA Extraction.

The bacterial pellet was resuspended in 10ml chilled resuspension buffer (50mM Tris-Cl pH 8.0, 10mM EDTA & 100 μ g/ml Rnase A.) The solution was then gently mixed with 10ml lysis buffer (200mM NaOH, 1% SDS w/v) at room temperature for no longer than 5 minutes to prevent shearing of the genomic DNA. To this 10ml of neutralisation buffer was added (3.0M potassium acetate pH 5.5) turning gently to

allow the buffers to mix completely and produce a white precipitate of genomic DNA, cell debris and protein. The plasmid DNA remains in solution.

2.1.3 DNA Filtration

The solution was incubated in a QIAfilter cartridge for 10 minutes at room temperature allowing the precipitate to float to the top of the cartridge. The solution was filtered through the cartridge using a plunger into a HiSpeed Maxi Tip previously equilibrated with equilibration buffer (750mM NaCl, 50mM MOPS (free acid) pH 7.0, 15% isopropanol v/v & 0.15% triton X-100 v/v). The filtrate was discarded as the plasmid DNA remains bound within the resin. Wash buffer (1.0M NaCl, 50mM MOPS pH 7.0 & 15% isopropanol v/v) was added to the Maxi Tip, discarding the filtrate.

2.1.4 DNA Elution.

The Maxi Tip was attached to a clean falcon and the DNA bound within the resin of the Tip was eluted using elution buffer (1.25M NaCl, 50mM Tris-Cl pH 8.5 & 15% isopropanol v/v.) The eluate was precipitated using 0.7 volume of isopropanol at room temperature for 5 minutes.

2.1.5 DNA Purification.

The precipitate was then spun at 15,000g for 30 minutes to allow the DNA to form a pellet. The supernatant was discarded and the pellet was washed in clean 70% ethanol

and spun again for 15 minutes at 15,000g. The supernatant was discarded and the pellet was resuspended in sterile distilled water at the desired concentration.

2.2 Micro preparation.

This is a procedure for rapid screening of large numbers of bacterial colonies, for the presence of recombinant clones within larger sized super-coiled plasmids.

2.2.1 Colony selection and pre-treatment.

A colony was picked directly from a plate using a yellow tip, and expelled into a tube containing 6 μ l protoplaster solution (30 mM Tris.Cl pH8, 5 mM Na_2EDTA , 50 mM NaCl, 20% sucrose, 50 mg/ml RNase A & 50 mg/ml lysozyme.) This was vortexed for 5-10 seconds while gently holding the top of yellow tip. The cells were resuspended in protoplaster, and left for 5-10 minutes, at room temperature.

2.2.2 Agarose gel preparation.

Agarose 0.7% running gel was prepared using 0.7% w/v SDS & agarose (Sigma), in 1x TAE buffer (40mM Tris Acetate pH 8.0, 1mM ethylenediamine tetraacetic acid EDTA.) Once the gel had set in the plastic running gel casts (BioRad) 3 ml of lysis solution (1x TAE buffer, 2% SDS, 5% sucrose & bromophenol blue) was loaded into each gel slot.

2.2.3 Agarose gel electrophoresis

The bacterial solution was placed carefully "under" the lysis solution and a control and non recombinant plasmid lane was also loaded. This was run in 1x TAE at 40 V for first 15min, then increasing the voltage to 100 V until the bromophenol had reached the end of the gel, at which point the gel was stained with Etidium Bromide and photographed under UV exposure. The supercoiled recombinant plasmids showed up larger in size from the control due to insert sequences.

2.3 The generation of silencing constructs.

The specific details of the vector and insert constructs are described and illustrated in Chapter 3.

2.3.1 Designing and preparing the plasmids

The PTP γ silencing constructs were designed using Ambion algorithms (www.ambion.com) (Michael Hurley). Six pairs of complimentary hairpin RNA encoding PTP γ -related cDNA oligonucleotides were annealed and ligated into the pSilencer 1.0 U6 vector (Ambion, USA). These were named Si1-6 and the sequence homologies to other off target genes were checked in Genbank, reducing the likelihood of off target effects and ensuring target specificity of the hairpins (M Hurley). This was repeated for PTP σ using the pSilencer 2.1 U6 vector (Ambion, USA) and the six new silencing constructs were named Sig1-6.

2.3.2 Annealing the PTP σ oligonucleotides.

The six complimentary pairs of hairpin encoding oligonucleotide inserts designed against PTP σ were diluted in molecular grade water (Sigma) to a final stock concentration of 100 μ M. To anneal the oligonucleotide sense and antisense strands, 50 μ l of annealing mix was prepared (2 μ l of sense DNA at 1 μ g/ μ l in TE (10 mM Tris, 1 mM EDTA), 2 μ l of antisense DNA at 1 μ g/ μ l in TE, 46 μ l 1x DNA annealing solution, Ambion.) This mixture was heated to 90°C in a heat block for three minutes and left to cool to room temperature, where the mix was incubated for an hour.

2.3.3 Ligation of templates.

In order to link the annealed hairpin encoding nucleotides to the silencing vector, two ligation mixes were prepared, one with and one without the insert as a control. 5 μ l of the annealed template mix was diluted into 45 μ l of molecular grade water. The ligation mixes comprised of the following:

	+ Insert	- Insert
Diluted annealed nucleotide mix (8ng/ μ l)	1 μ l	-
1x DNA Annealing solution (Ambion)	-	1 μ l
Nuclease free water (Sigma)	6 μ l	6 μ l
10X T4 DNA Ligase Buffer (Roche)	1 μ l	1 μ l
pSilencer 2.1-U6 Hygro Vector	1 μ l	1 μ l
T4 DNA Ligase (5U/ μ l)	1 μ l	1 μ l
Total	10 μ l	10 μ l

The ligation mixes were incubated at room temperature for 2 hours and then a stock was stored at -20°C and an aliquot set aside to proceed with the transformation. A negative control ligation without the insert was also set up that yielded no plasmids.

2.3.4 Culturing the clones

Following the ligation, 1µl of the ligation mix was transformed as previously described into competent DH5α bacterial cells and incubated in 1ml of LB solution without antibiotics at 37°C for one hour. 200µl of the cultures were plated onto pre-prepared agar plates (Sigma) with ampicillin antibiotics added as the silencing vector conferred ampicillin resistance and thus only bacteria that had taken up the silencing vector should form colonies on the agar plates.

These were left to culture overnight and the following day individual colonies (five clones for each silencing construct) were selected, expanded and mini-preps of DNA (Qiagen) conducted as previously described for sequencing. These DNA were initially digested and ran on 0.7% agarose gels to give an indication of the correct size for the plasmid before sequencing to ensure every insert was of the correct sequence.

2.3.5 Sequencing the constructs.

The DNA was then sequenced, where ~100ng was primed against a region of the vector upstream of the insert in a thermocycler (95°C 20'', 50°C 10'', 60°C 1'; for 25 cycles – Minicycler, MJ Research.) The reaction mix composed of (5µl DNA ~20ng, 3µl 1x sequencing dye, 2µl oligonucleotide and 5µl water) for each clone selected.

The product was extracted using 2 μ l 7.5M ammonium acetate and 55 μ l absolute ethanol. This was centrifuged for 15 minutes at 13,000rpm at room temperature and consequently detected using dye on a capillary machine, MEGAbase (Amersham) to check the correct orientation of the insert and for point mutations. The sequences were found to be correct.

2.4 Cell culture studies.

2.4.1 Creating a working stock.

Human Embryo Kidney 293T cells were cultured in 16.7g/L Dulbecco's Modified Eagle's Medium (DMEM) (Sigma, UK), 100U/ml penicillin/streptomycin & 10% foetal bovine serum (FBS) (Sigma, UK.) A working stock of cells was expanded from a starter culture, split into 10cm plates and incubated at 37°C, 5% CO₂ under sterile conditions.

2.4.2 Expanding the cells.

Once the cultures had reached 80% confluency, the medium bathing the cells was aspirated and cells washed with phosphate buffered saline (PBS). The PBS was then aspirated and 0.05% trypsin added for one to five minute to detach cells from the plate.

The cells were collected using the prepared DMEM at 37°C through pipetting and centrifuged at 1,000 rpm for one minute. The culture medium was aspirated and the

pellet of cells resuspended in fresh DMEM as previously prepared at 5% confluency and incubated again at 37°C, 5% CO₂.

2.4.3 Cell Transfections.

Once a confluency of 30% was reached (approximately 2 million cells per 10cm plate) the cultures were subsequently co-transfected with various silencing constructs and a PTP γ expression construct (The full length PTP γ cDNA was kindly provided by Lu Hai-Wang and was subcloned (A Stoker) in frame with the 3xFLAG tag into p3xFLAG-CMV14 (Sigma).) 10 μ g of total DNA (4 μ g PTP γ plasmid, 4 μ g silencing vector, 1 μ g GFP plasmid, 1 μ g luciferase reporter plasmid) was used per 10cm culture dish at 30% confluency (Concentrations - 2 μ l of 2 μ g/ μ l PTP γ , 2 μ l of 2 μ g/ μ l Silencing vector, 0.5 μ l of 2 μ g/ μ l GFP and 1 μ l of 1 μ g/ μ l luciferase construct). The total DNA was diluted in distilled water and 10% 2.5M CaCl₂ and added drop by drop into an equal volume of 2X HEPES buffered saline (pH7.05) (1ml total per 10cm plate) in a falcon whilst gently bubbling air into the buffer. The transfection mix was added to the cells drop wise and left in culture for 48 hours.

2.4.4 Protein Extraction.

Following 48 hours in culture the cells were lysed in 0.25% (v/v) TritonX-100, 150nM NaCl, 100mM NaCl, 50mM Tris-Cl pH 7.6 buffer with 1:100 v/v protease inhibitors (Complete, Roche) and centrifuged at 4,000rpm to remove cell debris. The supernatant containing soluble cellular proteins was collected.

2.4.5 Luciferase Assays.

A GFP Plasmid, pCA β IRES-GFP (Jon Gilthorpe) at a concentration of 2 μ g/ μ l and a Renilla Luciferase reporter construct, vector pRL-SV40-renilla (Promega, UK) encoding the firefly luciferase protein was also transfected (1 μ g/ μ l) to check for relative transfection efficiency amongst experiments in addition to the silencing and PTP γ plasmids described above. The shRNA was not tagged directly with GFP or other reporter constructs as these vectors were not commercially available at the time. The short hairpin encoding vectors that were available were driven by mouse U6 promoters rather than chick. 20 μ l aliquots of lysates were tested using the Renilla Luciferase assay system (E2810 Promega, USA).

The growth medium from cultured cells transfected as above were rinsed with PBS and 1ml 1X Renilla luciferase Assay Lysis Buffer (150mM HEPES pH8.0, 0.25% Triton X-100, 1mg/ml porcine gelatin, 10% glycerol and 0.05% antifoam 289) added to the cells. These lysates were then scraped from the culture dish to create a homogenous lysate. The lysate was then transferred to an eppendorph. The Renilla Luciferase assay substrate was then prepared at 1 μ l of 100X assay substrate to 100 μ l Assay buffer (0.5M NaCl, 0.1M potassium phosphate, 1.0mM Na₂EDTA, and 1mg/ml porcine gelatin pH7.6). For each sample, 100 μ l of Renilla luciferase assay reagent was added to the luminometer tube resting in the luminometer, and 20 μ l of cell lysate solution added.

The lysate mix and detection reagent consequently measured for luminescence rapidly within the first few seconds in a manual luminometer (Berthold Technologies Luminometer LUMAT LB 9507 – Bad Wildbad, Germany) The luminescence was

measured and recorded. In this reaction, light is produced through the formation of oxyluciferin. Firefly luciferase, a monomeric 61kDa protein, catalyzes luciferin oxidation and a flash of light is generated that decays rapidly after the enzyme and substrates are combined. This flash of light is subsequently detected by the luminometer.

2.5 Protein detection.

In order to detect the cellular proteins in our sample we used the Western blotting technique.

2.5.1 Cell Lysis

The transfected cells were lysed in 500µl lysis buffer (0.5% NP₄O, 25mM Tris pH 7.2, 150mM NaCl, 5mM MgCl₂, 5% Glycerol) and 1:100 v/v protease inhibitor (Complete, Roche.) The lysate was then kept on ice to prevent protein degradation whilst syringing up and down three times to ensure the cells were fully lysed.

2.5.2 Protein Reduction.

The lysates were centrifuged at 13,000 rpm at 4°C for 10 minutes and washed in wash buffer (50mM Tris pH 7.4, 150mM NaCl, 0.5% Tween20) and pulsed at full speed for 30 seconds. The cleared lysates were reduced using an equal volume of 2X loading buffer (0.1M Tris-HCl pH6.8, 2.5% Sodium Dodecyl Sulfate (SDS - Sigma), 10% glycerol, 10% b-Mercaptoethanol 14.2M (Sigma), 0.025% Bromophenoyl Blue BPB) at 100°C for 5 minutes then left to cool to room temperature.

2.5.3 SDS-PAGE Electrophoresis.

In order to separate the proteins according to their size, SDS gel electrophoresis was used whereby the binding of the protein products to SDS results in fractional separation by size as a current is passed through the gel.

The reduced samples were consequently loaded onto an SDS PAGE electrophoresis running gel prepared at 6% (30% Acrylamide, 1.5M Tris pH 8.8, 10% SDS, 10% ammonium persulphate (APS), 0.08%v/v NNN'N'-Tetramethylethylenediamine (TEMED - Sigma).) A stacking gel was prepared at 5.1% (30% Acrylamide, 1M Tris pH 6.8, 10% SDS, 10% APS and 0.08v/v TEMED.) The gel was allowed to polymerize and samples then loaded into the wells within the loading buffer. This was run at 40mA, <180V for an hour in an electrophoresis cell (BioRad, USA) filled with running buffer (25mM Tris, 0.2M Glycine, 0.1% SDS).

2.5.4 Gel Transfer

The gel was then transferred onto a polyvinylidene difluoride (PVDF) membrane (Sigma Immobilon-P) soaked in methanol and sandwiched in between 6 pieces of 3MM filter paper soaked in blot buffer (25mM Tris, 0.2M Glycine, 20% methanol) using a semi-dry transfer apparatus (Biorad) running at 400mA, <18V for 30 minutes.

2.5.5 Immunoblotting.

The membrane was then blocked in 10% milk/TBST (50mM Tris pH 7.4, 150mM NaCl, 0.2% Tween20) overnight at 4°C in preparation for immunoblotting. The

primary antibody was diluted in 10% Milk/TBST and incubated with the membrane at RT for 1 hour, then the membrane was washed with TBST for 5 minutes 5 times. The secondary HRP-conjugated antibody was also incubated in 10% Milk/TBST at RT for an hour and then washed in TBST for 5 mins 5 times.

2.5.6 Protein Detection.

Antibodies were detected through the use of chemical luminescence on the PVDF membrane, using the oxidation of lumenol by HRP with the ECL plus detection kit (Lumigen PS-3). Filters were exposed to Kodak light sensitive X-Ray film then developed in an x-ray developer machine.

2.6 In ovo electroporation

2.6.1 Microinjection

Silencing constructs were co-injected in ovo at final concentrations of $2\mu\text{g}/\mu\text{l}$ in PBS with $2\mu\text{g}/\mu\text{l}$ GFP in PBS (pCA β IRES-GFP, Jon Gilthorpe) in order to visualise the targeted region of electroporation. The total electroporation mix consisted of $2\mu\text{l}$ of $2\mu\text{g}/\mu\text{l}$ silencing vector, $0.5\mu\text{l}$ of $2\mu\text{g}/\mu\text{l}$ GFP and $0.2\mu\text{l}$ of 2% fast green. Microinjection needles made of 1mm glass capillary tubing were pulled using a KOPF needle puller Model 720 (David Kopf Instruments, USA) and were backfilled with DNA mix & 2% fast green dye (Sigma) and loaded onto micromanipulators (Narishige, Japan) attached to a cell microinjector (Microdata Instruments Inc PM1000).

2.6.2 Electroporation.

5mm Gold-plated electrodes (BTX Inc model 508) were placed 3mm apart and connected to a Square Wave Porator (BTX, Inc model ECM 830). DNA was injected into the neural tube at a pressure of 5 psi under a Ziess stereoscope (Steni SV11) The targeted region was then electroporated at 20V, for 5 pulses lasting 50ms, with 950ms intervals between pulses (parameters as outlined after Canatella et al, 2001). The embryos were then reared and GFP visualised using a Leica MZ stereomicroscope and Leica DC500 digital camera running Leica IM1000 software.)

2.6.3 Embryo Dissection and Storage.

Embryos were staged according to Hamburger & Hamilton, 1951, dissected out of their amniotic sacs and fixed in 4% PFA overnight at 4°C. 4g of paraformaldehyde was added to 80ml distilled water and heated to 70°C. Two drops of 1M NaOH was added to this while swirling until the solution went clear, and allowed to cool to room temperature. 10ml of 10x PBS was added and this was topped up to 100ml with distilled water. This 4% PFA was then stored at -20°C.

2.6.4 Cryoprotection and frozen sections.

The embryos were cryoprotected in 30% sucrose in PBS for another night at 4°C then snap frozen in OCT (Bright Inc) and stored at -80°C. 12µm cryosections were collected on superfrost plus slides (VWR) and stored at -20°C for further analysis.

2.7 Cell Death and Proliferation.

The purpose of the following treatments were to determine if interfering with PTP expression lead to reduced proliferation through the detection of BrdU introduced into the developing embryo, or increased cell death through the detection of cleaved Caspase 3 enzyme expressed in apoptotic cells. For both treatments embryonic sections were pre-treated to facilitate access of the probe to its intracellular target.

2.7.1 Apoptosis

Apoptosis is a programmed form of cell death, triggered through a cascade of proteolytic enzymes expression called Caspases. This results in the cleavage of protein substrates, causing the cell to disassemble. Caspase 3 acts as a key effector in the apoptotic pathway, present in numerous cell lineages and is responsible for the cleavage of various molecules such as actin. If cells were undergoing apoptosis during our silencing experiments then Caspase 3 detection would highlight the temporal and spatial pattern of cell death within the spinal cord.

2.7.1.1 Pre-treatment for Caspase 3 detection.

Cryosections were placed in freshly prepared 1x Declere (Cell Marque Corp, USA) for 40 minutes whilst steaming. The slides were then placed in fresh Declere that had been pre-heated in the steamer for 10 minutes to allow it to warm up and left at room temperature to cool slowly.

2.7.1.2 Peroxidase Quenching.

Once at room temperature, the slides were washed three times in Tris Buffered Saline (TBST) (100mM Tris pH7.5, 150mM NaCl, 0.1% Tween) for five minutes each wash. The endogenous peroxidase activity was then quenched with 3% H₂O₂ for ten minutes. This was followed by 3 subsequent washes in TBST for 5 minutes each.

2.7.1.3 Primary Antibody Application

The slides were blocked in blocking solution (0.15% Glycine, 2mg/ml BSA (Fraction V – Sigma), 5% Goat Serum and 0.1% TritonX) for 30 minutes at room temperature. The Caspase 3 primary antibody (see table for concentrations) was diluted in blocking solution and placed on the slides overnight at 4°C.

2.7.1.4 Secondary Antibody Application

The slides were then washed in TBST three times for five minutes each wash. The slides were then incubated at room temperature with a biotinylated secondary antibody to increase the signals detected within the cells, diluted in blocking solution for an hour at room temperature. Following incubation, 3 subsequent washes in TBST for 5 minutes each were carried out to remove residual secondary antibody.

2.7.1.5 Enhancing the Caspase signal.

To increase the Caspase 3 signal within the cells, the sides were incubated in freshly prepared ABC (Vector Labs) solution for half an hour. The ABC kit provides an immunoperoxidase procedure for antigens through a biotinylated enzyme and Avidin. Avidin has a very high affinity for biotin, where the binding of avidin to biotin through cross linking forms a stable and irreversible complex, allowing some biotin sites to remain free for binding. Three further washes in TBST were carried out to remove excess ABC reagent.

2.7.1.6 Detection

The HRP enzymes within the complex were detected visually as a brown precipitate using diaminobenzidine DAB+ reagent kit (DAKO, USA). The Caspase 3 antibody and its biotinylated complex reacts with horseradish peroxidase-conjugated streptavidin molecules and chromogen leading to the visible precipitate developing at the site of the antigen. The DAB+ solution was made in 5ml of PBS using 4 drops of the DAB+ reagent and 2 drops of hydrogen peroxide provided with the kit. This was applied directly to the sections at room temperature for 2 minutes. Three further washes in TBST were carried out to remove excess DAB+ reagent.

2.7.2 Proliferation.

The spatiotemporal pattern of dividing cells can be analysed using specific markers. Proliferating cells can be detected using Bromodeoxyuridine (BrdU) which is a

synthetic analogue of thymidine that uses nucleotide substitution to replace thymidine with uridine in the DNA structure of dividing cells. It is incorporated in newly synthesized DNA of dividing cells during the S phase of the cell cycle. Once the BrdU is incorporated into cells it can then be detected through antibodies specific to BrdU and usually antibody binding will require both acid and heat treatment to expose the BrdU antigens.

2.7.2.1 BrdU incorporation.

Embryos were treated with 100 μ l BrdU (Sigma, UK) 10mg/ml 2 hours prior to harvesting by dropping this directly on top of the embryo. The embryos were processed according to the protocol for Immunohistochemistry.

2.7.2.2 Pre-treatment

Cryosections were boiled within a slide box covered in cling film in the microwave, bathed in citric acid buffer (0.01M pH6.0) on medium heat for 4 times lasting 2 minutes, allowing 2 minute intervals between heating. The slides were allowed to cool to room temperature, then rinsed in PBS. The slides were then passed through 0.1M HCl for 30 minutes at RT. This was replaced with 2M HCl for 30 minutes at 37°C and finally in 0.1M sodium borate pH 8.5 for 10 minutes at RT followed by a rinse in PBS.

2.7.2.3 Peroxidase quenching.

The endogenous peroxidase was quenched with 2% H₂O₂ for 15 minutes followed by 2 subsequent washes in PBS for 5 minutes each. The slides were then blocked in 10% Normal Goat Serum (NGS) (Vector Labs) in PBS for an hour at room temperature.

2.7.2.4 Antibody Application.

The slides were then incubated in anti-BrdU (DSHB) diluted in blocking solution for an hour at room temperature, followed by 3 washes in PBS for 5 minutes each. The slides were then incubated with secondary antibody diluted in blocking solution in a humid chamber for an hour at RT followed by 3 washes in PBS for 5 minutes each.

2.7.2.5 Detection

DAB+ solution was then used to visualise the location of the antibody through biotin complexes as previously described. The slides were then rinsed in PBS and mounted in Floursave (Calbiochem) a glycerol free, ready to apply aqueous mounting medium that helps to preserve fluorescent markers within the tissue of the GFP electroporated embryos.

2.8 Immunohistochemistry

Slides were washed in PBS, then 1% H₂O₂/PBS for 20 minutes in order to quench the endogenous peroxidase. The sections were then blocked in 4% BSA (Fraction V, Sigma) in PBS for another 20 minutes at room temperature.

The primary antibody was added to fresh blocking solution and 200µl added to each slide which was incubated in a humid chamber for an hour at RT (see table for concentration of antibodies used). The slides were washed in PBST (0.2% Tween20) for 5 minutes three times.

The secondary HRP, biotinylated or fluorescent conjugated antibody was then applied and incubated for an hour at RT. The slides were washed in PBS and fluorescence observed with a conjugated secondary antibodies and Cy3 fluorescent tag (Amersham) or they were consequently detected using DAB (Vector Labs, USA).

Primary antibodies

Antibody	Donor species	Notes	Concentration
Neurofilament	Mouse	DSHB 3A10	1:100
β-Tubulin	Mouse	Babco	1:100
Islet1/2	Mouse	DSHB 39.4D5	1:100
Lim1/2	Mouse	DSHB 4F2	1:100
Nkx2.2	Mouse	DSHB 74.5A5	1:20
Mnr2/Hb9	Mouse	DSHB 81.5C10	1:400
Engrailed1	Mouse	DSHB 4G11	1:200
Lim3	Mouse	DSHB 67.4E12	1:5
Evx1	Mouse	DSHB 99.1.3A2	1:20
Hoxc9	Mouse	DSHB 5B5-2	1:20
Olig2	Guinea pig	S. Guthrie	1:400

P-Histone 3	Rabbit	Upstate	1:500
Caspase-3	Rabbit	Upstate 04-439	1:1000
BrdU	Mouse	DSHB	1:100
RPTP γ polyclonal	Rabbit (AB69)	A. Stoker (aa99-118)	1:5000 (Western)
RPTP σ polyclonal	Rabbit	A. Stoker	1:1000 (Western)
Anti-Flag M2	Mouse	Sigma	1:10,000 (Western)

- Polyclonal anti-avian PTP γ serum AB69 was generated locally using chick PTP γ peptide YQELDGFDNNESSNKTWMK aa99-188, by M Hurley & A Stoker.

Secondary antibodies

Antibody	Donor species	Conjugation	Concentration
Anti mouse	Rabbit	TRITC	1:50 (DAKO)
Anti mouse	Rabbit	FITC	1:50 (DAKO)
Anti guinea pig	Rabbit	HRP	1:100 (Abcam)
Anti rabbit	Goat	HRP	1:100 (DAKO)
Anti mouse	Rabbit	HRP	1:100 (DAKO)
Anti rabbit	Goat	Biotinylated	1:250 (DAKO)
Anti mouse	Rabbit	Biotinylated	1:100 (DAKO)
Cy3	Mouse	Streptavidin (3°)	1:400 (Amersham)

2.9 Histological staining

Slides were washed in PBS and stained with 1% Haematoxylin (Ehrlich's - Sigma) for 5 minutes then rinsed with running tap water. The slides were then quickly dipped in acid alcohol (1% HCl in 70% ethanol) and rinsed again under running tap water and counterstained with 1% Eosin (Raymond Lamb) for 2 minutes, and then rinsed under running tap water, dried and mounted in Floursave as previously described.

2.10 Non-radioactive in situ hybridisation with digoxigenin (DIG) labelled probes.

Embryos were processed for cryosectioning, as previously described, only using DEPC treated reagents to prevent RNA degradation. The slides were stored in black slide boxes with silica gel to remove moisture. The treatment took place over three days. RNA probes were produced against cellular targets namely PTP mRNA, giving an indication of the gene expression profile throughout the spinal cord at different embryonic ages.

2.10.1 DNA Linearisation.

1µg of DNA was linearised with appropriate restriction enzymes at 37°C for 2 hours in a total of 40µl volume (34µl DNA & dH₂O, 4µl specific buffer, 2µl enzyme) which was then purified using a PCR purification column (Qiagen). High salt binding buffer was added to the linearised mix and this was centrifuged at full speed for one minute in the spin column. This resulted in the DNA binding to the silica gel membrane within the spin column and impurities being washed away. The DNA was then eluted off in

50 μ l molecular grade water (Sigma) through centrifugation at full speed for a minute, collecting the eluate in a sterile eppendorf. The sizes of the digested DNA were then checked on 0.7% agarose gel as previously described.

2.10.2 Probe Synthesis

The probe synthesis mix was made up to a total volume of 20 μ l & incubated at 37°C for 2 hours. 47 μ l of ddH₂O was added and this was purified by centrifuging the probe mixture using an RNA purification column (Qiagen) and collecting the eluate containing the desired RNA probe. To this eluate, 33 μ l of formamide was added taking the total volume to 100 μ l of probe which was stored at -20°C. The following plasmids were used to prepare the RNA probes: Chick NeuroM, pBSK-NeuroM (M Gullivet 1997); Chick PTP σ , pCRYPmyc1 (A Stoker 1994); Chick PTP γ 3xFlagGamma-CMV14 (Ledig et al 1999), full length PTP γ cDNA provided by Lu Wang.

Probe synthesis was initiated using:

13 μ l	linear DNA template in H ₂ O 0.25 μ total
2 μ l	5x transcription buffer
2 μ l	DIG RNA labelling mix (Roche)
1 μ l	RNA inhibitor (Roche)
2 μ l	RNA polymerase (T3, T7, Sp6 Roche)

2.10.3 Hybridization.

2-5 μ l of probe per 1ml of hybridisation buffer (1x salts (10x stock: 2M NaCl, 50mM EDTA, 100mM Tris-HCL pH7.5, 50mM NaH₂PO₄.2H₂O, 50mM Na₂PO₄), 50% formamide, 0.1mg/ml yeast tRNA, 10% dextran sulphate, 1x Denharts solution) was denatured for 5 minutes at RT and allowed to stand for 5 minutes on the bench. 150 μ l of this dilution was added to each slide and a coverslip placed on top. This was hybridised in a humid chamber with tissues soaked in 2x SSC/Formamide at 70°C overnight.

2.10.4 Antibody Treatment.

The following day post hybridisation, the slides were washed in wash buffer (1x SSC, 50% Formamide, 0.1% Tween20) at 65°C for 30 minutes three times. 3 consequent washes in TBST were carried out for 30 mins each at room temperature. The slides were dried and blocked (TBST, 2% nucleic acid blocking reagent – Roche, 10% heat inactivated sheep serum) for 1 hour at RT. Anti-Digoxigenin AP-conjugated antibody (Roche) was diluted 1:1500 in blocking solution and the slides were incubated with this in a humid chamber overnight at 4°C.

2.10.5 Signal Detection.

Following overnight incubation, the slides were washed 3 times in TBST for 10 minutes each, then washed in pre-staining buffer (100mM Tris pH9, 100mM NaCl, 5mM MgCl₂) for 10 mins twice. Staining buffer was prepared using and equal volume

of prestaining buffer with 10% (w/v) polyvinyl alcohol and 18 μ l/ml of combined NBT/BCIP (Roche). The slides were then incubated at 37°C in the dark until a satisfactory signal was achieved. They were then rinsed in distilled water and mounted in Floursave.

2.11 Quantification of cell numbers from spinal cord sections.

Quantification of cell numbers in different regions of the neural tube stained with respective neuronal specific antibodies, as well as apoptosis markers and proliferation markers, Caspase 3, pH3 and BrdU respectively were carried out on spinal cord sections. The embryos analysed for PTP γ and PTP σ loss of function and PTP γ over expression as well as control sets were stained against Islet1/2, Lim1/2, MNR2, Lim3, Caspase3, p-Histone3 and BrdU antibodies.

The counts were carried out 'blind' using the Openlab software, where the region of cells to be counted was outlined, marked and compared against its control side within the same embryo. Three serial sections per embryo analysed were counted to ensure accurate results. The mean ratio between the control and electroporated sides of the neural tube of stained cells was determined for each embryo in the silenced group and control group. The average ratios of cells amongst experimental sets were then determined as an average of the individual embryo counts and tabulated.

Chapter 3: Testing shRNA knockdown of PTPs in culture.

3.1 RNA Interference in the chick.

Since its discovery in 1998 (Fire et al, 1998) RNAi has allowed researchers to test the post-transcriptional effects of genes spatially and temporally in vivo, without the need to create a genetic knock-out organism. A number of studies had previously validated the chick as a model system for RNAi technology (Mette et al, 2000; Katahira & Nakamura, 2003; Bourikas & Stoeckli, 2003). These studies demonstrated the effective silencing of target genes during embryonic development.

RNA interference has many advantages over conventional methods of gene analysis and is becoming a powerful tool in deciphering genetic interactions during development. Moreover, studies have demonstrated the use of short hairpin RNA plasmids in the chick neural tube (Chesnutt & Niswander, 2004). The use of small-interfering RNA and short-hairpin RNA molecules to deliver silencing of the genes involved in proliferation, both in human and murine cell types, has also been investigated (Berns et al, 2004; Gupta et al, 2004).

During and after this project, several more studies have further validated shRNA use in the chick. These studies have utilized the vector-based approach using avian retroviruses or U6 promoters, to drive shRNAs during commissural axon development, neural tube development and in the developing eye (Bourikas et al, 2005; Bron et al, 2004; Harpavat & Cepko, 2006).

Together, these results have set precedent and validated the use of short-hairpin/small-interfering RNA molecules using U6 promoters in the chick nervous system directed against Protein Tyrosine Phosphatases.

3.2 Designing the RNAi constructs

Using the chick as a model organism allowed the screening of the effects of multiple double stranded RNA molecules over a short space of time, with sequences specifically targeting the mRNA of members of the RPTP family without the need to create knock out organisms. Initially, the hairpin-encoding constructs were designed and assembled and their efficacy tested in culture.

3.2.1 Designing the target sequences.

Six target sequences were selected at different locations on the chick PTP σ cDNA (Figure 3.1A), using the online manufacturers algorithm for creating the silencing vectors (www.ambion.com) (Ambion, USA). Once the target sequences were determined the sense and anti-sense oligonucleotides encoding the short-hairpin molecules were designed (Figure 3.1B). These were then obtained directly from Operon UK.

The activity of six RNAi encoding vectors against PTP γ , previously constructed using the p-silencer1.0 U6 vector (Ambion) by M Hurley, were also used (Figure 3.2A). The target sequences of the PTP γ cDNA were also designed using the Ambion algorithm (Figure 3.2B & 3.2C).

Figure 3.1 (A) Table of the 6 anti-sense cDNA target sequences for PTP σ , Sig 1-6 and the location of the various target sequences along the length of the cDNA. The corresponding GC content for each target sequence is also listed. (B) The full sense and anti-sense pairs of hairpin sequences constructed for the six PTP σ cDNA targets. Key: White- Target sequence, Yellow – Hairpin loop sequence, Green – AA/TT target sequence overhangs, Blue - 5' GATCC terminus, Red- RNA pol III terminator sequence on antisense strand and Pink- its complimentary sense strand RNA pol III terminator sequence.

A

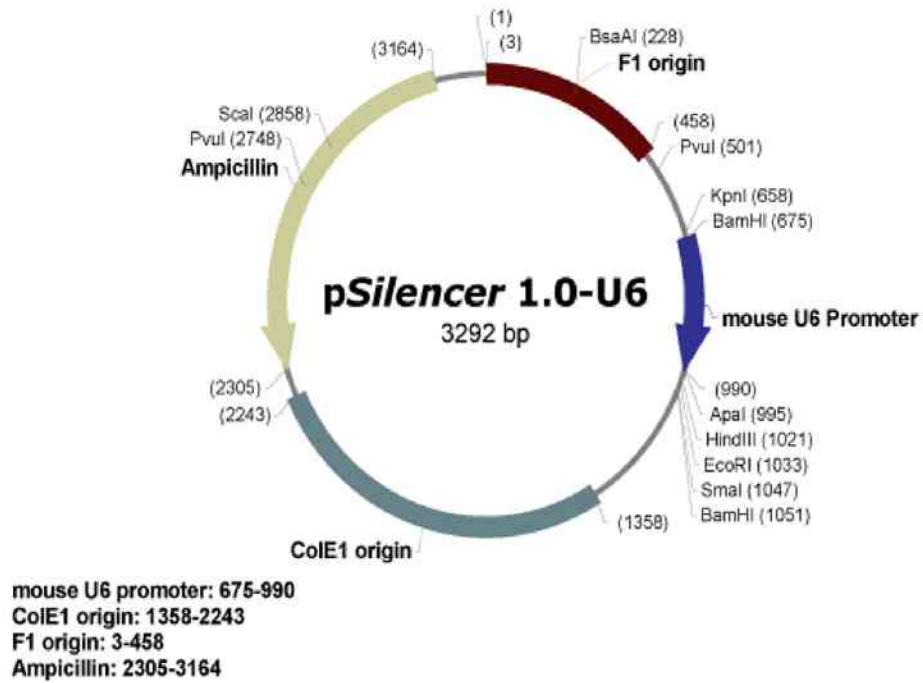
shRNA	cDNA	Target Sequence	GC Content
Sig1	313	AGGGAAGAAAGTGA ACTCT	38.1%
Sig2	348	TTGAATTTGATGAAAGTGC	28.6%
Sig3	1942	GATGGTGACAAAGACATCT	38.1%
Sig4	2923	AGCTAATGATAACCTGAAA	28.6%
Sig5	3212	CGTTCAGCTACTATTGTTA	33.3%
Sig6	3880	CAAATTCAAGAATCGTCTT	28.6%

B

Sig1 Sense	5'-GATCC AGGGAAGAAAGTGA ACTCT TTCAAGAGA AGAGTTCAC TTTCTCCCTTT TTTGGAAA-3'
Sig1 Antisense	5'-AGCTTTTCCAAAA AAAGGGAAGAAAGTGA ACTCT TCTCTTGAA AGAGTTCAC TTTCTCCCTG-3'
Sig2 Sense	5'-GATCC GTTGAATTTGATGAAAGTGC TTCAAGAGA GCACTTTCATCAAATTCAA TT TTTGGAAA-3'
Sig2 Antisense	5'-AGCTTTTCCAAAA AATTGAATTTGATGAAAGTGC TCTCTTGAA GCACTTTCATCAAATTCAAACG-3'
Sig3 Sense	5'-GATCC GATGGTGACAAAGACATCT TTCAAGAGA AGATGTCTTTGTCCACCATCT TTTGGAAA-3'
Sig3 Antisense	5'-AGCTTTTCCAAAA AAGATGGTGACAAAGACATCT TCTCTTGAA AGATGTCTTTGTCCACCATCG-3'
Sig4 Sense	5'-GATCC AGCTAATGATAACCTGAAA TTCAAGAGA TTTTCAGGTTATCATTAGCTTT TTTGGAAA-3'
Sig4 Antisense	5'-AGCTTTTCCAAAA AAGCTAATGATAACCTGAAA TCTCTTGAA TTTTCAGGTTATCATTAGCTG-3'
Sig5 Sense	5'-GATCC GCGTTCAGCTACTATTGTTA TTCAAGAGA TAACAATAGTAGCTGAACGTT TTTGGAAA-3'
Sig5 Antisense	5'-AGCTTTTCCAAAA AACGTTCAGCTACTATTGTTA TCTCTTGAA TAACAATAGTAGCTGAACGCG-3'
Sig6 Sense	5'-GATCC GCAAATTCAAGAATCGTCTT TTCAAGAGA AAGACGATTCTTGAATTTGTT TTTGGAAA-3'
Sig6 Antisense	5'-AGCTTTTCCAAAA AACAAATTCAAGAATCGTCTT TCTCTTGAA AAGACGATTCTTGAATTTGCG-3'
Con Sense	5'-GATCC GGTATGTACAGGAACGCA TTCAAGAGA TCGTTCCTGTACATAACCTTT TTTGGAAA-3'
Con Antisense	5'-AGCTTTTCCAAAA AAGGTATGTACAGGAACGCA TCTCTTGAA TCGTTCCTGTACATAACCG-3'

Figure 3.2 (A) The pSilencer 1.0-U6 plasmid used to drive shRNAi molecules against PTP γ . Reproduced from Ambion. (B) Example of hairpin oligonucleotides and orientation for the pSilencer 1.0-U6 plasmid. Reproduced from Ambion. (C) PTP γ cDNA target sequences after M Hurley.

A



B

	Sense	Loop	Antisense	
	5'-N(19)	TTCAAGAGA	N(19)	TTTTTT-3' (53 bases)
	3'-CCGG N(19)	AAGTTCTCT	N(19)	AAAAAATTAA-5' (61 bases)
	Apa I			Eco R I

C

Si1	132	GTTCTGTGCAGATACGGAG	47.6%
Si2	1075	CAGGACAGCGTTGCTTGTA	47.6%
Si3	2102	CCTCTCCCAAAGGACAACA	47.6%
Si4	502	GAGGTTCCCCGTTGAGATG	52.4%
Si5	1359	TTGTGAAAACAGGAGTGCC	42.9%
Si6	3537	CCCAACATCCGCTGCCACA	57.1%

3.2.2 The optimum parameters.

The hairpin-encoding complimentary DNA oligonucleotides were designed according to the guidelines from Ambion, ensuring the loop sequences and orientation were in the correct alignment. Amongst these parameters were a low GC content and an avoidance of long AAAA repeats within targets. The sequences would ultimately span targets including regions encoding the intra-cellular and extra-cellular domains of the receptor. These would all be expected to result in degradation of the mRNA transcript.

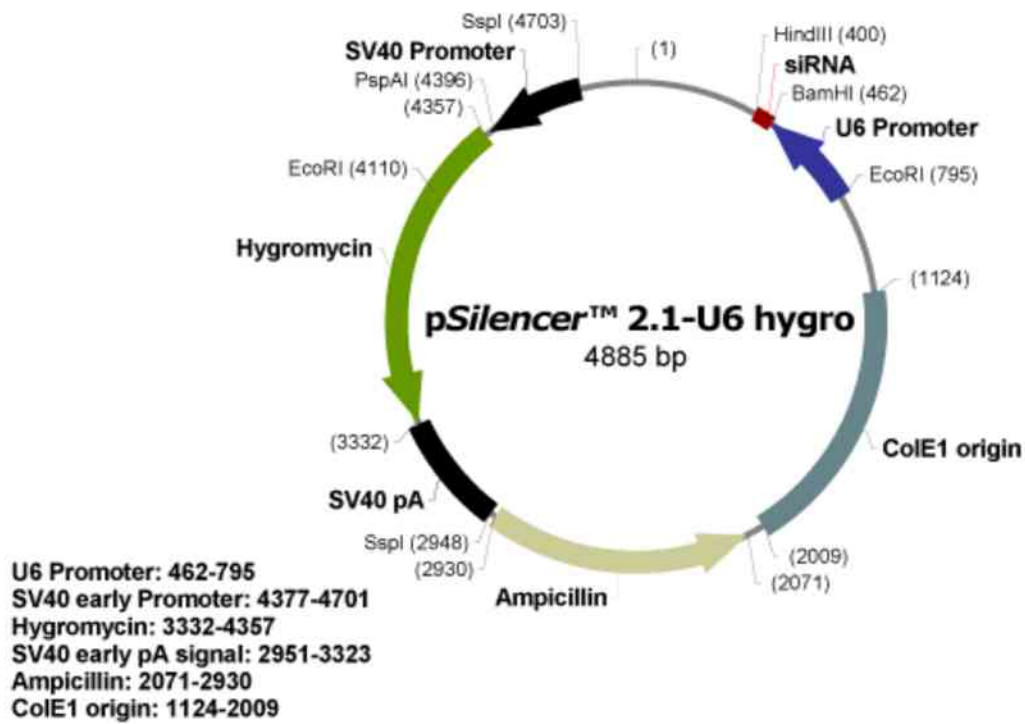
3.2.3 Building the PTP σ silencing vectors.

The six complimentary sequences against PTP σ were annealed and ligated into the pSilencer-2.1 plasmid (Ambion) (Figure 3.3A & 3.3B). A negative control pSilencer-2.1 U6 Hygro plasmid containing an RNA sequence of no homology to any specific gene was supplied by Ambion. The sequence had been checked against the emerging chick genome database, with no homologies found.

This negative control vector controls for the non-specific effects of a hairpin in our system. Numerous studies have indicated this requirement to provide another level of evidence against off-target effects and non-specific activation of the RNAi machinery and specificity of target gene silencing (Ohkawa et al, 2000; Sui et al, 2002; Brummelkemp et al 2002; El-Bashir et al, 2001).

Figure 3.3 (A) The pSilencer 2.0-U6 hygro plasmid used to drive shRNAi expression against PTP σ . Reproduced from Ambion. (B) Schematic representation of an example target sequence, annealed hairpin DNA insert and the resulting hairpin siRNA structure and orientation. Star denotes a GC overhang. Reproduced from Ambion.

A



B

Example Target Sequence (AA plus 19 nt)

5' AA GTCAGGCTATCGCGTATCG 3'

Annealed Hairpin siRNA Template Insert (order these 2 oligonucleotides)

<i>Bam</i> HI	Sense Strand	Loop	Antisense Strand	RNA pol III Terminator	<i>Hind</i> III
5'-GATCC	GTCAGGCTATCGCGTATCG	TTCAAGAGA	CGATACGCGATAGCCTGAC	TTTTTTGGAAA-3'	
	3'-G CAGTCCGATAGCGCATAGC	AAGTTCTCT	GCTATGCGCTATCGGACTG	AAAAAACCTTTTCGA-5'	

*G
C

Hairpin siRNA Structure

sense sequence
 5'-GUCAGGCUAUCGCGU AUCG UUC A
 3'-UU CAGUCCGAUAGCGCAUAGC A G A G
 antisense sequence

3.3 In vitro assays.

The silencing vectors used to knock down the RPTP genes in the following experiments were all based on short-hairpin (sh) RNA molecules. To validate the shRNA expression vectors and find the most effective ones for use in ovo, the silencing vectors were tested for knock-down efficiency in a cell culture system using HEK 293T cells. In the following paragraphs, the results of the biochemical analysis of knocking down PTP σ and PTP γ using shRNAi in vitro are discussed further.

3.3.1 PTP γ

When considering levels of plasmid expression in the culture system, it is worthy to note that although the co-transfected PTP σ (Figure 3.6D) and PTP γ (Figure 3.6B) plasmids were amplifiable in HEK 293T cells, the silencing plasmids were not. A number of the vectors demonstrated an efficient and reproducible reduction of protein levels (Figure 3.4A & 3.4B), when compared against a negative control silencing plasmid co-transfected with PTP γ . The level of target gene expression was detected using an anti-PTP γ 69 antibody (M Hurley & A Stoker, unpublished data).

3.3.2 Setting the control experiments.

All the silencing cultures were co-transfected with a firefly luciferase construct in order to normalise the intensity of protein expression on western blots, against the transfection efficiency within experimental groups (Appendix I).

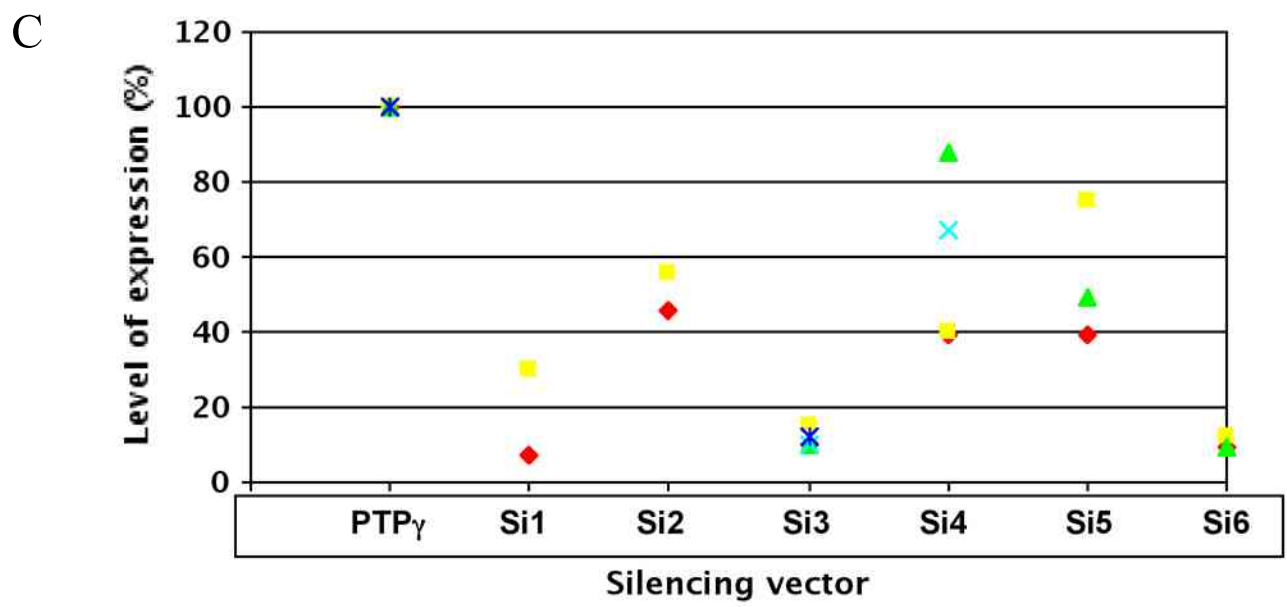
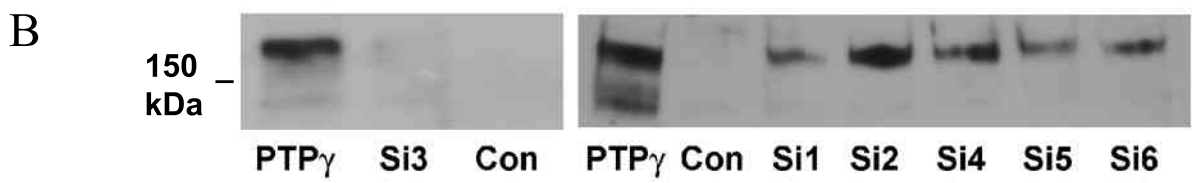
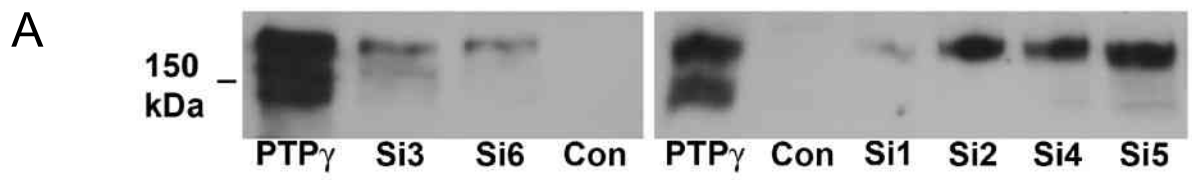
The level of expression of the luciferase reporter in culture allowed its detection through measuring the degree of luminescence from a small sample of cell lysate, using the Renilla Luciferase Assay (Promega). Once the transfection efficiency was determined, the values were then used to normalise results within each sample group against the density of the protein bands obtained, in order to give an accurate indication of the level of silencing.

Control transfections using only a proportional amount GFP (Figure 3.6A), were established as a negative control against the non-specific binding of the PTP γ 69 antibody in non PTP γ transfected cultures (Figure 3.4A & 3.4B). Equal volumes of the cell lysates per experimental group were processed further for western blotting, the results of which are described below.

3.3.3 Quantifying the level of mRNA knock down.

Amongst independent experimental sets Si1, Si3 and Si6 consistently demonstrated very effective PTP γ protein knock down by approximately 90 % (Figure 3.4C). These data then allowed us to select these three vectors and test their effects within the chick spinal cord. The results also gave an indication of silencing plasmids that did not reduce the levels of PTP γ expression so effectively, which could then be used as controls in our in vivo experiments where they would be predicted to be less effective than Si1, Si3 and Si6.

Figure 3.4 (A) Level of PTP γ protein expression on western blots detected by anti PTP γ 69 (A Stoker, Unpublished.) In order to determine this, the protein gels were scanned on a BIORAD scanner, and values of expression intensity normalised against the luciferase readings for each sample. Equal amounts of protein from the lysates were added to each lane as determined by Coomassie Brilliant Blue R-250 staining of gels run once they had been developed. These consistently showed proportional amounts of protein within the 20 μ l aliquots of lysate used (data not shown). The expression intensities on film were compared to the PTP γ control at 100%. Strong PTP γ expression is evident in the PTP γ labelled lane containing the negative control silencing vector and chick PTP γ . The sample containing no PTP γ DNA (con) shows no antibody binding as expected. A strong level of knock down of PTP γ is seen from Si1, Si3 and Si6 when compared to the PTP γ lane. The level of knock down achieved from Si2, Si4 and Si5 is not as pronounced. (B) The previous set of experiments were repeated with similar results with Si2 remaining the least efficient PTP γ silencing vector. (C) Table of quantified PTP γ knock-down by the silencing vector, normalised against the luciferase assay results and taking the expression of the PTP γ control lane as 100%. (Each vector was tested the following number of times: n=4; Si1 n=2; Si2 n=2; Si3 n=4; Si4 n=4; Si5 n=3; Si6 n=3) (Each colour marker, Green, Blue, Red, Yellow indicates an experimental set analysed per western blot for instance amongst the yellow sample set, expression intensities for PTP γ , Si1, Si2, Si3, Si4, Si5 and Si6 were recorded) (Raw data in appendix).



3.3.4 PTP σ

The RNAi vectors constructed against PTP σ were tested in cell culture for their efficiency in reducing the level of PTP σ protein in HEK 293T cells. PTP σ was detected using an anti-PTP σ antibody (Stoker et al, 1995). The results show that amongst independent experimental sets, when compared to the expression of PTP σ (Figure 3.7D), that were treated with the negative control RNAi hairpin, Sig1, Sig5 and Sig6, proved particularly effective at reducing the expression of its target protein (Figure 3.5A & 3.5B). The results indicated that using Sig1, Sig5 and Sig6, could significantly knock down the level of PTP σ protein expression in the culture system.

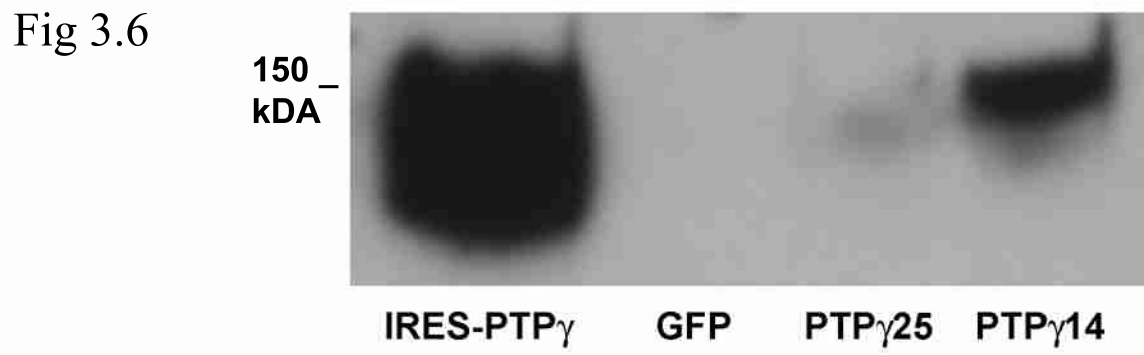
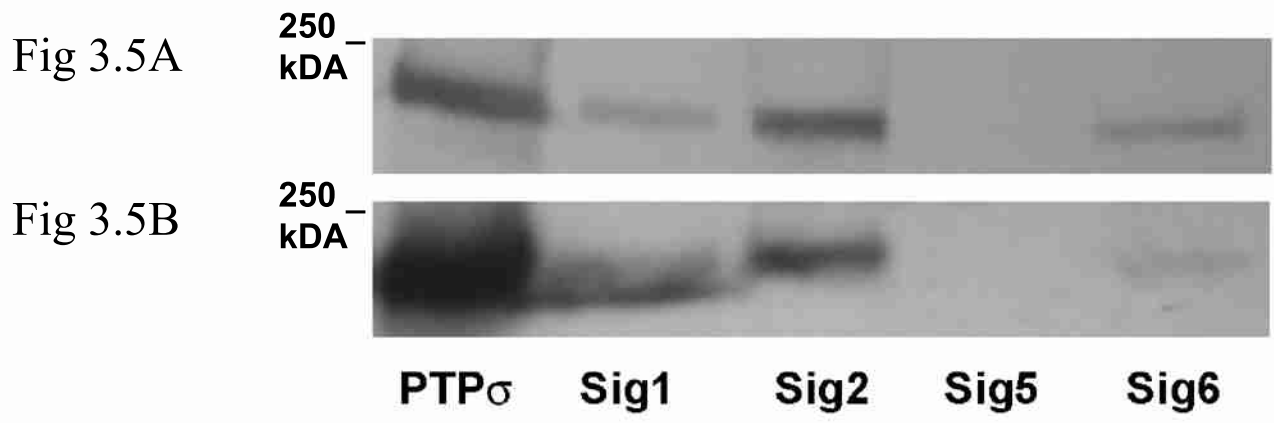
3.3.5 PTP γ over-expression vectors.

Once the most suitable vectors for silencing were determined, the converse experiment for PTP γ was designed. An over-expression vector for PTP γ was used to demonstrate that the PTP γ protein could be significantly over-expressed in culture. This would then serve as a useful indicator of PTP γ gain of function during development, and may prove useful for any future studies attempting to rescue the effects of silencing.

An over-expression construct was generated using chick PTP γ cDNA (previously generated by M Hurley and A Stoker) driven by a β -actin promoter in the IRES-GFP vector (Figure 3.7C). This was transfected in HEK 293T cells to test the levels of its expression along with the previous PTP γ CMV25 and PTP γ CMV14 expression plasmids generated by M Hurley.

Figure 3.5 (A) Level of PTP σ protein expression on western blots detected by anti PTP σ (Stoker et al, 1995). Equal amounts of protein from the lysates were added to each lane as determined by Coomassie Brilliant Blue R-250 staining of gels run once they had been developed. These consistently showed proportional amounts of protein within the 20 μ l aliquots of lysate used (data not shown). Strong PTP σ expression is evident in the PTP σ labelled lane containing the negative control silencing vector and chick PTP σ . A strong level of knock down of PTP σ is seen from Sig1, Sig5 and Sig6 when compared to the PTP σ lane. The level of knock down achieved from Sig2 is not as pronounced. (B) The previous set of experiments were repeated with similar results with Sig2 remaining the least efficient PTP σ silencing vector and Sig5 the most efficient (n=4 for each Sig vector).

Figure 3.6 Level of PTP γ protein expression on western blots detected by anti PTP γ 69 (A Stoker Unpublished). Equal amounts of protein from the lysates were determined by Coomassie Brilliant Blue R-250 staining of gels. These showed proportional amounts of protein within the 20 μ l aliquots of lysate used per sample set (data not shown). Strong PTP γ expression is evident in the IRES-PTP γ labelled lane containing the new IRES vector when compared to the previous PTP γ 14 CMV expression vector, and less efficient expression is observed from the PTP γ 25 expression vector (M Hurley). As expected the control GFP labelled lane containing only IRES-GFP does not show a signal when treated with anti-PTP γ 69 antibody (n=3).



The PTP γ protein was detected on a western blot using anti-PTP γ 69 antibody. This was tested alongside the original PTP γ 14 and PTP γ 25 plasmid (Figure 3.7B), to compare their relative levels of expression for the same total amount of transfected vector. A high level of gene expression of IRES-PTP γ was detected when compared to the PTP γ 14 expression vector and least efficient PTP γ 25 vector (Figure 3.6). This was most likely the result of the β -actin promoter, which was more efficient at gene expression than the previous CMV promoter, which is generally considered to be an unreliable promoter in ovo. This then allowed us to proceed with the gain-of-function studies in vivo.

3.3.6 Conclusions of in vitro assays.

The results of the cell culture experiments using shRNAi directed against PTP γ and PTP σ suggest that Si1, Si3 and Si6 are the most efficient silencing vectors for knocking down PTP γ and that Sig1, Sig5 and Sig6 provide the greatest levels of knock down directed against PTP σ . Furthermore a set of controls were established to test the integrity of the RNAi process, that all returned negative results providing confidence that the silencing effects were target specific. Furthermore an IRES over expression vector for PTP γ proved successful at lifting the levels of PTP γ protein in culture when compared to a similar quantity of a PTP γ encoding vector utilising the CMV promoter. These results together provided a good foundation upon which to test the efficacy of the silencing vectors in vivo, providing loss-of-function, and the PTP γ expression vector providing gain-of-function.

Figure 3.7 RPTP Expression vectors used in the cell culture studies (A) pCABetaIRESGFP vector expressing GFP (Gift of John Gilthorpe). (B) 3xflagGamma-CMV14 vector (Sigma, UK) expressing PTP γ (M Hurley). (C) cPTPGam-IRESGFPgrip vector over-expressing PTP γ (A Stoker). (D) p3xFLAG-CMV25-PTPs-Myc vector expressing PTP σ (A Stoker).

Chapter 4: Defining the PTP γ and neuronal expression domains.

4.1 Introduction

Neurons within the spinal cord arrange in pool-specific identities during their initial outgrowth, indicating that they must have cell surface differences which allows them to fasciculate with like axons and recognize path-finding guidance cues during axonogenesis (Tessier-Lavigne & Goodman, 1996). The LIM-Homeodomain family of transcription factors plays an important role in the development of motor neurons with pool-specific identities (Tsuchida et al, 1994). Members of this family set up various neuronal subtypes within the spinal cord and refine the initial patterns that are already established.

Cell movements within the spinal cord are subsequently critical to determining the final location of these neuronal subtypes. It is during the refinement of initial patterns and during axonogenesis that neurons acquire transcription factor specific columnar identities, that strongly relate to their fate and function. The cells located within these neuronal pools project their axons towards the limbs and axial components of the body.

In the following paragraphs, I will describe in more detail how such transcription factors interact and demonstrate expression profiles of those members of the LIM-HD family implicated in motor neuron development, and why PTP γ could, based on its expression profile, play an important role in the generation and migration of spinal neurons.

4.2 Axonogenesis

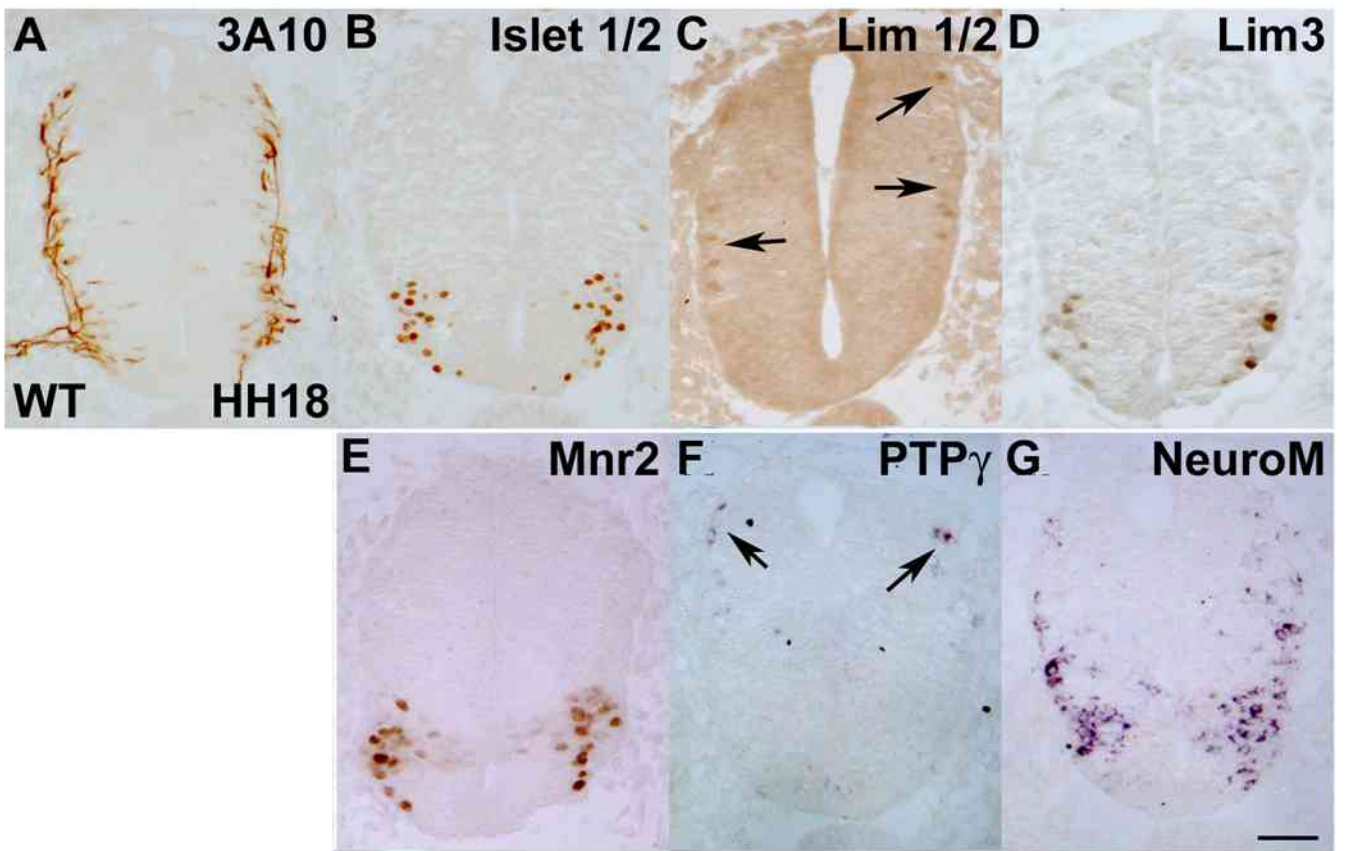
The progression of axonogenesis follows the birth of the first spinal motor and interneurons, and tracing the axonal architecture of the spinal cord highlights the route axons of differentiated neurons take towards their targets. 3A10, a neurofilament marker was used for this purpose at HH stages 18, 20, 22 and 26 in order to gauge the degree of axon outgrowth.

This is also as a general indicator of axonal circuitry, and therefore correct path finding of differentiated neuronal projections. At HH18, interneuronal populations have extended their axons dorsoventrally, and the first sensory and motor neurons have exited the ventral nerve roots (Figure 4.1, Panel A).

From HH stages 20 and 22 the decussation of commissural axons is visible along the ventral-most aspect of the spinal cord as well as extensive dorsal and ventral root innervations (Figure 4.2, Panel A and Figure 4.3, Panel A). At stage 26, the prominent dorsal root entry zones and extensive dorsal root ganglion neurons are highlighted (Figure 4.4, Panel A).

Within the spinal cord, interneurons can be observed associated with axons that run anteroposteriorly along the embryo and within the outer perimeter of the ventral horns within the white matter, ventral to the commissural plate. 3A10 thus serves as a good indicator of correct axonal trajectories from pool specific interneurons and motor neurons of the spinal cord at all dorsoventral and mediolateral levels.

Figure 4.1 Expression of neuronal markers in transverse sections of wild type HH18 chick brachial spinal cord sections. Immunocytochemical staining of (A) 3A10, (B) Islet1 & Islet2 expression in ventral motor neurons, (C) Lim 1 & Lim2, arrows denote Lim1/2 positive dorsal interneurons, (D) Lim 3 expression in ventral motor neurons, and (E) Mnr2 protein expression in motor neurons. Dig-labelled mRNA in situ hybridization to (F) PTP γ in dorsal spinal cord, arrows denote dorsal interneurons and (G) NeuroM expression predominantly in the ventral spinal cord. Scale bar is 0.5mm.



4.3 Lim-HD expression profiles of differentiating neurons.

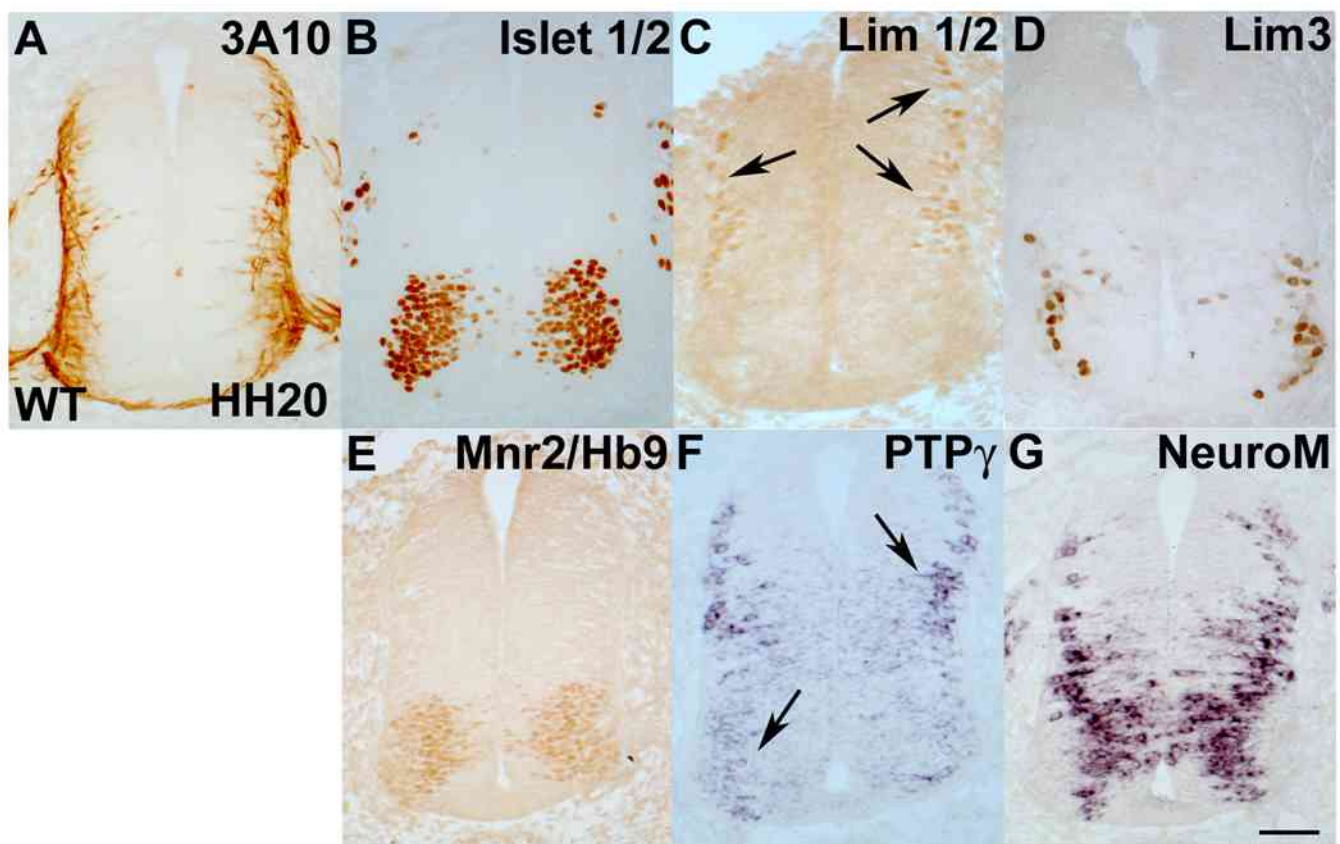
4.3.1 Islet1/2

Islet 1 is a LIM HD transcription factor expressed by all motor neurons by stage HH 18. Islet 1 determines the mediolateral position of motor neurons providing an indication of the time that has elapsed from their birth, whereby they exit the cell cycle and initiate the expression profile of differentiated neurons (Karlsson et al 1990, Ericson et al 1992). At stage 18 the expression of Islet 1 in the motor neurons fated to form part of the medial branch of the LMC is evident. At this stage, cells occupy both medial and lateral positions distal to the ventricular zone (Figure 4.1, Panel B).

At HH20, Islet-1 positive cells occupy the ventral spinal cord within groups fated to form the LMC, as newly differentiated migratory motor neurons. The early born neurons prior to HH18, predominantly populate the medial branch of the LMC and later born neurons occupy the lateral branch of the LMC (Tsuchida et al, 1994). It is worthy to note that at this stage, these LMC cells express a combination of Islet 1 and Islet 2 but not Lim1/2 (Figure 4.2, Panel B).

By stage HH22, Islet 1 is expressed in the medial zone proximal to the ventricular zone (Tsuchida et al, 1994). As the cells within the motor column start to express Islet 2, Islet 1 expression is maintained in the medial branch of the LMC. The motor columns are now anatomically clearly evident, and a few Islet 1 positive dorsal interneurons are visible (Figure 4.3, Panel B). Towards HH26, this dorsal expansion is more evident, whereby Islet 1 and Islet 2 occupy dorsal, intermediate and ventral locations along the outer edges of the spinal cord (Figure 4.4, Panel B).

Figure 4.2 Expression of neuronal markers in transverse sections of wild type HH20 chick brachial spinal cord sections. Immunocytochemical staining of (A) 3A10, (B) Islet1/2 clearly highlighting the ventral column motor neurons, (C) Lim 1/2 positive interneurons dorsally, arrows (D) Lim 3 in the outer lateral segments of the motor columns, and (E) Mnr2 protein expression in the motor pools. Dig-labelled mRNA in situ hybridization to (F) PTP γ across the dorsoventral aspect of the spinal cord, arrows denote regions of strong expression ventrally and dorsally and (G) NeuroM expressing strongly in the ventral spinal cord and weakly in dorsal mantle zone. Scale bar is 0.5mm.



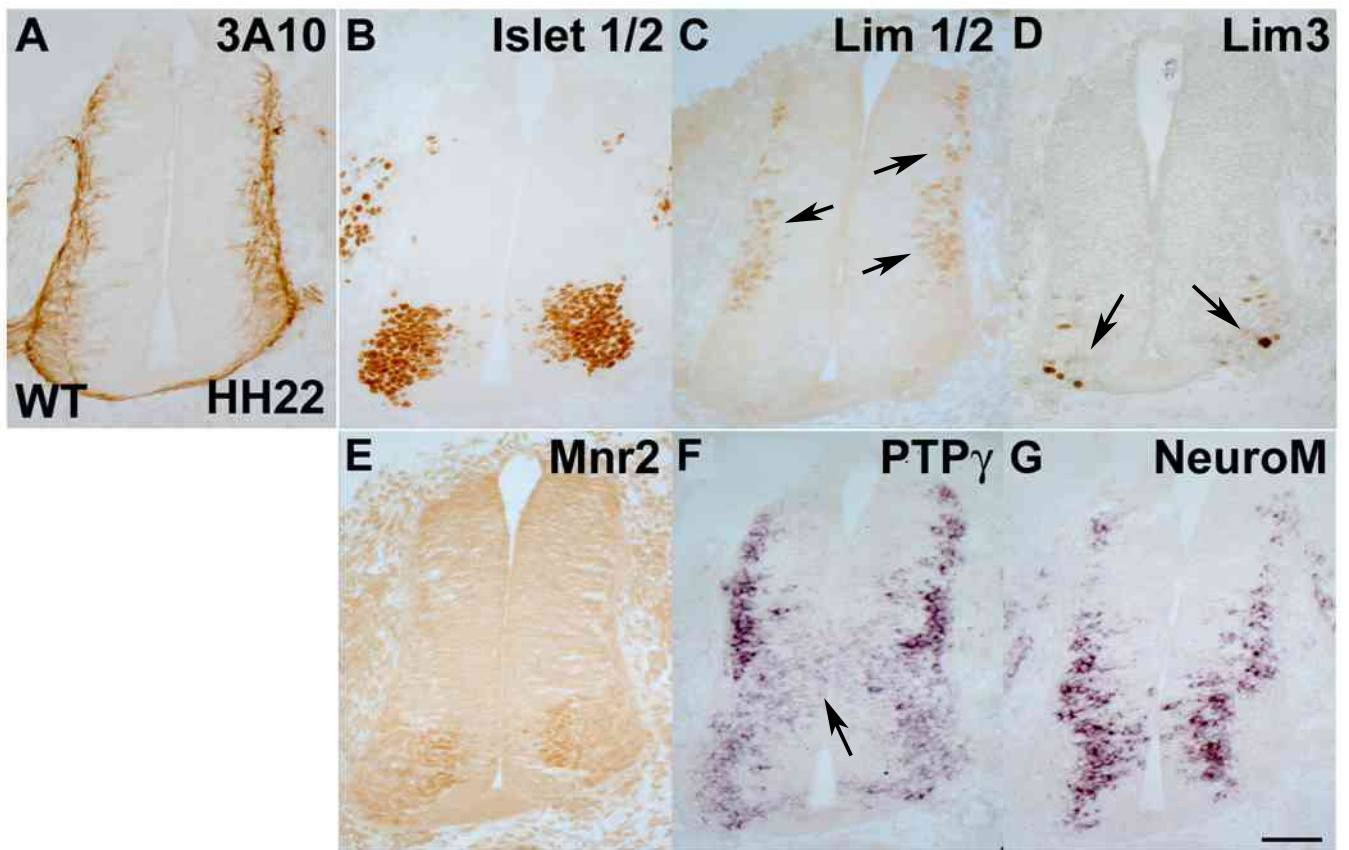
Although the antibody used highlights both Islet 1 and Islet 2 positive cells indistinguishably, it is worthy to note that as the neurons migrate laterally within the lateral motor column they begin to express Lim 1 and Islet 2. The transient period of expression of Islet 1 ends once cells occupy this more lateral columnar location. The cells within the medial branch of the LMC maintain the expression of Islet 1 as well as Islet 2 (Tsuchida et al, 1994).

4.3.2 Lim 1/2

Lim 1 and Lim 2 are two further members of the LIM HD family, expressed in motor neurons and interneurons (Tsuchida et al 1994). Their expression begins by HH18 in the first-born interneurons, where a few cells are evident in the dorsal and intermediate margins of the spinal cord (Figure 4.1, Panel C).

By HH 20 and HH 22 this expression domain progressively extends ventrally towards the intermediate zone yet persists along the lateral edges of the mantle zone, with interneurons located dorsally and medially along the dorsovental length of the spinal cord (Figure 4.2, Panel E; Figure 4.3, Panel E). These Lim 1/2 positive cells also co-express Pax 2, but not Pax 6 or Pax 7 (Burrill et al, 1997; Tsuchida et al 1994). Toward HH 26, Lim 1/2 expression continues to extend ventrally as new cells arise to occupy ventral motor neuron populations of the lateral branch of the LMC (Figure 4.4, Panel C). These Lim 1/2 LMCI positive motor neurons also express Islet 2 at this developmental stage (Tsuchida et al, 1994). It is worthy to note that in this ventral location a Lim 1/2 expression profile is initiated only once cells have cycled through Islet 1 and then Islet 2 expression.

Figure 4.3 Expression of neuronal markers in transverse sections of wild type HH22 chick brachial spinal cord sections. Immunocytochemical staining of (A) 3A10, (B) Islet1/2 clearly marking the ventral motor pools, (C) Lim 1/2 in the mantle zone, arrows, (D) Lim 3 in a few cells in the ventral motor pools, arrows and (E) Mnr2 ventrally within post mitotic neurons protein expression. Dig-labelled mRNA in situ hybridization to (F) PTP γ across the dorsoventral aspect of the spinal cord, and diffusely in the ventricular zone, arrows and (G) NeuroM in the ventral spinal cord and dorsal mantle zone. Scale bar is 0.5mm



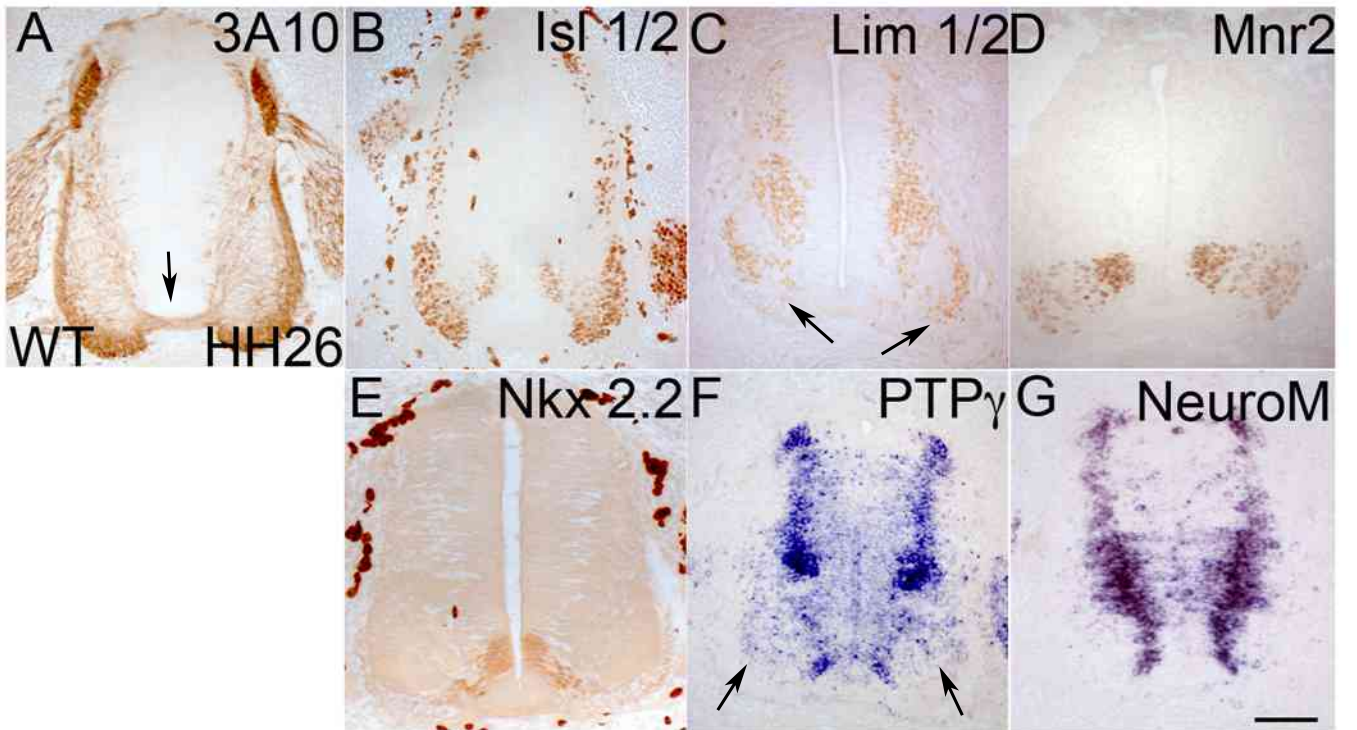
4.3.3 Lim3

A further member of the cysteine-histidine rich Lim HD family, Lim-3 is transiently expressed by ventrally located neurons in the spinal cord in the most lateral positions. This suggests that these cells are acquiring their terminally differentiated identities following cycling of Islet 1/2 states albeit at a lower frequency than the Islet 1/2 cells (Tsuchida et al 1994). Lim 3 expressing neurons arise at HH 18 from the pMN domain predominantly, where Lim3 is expressed in the cells on the extreme lateral edges of the spinal cord (Figure 4.1, Panel D). It is expressed by motor neurons laterally and reaches a peak in expression at HH 20 (Figure 4.2, Panel D). However, at this early stage and within the brachial region, Lim 3 positive motor neurons also express other markers as these cells transit through their Lim-3 differentiation state. The number of cells expressing Lim-3 decreases in number by HH 22 (Figure 4.3, Panel D), and is absent by HH 26 altogether (data not shown). Its expression returns to the MMC later during development at brachial levels (Tsuchida et al, 1994).

4.4 Mnx-HD and Nkx-HD transcription factor profiles of nascent motor neurons.

The Mnx group of HD transcription factors are expressed by post mitotic motor neurons, their functions are evolutionary conserved and well documented. Two members of this family, Mnr2 and Hb9 have been implicated in the generation of motor neurons (Tanabe et al, 1998; Arber et al, 1999).

Figure 4.4 Expression of neuronal markers in transverse sections of wild type HH26 chick brachial spinal cord sections. Immunocytochemical staining of (A) 3A10, arrow shows ventral commissure (B) Islet1/2 clearly marking the ventrally located lateral motor pools, (C) Lim 1/2 in the ventral motor pools, medially and dorsally in distinct segments, arrow shows lateral aspect of LMC (D) Mnr2 protein expression ventrally within the lateral and medial motor columns, (E) Nkx2.2 in a thin stripe just above the floor plate. Dig-labelled mRNA in situ hybridization to (F) PTP γ in the dorsoventral aspect of the spinal cord, and diffusely in the ventricular zone and motor columns shown by the arrows, with stronger expression in the dorsal most region of the spinal cord and a strong level of expression medially and (G) NeuroM in the ventral spinal cord, just outside of the ventricular zone and dorsal mantle zone. Scale bar is 0.5mm



All motor neurons express Mnr2 initially, and all Mnr2 expressing cells arise from the pMN domain. In motor neuron progenitors, Mnr2 has functions in the initial specification of motor neuron identity and a later wave of expression regulates motor neuron columnar identities, where it plays a role as a transcriptional repressor directing motor neuron identity whilst inhibiting interneuronal identities (William et al 2003).

At HH18, Mnr2 expression is restricted to the ventral spinal cord as its cells arise from the pMN domain (Figure 4.1, Panel E.) The antibody used in these experiments detects both Mnr2 and Hb9, however we shall refer to the results in the context of Mnr2. From HH20 to HH22, the expression of Mnr2 lies sandwiched between the outer pial edge and inner ventricular layer in the ventral spinal cord at the level of the pMN domain. Interestingly the expression of Lim3 lies outside of the Mnr2 expression domain (Figure 4.2, Panel E; Figure 4.3, Panel E). This expression persists through to HH 26, where at axial levels it is also expressed in the Column of Ternii neurons (Figure 4.4, Panel D).

Mnr2 has been shown to act as a transcriptional repressor during the acquisition of motor neuron fate (William et al, 2003). Hb9 expression is activated and maintained by an enhancer region within the Hb9 regulatory region that contains 'cis' elements for 'positive' factors such as Islet1, Ngn2, NeuroM & NeuroD. Hb9 therefore maintains its own expression via a positive feedback loop. Synchronization of neurogenesis and motor neuron specification then occurs via β HLH and homeodomain transcription factors (Lee & Pfaff, 2003).

Nkx2.2 is expressed by the ventral most progenitor domain dorsolateral to the floor plate, giving rise to the ventral most V3 neurons where it is required for their generation and maintenance (Briscoe et al 1999). These cells repress their potential for somatic motor neuron generation, whilst they are required for the development of oligodendrocytes that arise from progenitors within the Nkx2.2 expressing domain. Nkx2.2 thus marks the ventral most cells, and is a useful marker as its expression coincides, in part with that of PTP γ at HH26 (Figure 4.4, Panel E).

4.5 The expression of PTP γ in the chick spinal cord

PTP γ is a member of the RPTP type V group. These molecules have extra-cellular domains similar to cell adhesion molecules implicating their role in axonogenesis and path-finding. Differences in these extracellular domains suggest they have specific ligands and studies have led to the emergence of both heterophilic and homophilic ligands for these molecules. The onset of PTP γ expression begins at around HH18, where this gene displays an interesting pattern of expression within the spinal cord, whose onset of expression overlaps with neurogenesis.

Chick PTP γ was first described in 1996 (Xiong et al, 1996). The protein exists as both transmembrane and secreted isoforms (Shintani et al, 1997). PTP γ expression in the chick is predominantly seen in the nervous system from gastrulation onwards with low level expression in the primitive streak and the first formed somites.

Within the neural tube PTP γ is first clearly detected at HH18, where it is initially expressed in the dorsal interneuron domain (Gustafson & Mason, 2000) (Figure 4.5,

Panel B). Traces of PTP γ expression can however be observed as early as HH16 within the spinal cord (Figure 4.5, Panel A). By HH20, PTP γ is expressed in the medio-ventricular region. This expression domain expands ventrally from HH20 to HH23 within the intermediate zone (stronger expression) and is seen in the cells just above the floor plate and within the lateral motor columns (weaker expression) (Figure 4.5, Panels C, D, E & F respectively). PTP γ is also expressed at lower levels in the ventricular progenitors of motor neurons and interneurons by HH20, at least three quarters of the way up the spinal cord (Figure 4.6, Panel C). Dbx1 and Dbx 2 homeobox genes define the fate of V0 and V1 interneurons from progenitors, whereby Dbx1 loss of function mutants fail to produce V0 interneurons (Pierani et al, 2001). Dbx1/2 however was not used as a marker as the onset of its expression within interneuronal populations was much earlier than that of PTP γ expression. Furthermore we had initially set about identifying motor neuron markers of the motor pools and dorsal interneurons (the populations of cells that were used in our cell counts). This however would prove useful in future studies in determining the effect of PTP γ expression on V0 and V1 interneurons and their development.

Looking closely at the expression of PTP γ within individual cells (presumed to be bipolar in morphology or daughters of bipolar cells retaining trailing processes) at high magnification, intense regions of staining are seen within the cytoplasm of the cell outside of the nucleus yet intimately associated with it. As the PTP γ mRNA is being detected within these sections, this is presumed to be the often enlarged Rough Endoplasmic Reticulum amassed with ribosomes and thus a hub for the translational machinery of cells with bipolar morphology (Moreels et al, 2005).

Figure 4.5 Expression of PTP γ and NeuroM in transverse sections of wild type chick brachial spinal cord sections from HH16-23. DIG-labelled mRNA in situ hybridization to (A) PTP γ which is expression absent at HH16 at brachial level, shown by the arrows(B) PTP γ at HH18 and the onset of expression in dorsal regions, arrows, (C) PTP γ at HH20 showing an expression domain diffusely across the dorsoventral aspect and ventricular zone, arrows, (D) PTP γ at HH21 with expression persisting dorsoventrally however with higher expression levels in the dorsal mantle layer and as a stripe just above the floor plate, (E) PTP γ expression persists through HH22 with weaker expression in the ventricular zone, arrows and (F) PTP γ expression intensifies by HH23 in similar regions to HH21 and HH22. Dig-labelled mRNA in situ hybridization to NeuroM (G) HH16 where expression is predominantly in the ventral region, (H) HH18 where this expression extends dorsally, (I) HH20 expression is evident in two lateral stripes dorsoventrally with stronger expression ventrally, (J) HH21 expression persists ventrally with some dorsal neuronal staining in a complimentary pattern to PTP γ expression, (K) HH22, (L) HH23. Scale bar is 0.5mm.

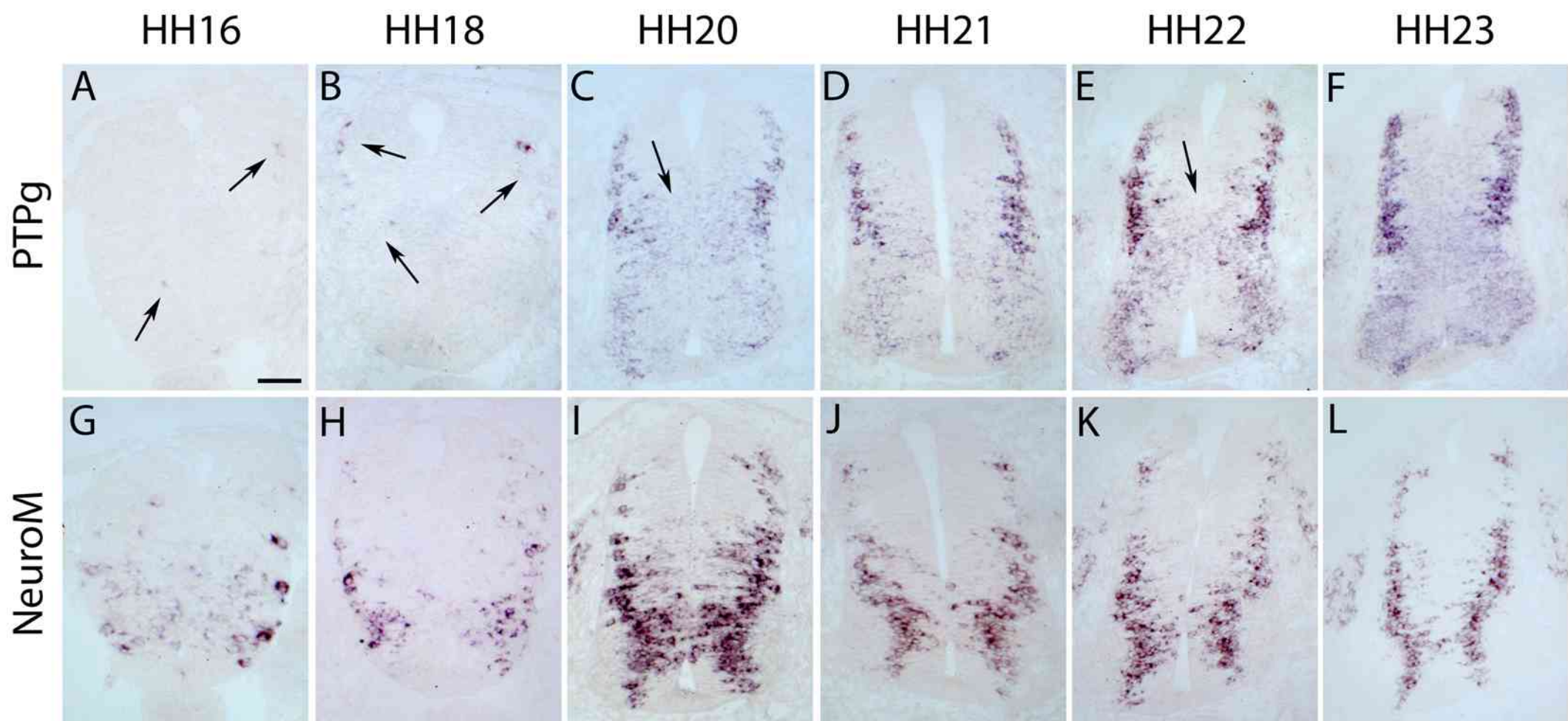
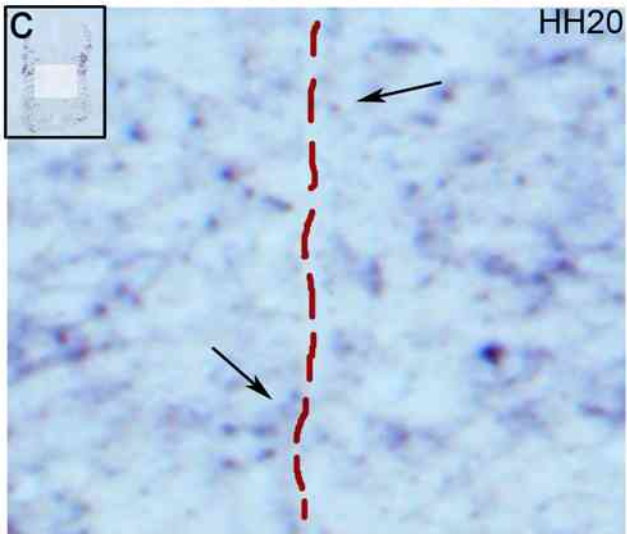
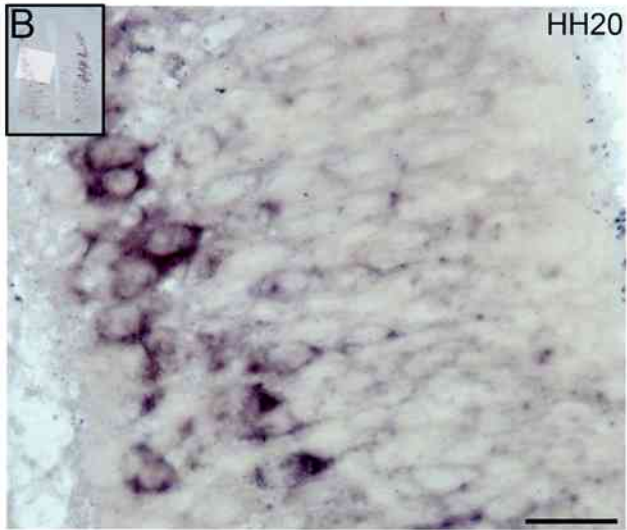
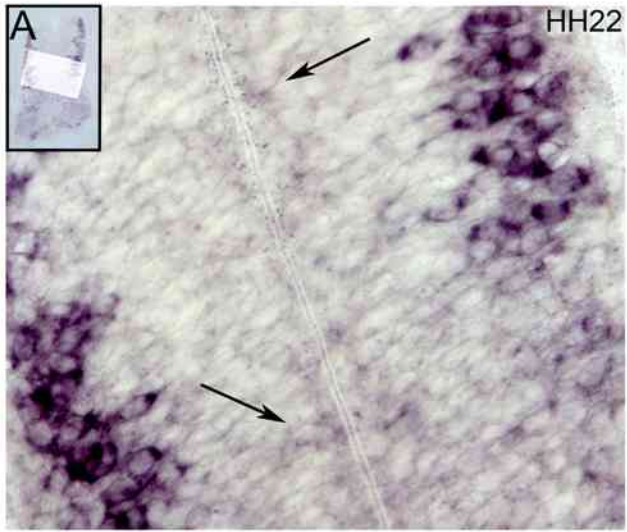


Figure 4.6 Expression of PTP γ in transverse sections of wild type chick brachial spinal cord sections from in two different embryos. DIG-labelled mRNA in situ hybridization to (A) PTP γ at HH22 showing clear mRNA expression amongst post mitotic cells and evident ventricular staining, arrows (B) PTP γ at HH20 showing c mRNA expression amongst post mitotic cells in the mantle zone (C) PTP γ expression in the ventricular progenitors and pMN domain, arrows. Scale bar is 0.5mm.



At higher magnifications, bipolar cells clearly express PTP γ mRNA at HH22 and HH20 (Figure 4.6, Panels A & B respectively – inserts show area of enlargement). Further into development and at HH26, PTP γ expression is evident along the dorsoventral aspect of the spinal cord in two lateral stripes within the intermediate zone that partially overlaps with Lim1/2 expression, and just above the floor plate in an inverted smile. A prominent area of expression is seen in the dorsolateral regions of spinal cord and a ball of strong expression is observed the equator of the spinal cord distal to the luminal surface.

Diffuse gene expression is seen elsewhere when compared to a clean background outside of the spinal cord. These observations were then analysed in context of the previously described motor neuron markers and of the neurogenic marker NeuroM .

4.6 Signalling neurogenesis.

NeuroM is a β HLLH transcription factor whose transient expression is restricted to the cells lining the ventricular zone following proliferation. Its role has been implicated in defining the transition between undifferentiated, premigratory and differentiated migratory neural precursors (Roztocil et al, 1997). NeuroM expression is located at the interface of the proliferative and non-proliferative zones of the neural tube. Its expression is initially seen in the first post-mitotic primary interneuronal cells. This expression gradually forms a bilateral stripe between the ventricular zone and the subpial zone. This pattern becomes more apparent with the highest expression in the ventral neural tube (Roztocil et al, 1997). This gene is therefore a good marker of

nascent neurons embarking on their migration and highlights a key stage in every neuron's life.

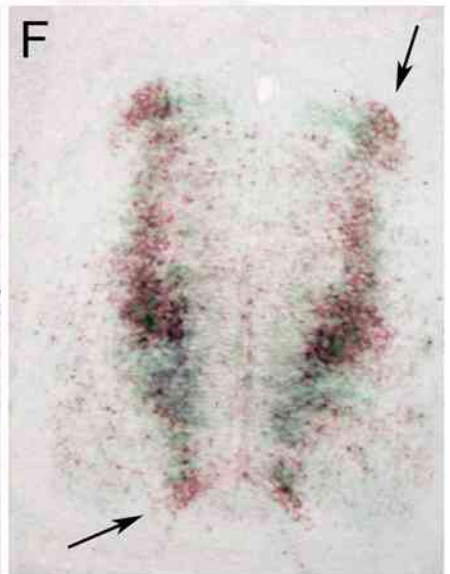
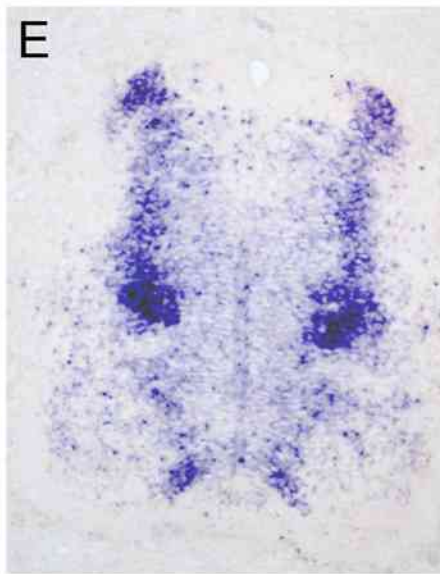
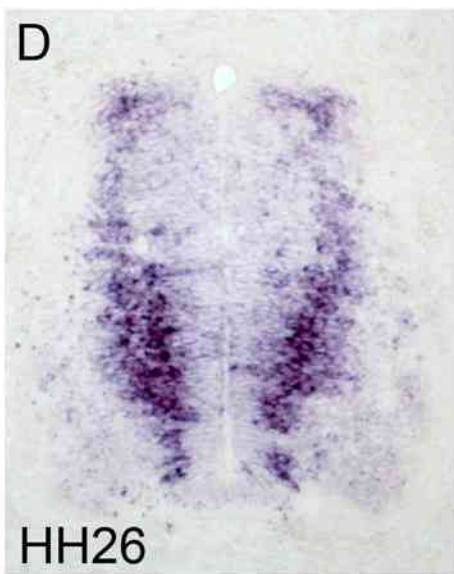
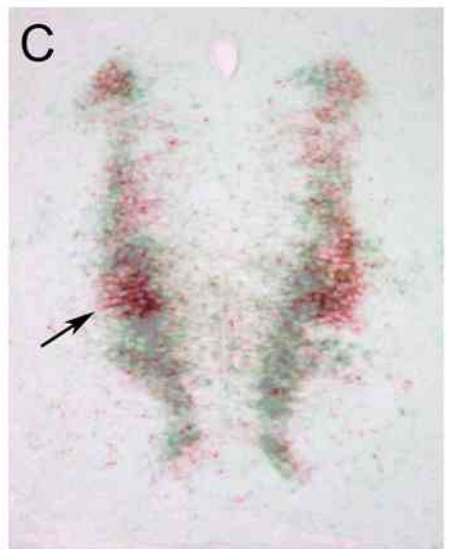
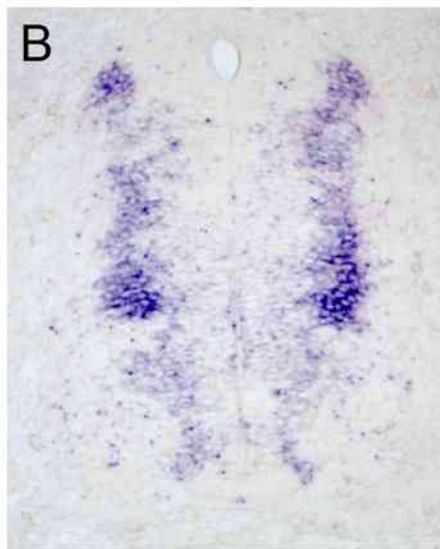
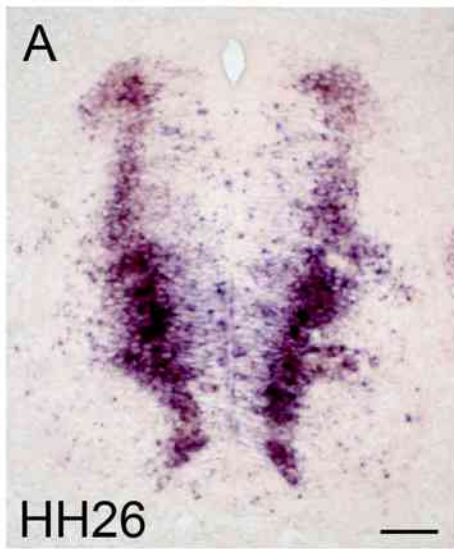
The expression of NeuroM begins at around HH16, coinciding with the generation of the first primary interneurons and motor neurons, essentially the first post mitotic cells in the spinal cord (Figure 4.5, Panel G). Towards HH 18, NeuroM is expressed along the pial surface and in the ventricular zone level to the pMN domain (Figure 4.5, Panel H).

NeuroM forms direct molecular complexes with Islet 1/2 in motor neurons and is involved in their differentiation (Lee & Pfaff, 2003). From HH 20, NeuroM appears adjacent to the ventricular zone in the intermediate zone along the entire dorsoventral aspect of the spinal cord. (Figure 4.5, Panel I).

From HH21 to HH23, NeuroM expression becomes prominent within the ventricular layer at the level of the pMN domain and a dampening of expression is evident within the dorsal spinal cord although still present (Figure 4.5, Panels J, K & L respectively). The expression of NeuroM is reduced to two prominent stripes within the ventricular zone of the ventral spinal cord from HH 26 (Figure 4.7, Panels A & D).

Moreover, a similar dorsal expression domain is seen to that of PTP γ , however when the expression of NeuroM and PTP γ were overlapped using serial sections, a complementary expression pattern was observed at HH 26 in all dorsoventral regions except for a slight overlap within the dorsal and intermediate zones of the spinal cord. This is shown amongst two individual examples (Figure 4.7, Panels C & F, arrows).

Figure 4.7 Expression of PTP γ and NeuroM in transverse sections of wild type chick brachial spinal cord sections from HH26 in two different embryos. DIG-labelled mRNA in situ hybridization to (A) NeuroM, (B) PTP γ , (C) Overlap of in situ staining on different serial sections of PTP γ (Red) and NeuroM (Green) demonstrating a complementary pattern of expression and a slight overlap medially, arrows (D) NeuroM, (E) PTP γ (F) Overlap of PTP γ in situ staining on different serial sections (Red) and NeuroM (Green) demonstrating a complementary pattern of expression and a slight overlap medially. Arrowhead shows more medial expression of NeuroM and arrow indicates NeuroM expression in absence of PTP γ expression. Scale bar is 0.5mm.



In several places, the strongest PTP γ expression is lateral to NeuroM, however weak expression of PTP γ overlaps with NeuroM elsewhere. The complimentary patterns of PTP γ and NeuroM are also evident at HH20 and HH22 (Figure 4.8, Panels E & J respectively).

4.7 PTP γ in the context of cellular differentiation.

The expression profile of PTP γ within the spinal cord during neurogenesis reveals an interesting pattern when compared with different neuronal markers at HH 20 and HH 22. The expression analysis data highlights potential interactors and non-interactors of PTP γ based purely on their corresponding regions of expression with respect to PTP γ gene expression from adjacent overlapped serial sections of the same embryo. These findings are briefly discussed here with the aim of providing directions for the study of PTP γ gene function with the spinal cord tissue.

PTP γ expression at HH20 is present but relatively faint within the ventral spinal cord around the pMN domain proximal to the ventricular lumen (Figure 4.8, Panel A). By HH22 expression of PTP γ is almost absent from this region (Figure 4.8, Panel F). This deficit in PTP γ expression seems to be filled by an early wave of the bHLH gene, Olig2 expression (Figure 4.8, Panels B & G).

Olig2 is implicated in the generation of motor neurons within the spinal cord at this early stage of development, and is expressed during neurogenesis (Takebayashi et al, 2000). This observation may suggest that Olig2 suppresses the expression of PTP γ to

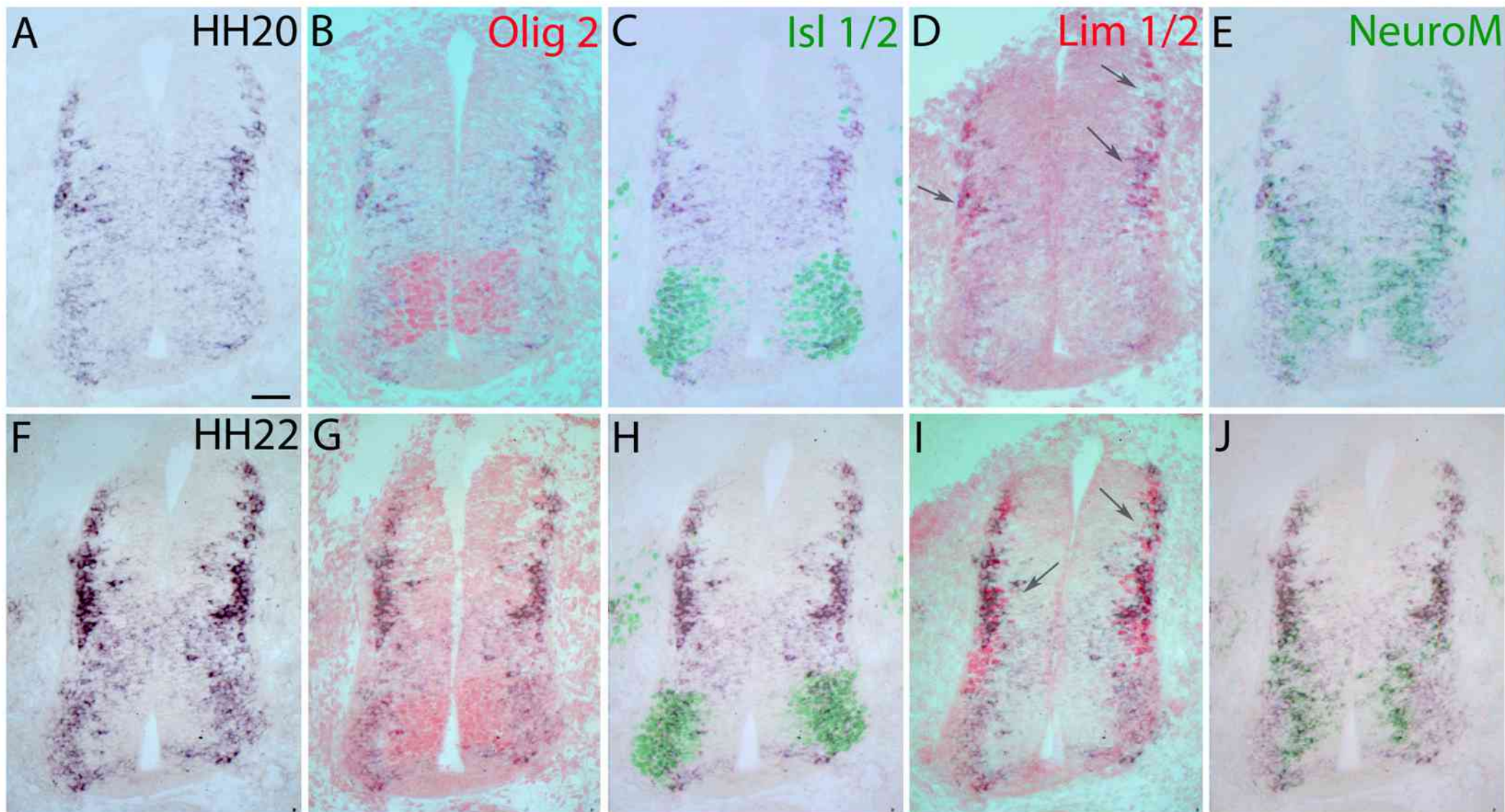
an extent within this domain, or that the two genes have for the most part divergent functions from each other, however this is purely speculation.

Analysis of *Islet1/2* expression and *PTPγ* show a ventral region of overlap within the lateral branch of the LMC at brachial levels, that is not present in the distal most cells of the LMC, whereby *PTPγ* expression is sandwiched within the *Islet1/2* positive LMC. Dorsal *Islet1/2* cell populations show regions of partial overlap with *PTPγ* when comparing serial sections of the same embryo at HH 20 and HH 22 (Figure 4.8, Panels C & H respectively). The few cells dorsally positive for *Islet1/2* may or may not be expressing *PTPγ* as in Figure 4.8 different serial sections were used to achieve overlaps.

This may suggest an interaction of *PTPγ* with either *Islet1* or *Islet2* expressing cells and their arrangement during LMC development and dorsal interneuronal specification. Once again this is a prediction based upon the expression domains of these factors.

Further analysis of the LIM HD genes *Lim1/2* and *PTPγ* from HH 20 to HH 22 within the dorsal spinal cord reveals a striking pattern of overlapping expression. Most of the dorsal *PTPγ* expression is seen within the domain of *Lim1/2* expressing differentiated neurons. A small population of the ventral most *Lim1/2* expressing cells are for the most part outside of the region of strong *PTPγ* expression both at HH 20 and HH 22 (Figure 4.8, Panels D & I respectively).

Figure 4.8 Expression of PTP γ and various neuronal markers in transverse sections of wild type chick brachial spinal cord sections at HH20 and HH22. DIG-labelled mRNA in situ hybridization to (A) PTP γ at HH20 showing an expression domain diffusely across the dorsoventral aspect, in situ hybridization to PTP γ and overlap of PTP γ in situ and immunohistochemical staining on different serial sections (B-E) at HH20 of (B) Olig 2 at HH20 within the motor neuron progenitor domain, (C) Islet 1/2 at HH20 showing complimentary expression dorsally, arrows, and slight overlap ventrally within the motor pools, (D) Lim 1/2 at HH20 showing strong overlap of expression medially ventrally and dorsally with PTP γ mRNA, arrows, and (E) NeuroM and PTP γ mRNA at HH20 showing complimentary expression patterns. DIG-labelled mRNA in situ hybridization to (F) PTP γ at HH22 showing an expression domain dorsoventrally along the mantle layer with strong expression medially, in situ hybridization to PTP γ and overlap of PTP γ in situ and immunohistochemical staining on different serial sections (G-J) at HH22 (G) Olig 2 at HH22 within the motor neuron progenitor domain, (H) Islet 1/2 at HH22 showing slight expression dorsally and stronger overlap ventrally within the motor pools with PTP γ , (I) Lim 1/2 at HH22 showing strong overlap of expression medially, dorsally, and ventrally with PTP γ mRNA, arrows, and (J) NeuroM and PTP γ mRNA at HH22 showing complimentary expression patterns with NeuroM mRNA being expressed closer to the ventricular zone ventrally. Scale bar is 0.5mm.



This observation suggests that at these stages and in fact at earlier time points, the expression of PTP γ coincides with the expression of Lim1/2 in differentiating neurons both temporally and spatially. This highlights the potential interaction of the Lim1/2 genes with PTP γ .

Together these results suggest that the markers studied can effectively be used to delineate cell populations during neuronal development within the chick spinal cord, and that the expression of PTP γ within certain neuronal cell domains suggest this may be an area where PTP γ may be functionally active amongst these post mitotic cells types. Moreover, the expression of PTP γ within the regions of Islet1/2, Lim3 and Mnr2 expression may also suggest a role for PTP γ in the positioning, development or maintenance of these cell populations.

Chapter 5: PTP γ Loss-Of-Function.

5.1 Introduction.

Biochemical studies on PTP γ reveal that Si1, Si3 and Si6 were the most effective at knocking down levels of PTP γ expression in HEK 293T cells. Experiments were then conducted in ovo to determine the effect of silencing PTP γ in the spinal cord, initially using the aforementioned silencing constructs based on their knock-down ability in cell culture. The aim of these of experiments was to determine to what extent perturbing the level of PTP γ expression would affect the generation of patterns and survival of neurons, as defined through the expression patterns of the neural markers in Chapter 4.

5.1.1 Silencing RPTP's in ovo.

During the initial stages of this study, there had been little further use of shRNAi, although it had been successfully used in many other cell and tissue systems (Bron et al, 2004; Sui et al, 2002). As my study progressed and soon afterwards, there have been several uses of RNAi and miRNA in ovo, all of which have proven that, if carefully controlled, this is a reliable technology for gene knockdown (Das et al, 2006; Harpvant & Cepko, 2006). shRNA does therefore provide a powerful tool to study the functions of RPTP's transiently and spatially in the chick neural tube, without any obvious off target effects and therefore delivering specific effects relative to the genes perturbed.

5.1.2 Taking a closer look at PTP γ .

The functions of RPTPs are still poorly understood during neural development, particularly, in the development of the spinal cord. In situ data reveal striking patterns of expression in the spinal cord suggesting that they may play a role in the development of these tissues (Chilton & Stoker, 2000).

Developmental roles for PTP γ have been previously described. In experiments where Rat PC12 cells were transfected with PTP γ , NGF-induced neurite outgrowth was inhibited as PTP γ is also expressed in peripheral tissues. This did not occur when these cells were transfected with PTP ζ , suggesting a specific inhibitory effect of this gene on neurite outgrowth (Shintani et al, 2001). Furthermore in vitro studies have also shown PTP γ to inhibit anchorage-dependent growth of breast cancer cells suggesting that this phosphatase may have an important role during proliferation and regulation of tumorigenesis (Liu et al, 2004).

In the murine brain, PTP γ is normally expressed in pyramidal neurons of cortical layers II and IV and sensory neurons, suggesting this gene may play a role in neuronal development, or maintenance. PTP γ loss of function mice showed that the gene was not necessary for normal development, however expression of this gene varies amongst model organisms and these genes may exhibit a certain level of functional redundancy over conserved cellular functions (Lamprianou et al, 2006). Further expression of PTP γ is evident in the sensory cells of the retina, ear and tongue yet the mutants appeared normal despite gene expression in such organs, suggesting functional redundancy where other phosphatases may rescue PTP γ function

(Lamprianou et al, 2006). It is also worthy to note that in the mouse PTP γ is expressed very weakly in the spinal cord, in contrast to the chick.

PTP γ expression in the chick nervous system is seen from gastrulation onwards with a low level of expression in the primitive streak and somites. In the neural tube PTP γ is first observed in the neural folds of the presumptive forebrain. During neurogenesis, this expression remains robust within the dorsal interneuron domain that gives rise to interneurons (Gustafson and Mason, 2000; Chilton & Stoker, 2000). By E5, PTP γ expression expands along the dorsoventral aspect of the spinal cord in two lateral stripes within the intermediate zone, and just above the floor plate in an inverted smile (Gustafson and Mason, 2000). At brachial levels strong expression is also detected within the lateral motor columns. The expression profile of PTP γ is described in detail in Chapter 4.5.

5.1.3 Experimental Aims.

The effect of silencing PTP γ using siRNA in the chick spinal cord was observed, and in particular the effect this would have on the generation of different neuronal populations and their migration. Furthermore, the proliferation of such cells from radial glial progenitors at the ventricular lumen were studied, focussing on two distinct stages of the cell cycle. The final aim of the experiments was to determine whether reducing levels of PTP γ would initiate a programme of apoptosis in cells whose survival was perhaps dependent upon sustained levels of PTP γ expression. If so, was there a particular spatial pattern that dying cells would follow, reflecting neuronal progenitor populations and their associated differentiated domains?

5.2 Establishing the RNAi system in ovo.

5.2.1 Electroporation efficiency.

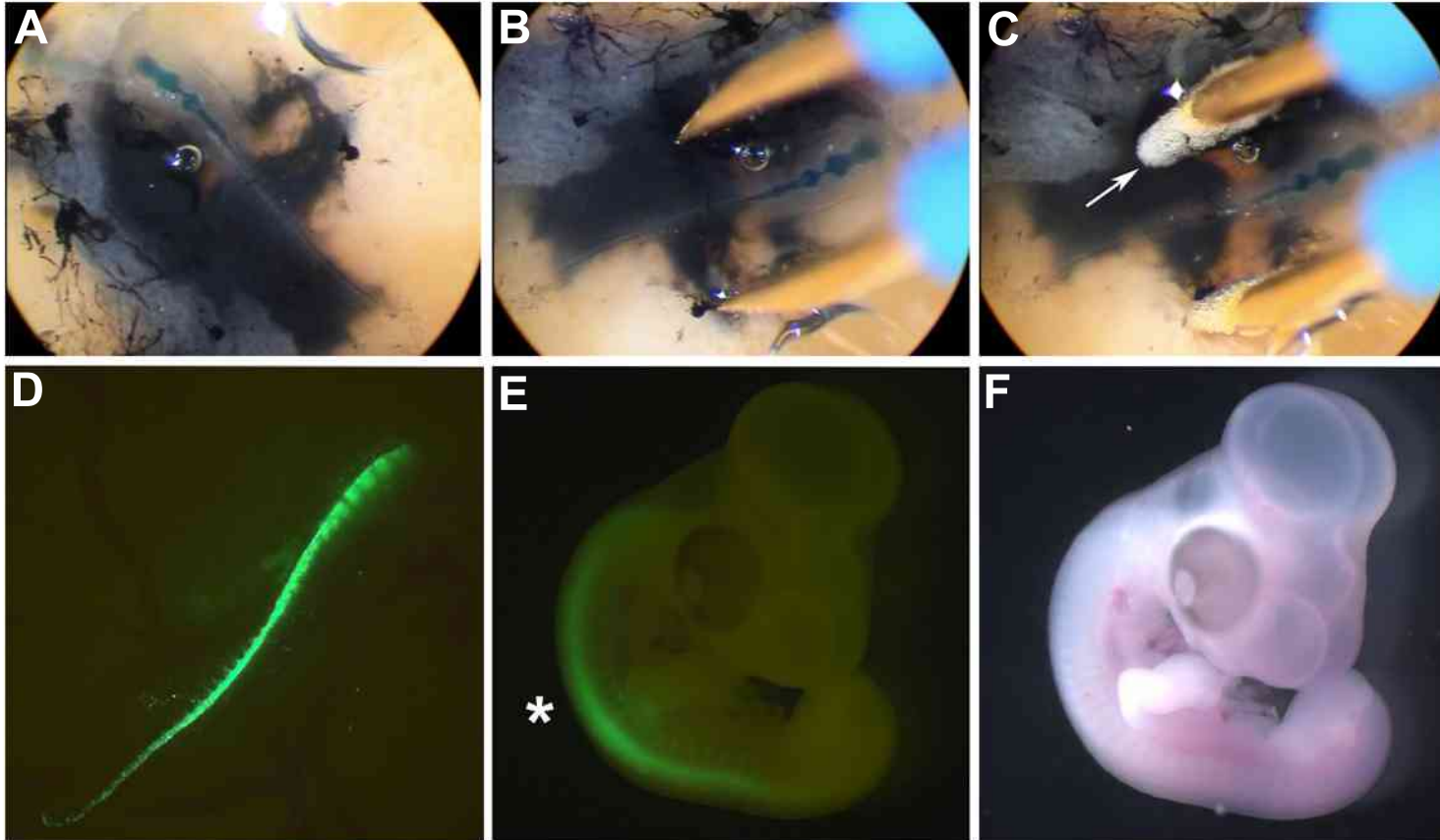
To establish RNAi as a reliable approach for analysing gene function, a set of control experiments were designed to test uptake of the plasmids injected within the targeted region. This was to determine whether the embryos developed normally following microinjection and electroporation in ovo at HH10 (Figure 5.1, Panels A-C). These embryos were co-injected with a negative control siRNA vector containing a random sequence with no homology to any gene, together with GFP, to visually determine the efficiency and spatial specificity of the electroporation.

The embryos were injected at HH10 with DNA directly into the neural tube and the presumptive brachial region was targeted for electroporation. Strong GFP expression was achieved within the brachial region and along the length of the spinal cord indicating that the vector was efficiently expressed from a few hours after electroporation (Figure 5.1, Panel D). GFP expression could be sustained until both E5 and E7, the two time points that were initially studied. Control groups appeared to be viable with no gross non-specific abnormalities (Figure 5.1, Panels E & F).

5.2.2 Embryo Viability and Controls.

Of the eggs injected and electroporated, approximately 50% survived to the time points at which they were harvested, whilst also displaying strong GFP expression, to help visualize the targeted region (Figure 5.1, Panel E–Asterix).

Figure 5.1 Microinjection & Electroporation at HH10 (A) Microinjection of the plasmid into the chick neural tube at HH10, along with fast green dye. The spinal lumen contains the injected solution along its length (B) Aligning the electrodes either side of the neural tube around the presumptive brachial region, (C) Electroporation of the vector, and uptake in the neural tube, where bubbles forming on the electrodes confirming the flow of current, arrow. Embryo viability and vector expression (D) Active GFP expression along the length of the neural tube at HH 16, (E) GFP expression persists until E5 within the brachial region denoted by the asterisk and (F) A viable electroporated embryo in bright field at E5.



Brachial sections from treated embryos were assessed on the degree of vector uptake and hence GFP expression. The embryos obtained at E5 and E7 were further analysed both histologically and immunohistochemically for any defects (Table 5.1).

To ensure that the RNAi hairpins were not inducing off-target effects, a set of control embryos treated with a random hairpin encoding pSilencer vector were analysed in more detail at E5 and E7 through expression of 3A10, Nkx2.2 and Islet1/2 (Figure 5.2). Overall, it was confirmed that introducing a scrambled silencing vector encoding hairpin with no homology to any known sequence in vivo does not trigger any off target effects.

5.3 PTP γ silencing induces a range of ectopic phenotypes at E5 & E7.

5.3.1 Classification of phenotypes.

To begin examining the role of PTP γ in spinal cord development, we went about silencing this gene in ovo, through the use of 6 different silencing constructs, of which three were shown to significantly knock down target protein levels (Figure 5.12 M; Figure 5.14 M; Figure 5.16M). Spinal cord sections were analysed for their overall histology and structure, visually through specific neuronal markers.

A total of five PTP γ silencing vectors were studied from HH18 to E7 and a total of 197 embryos were analysed at the different developmental stages and classified according to their phenotypes. Only embryos with strong electroporation spanning the entire DV axis of the neural tube were used for analysis as visualised by GFP (Table 5.1).

Figure 5.2 Expression of neuronal markers in transverse sections of E5 (A-D) & E7 (E-G) chick brachial spinal cord in control embryo shRNA treated embryos, showing normal patterns of Immunocytochemical staining to (A) 3A10, (B) Islet 1/2 , (C) Nkx2.2, (D) Lim1/2. (E) 3A10. (F) Islet1/2, (G) Nkx2.2. Scale bar is 0.5mm.

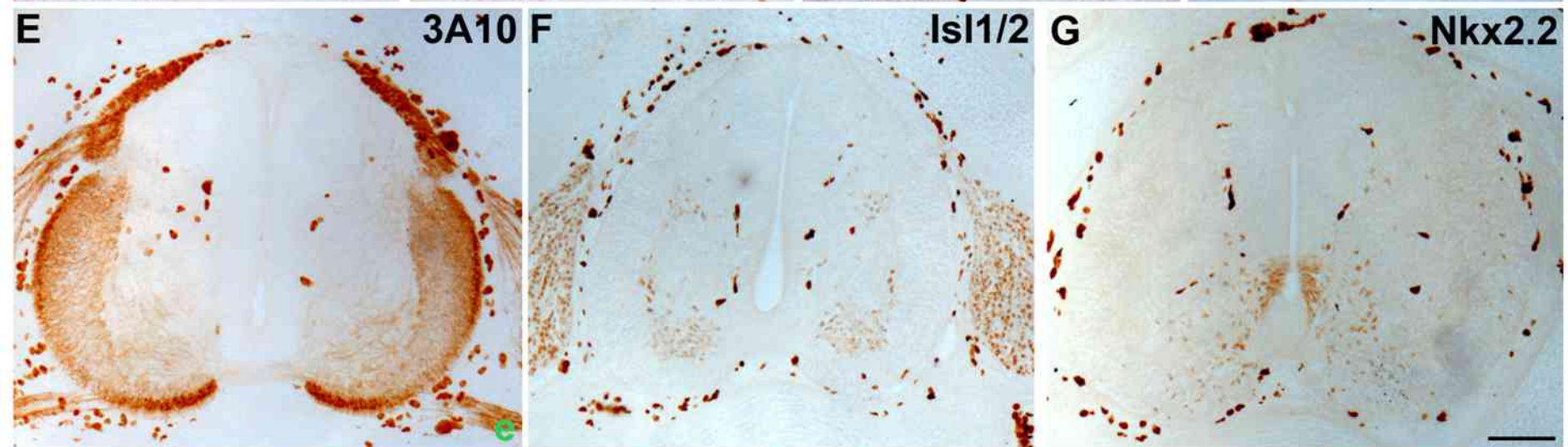
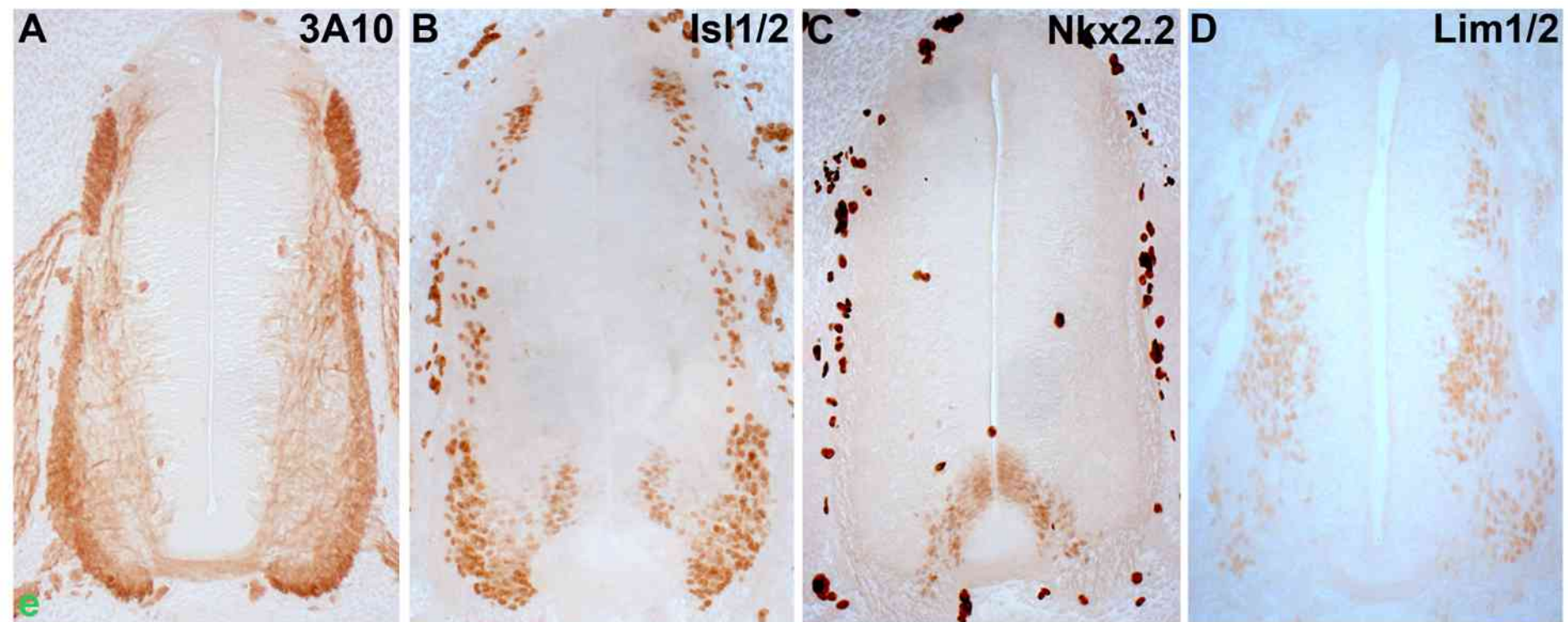


Table 5.1 Table of embryos electroporated with the negative control silencing vector, GFP and Si1-6 at E5 and E7. These are pooled according to normal, truncated and heterotopic phenotypes.

Experiment/Stage	Normal Phenotype	Truncated Phenotype	Heterotopia Phenotype	Total
<i>p-Silencer negative control</i>				
E5	21	0	0	21
<i>GFP</i>				
E5	38	0	0	38
E7	4	0	0	4
<i>Si1</i>				
E5	7	4	0	11
<i>Si3</i>				
E5	30	23	3	56
E7	3	1	2	6
<i>Si4</i>				
E5	10	0	0	10
<i>Si5</i>				
E5	12	0	0	12
<i>Si6</i>				
E5	12	8	0	20
E7	4	2	0	6

Initial analysis using the silencing vectors provided a set of phenotypes classified as either normal, mild (truncated) or invasive (heterotopic). The mild phenotype represented an obvious truncation in the ventral area of the spinal cord while the severe invasive heterotopia phenotype presented with an ectopic displacement of neuronal cells into the ventricular lumen of the spinal cord (Figure 5.3).

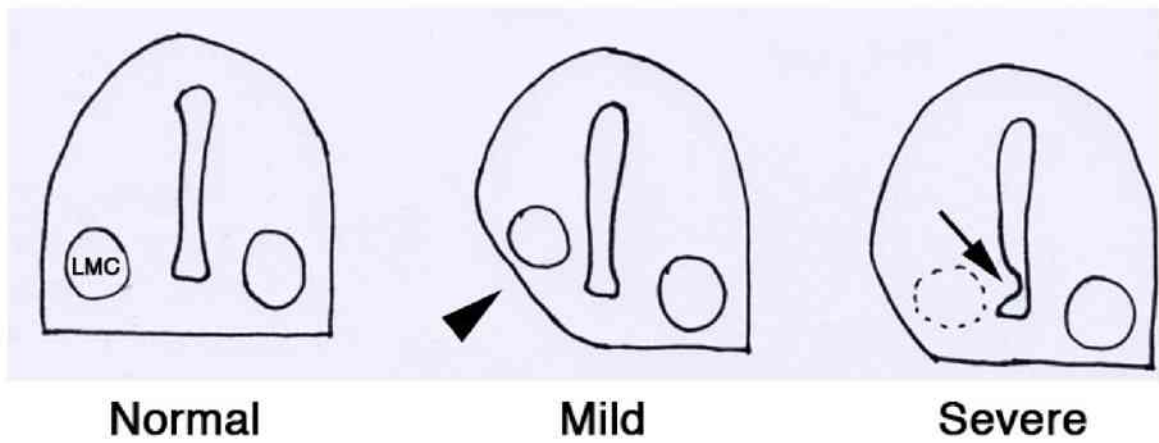
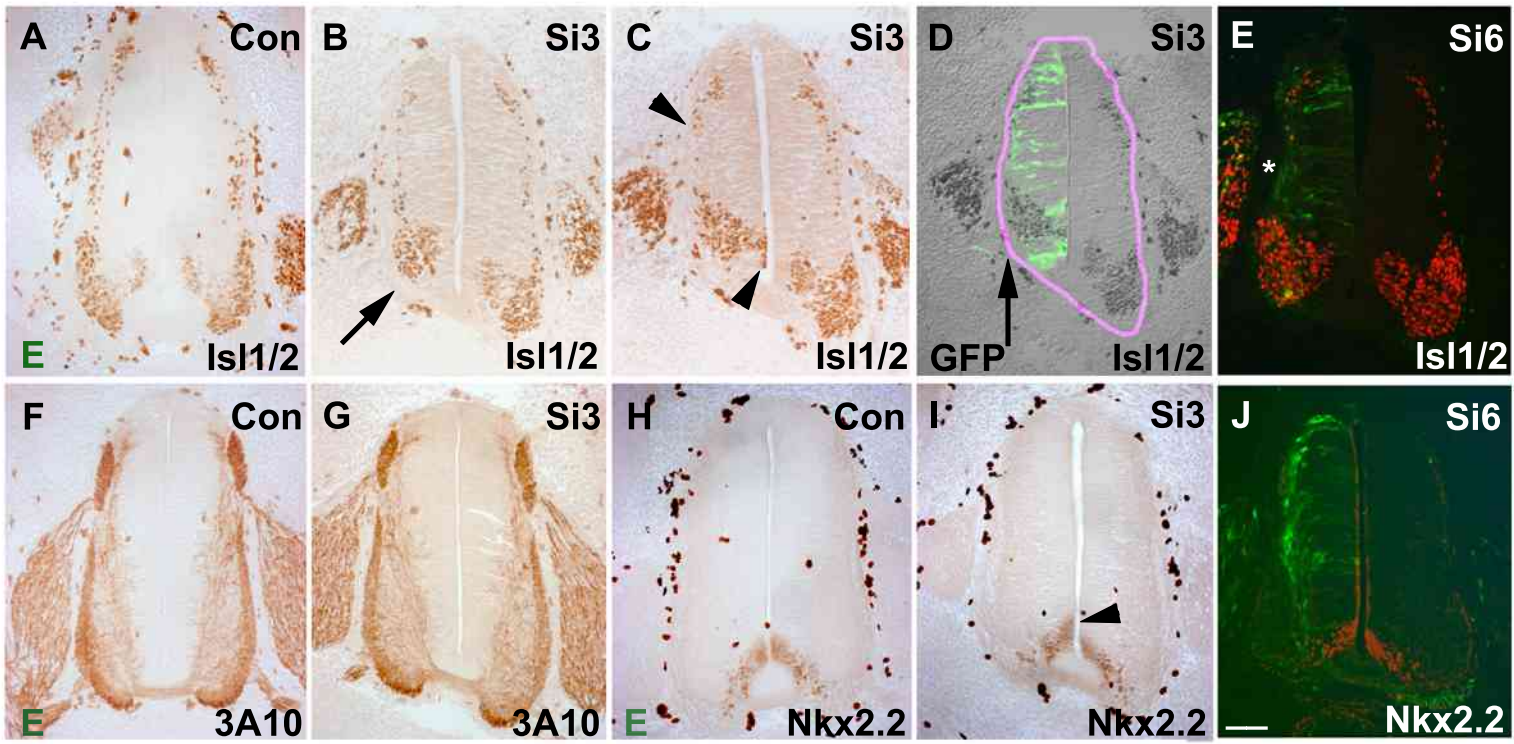
5.3.2 Silencing PTP γ and resulting gross phenotypes in ovo.

By E5, Si3 injected embryos showed a mild phenotype in nearly half the samples, with a slight shift of the spinal cord territory dorsally as shown by the neurofilament marker 3A10, along with the expression domains of Islet1/2 and Nkx2.2 (Figure 5.4 – Panels G, B & I respectively). A similar observation was made with Si6 at E5 as shown by Islet1/2 and Nkx2.2 immunoreactivity (Figure 5.4, Panels E & J). A more severe phenotype was demonstrated by Islet1/2 that included a mild disruption in the dorsal groups of Islet1/2 cells, a more profound shift dorsally of the spinal cord territory, a ventral truncation and an ectopic ventricular localisation of neurons, whose cells were also Islet1/2 positive (Figure 5.4, Panels C & D).

At both E7 and E5, histological staining highlighted a disruption in the ependymal cell layer amongst ectopic embryos (Figure 5.5, Panels B & G respectively). The ependymal layer appeared to be missing in extreme cases, replaced by neuronal precursors. At E5, the example shows that what should be a smooth inner luminal ependymal cell lining, was uneven and ruffled on the electroporated side, with an absence of the ependymal cell layer structure in the region of the ingrowth (Figure 5.5, Panel G, arrows).

Figure 5.3 Schematic representation of the two main phenotypes observed amongst PTP γ silenced embryos showing the normal, truncated and heterotopic examples.

Figure 5.4 Expression of neuronal markers in transverse sections of E5 chick brachial spinal cord. Immunocytochemical staining of (A) Islet 1/2 in a control embryo, (B) Islet 1/2 in an Si3 treated embryo. Arrow indicates region of truncation; (C) Islet 1/2 Si3 treated embryo showing a heterotopic phenotype indicated by the lower arrowhead. Upper arrowhead shows the region of mild cell loss dorsally, (D) Copy of plate C showing the boundary of the neural tube, highlighted in pink. The arrow indicates the degree of truncation on the electroporated side in green, when compared to the right hand side of the neural tube. (E) Islet 1/2 Si6 treated embryo showing cell loss on the treated side in green. (F) 3A10 in a control embryo, (G) 3A10 in a Si3 treated embryo, (H) Nkx2.2 in a control embryo, (I) Nkx2.2 in a Si3 treated embryo is expressed above the floor plate and shows a disrupted expression pattern, (J) Nkx2.2 in a Si6 treated embryo displaying a truncated phenotype and disruption of the Nkx2.2 domain. Scale bar is 0.5mm.



At E7, H&E staining showed that the normal ependymal tissue appears to be missing. The cells within the lumen instead stained positive for the neuronal marker 3A10, and there was a general distortion in the neurofilament pattern elsewhere in the ventral spinal cord. (Figure 5.5, Panel C). These cells were also positive for Islet1/2 and Nkx2.2 (Figure 5.5, Panels D & E respectively). These enlargements are shown within the spinal cord at lower magnifications in Figure 5.4, Panels D, E and F. The ectopic effect on Nkx2.2 cells maybe as a consequence of breakdown of the ependymal layer and not a direct consequence of PTP γ targeting. These results led to further studies to determine what has lead to the truncation of the spinal cord, and a number of different markers were used.

At E5, the luminal invasion of cells occurred in a region of strong eGFP expression (Figure 5.5, Panel F), and numerous cells here were shown to be Islet1/2 positive (Figure 5.5, Panel H). However, when the same embryo, a few sections higher in the region of the ingrowth was stained with Lim1/2, cells within and surrounding the luminal region failed to stain with Lim1/2 (Figure 5.5, Panel I). Interestingly, ectopic luminal Nkx2.2 positive cells were again observed (Figure 5.5, Panel J).

5.3.3 Explaining the phenotypes.

When Lim 1/2 positive neurons were studied, a more significant reduction in these cells compared to Islet 1/2 expressing cells were observed at E5, consistently seen using 3 different vectors Si1, Si3 and Si6 (Figure 5.7, Panels A – E). Two other vectors studied, Si4 and Si5 did not yield any abnormal phenotypes, supporting the knock down results in vitro (22 embryos studied – data not shown).

Figure 5.5 Expression of histological & neuronal markers in transverse sections of E7 (A-E) and E5 (F-J) chick brachial spinal cord in a Si3 treated embryo. (A) H&E staining, boxed region is magnified in panels B-J. (B) H&E, arrow indicates heterotopic phenotype and loss of ependymal layer, (C) 3A10, arrow indicates ectopic presence of neurofilament in the lumen, dashed line represents the luminal boundary; (D) Islet 1/2, arrow showing ectopic location of cells in the lumen; (E) Nkx2.2, arrow indicates presence of these cells within the lumen; (F) Strong GFP expression in ectopic region, arrow; (G) H&E staining, arrows indicate abnormal structure of the ependymal layer; (H) Islet 1/2, arrowhead indicated the ectopic location of cells within the lumen, (I) Lim 1/2 arrowhead indicated complete absence of Lim 1/2 cells within the ectopic luminal cells and within the ventral spinal cord; (J) Nkx2.2, ectopic cells stain positive within the lumen. All embryos shown were electroporated on the right hand side of the neural tube as denoted by the green E in sections A & F. Scale bar is 0.5mm.

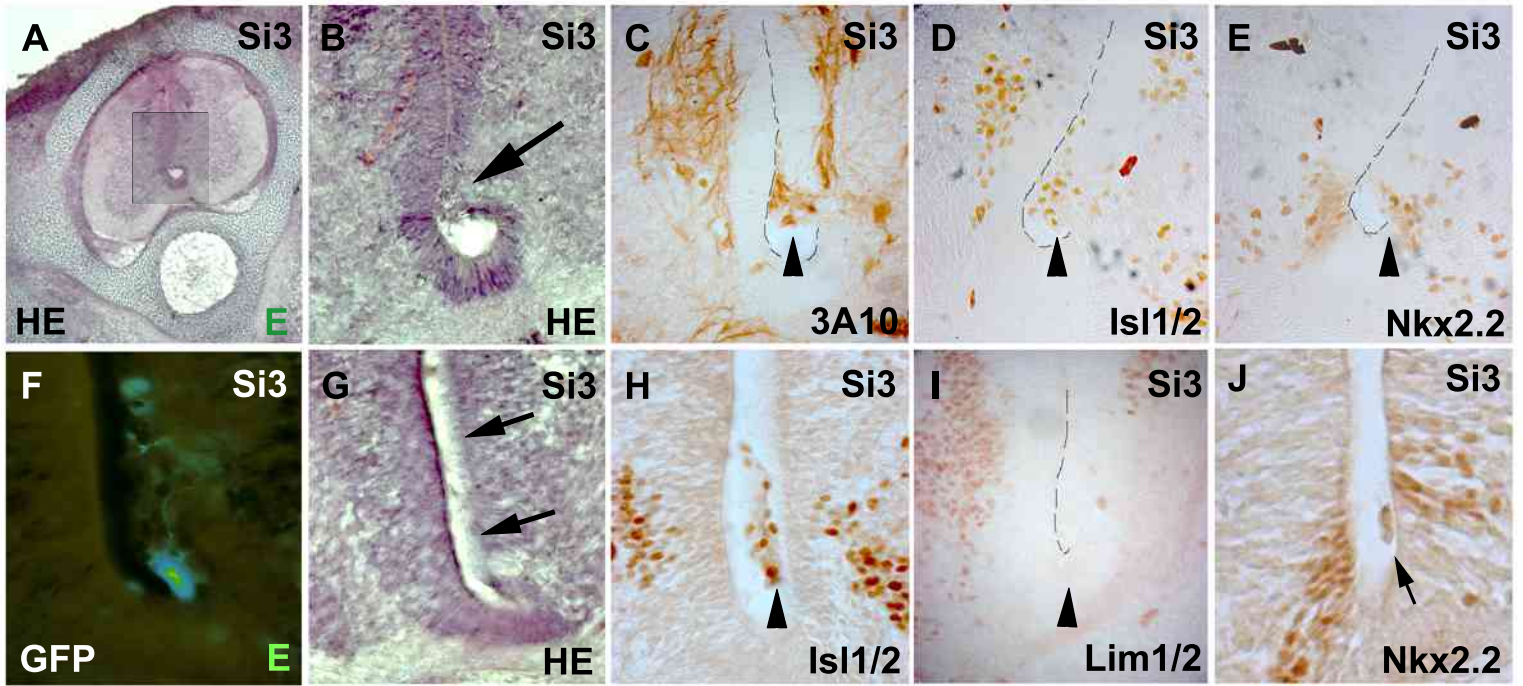


Figure 5.6 (A-C) Expression of neuronal markers in transverse sections of E7 control chick brachial spinal cord. Immunocytochemical staining of (A) 3A10 in a control embryo, (B) & (C) Isl 1/2 in a control embryo. (D-F) Whole transverse sections of E7 Si3 treated chick brachial spinal cord. Immunocytochemical staining of (D) 3A10, arrows showing abnormal neurofilament staining; (E) Islet 1/2 positive cells abnormally located in the lumen of the spinal cord as shown by the arrow; (F) Islet 1/2, further example of the heterotopic phenotype. Embryos were electroporated on the right hand side of the neural tube, denoted by the green “e” in section D. Scale bar is 1mm.

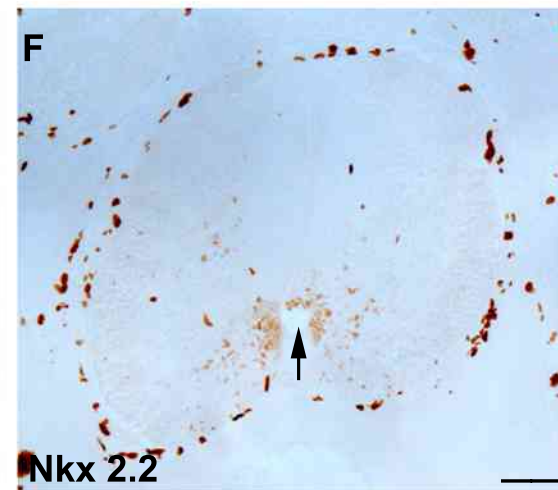
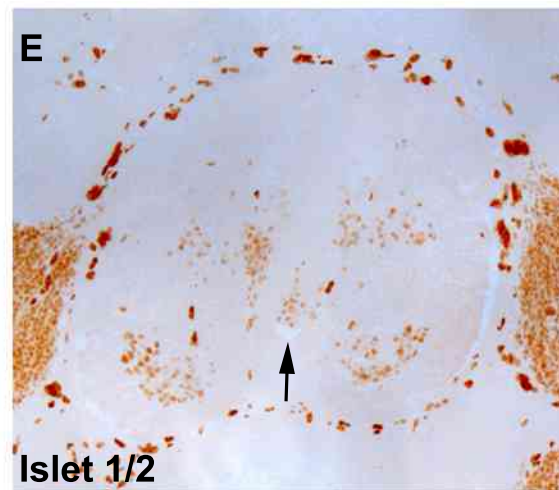
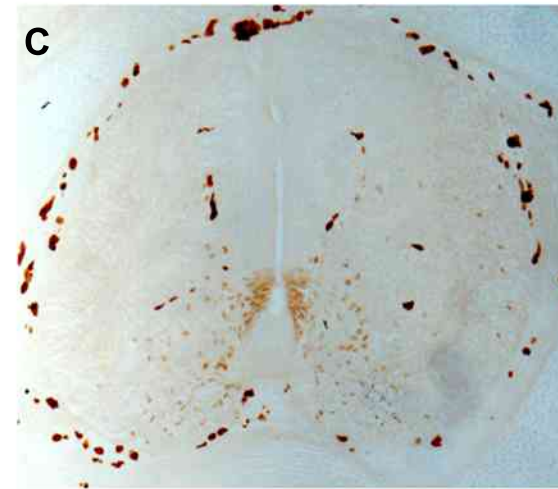
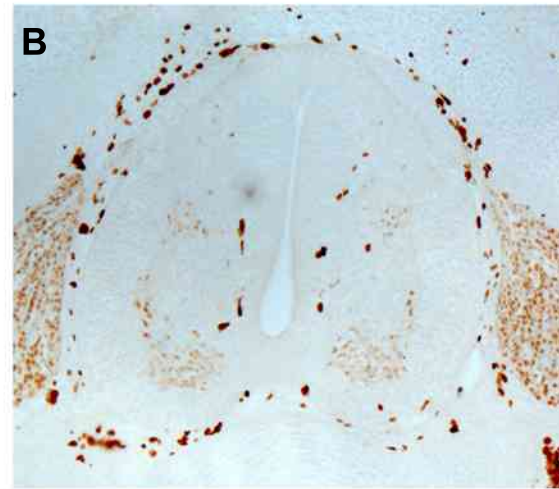
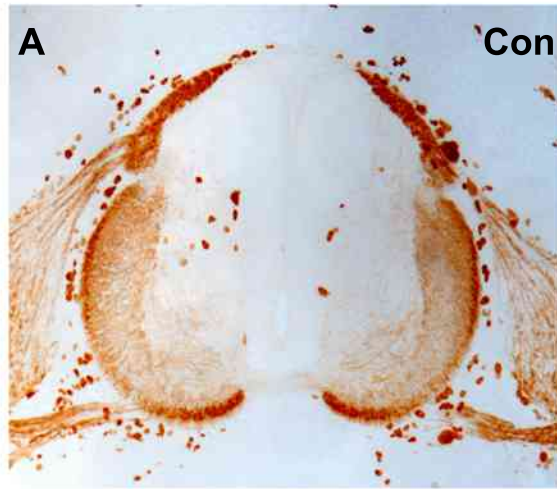
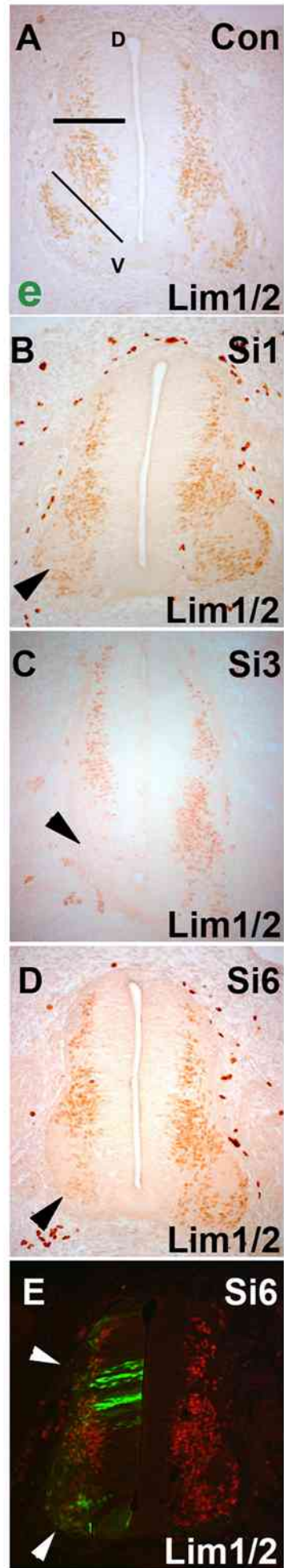


Figure 5.7 Expression of neuronal markers in transverse sections of E5 chick brachial spinal cord. Immunocytochemical staining of (A) Lim 1/2, in a control embryo showing the dorsal, intermediate and ventral regions of expression, (B) Lim 1/2, in an Si1 treated embryo. Arrowhead indicates region of truncation; (C) Lim 1/2, Si3 treated embryo, arrowhead showing a complete absence of the motor pool in the ventral region; (D) Lim 1/2, Si6 treated embryo arrowhead shows a loss of the motor pool; (E) Lim 1/2, Si6 treated embryo with a small loss of dorsal and intermediate Lim1/2 positive (top arrowhead) cells and the ventral motor pool is absent as indicated by the bottom arrowhead on the treated side, green. Scale bar is 0.5mm.



The loss and mislocation of certain cell types led to the use of different neuronal markers to indicate which other cell populations could also be affected by PTP γ silencing. Mnr2 is a motor neuron marker within the ventral neural tube and is expressed in the cells of the LMC and Column of Terni (CT). Its expression was also slightly affected in embryos treated Si1, Si3 & Si6 at E5, with a slight shift in the expression domain, in cases with Si3 & Si6 (Figure 5.8, Panels A - D).

A further more dorsal phenotype was observed at E5 in only one case, however it is perhaps worth mentioning. In one embryo treated with Si3, a reduction in the number of Lim1/2, Islet1/2 positive cells were observed, and mislocated neurons expressing those markers outside of the periphery of the spinal cord (Figure 5.9, Panels E & F respectively). 3A10 staining also reveals the ectopic projection of axons dorsally towards the ventricular lumen of the neural tube within the same embryo (Figure 5.9, Panel D – boxed region), and a potentially fused dorsal root ganglia to the spinal cord (Figure 5.9, Panel C - arrow).

Together these data suggest that loss of PTP γ causes a mislocation of ventral spinal cord cells, amongst which are Islet1/2 and Nkx2.2 positive cells in ectopic locations. These cells are presumed to be motor neurons. Of these cells, the Islet1/2 cells also seem to project their axons radially in a somewhat disorganised pattern, suggesting PTP γ silencing may also induce migrational defects amongst certain spinal cord cell types. The indication that the luminal cells were Lim1/2 negative suggested that PTP γ silencing may be causing a mislocation of selected groups of neurons for example Islet 1/2 positive, Lim 1/2 negative.

Figure 5.8 Expression of Mnr2 in transverse sections of E5 chick brachial spinal cord. Immunocytochemical staining of Mnr2 to (A) Control embryo showing the lateral motor column LMC and Column of Ternii CT, (B) Si1 treated embryo showing little effect; (C) Si3 treated embryo, showing a disruption of the normal Mnr2 expression patten, arrows, (D) Si6 treated embryo showing little effect. The embryos are electroporated on the right hand side of the neural tube as denoted by the green “E” in panel A. Scale bar is 0.5mm.

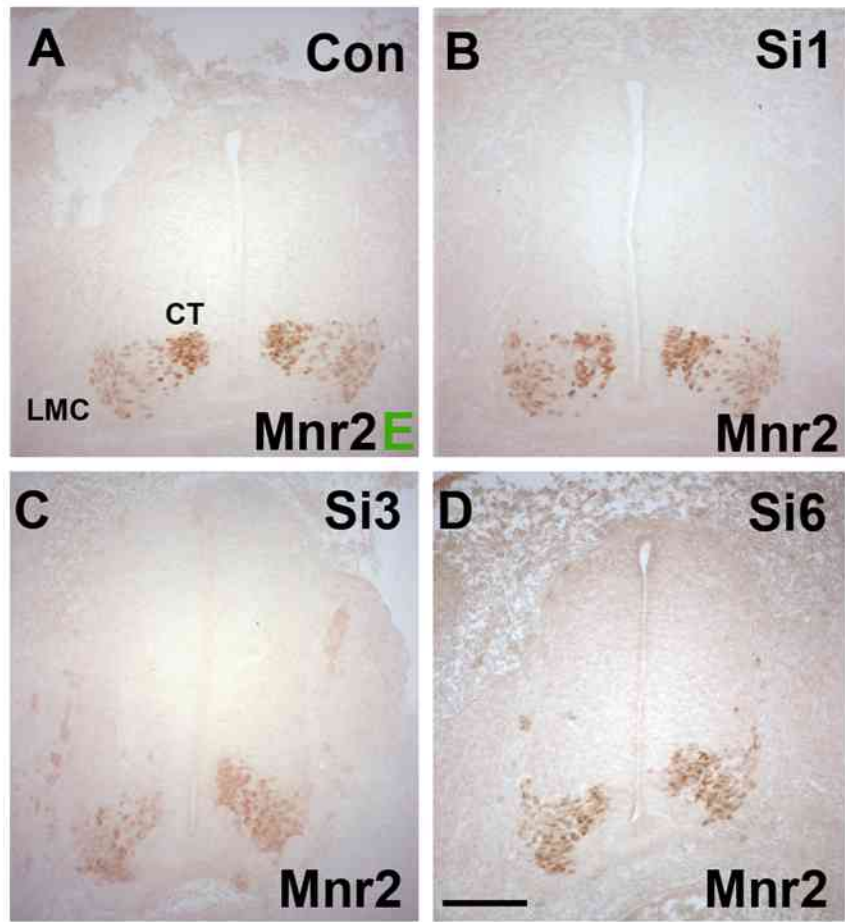
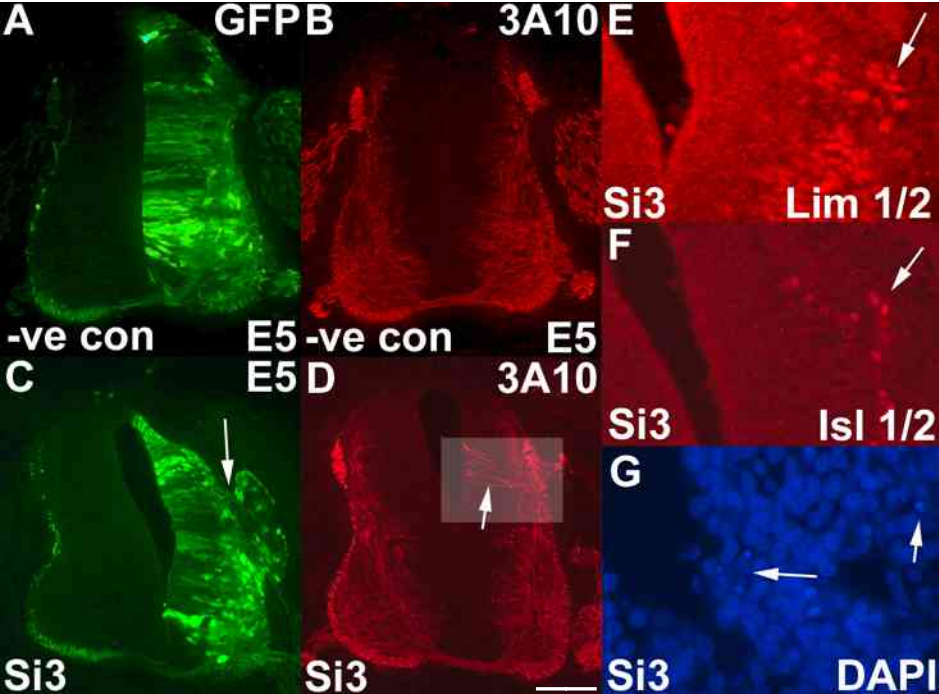


Figure 5.9 Expression of neuronal markers in transverse sections of E5 chick brachial spinal cord. (A) GFP in a control embryo, (B) 3A10 in a control embryo, (C) GFP in Si3 treated embryo, arrow indicates dorsal fusion of the DRG to the neural tube; (D) 3A10 in Si3 treated embryo arrow showing misguidance of axons in boxed region dorsally, this region studied in panels E-F in the same embryo; (E) Lim1/2 in ectopic locations outside of the neural tube, arrow; (F) Islet1/2 in similar ectopic locations, arrow; (G) DAPI staining showing location of apoptotic nuclei within that region. Scale bar is 0.5mm.



5.4 Quantitative analysis of neuronal pools.

5.4.1 Effects on Islet1/2 positive neuronal populations.

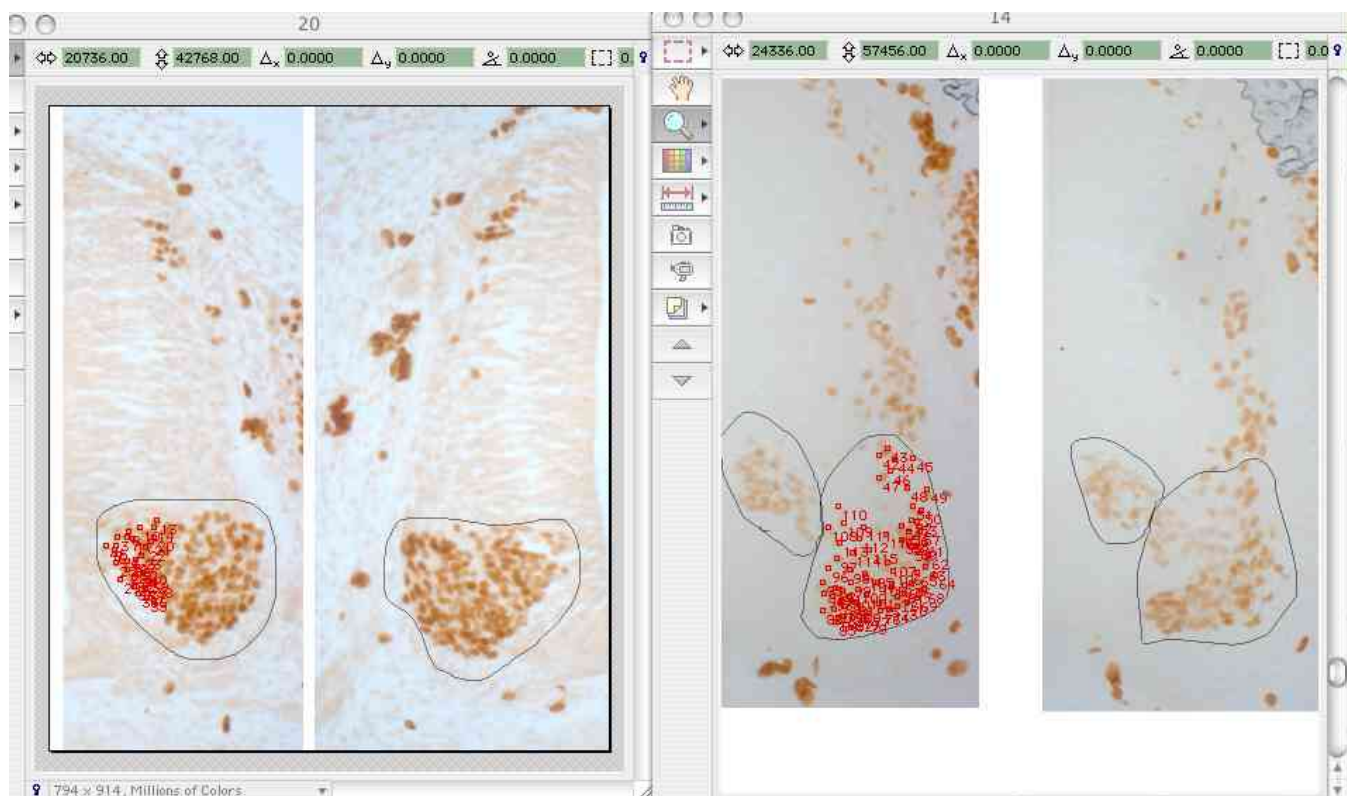
Of the embryos where a spatial disruption of the Islet1/2 cell pattern was observed, initial observations indicated a possible loss of these cells from the LMC that would explain the shift or perhaps loss of the spinal cord tissue from the ventral region. Cell counts of Islet positive cells from the ventral most Islet1/2 positive cell populations were conducted.

The counts were carried out 'blind' using the Openlab software (Figure 5.10), where the region of cells to be counted was outlined, marked and compared against its control side within the same embryo. The mean ratio between the control and electroporated sides of the neural tube of Islet1/2 cells was determined for each embryo in the silenced group and control group. Interestingly, the results showed no overall change in the ratio of these cells between the 2 sides of the neural tube compared to the control groups (Figure 5.11, Chart A). However, as stated in previous sections, there were defective patterns of Islet 1/2 cells in some embryos.

5.4.2 Effects on Lim 1/2 positive neuronal populations.

The motor horns contain many distinct types of motor neurons, some expressing Islet 1/2, others expressing factors such as Lim 1/2 (Tsuchida et al 1994). Further analysis examined whether motor neurons expressing Lim 1/2, a LMCI marker, were altered spatially or numerically amongst PTPy silenced embryos.

Figure 5.10 Screenshot of the Openlab software and method of counting cells.



At E5, the broad expression domain of Lim1/2 could be split into 3 main areas, a dorsal, intermediate and ventral cell (motor horn) grouping, as previously described. Embryos treated with Si3 showed a consistent loss of Lim1/2 cells predominantly from the ventral LMC populations. Furthermore, a significant loss of cells was observed amongst the dorsal group of Lim1/2 cells (Figure 5.11, Chart B).

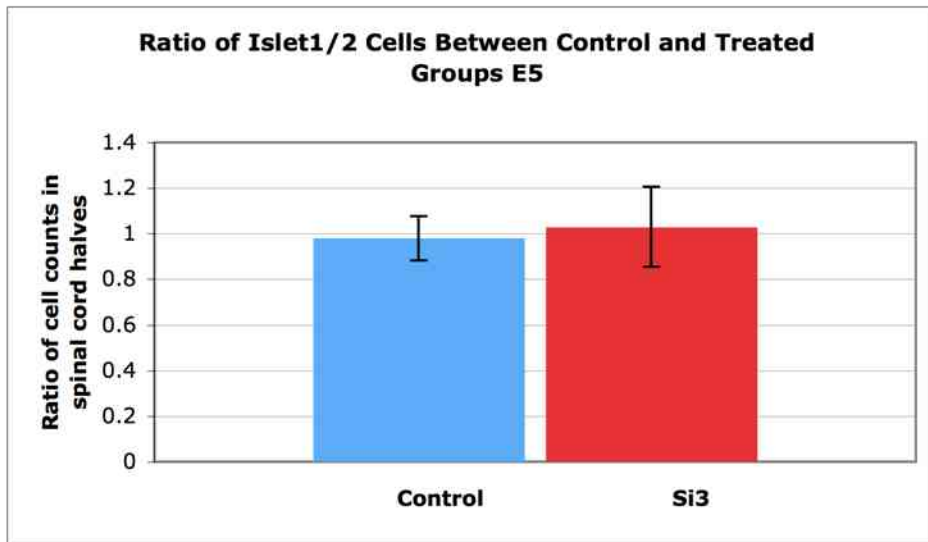
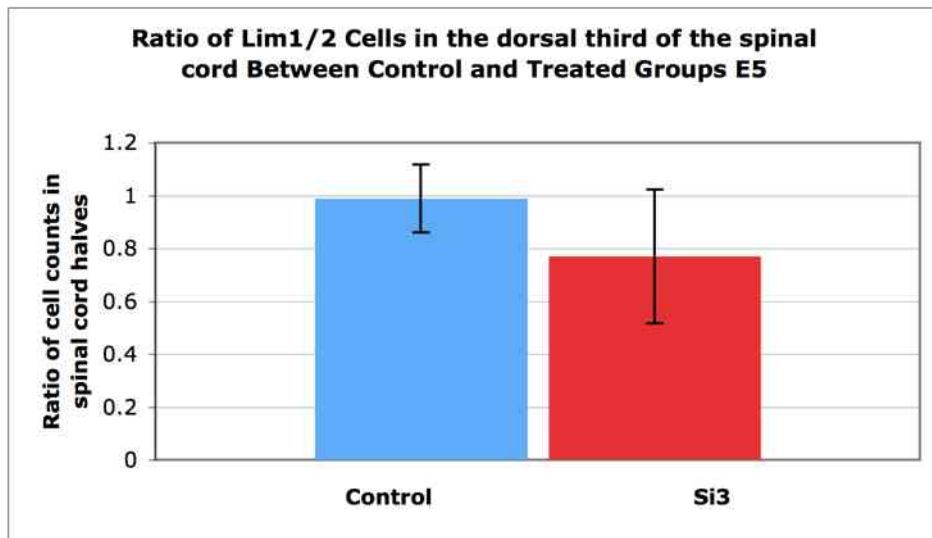
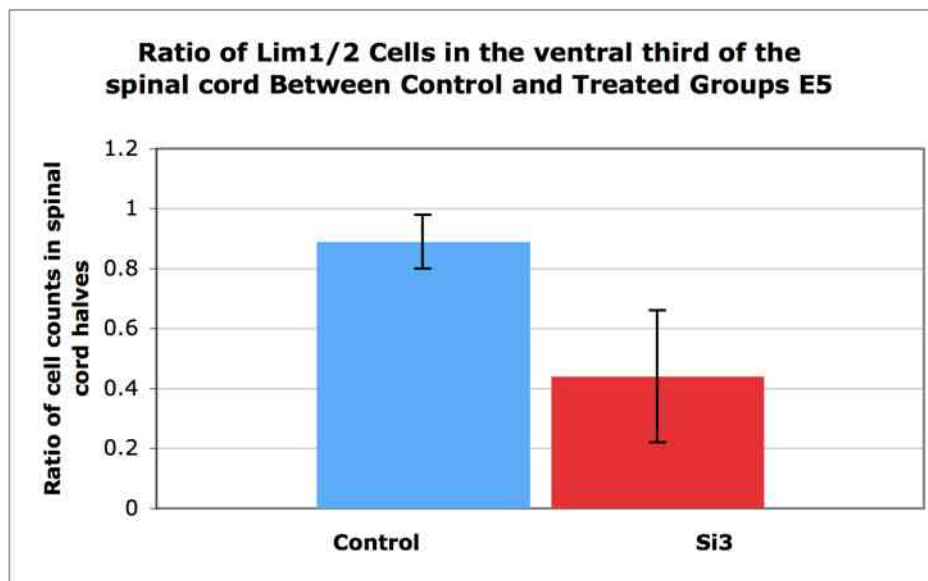
These results were corroborated with cell counts of the ventral most and dorsal most Lim1/2 positive cell populations, and carried out in a similar way to the Islet1/2 cell counts. The results indicated PTP γ loss-of-function causes a significant loss of Lim1/2 cells, over 50% reduction of Lim1/2 cells in the motor horns when compared to the control groups (Figure 5.11, Chart C).

5.4.3 Summary

In summary, PTP γ loss-of-function starting from HH10 induces a loss of Lim1/2 cells by E5. Embryos treated with Si1, Si3 and Si6 clearly demonstrate the loss of Lim1/2 cells. This raises many questions as to what is exactly happening with these cell types. Are we seeing a death of cells or do they in fact fail to proliferate?

Apparent mislocation defects are presented, and so what role does PTP γ play in the specification and positioning of the various cell types within the neural tube? In order to understand at what point the cellular defects were being initiated, further analysis on PTP γ silenced embryos was carried out at earlier time points.

Figure 5.11 Chart A- Ratio of Islet 1/2 cells between control (Blue) (n=6) and Si3 (n=19) treated (Red) groups at E5. No real difference in the number of Islet positive cells can be observed between treated and control groups. Chart B- Ratio of Lim 1/2 cells in the dorsal third of the spinal cord between control (Blue) (n=6) and Si3 (Red) (n=12) treated groups at E5. A significant reduction is evident in the number of Lim 1/2 positive cells between treated and control groups ($P < 0.01$; Student T Test). Chart C - Ratio of Lim 1/2 cells in the ventral third of the spinal cord between control (Blue) (n=6) and Si3 (Red) (n=14) treated groups at E5. A larger reduction is evident in the number of Lim 1/2 positive cells between treated and control groups ventrally ($P < 0001$; Student T Test) (Error Bars show SD).

A**B****C**

Key (A-C): **Blue Bars** denote ratio of cells between treated and non-treated sides of the spinal cord among control shRNA samples. **Red Bars** denote ratio of cells between treated and non-treated sides of the spinal cord among Si3 shRNA samples.

5.5 Studying PTP γ loss-of-function at earlier embryonic time points.

5.5.1 HH18

The onset of PTP γ expression within the dorsal marginal zone of committed neurons in the spinal cord coincides temporally with the birth of the first motor and interneurons, and onset of neurogenic activity generally throughout the cord at around HH14-15 (Landmesser, 2001, Briscoe & Novitch, 2008; Bertrand et al, 2002). The earliest time point studied in detail was HH18, when PTP γ is still only expressed in interneurons (Table 5.2).

Within samples treated with Si3, a small number of cells expressing Islet1/2, Lim1/2, Lim3 and Mnr2 appeared to show no significant change in number when compared against Wild Type embryos (Figure 5.12, Panels A-N). This was confirmed with cells counts of Islet1/2, Lim1/2, Lim3 and Mnr2 positive neurons (Figure 5.13).

5.5.2 HH20

Two later stages of development, HH20 and HH22 were studied to ascertain what was happening to the neuronal profiles within the spinal cord following PTP γ silencing. These time points were chosen, as at those stages PTP γ expression was prevalent throughout the spinal cord. At HH20, a shortening of the spinal cord on the targeted side become apparent, consistent with a loss of Islet1/2, Lim1/2, Lim3 and Mnr2 fated cells and slight reduction in PTP γ expression (Figure 5.14 A-N).

Table 5.2 Table of embryos at HH18, HH20 and HH20 between control and PTP γ loss of function experiments.

Experiment/Stage	Normal Phenotype	Truncated Phenotype	Heterotopia Phenotype	Total
<i>p-Silencer negative control</i>				
HH18	8	0	0	8
HH20	7	0	0	7
HH22	8	0	0	8
<i>Si1</i>				
HH22	4	3	0	7
<i>Si3</i>				
HH18	9	2	1	12
HH20	12	13	2	27
HH22	13	10	1	24
<i>Si6</i>				
HH22	5	5	0	10

Figure 5.12 Immunocytochemical and DIG-labelled mRNA in situ hybridisation in transverse sections of HH18 chick brachial spinal cord in a WT control (A-G) and a Si3 treated embryo (H-N) to (A) 3A10 (B) Islet 1/2, (C) Lim 1/2; (D) Lim3; (E) Mnr2; (F) In situ of PTP γ ; (G) In situ of NeuroM; (H) 3A10, the Si3 treated side is shown in green by its GFP fluorescence (I) Islet 1/2, (J) Lim 1/2; (K) Lim3; (L) Mnr2; (M) In situ of PTP γ ; and (N) In situ of NeuroM. Scale bar is 0.5mm.

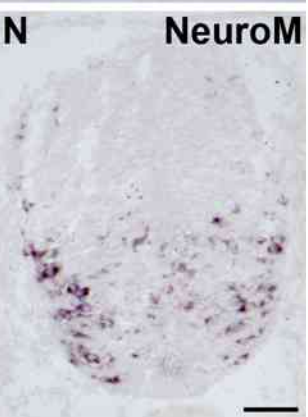
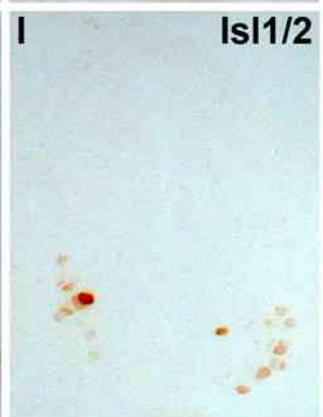
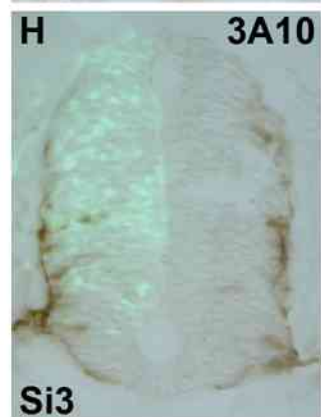
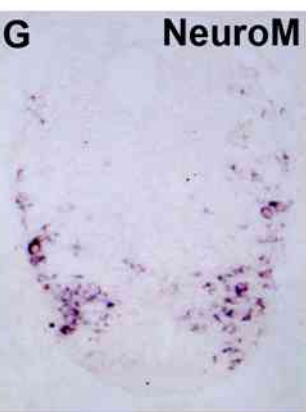
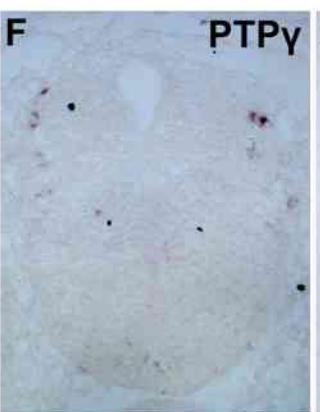
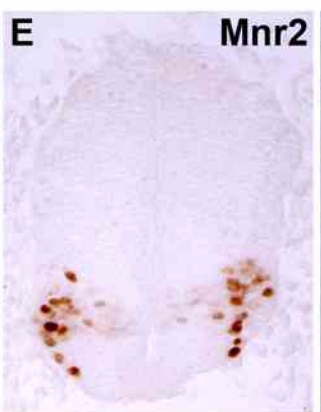
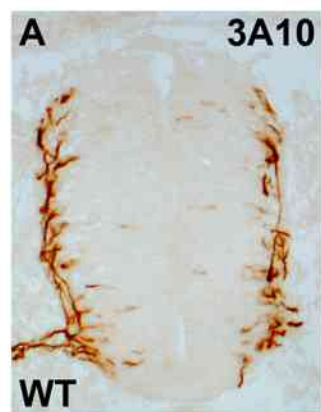
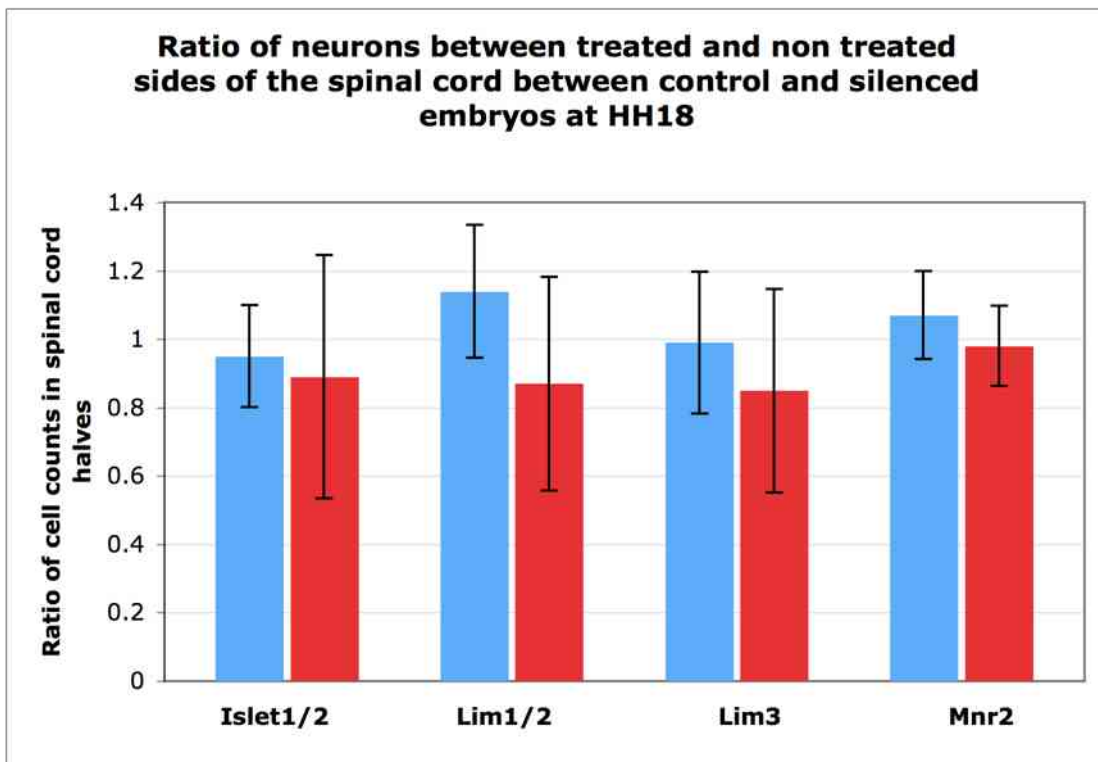


Figure 5.13 Chart of LIM-HD positive cell numbers. Ratio of neurons compared between treated (Red) and non treated (Blue) sides of the spinal cord between shRNA control and PTP γ silenced embryos at HH18. All four markers studied, Islet 1/2 (n=7), Lim 1/2 (n=7), Lim 3 (n=6) and Mnr 2 (n=6) showed no significant reduction in their cell numbers in PTP γ silenced groups ($P < 0.01$; Student T Test) (Error Bars show SD).



Key: **Blue Bars** denote ratio of cells between treated and non-treated sides of the spinal cord among control shRNA samples. **Red Bars** denote ratio of cells between treated and non-treated sides of the spinal cord among Si3 shRNA samples.

This effect extends along the entire dorsoventral aspect of the spinal cord. Cell counts reveal an average reduction in Islet1/2 cell number by 43% when comparing ratios between embryos. The number of Lim1/2 cells were reduced by 39%, and Lim3 cells demonstrated a reduction of 48%. Mnr2 cells reduced in number by the least percentage, on average a reduction of 31% (Figure 5.15).

5.5.3 HH22

Two developmental stages later at HH 22, ectopically located Islet1/2 and Mnr2 cells were observed very close to or at the site of the ventricular lumen (Figure 5.16, Panels I & L respectively – arrows). This observation further supports the invasive phenotypes observed at E5 suggesting that silencing PTP γ triggers their occurrence at earlier embryonic stages.

A truncated spinal cord develops with lower levels of PTP γ expression (Figure 5.16 A-N). Cell counts reveal an average reduction in Islet1/2 cells by 32% when comparing ratios between embryos. The number of Lim1/2 cells is reduced by 48%, and the Lim3 positive cells by 46%.

Mnr2 cells did not show any significant reduction in cell number on average at this developmental stage (Figure 5.17). There seemed to be a recovery of the Islet1/2 and Mnr2 patterns at this point when compared to cell counts at HH20. The expression profiles of Lim1/2/3 together displayed a greater reduction jointly than at HH20. It is worthy to note that at earlier stages to HH22, Lim 3 and Islet 1 cells are all motor neuron precursors whilst Lim 1/2 cells are predominantly interneurons at this stage.

Figure 5.14 Immunocytochemical and DIG-labelled mRNA in situ hybridisation in transverse sections of HH20 chick brachial spinal cord in a WT control (A-G) and a Si3 treated embryo bearing a truncated phenotype (H-N) to (A) 3A10 (B) Islet 1/2, (C) Lim 1/2; (D) Lim3; (E) Mnr2; (F) In situ of PTP γ ; (G) In situ of NeuroM; (H) 3A10, the Si3 treated side is shown in green by its GFP fluorescence (I) Islet 1/2, (J) Lim 1/2; (K) Lim3; (L) Mnr2; (M) In situ of PTP γ ; and (N) In situ of NeuroM. Scale bar is 0.5mm.

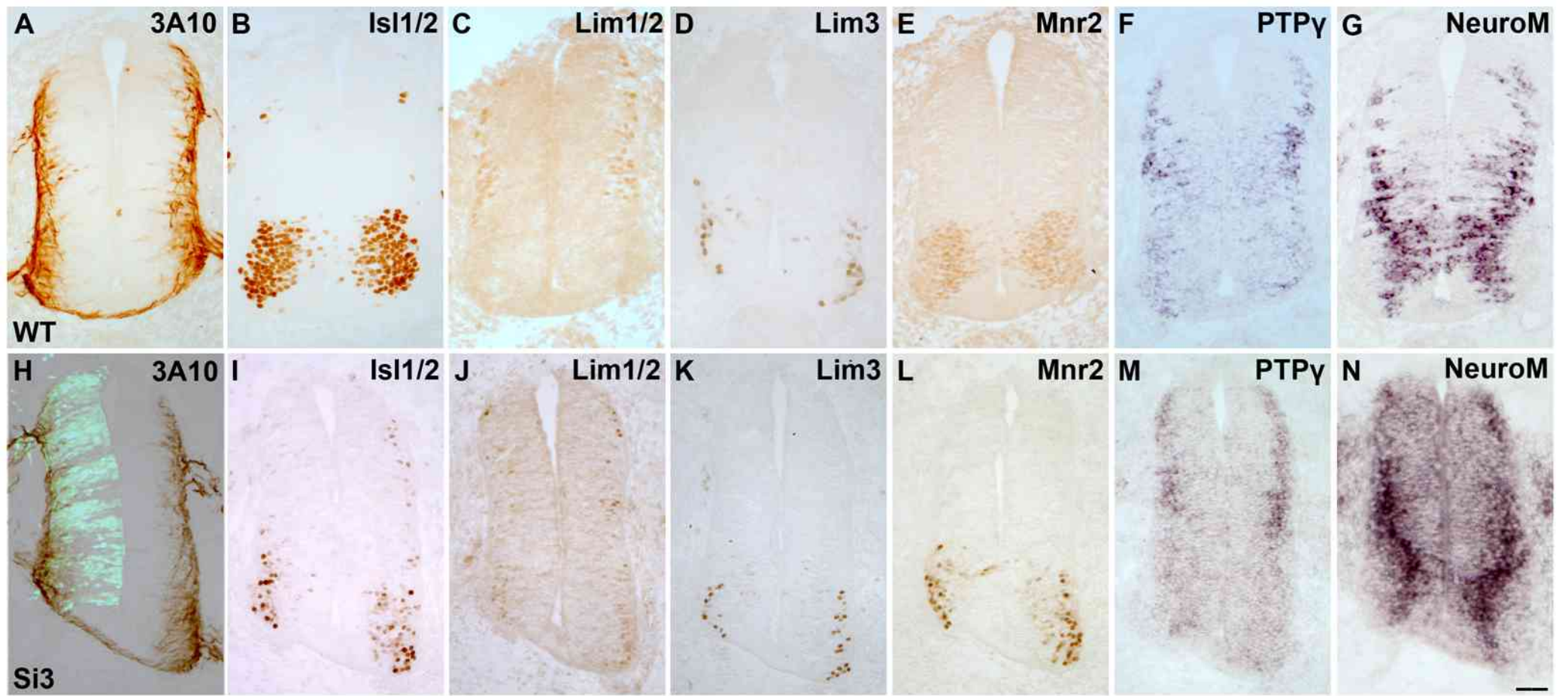
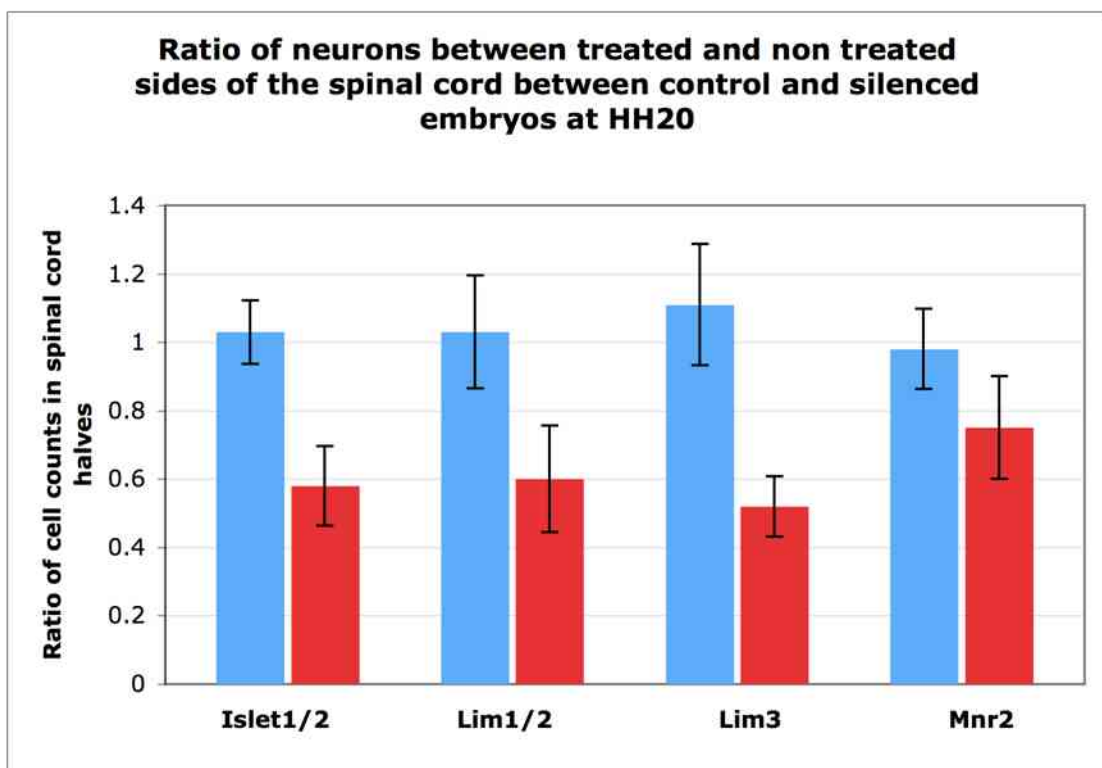


Figure 5.15 Chart of LIM-HD positive cell numbers. Ratio of neurons compared between treated (Red bars) and non treated (Blue bars) sides of the spinal cord between shRNA control and PTP γ silenced embryos at HH20. All four markers studied, Islet 1/2 (n=13)(P<0.0001; Student T Test), Lim 1/2 (n=11)(P<0.001; Student T test), Lim 3 (n=12)(P<0.0001; Student T Test) and Mnr 2 (n=9)(P<0.01: Student T test) showed a significantly larger reduction in their cell numbers in PTP γ silenced groups (Error Bars show SD).



Key: **Blue Bars** denote ratio of cells between treated and non-treated sides of the spinal cord among control shRNA samples. **Red Bars** denote ratio of cells between treated and non-treated sides of the spinal cord among Si3 shRNA samples.

Figure 5.16 Immunocytochemical and DIG-labelled mRNA in situ hybridisation in transverse sections of HH22 chick brachial spinal cord in a WT control (A-G) and a Si3 treated embryo (H-N) to (A) 3A10 (B) Islet 1/2, arrow indicates ectopically located cell close to the ventricular zone, (C) Lim 1/2; (D) Lim3; (E) Mnr2; (F) In situ of PTP γ ; (G) In situ of NeuroM; (H) 3A10, the Si3 treated side is shown in green by its GFP fluorescence (I) Islet 1/2, (J) Lim 1/2; (K) Lim3; (L) Mnr2, arrow indicates ectopic luminal cell; (M) In situ of PTP γ showing a significant reduction in its expression compared to the control side and expression seen in panel F; and (N) In situ of NeuroM. Scale bar is 0.5mm.

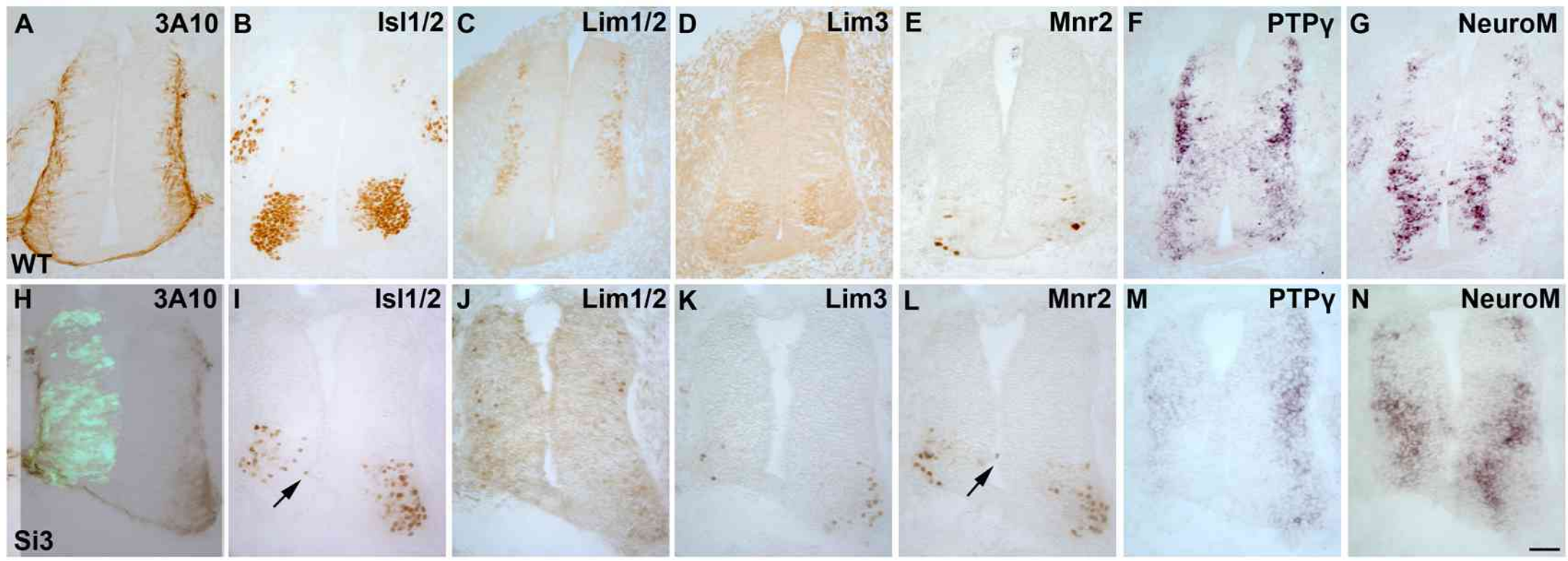
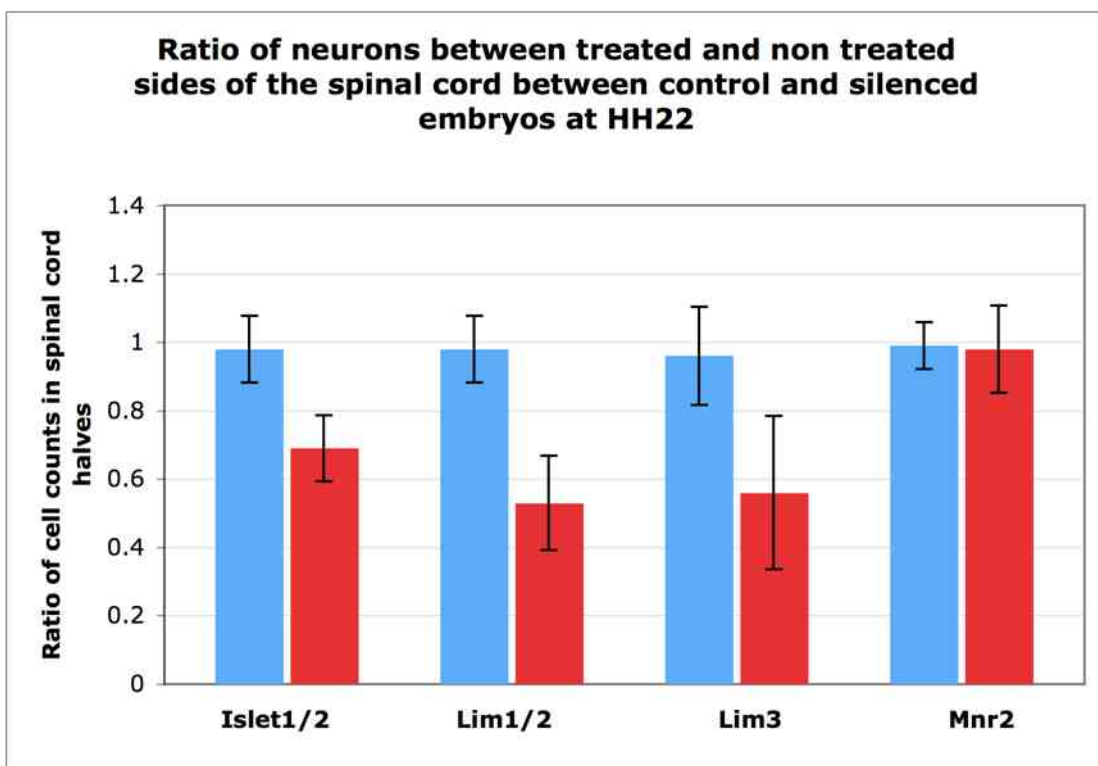


Figure 5.17 Chart of LIM-HD positive cell numbers. Ratio of motor neurons compared between treated (Red bars) and non-treated (Blue bars) sides of the spinal cord between shRNA control and PTP γ silenced embryos at HH22. Three out of four markers studied, Islet 1/2 (n=10)(P<0.0001; Student T Test), Lim 1/2 (n=10)(P<10⁻⁷; Student T test), and Lim 3 (n=10)(P<0.001; Student T test) showed a significantly larger reduction in their cell numbers in PTP γ silenced groups. There was no significant change in the number of Mnr2 (n=10) cells at this stage amongst experimental sets (Error Bars show SD).



Key: **Blue Bars** denote ratio of cells between treated and non-treated sides of the spinal cord among control shRNA samples. **Red Bars** denote ratio of cells between treated and non-treated sides of the spinal cord among Si3 shRNA samples.

5.6 PTP γ silencing induces a reduction in the proliferative capacity of LIM-HD expressing progenitors.

The results described above show a reduction in the number of cells at HH20 and HH22. In order to determine the cause of this reduction, the proliferative activity of progenitor cells within silenced embryos was taken into account. The number of radial glia undergoing Mitosis were studied through the activity of phosphorylated Histone 3 within those treated at HH20 & HH22 (Figure 5.18, Panels D - F) (Figure 5.19, Panels F – J).

Cells were observed at different locations along the dorsoventral range of the ventricular layer and their distribution and number were gauged comparing the treated and control side of the spinal cord at HH 20. The number of cells during mitosis was reduced in number by the greatest percentages along the top third of the spinal cord and bottom third (Figure 5.20). The total numbers of mitotic cells were reduced by 30% when comparing ratios of cells between 10 independent embryos (Fig 5.21). There was no clear evidence of any significant bias in the location of reduced mitoses.

5.7 PTP γ silencing induces apoptosis at HH20 and HH22.

The previous studies on the proliferative capacity of silenced embryos reveal a reduction in the number of M-phase cells. However PTP γ silencing may also be inducing cell death. I set about this study by determining the apoptotic activity at stages HH20 and HH22 using an antibody against activated Caspase-3.

Figure 5.18 Immunocytochemical cell death and proliferation markers in transverse sections of HH20 chick brachial spinal cord shRNA control (A & D), and two Si3 treated embryos (B-C) & (E-F) to (A) Caspase3 (B) Caspase3, arrow indicates location of dying cells close to the ventricular lumen, (C) Caspase3, arrow indicates a trail of apoptotic cell debris in the ventricular zone; (D) pHistone3; (E) pHistone3; (F) pHistone3, arrow showing a reduced number of mitotic cells. Scale bar is 0.5mm.

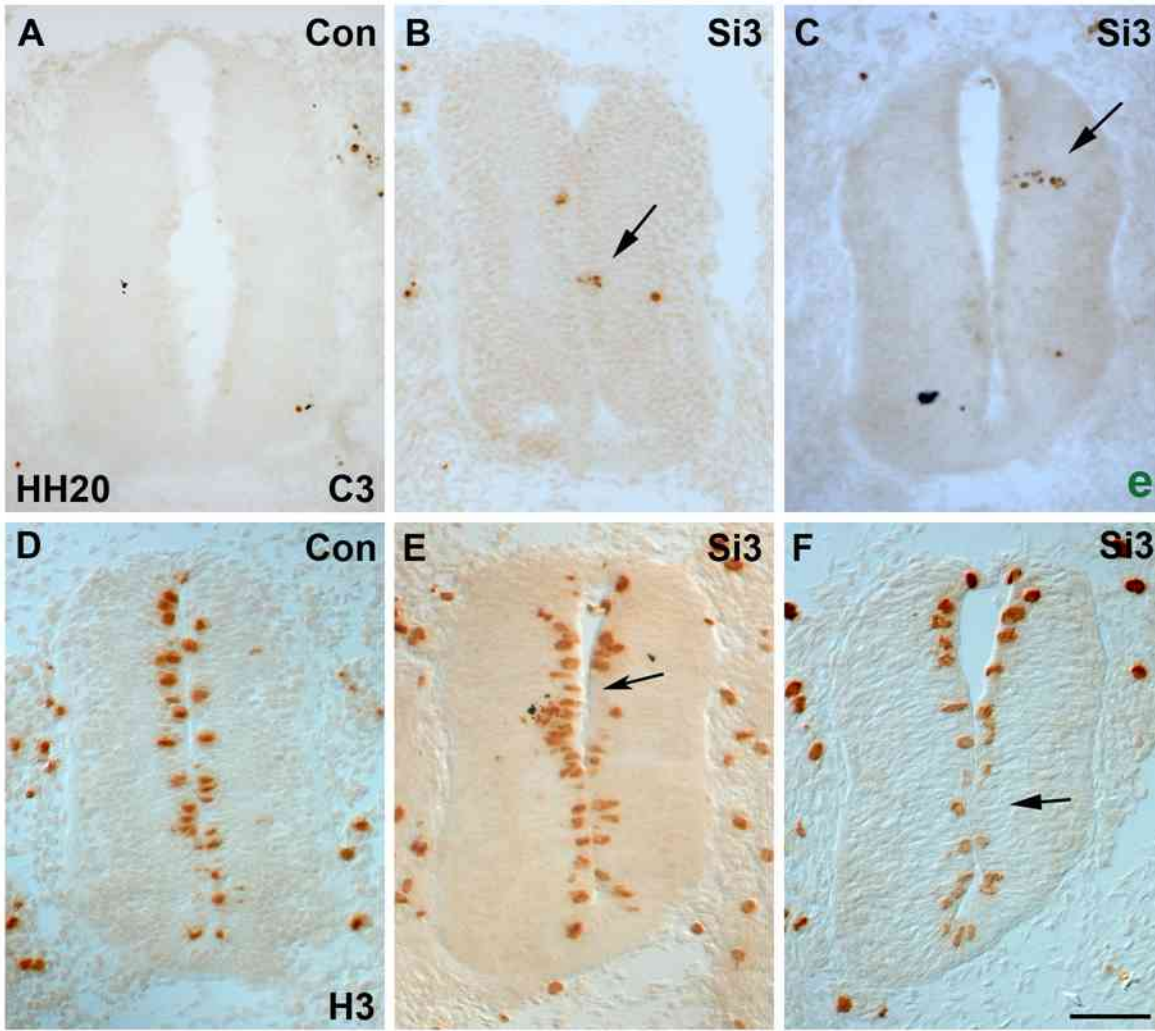


Figure 5.19 Immunocytochemical cell death and proliferation markers in transverse sections of HH22 chick brachial spinal cord shRNA control (A & F), and Si3 treated embryos (B-E) & (G-J) in serial sections of the same embryo to (A) Caspase3 (B-E) Caspase3, arrows indicates location of dying cells close to the ventricular lumen in strings at different locations dorsoventrally in four samples; (F) pHistone3; (G-J) pHistone3, arrows indicate a reduced number of mitotic cells at different dorsoventral locations. Scale bar is 0.5mm.

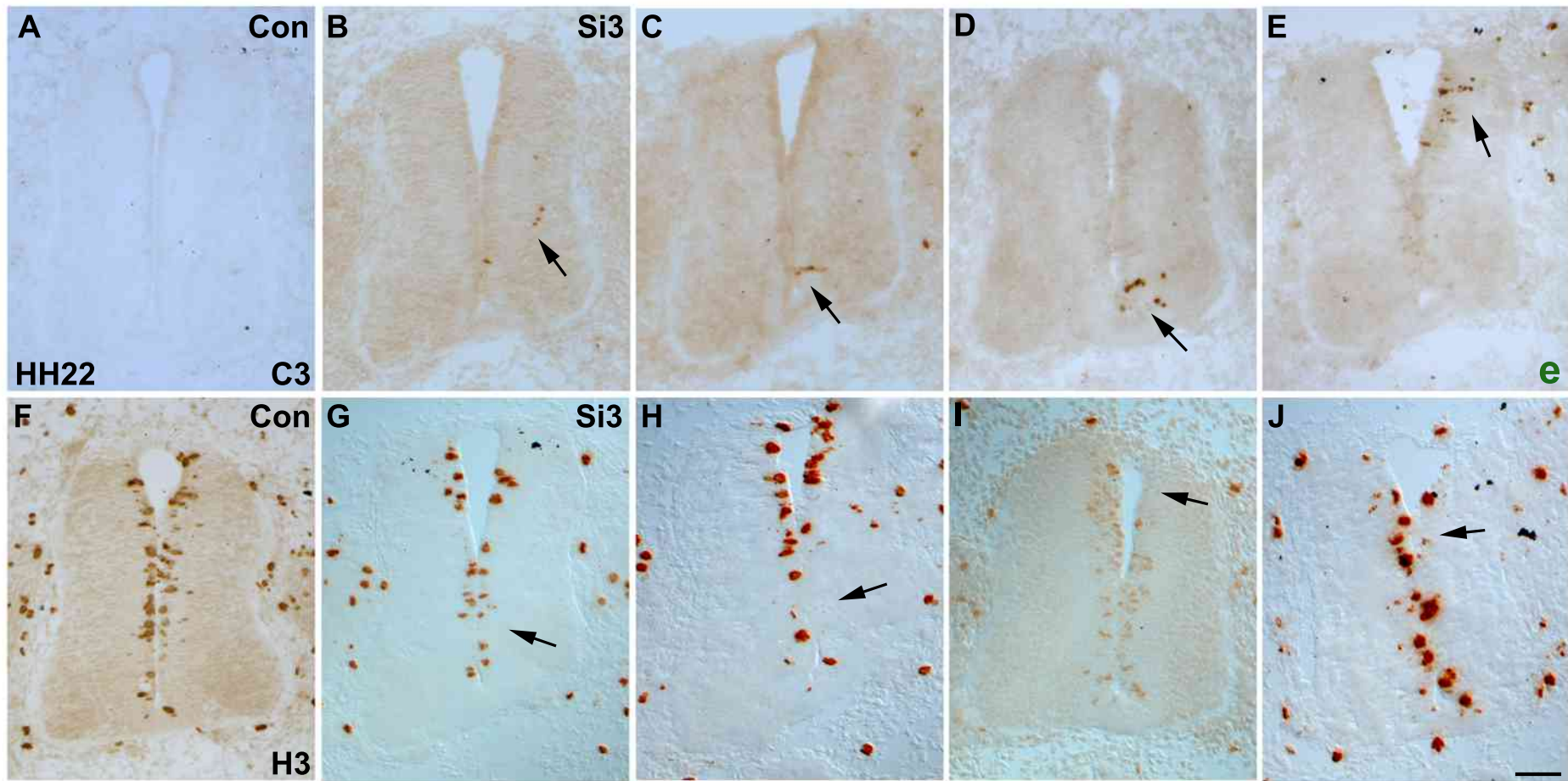
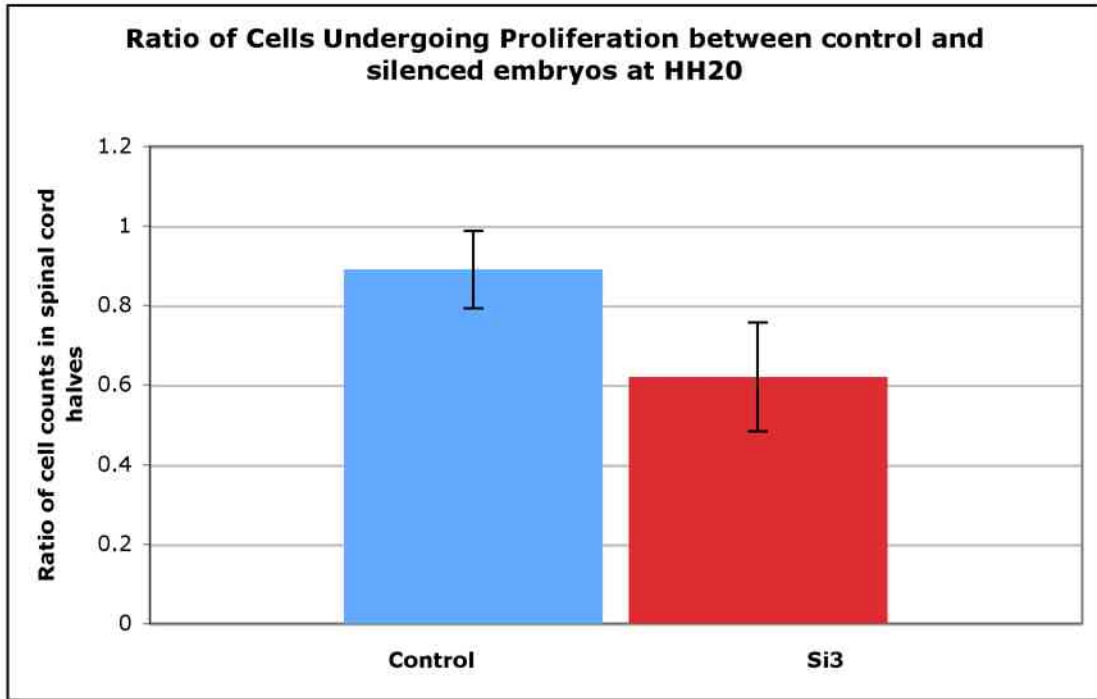
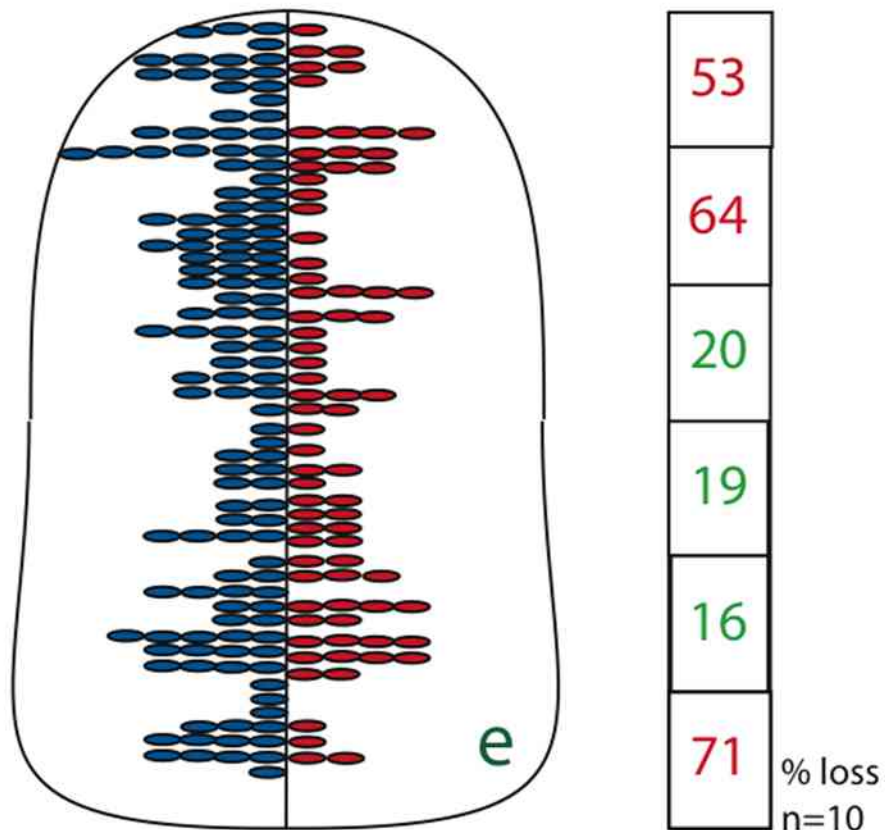


Figure 5.20 Chart of proliferating cell numbers. Ratio of cells undergoing proliferation between treated and non treated sides of the spinal cord between control (Blue bar) and PTP γ silenced (Red bar) embryos at HH20 (n=10)(P<0.001; Student T test) (Error Bars show SD).

Figure 5.21 Schematic representation of proliferating cells in PTP γ silenced embryos at HH20 (n= 10). Red spots indicate location of individual proliferating cells along the ventricular zone. Blue spots indicate pattern of proliferating cells on the control side of the neural tube in silenced embryos. The ventricular zone was split into six zones (boxed) and the percentage loss of proliferating cells on the electroporated side compared to the control side was recorded.



Blue Bars denote ratio of cells between treated and non treated sides of the spinal cord among control shRNA samples. Red Bars denote ratio of cells between treated and non treated sides of the spinal cord among Si3 shRNA samples.



This revealed an interesting pattern with cells in treated tissue undergoing apoptosis either individually or as clusters along radial spoke-like units at different dorsoventral levels of the spinal cord, but predominantly within or neighbouring the ventricular zone (Figure 5.18 Panels A – C - Arrows) (Figure 5.19, Panels A – E – Arrows). Although a few caspase cells were stained at any one time, we were confident this was a genuine signal. Control embryos showed no staining other than the odd cell and the antibody used gave a very clean and clear signal with no background staining. Furthermore the resultant staining was indicative of apoptotic structures.

This suggested that the integrity of clonally related progenitor neurons was compromised leading to an apoptotic programme. The general distribution of Caspase 3 positive cells was recorded amongst 6 control embryos (Figure 5.23 - A) and 14 PTP γ silenced embryos at HH20 (Figure 5.23). This showed a distinct pattern of apoptotic cells arising predominantly from the p1 domain and the dorsal D3 domain (Muller et al 2002). These patterns of clustering were not observed on the control side or with the negative control shRNA treatments. Compared to these control embryos, with less than one apoptotic cell evident per section, loss-of-function embryos showed on average 5 apoptotic cells per section at HH22 on the treated side (Figure 5.23, Panel B).

The rate of apoptosis at stage HH22 appeared reduced from the previous stage studied, with a halving of the rate recorded on average within the treated side of silenced embryos (Figure 5.23.) When the cumulative distribution amongst 6 control embryos and 14 silenced embryos at HH22 was compared, this consistently showed apoptotic activity arising from the pMN domain and dorsal D3 domain (Figure 5.23, Panel B).

Caspase3 positive cell counts at stage HH20 reveal 5 apoptotic cells on the silenced side of the spinal cord compared with 2.25 cells on average observed at stage HH22 (Figure 5.23, Panel A). Amongst control embryos less than one caspase 3 positive cells were observed on either the control or treated samples. It is worthy to note that the control shRNA vector did not induce Caspase3 activity itself.

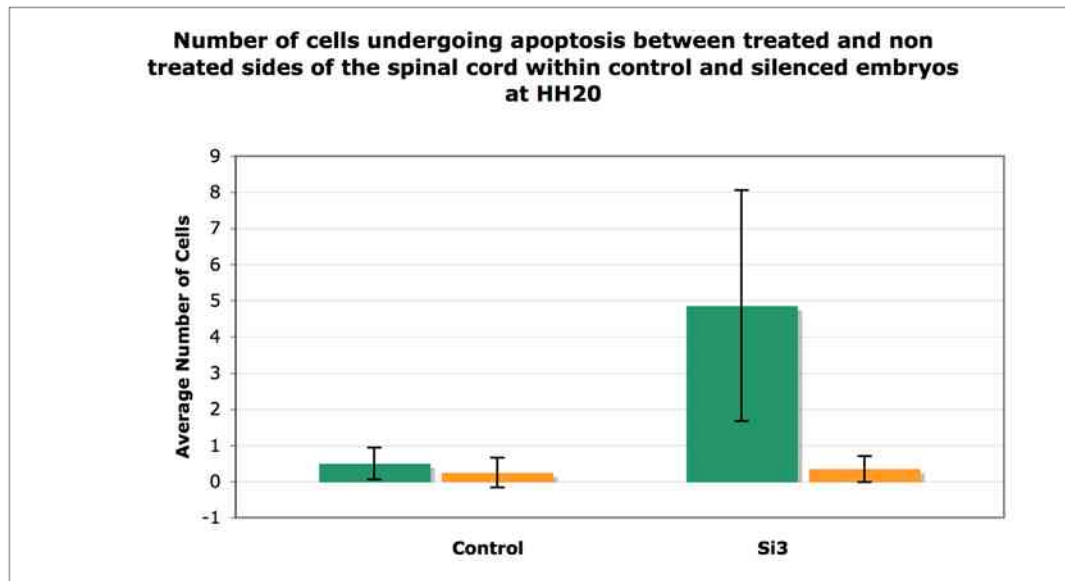
5.8 Summary

Altogether these data indicate that silencing PTP γ leads to the mislocation of cells starting from HH20 onwards during the progression of development within the chick and a reduction of LIM-HD transcription factor expressing cells up to HH22. The development of the ependymal layer of cells on the treated side of the embryo is also disrupted suggesting that there is a defect in progenitor cell maintenance.

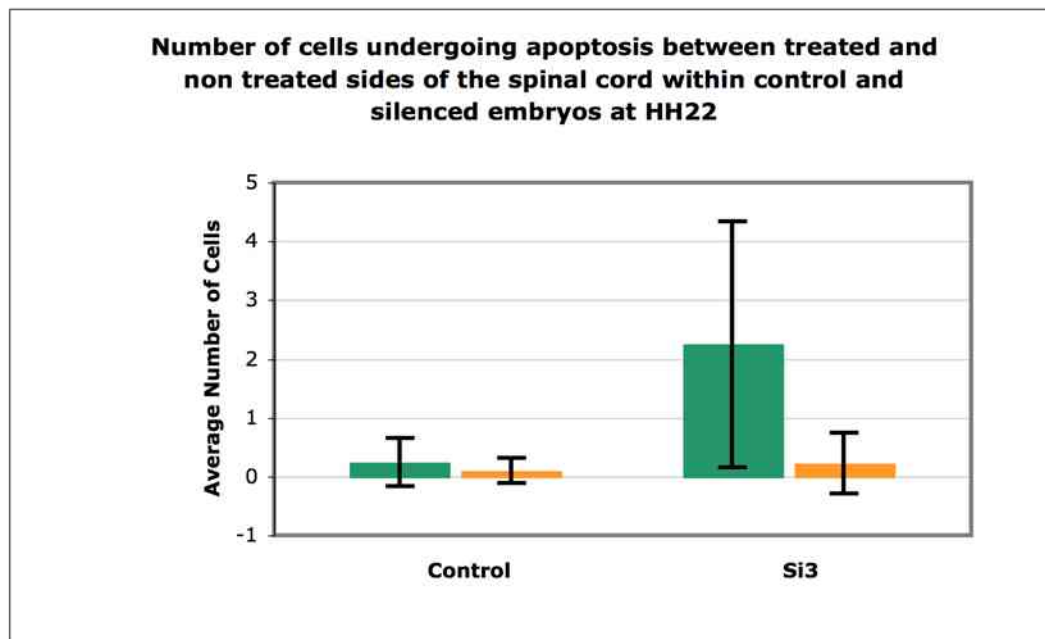
A sustained loss of Lim1/2 expressing cells is maintained until E5, the latest time point studied. The loss of cells may arise through a reduction of the proliferative capacity of radial glial cells or a triggering of the apoptotic programme, which occurs at a higher rate at HH20 than HH22. These results will be discussed in more detail in the concluding chapter.

Figure 5.22 A - Chart of Caspase 3 positive cell numbers. Number of cells undergoing apoptosis between treated (Green bars) and non treated (Yellow bars) sides of the spinal cord between control and PTP γ silenced embryos at HH20. Three different serial sections per embryo were analysed, the mean cells per embryo recorded on respective spinal cord halves. The average of the data from all the embryos in the experimental set were then tabulated. The control embryos showed no significant change in the number of dying cells, however this was significantly increased in PTP γ silenced groups, observing around 5 cells on average on the treated half of the neural tube (n=18)($P < 10^{-5}$; Student T test). B -Chart of cell numbers undergoing apoptosis. Ratio of cells undergoing apoptosis between treated (Green bars) and non treated (Yellow bars) sides of the spinal cord between control and PTP γ silenced embryos at HH22. At least two dying cells are observed per section in PTP γ silenced embryos (n=11)($P < 0.01$; Student T Test) (Error Bars show SD).

A

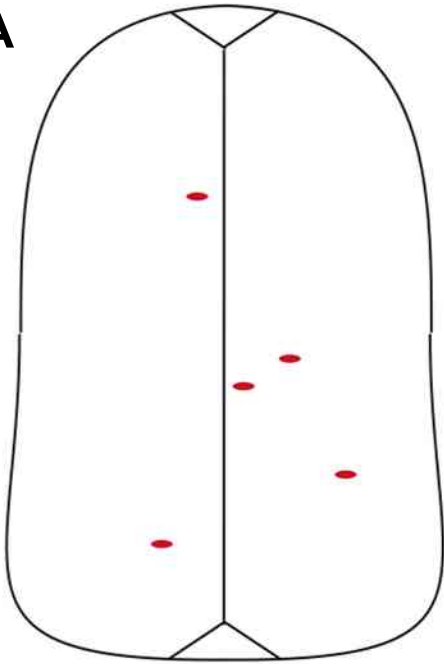
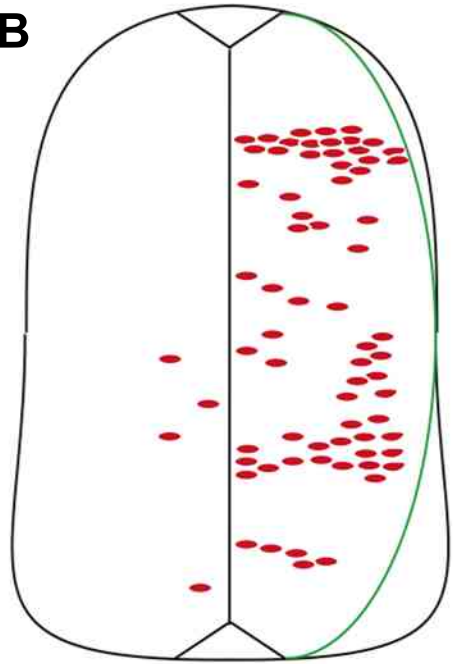
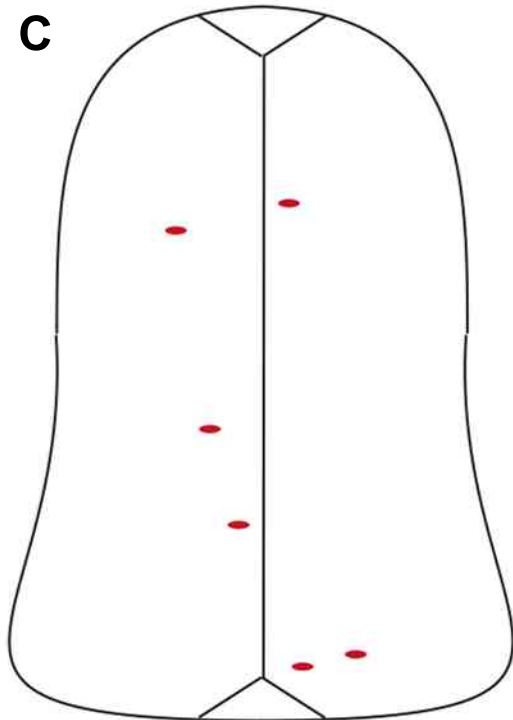
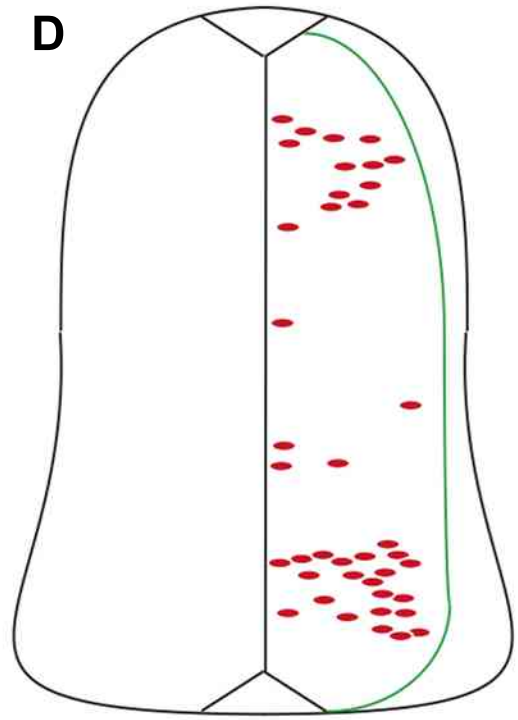


B



Key (A & B): **Green Bars** denote the average number of cells on the treated sides of the spinal cord among control shRNA & Si3 sample groups. **Orange Bars** denote the average number of cells on the non-treated sides of the spinal cord among control shRNA & Si3 sample groups.

Figure 5.23 A- Schematic representation of apoptotic cells in control embryos at HH20 (n= 6). Red spots indicate location of individual cells. B - Schematic representation of apoptotic cells in PTP γ silenced embryos at HH20 (n= 18). Red spots indicate location of individual randomly located apoptotic cells. Green line represent approximate loss of tissue following loss of function treatment. C - Schematic representation of apoptotic cells in control embryos at HH22 (n= 6). Red spots indicate location of individual cells. D - Schematic representation of apoptotic cells in PTP γ silenced embryos at HH22 (n= 11). Red spots indicate location of individual apoptotic cells. A distinct pattern of cell death develops at various dorsoventral locations. Green line represent approximate loss of tissue following loss of function treatment. Note that panels B and D represent the cumulative results from all experimental sets of embryos observed rather than data from one embryo.

A**B****C****D**

Chapter 6: PTP γ gain-of-function.

6.1 Introduction

The aim of the experiments in this chapter was to determine the effect of PTP γ gain-of-function on the generation of differentiated neurons and progression of the cell cycle, by studying the number of proliferation cells at S and M Phases of the cell cycle. This gain-of-function test would serve to complement the studies presented in Chapter 5, where the results showed missing and ectopically located cells within the spinal cord. This set of experiments would indicate if the gain-of-function of PTP γ did have an impact on the expression profiles of the LIM-HD genes and cell cycle markers.

6.2 PTP γ over expression causes a broad reduction in the number of Lim-HD expressing neurons along the entire DV aspect of the spinal cord.

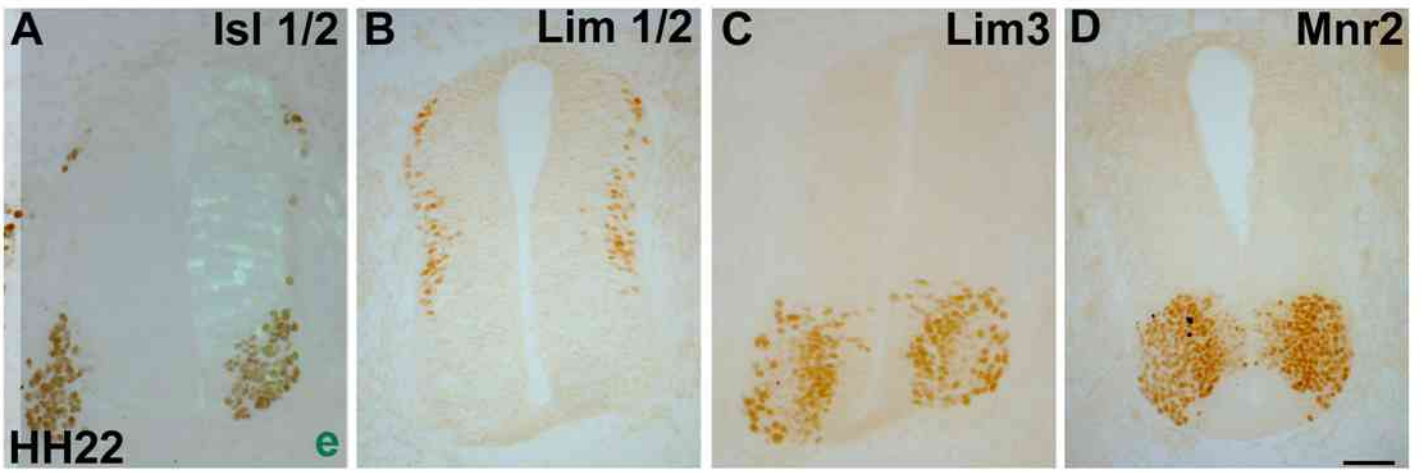
In order to gain more insight into which populations of neurons were affected by PTP γ over expression, the expression profiles of motor neuron markers, states of proliferative activity and cell death at stages HH 20 and 22 were studied. The total number of embryos studied for each developmental stage is shown in Table 6.1.

A set of control embryos were treated with IRES-GFP plasmid at HH20, and of the neuronal markers observed, all displayed a normal pattern of development (Figure 6.1, Panels A-D).

Table 6.1 Table of IRES-GFP and PTP γ -IRES-GFP treated embryos at HH18, HH20 and HH22. These are pooled according to normal, truncated and heterotopic phenotypes.

Experiment/Stage	Normal Phenotype	Truncated Phenotype	Displacement Phenotype	Total
<i>IRES-PTPγ-GFP</i>				
HH18	1	10	0	11
HH20	1	12	0	13
HH22	3	19	1	23
<i>IRES-GFP</i>				
HH18	5	0	0	5
HH20	6	1	0	7
HH22	6	0	0	6

Figure 6.1 Immunocytochemical and DIG-labelled mRNA in situ hybridisation in transverse sections of HH22 chick brachial spinal cord in a control IRES-GFP treated embryo to (A) Islet 1/2, (B) Lim 1/2, (C) Lim 3; (D) Mnr2. Scale bar is 0.5mm.



At HH 20, of the 4 neuronal markers observed, *Islet1/2*, *Lim1/2*, *Lim3* and *Mnr2*, all demonstrated a reduction in the total number of cells marked, along with a significant shortening and narrowing of the spinal cord in many cases (Fig 6.2, Panels A-D). No significant differences in Caspase-3 cells were observed between samples, with only one or two isolated cells appearing within each section (Fig 6.2, Panel E, arrows.)

There appeared to be a slight reduction in the number of mitotic cells in tissues treated with IRES-PTP γ , shown by phosphorylated Histone3 activity at the ventricular lumen, although only the HH22 samples were quantified (Fig 6.2, Panel F & Panel G) (Figure 6.3).

6.3 The reduction in LIM-HD cell expression persists to HH 22

At HH 22, the effect of IRES-PTP γ gain of function on differentiating neurons expressing LIM-HD identities was similar to that at HH20, with a reduction of differentiated cells (Fig 6.3, Panels A-D).

6.3.1 LIM-HD cell counts

Cell counts at HH 22 reveal a reduction in the total number of *Islet1/2* cells amongst PTP γ -IRES-GFP and IRES-GFP treated embryos representing a ratio of 0.61 (relative to 0.92) when comparing treated and non-treated sides of the embryos amongst PTP γ -IRES-GFP sets relative to IRES-GFP sets (Fig 6.4 Chart A).

Figure 6.2 Immunocytochemical and DIG-labelled mRNA in situ hybridisation in transverse serial sections of HH20 chick brachial spinal cord in a PTP γ -IRES-GFP treated embryo to (A) Islet 1/2 labelling, showing a reduction of the motor pool cells. (B) Lim 1/2 labelling, showing a clear loss of all ventral and most intermediate cell populations. (C) Lim 3 labelling, showing a significant reduction in the number of cells and absence of the ventral most Lim 3 population. (D) Mnr2 labelling, showing a sustained loss of cells. (E) Caspase3 labelling, arrows indicate the location of the dying cells. (F) pHistone3 labelling. (G) In situ to PTP γ showing a reduction in spinal cord tissue ventrally and in intermediate levels, and a modest increase in PTP γ signal in the electroporated side of the spinal cord. (H) Schematic outline of the spinal cord to highlight the reduction in spinal cord area. “e” denotes electroporated side of the neural tube. Scale bar is 0.5mm.

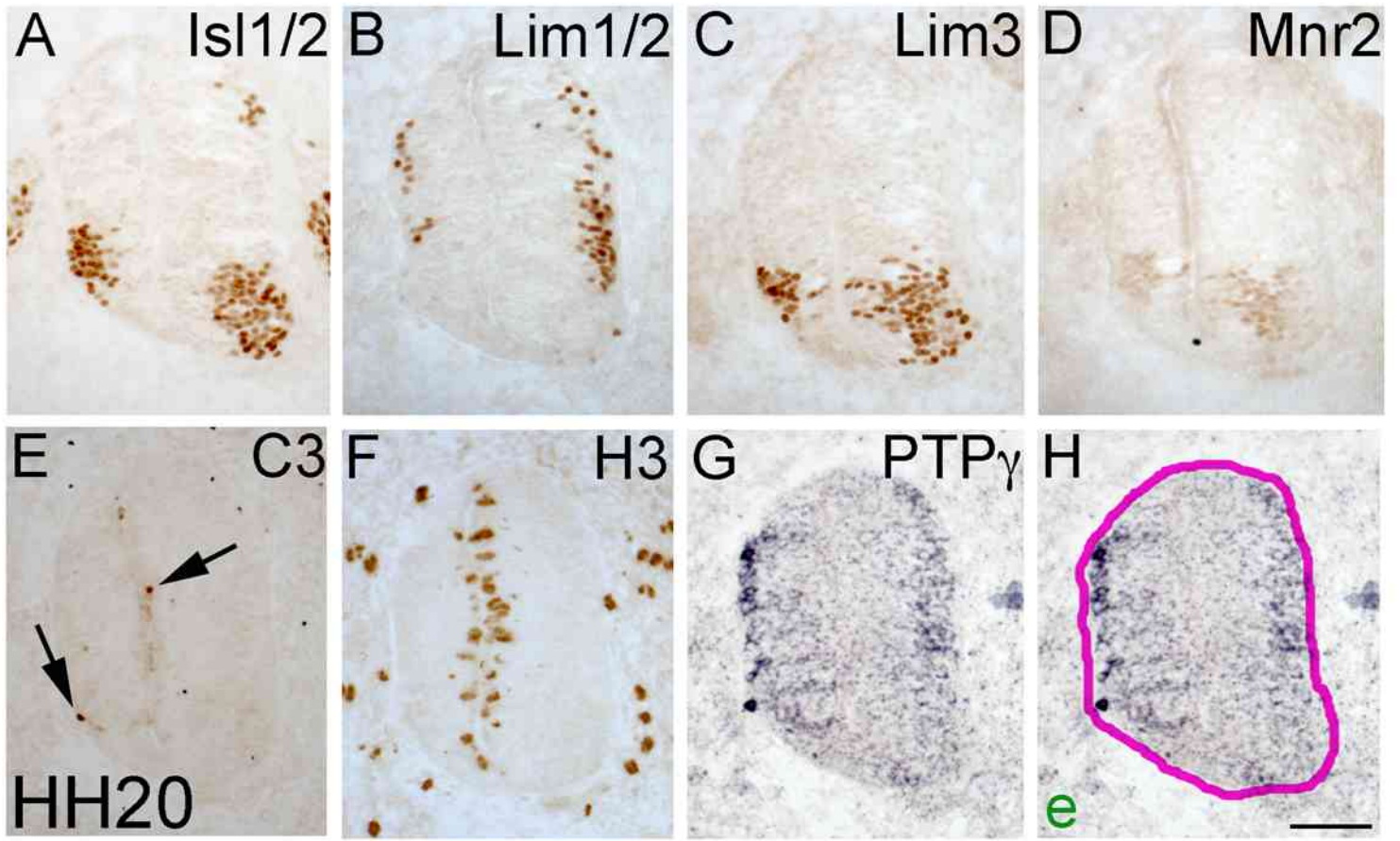
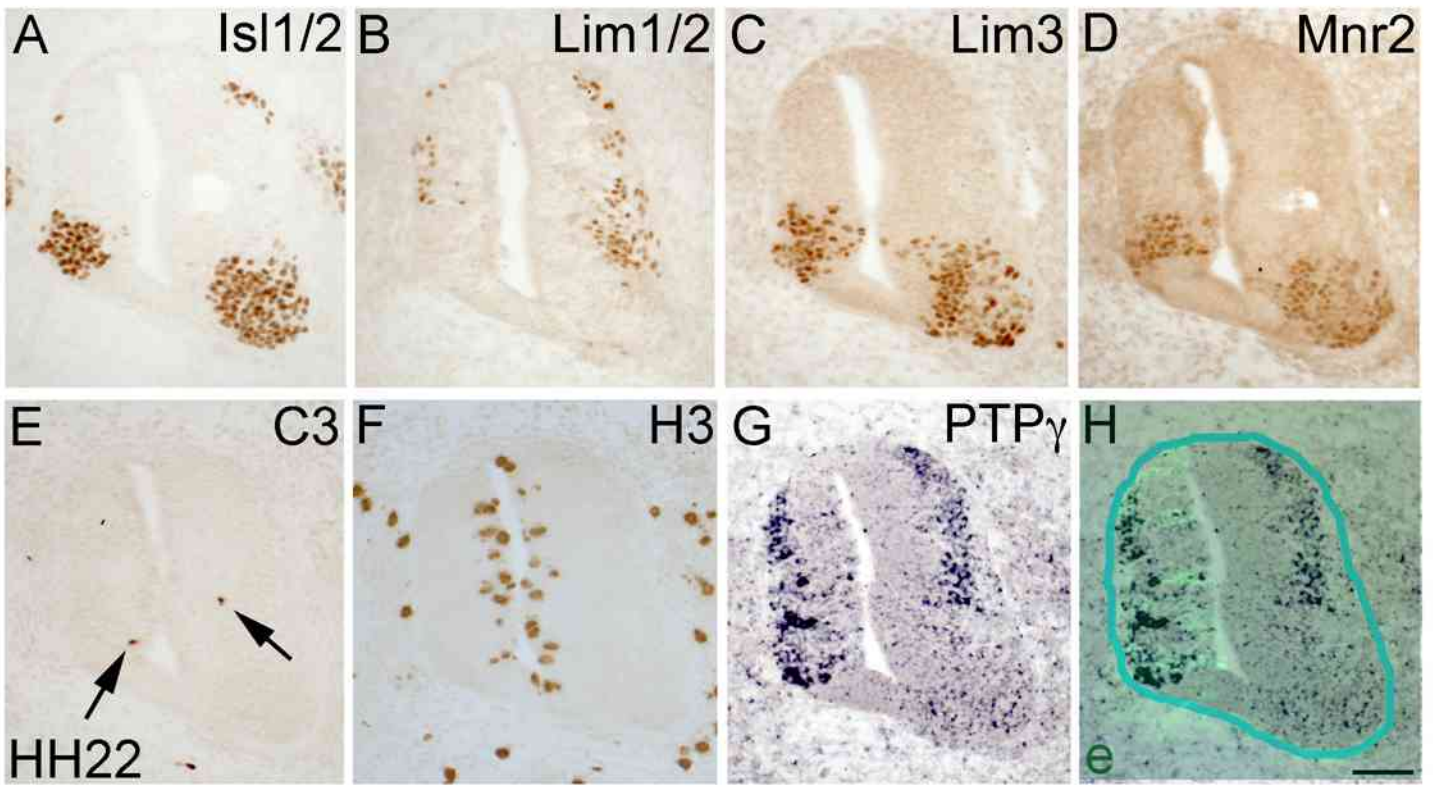


Figure 6.3 Immunocytochemical and DIG-labelled mRNA in situ hybridisation in transverse sections of HH22 chick brachial spinal cord in a PTP γ -IRES-GFP treated embryo (in serial sections). (A) Islet 1/2 labelling, showing a reduction of motor pool cells. (B) Lim 1/2 labelling, showing a clear loss of all ventral and most intermediate and dorsal cell populations on the treated left hand side of the neural tube. (C) Lim 3 labelling, showing a significant reduction in the number of cells especially the lateral aspect of the LMC. (D) Mnr2 labelling, showing a significant loss of cells. (E) Caspase3 labelling, arrows indicate the location of the dying cells. (F) pHistone3 labelling. (G) In situ to PTP γ showing an increase in RNA levels on the electroporated side, and sustained shortening and narrowing of the neural tube. (H) Schematic outline of the spinal cord to highlight the reduction in spinal cord area on the electroporated side. “e” denotes electroporated side of the spinal cord. Scale bar is 0.5mm.



Similar counts for Lim1/2 indicate a reduction of cells on average corresponding to a ratio of 0.61 (relative to 0.98) (Fig 6.4, Chart B). Lim 3 positive cells also demonstrate a reduction of cell numbers representing a ratio of 0.64 (relative to 0.98) (Fig 6.4, Chart C). Overall, we see a consistent global reduction in the number of Lim-HD expressing cells following PTP γ over expression.

6.3.2 Further patterns at HH22 in IRES-PTP γ treated embryos.

Very few cells appear to undergo apoptosis and the number of progenitor cells at M-phase of the cell cycle appear reduced as shown by phosphorylated Histone 3 expression (Fig 6.3, Panels E & F). The mRNA distribution of PTP γ confirms the persistent over expression of PTP γ within the spinal cord tissue despite the reduction in overall spinal cord area on the treated side (Fig 6.3, Panel G). The truncation may arise as a result of a reduction in the mitotic activity of progenitors whereby the ectopic expression of PTP γ in areas it is not normally expressed may disrupt the balance of normal gene expression and therefore neuronal development.

Most of the affected embryos demonstrated a truncation of the spinal cord tissue on the treated side. However, in only one case we did see a displacement of cells within the lumen of the spinal cord. These cells were positive for Islet 1/2 (Fig 6.5, Panels A – C). The significance of this example is uncertain since this was an isolated observation, but it does look similar to what was found following PTP γ knockdown. Nevertheless, it contrasts with the high frequency of ectopically-placed precursors following PTP γ loss-of-function (Table 5.2).

Figure 6.4 Charts of LIM-HD expressing cell numbers at HH22 between IRES-GFP and PTP γ -IRES-GFP treated embryos (A) Ratio of Islet1/2 cells between control and treated groups demonstrated a reduction in cell number amongst over PTP γ expressed samples (n=19)(P<0.001; Student T test). (B) Ratio of Lim1/2 cells between control and treated groups showing a reduction in cell number amongst over PTP γ expressed samples (n=8)(P<0.001; Student T Test). (C) Ratio of Lim3 cells between control and treated groups again showing a reduction in cell number amongst over PTP γ expressed samples (n=11)(P<0.01; Student T Test) (Error bars show SD).

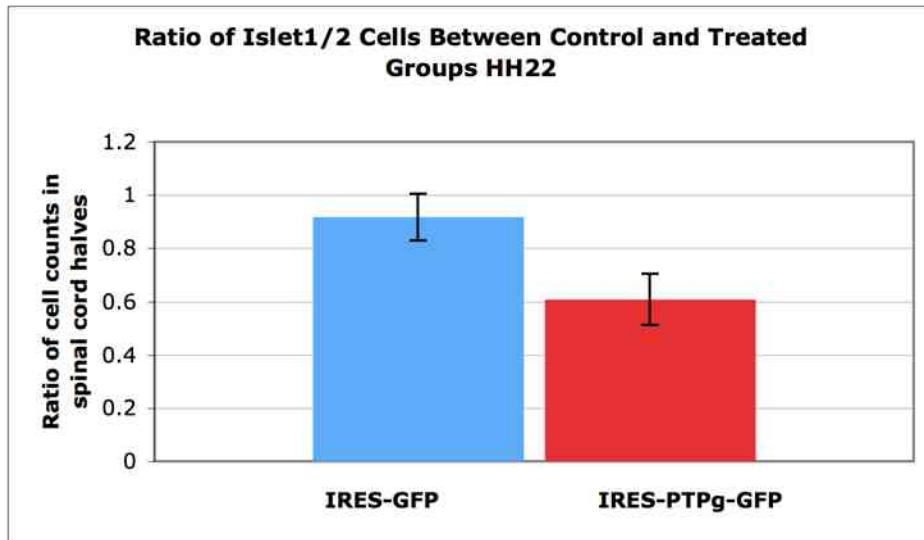
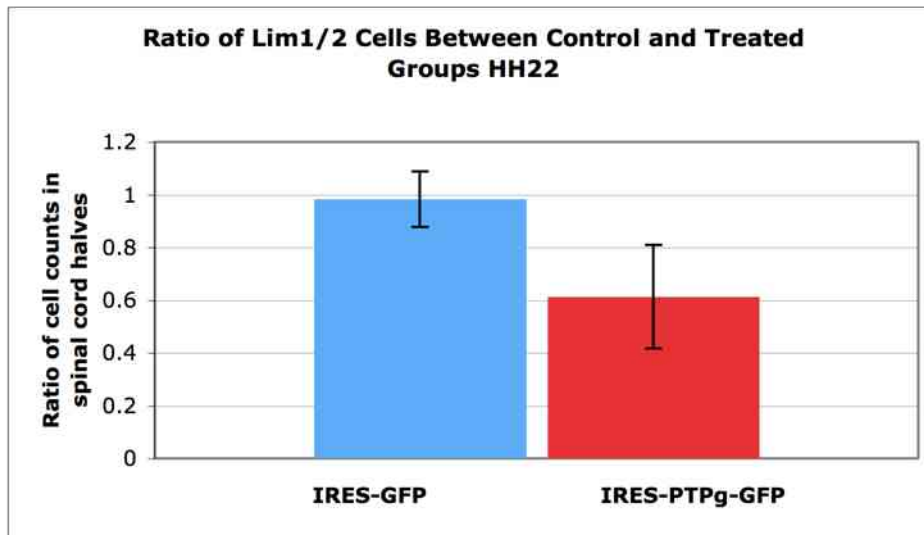
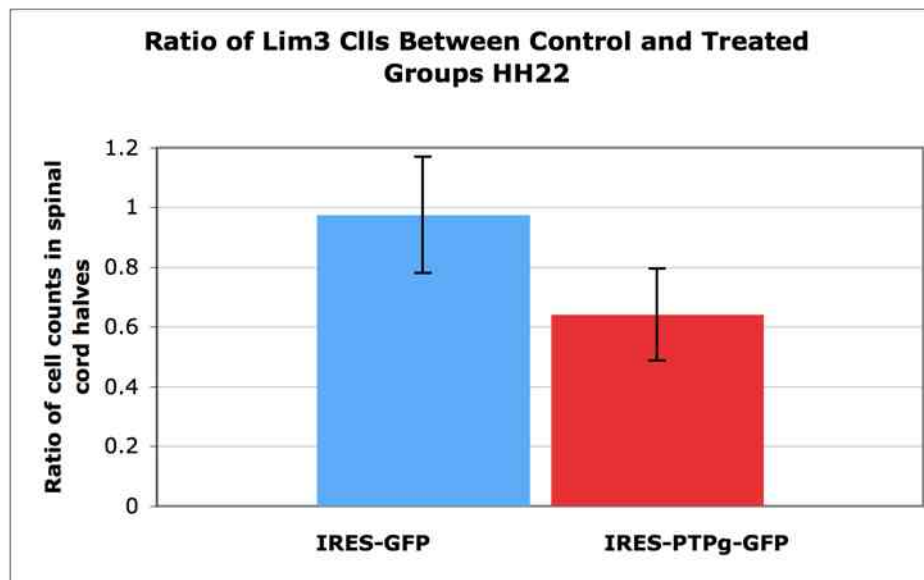
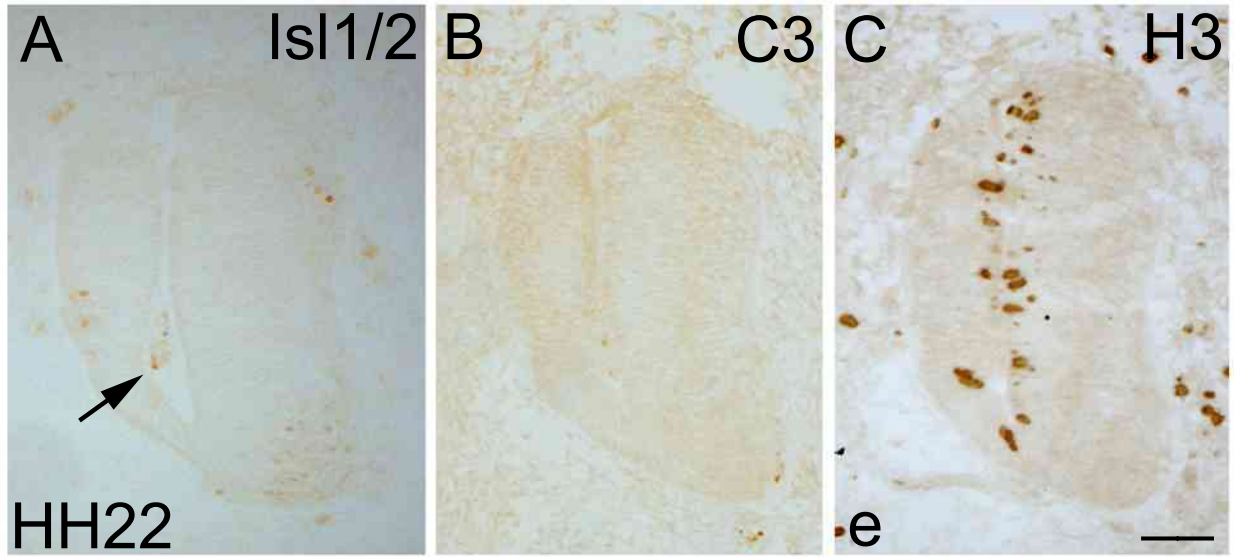
A**B****C**

Figure 6.5 Immunocytochemical markers in transverse sections of HH22 chick brachial spinal cord in a PTP γ -IRES-GFP treated embryo to (A) Islet 1/2, showing the ectopic expression of this marker within an island of cells in the ventricular lumen (B) Caspase 3, showing no cell death in serial sections of the same embryo and (C) pHistone3 in serial sections. Scale bar is 0.5mm.



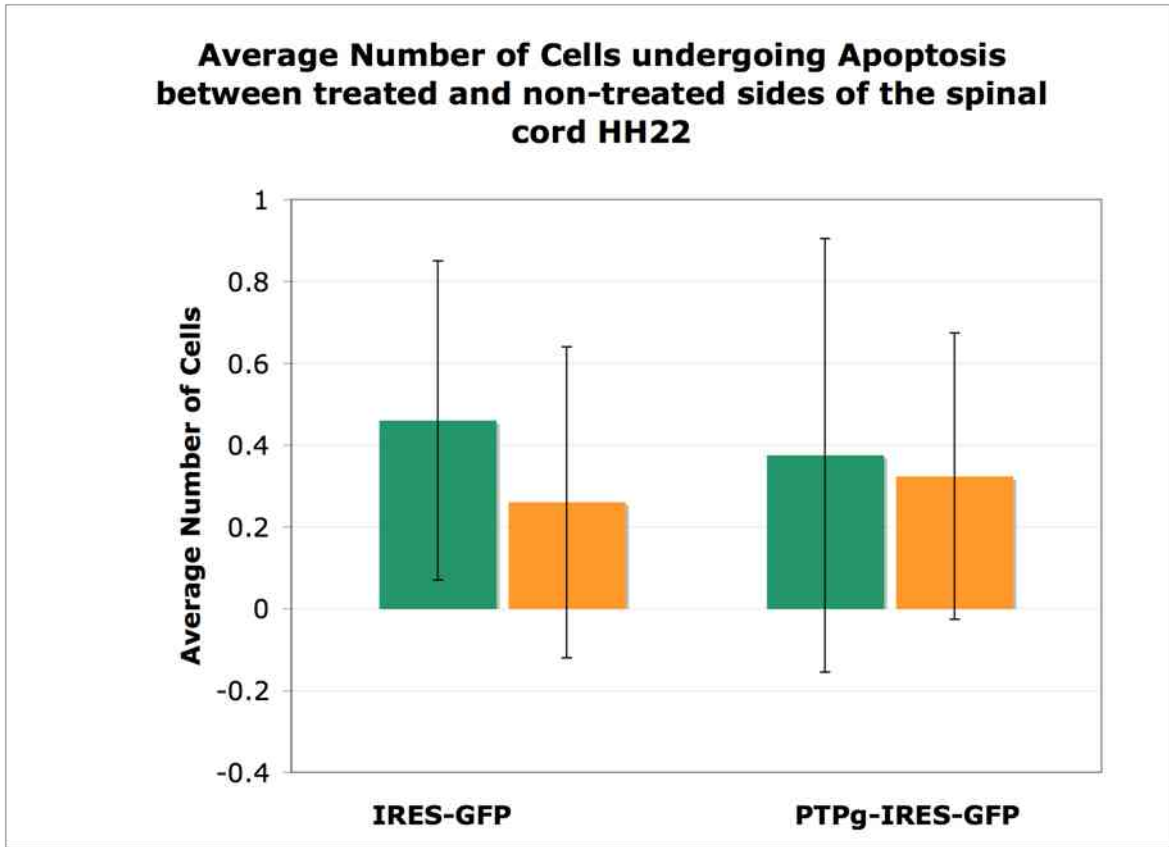
6.4 PTP γ gain-of-function does not lead to apoptosis.

To gauge whether PTP γ gain-of-function was triggering apoptosis, the number of apoptotic cells amongst our experimental groups at HH 22 were quantified using activated Caspase-3 as a marker for cell death. Within PTP γ -IRES-GFP treated embryos, on average there were 0.38 and 0.32 cells observed between treated and non-treated sides of the spinal cord respectively. Amongst control IRES-GFP treated embryos this value remained very low at 0.46 and 0.27 between treated and non-treated sides respectively (Figure 6.6).

Essentially there was no significant difference in apoptosis levels between sample sets, with each embryo having less than one apoptotic cell on average between the 3 sections counted for each embryo. In conclusion, the over-expression of PTP γ does not trigger apoptosis and the lack of apoptotic cells in any location at HH 20-22 reveals that cells, either in a radial glial state or as differentiating neurons, are not dying at a significant rate (Homma et al, 1994; Li et al, 1998).

These findings lead us to ask a further question to account for the loss of spinal cord tissue and LIM HD positive neurons in tissue over-expressing PTP γ . If no cell death programme has been initiated one could either assume that a minority of LIM HD fated cells were not being born, or that the radial glial cells giving rise to such neurons were blocked at some stage of the cell cycle whereby they were not able to self renew or proliferate.

Figure 6.6 Chart – Average numbers of cells undergoing apoptosis as measured by Caspase3 between treated and non-treated sides of the spinal cord at HH22. IRES-GFP (n=6) ($P < 0.001$; Student T test) and PTP γ -IRES-GFP (n=23) ($P < 0.001$; Student T test) samples compared, showing no significant change in the number of dying cells amongst the sample groups. The green bars represent the treated half of the spinal cord and the yellow bars the non-treated half of the spinal cord among the two experimental sets of embryos treated with IRES-GFP as a control and PTP γ -IRES-GFP to drive the over expression of PTP γ (Error bars show SD).



Key : **Green Bars** denote the average number of cells on the treated sides of the spinal cord among control IRES-GFP & PTP⁻-IRES-GFP sample groups. **Orange Bars** denote the average number of cells on the non-treated sides of the spinal cord among control IRES-GFP & PTP⁻-IRES-GFP sample groups.

6.5 Measuring the mitotic activity at HH22

The mitotic activity of samples was measured at HH 22 using p-H3 as a marker of M-phase of the cell cycle. Representative samples within the sets that demonstrated a reduction of motor neuron phenotype and high PTP γ over expression levels were studied further to gauge the proliferation state of progenitor cells. (Figure 6.3, Panel F).

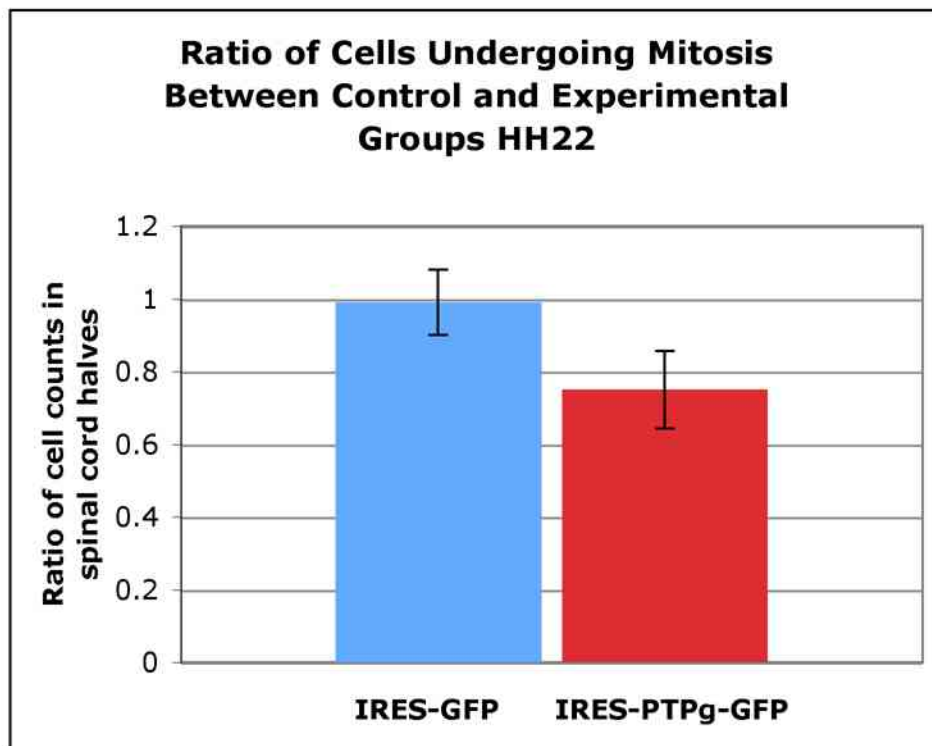
Amongst 11 embryos at HH 22 treated with IRES-GFP and 15 embryos treated with PTP γ -IRES-GFP, pH3 activity was reduced 25% in PTP γ treated cases, compared with a 1% reduction in control samples (Figure 6.7). This finding suggests that the proliferative potential of LIM-HD fated neuronal progenitors was indeed decreased after PTP γ gain-of-function.

A significant reduction of cells undergoing mitosis is observed. This may favour a hypothesis that a number of radial glial progenitors are either arrested at a stage of the cell cycle, or that some other phase of the cycle is lengthened by high levels of PTP γ .

6.6 PTP γ over-expression does not affect the rate of S-phase.

Radial glial cells have a distinct morphology during S-phase of the cell cycle, whereby their nuclei shuttle back and forth in the mantle zone whilst synthesising DNA. Embryos injected with the BrdU tracer prior to harvesting will incorporate the molecule as they synthesise new DNA strands and this can be detected with an antibody against BrdU.

Figure 6.7 Chart Showing the ratio of cells detected with pH3 at HH22 between treated and non-treated sides of the spinal cord amongst IRES-GFP (n=11) and PTP γ -IRES-GFP (n=15) treated samples. A slight reduction is evident in the number of cells at M Phase of the cell cycle between treated and control groups ($P < 0.0001$: Student T Test) (Error bars show SD).



Blue Bars denote ratio of cells between treated and non treated sides of the spinal cord among control IRES-GFP samples. Red Bars denote ratio of cells between treated and non treated sides of the spinal cord among PTP γ -IRES-GFP samples.

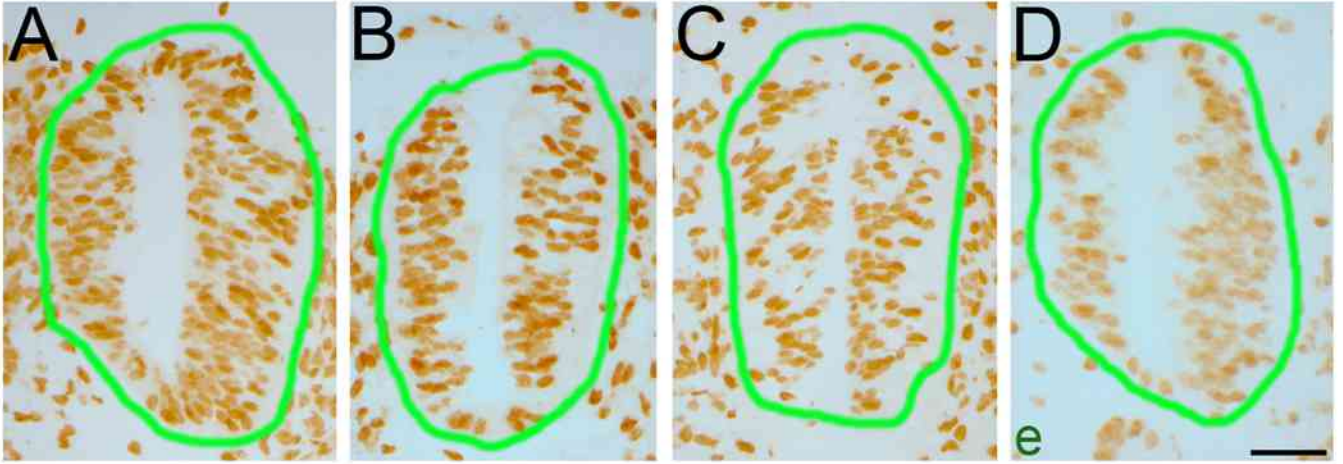
In a preliminary study, stage HH 10 embryos injected with IRES-PTP γ were treated with BrdU for half an hour prior to harvesting at HH 18. The treated side of the spinal cord revealed a reduction in the number of BrdU positive S-phase cells along with a corresponding reduction in the spinal cord area (Fig 6.8, Panels A-D). The BrdU labelled cells occupied the entire length of the spinal cord albeit in reduced numbers. The total number of cells and areas of the spinal cord were measured in Open Lab (Figure 6.9). The sample set at HH 18 consisted of 10 treated embryos over-expressing PTP γ and 5 control Embryos expressing the IRES-GFP vector. Two to three sections from each embryo were measured and an average for each embryo was obtained. These values were then compared amongst the representative groups and an average number of cells and ratios obtained.

The average number of BrdU and therefore S-phase cells was reduced to a ratio of 0.76 (relative to 0.97). This was true when comparing the average ratio of cells on the treated and non-treated sides of the spinal cord within the PTP γ -IRES-GFP and IRES-GFP samples sets respectively (Figure 6.10, Chart A). The corresponding area of the spinal cord was also reduced by a ratio of 0.79 (relative to 1.04) (Figure 6.10 Chart B). Raising PTP γ levels non-physiologically after HH10 and before its normal expression by HH18 may have an impact on the proliferative activity of the neural tube.

When the ratio of cells on treated and non-treated sides amongst sample groups were corrected against the ratio of their corresponding areas, we obtained a value close to 1 (Figure 6.10, Chart C), indicating that we were not observing proportionally less S-Phase cells per unit area, despite the loss of tissue. Thus the process of DNA replication within progenitor cells seems unaffected at this embryonic stage.

Figure 6.8 BrdU labelling in transverse sections of HH18 chick brachial spinal cord treated with PTP γ -IRES-GFP, labelled with BrdU prior to sectioning. Immunocytochemical staining of BrdU (A-D) Outline indicates boundary of the neural tube and the cells within this were quantified in four different examples. Scale bar is 0.5mm.

Figure 6.9 Screenshot of the Openlab software and method of counting the proliferating cells. The floor plate and roof plate regions were not counted.



Grab File Edit Capture Window Help

ires-a1

ires-a1 Measurements

No.	Line Name	No.	R...	Area	Perimeter	Width	Height	No.	Point
1				152606592.000	51869.246	7848.000	24552.00		
3				116323776.000	47458.898	6552.000	22392.00		

302 x 592, Millions of Colors

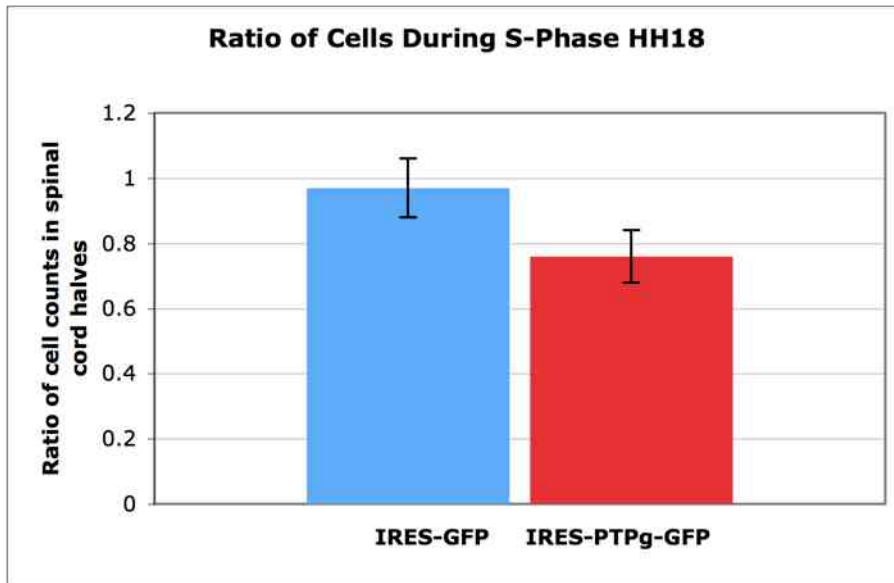
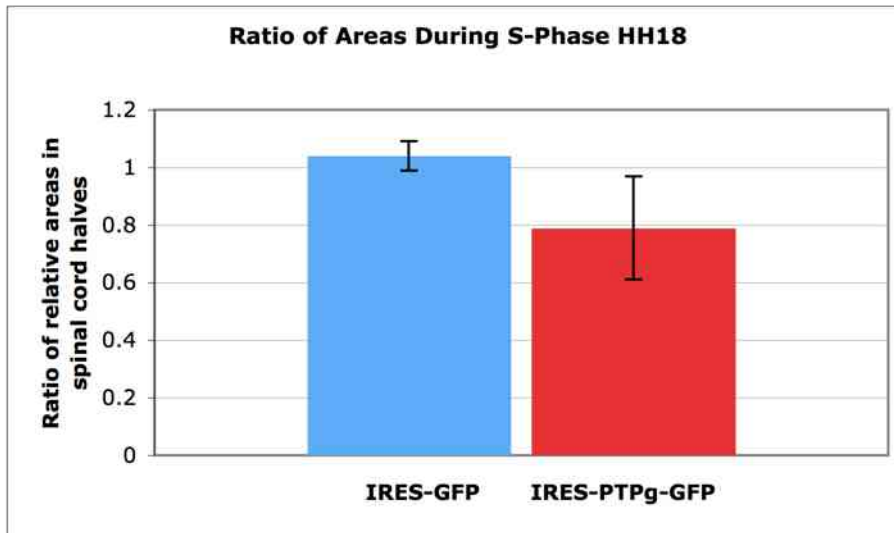
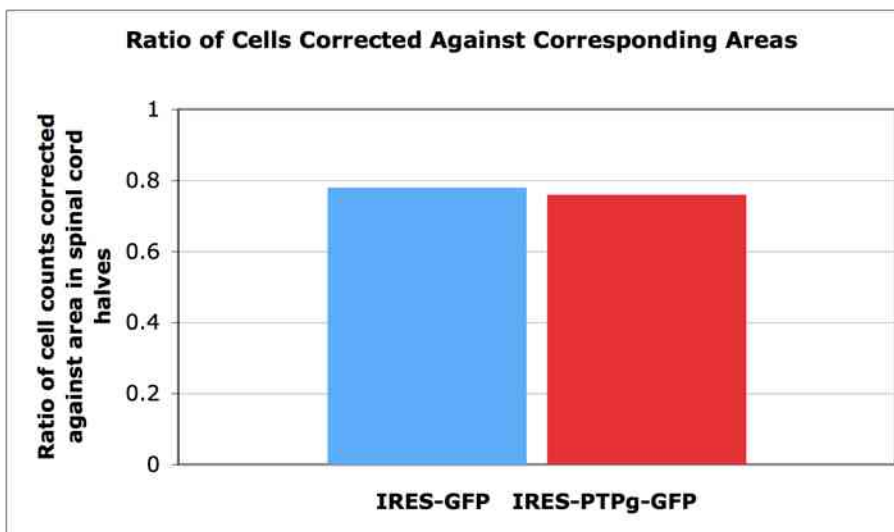
Windows XP - Parallels Desktop

start EN 15:26

Click inside OS Window to capture mouse

The screenshot shows a software interface for image analysis. The main window displays a histological image with two red outlines. A 'Grab' application window is open, showing the image with various toolbars and a status bar. A 'Grab File Edit Capture Window Help' menu is visible at the top. A 'Grab' toolbar is on the left. The 'Grab' status bar shows coordinates: -1008.00, 6840.000, 0.0000, 0.0000. A 'Grab' window titled 'ires-a1' is open, showing the image with two red outlines. A 'Grab' window titled 'ires-a1 Measurements' is open, showing a table with columns: No., Line Name, No., R..., Area, Perimeter, Width, Height, No., Point. The table contains two rows of data. The 'Grab' status bar shows '302 x 592, Millions of Colors'. The background shows a Windows XP desktop with a 'Recycle Bin' icon and a taskbar with the 'start' button, 'EN' language indicator, and '15:26' time. A 'Click inside OS Window to capture mouse' message is at the bottom.

Figure 6.10 Charts of LIM-HD BrdU positive cell numbers at HH18 between IRES-GFP (n=6) and PTP γ -IRES-GFP (n=10) treated embryos. (A) Ratio of cells during S-phase between control and treated groups demonstrated a reduction in proliferating cell number amongst PTP γ gain-of-function samples. (B) Ratio of spinal cord areas in corresponding samples between control and treated groups shows a reduction in the area of the spinal cord in PTP γ over-expressed samples. (C) Ratio of proliferating cells corrected against the corresponding areas shows no change in the overall number of cells undergoing S-Phase in sample sets (Error bars show SD).

A**B****C**

6.7 Discussion

The impact PTP γ gain-of-function had on spinal cord tissues at HH20 and HH22 was determined through the expression on neuronal markers following PTP γ -IRES-GFP treatment and electroporation of the neural tube. The results indicate that PTP γ gain-of-function led to a reduction in the total number of Lim1/2, Lim3, Mnr2 and Islet1/2 cell populations through to HH22. The area of the spinal cord also appeared reduced in treated samples and this reduction was not thought to be a result of cell death as activated Caspase3 staining revealed no significant differences in cell death when compared to control samples.

The mitotic activity, at M-Phase of the cell cycle within the sample groups was measured, revealing a decrease in the proliferative activity of neural progenitors as a result of PTP γ gain-of-function. This suggested that the radial glial progenitors were either arrested at a particular point in the cell cycle, or that PTP γ gain-of-function resulted in a lengthening of a phase of the cell cycle ultimately reducing the proliferative capacity of the spinal cord. Further preliminary studies using BrdU labelling to measure the number of cells undergoing S-Phase between control and PTP γ gain-of-function groups revealed that the process of DNA replication within progenitors seemed unaffected. During PTP γ gain-of-function, the gene acts in regions it is not normally expressed and proportionally affects a larger number of cells which maybe an important consideration. The role PTP γ may have during the progress of the cell cycle and interaction with the cell matrix will be discussed further in the concluding chapter.

Chapter 7: Silencing PTP σ

7.1 Introduction.

A structurally different member of the PTP family to PTP γ , PTP σ , has been implicated in neuronal development and its expression is localised on axonal growth cones and among spinal motor neurons (Stoker et al, 1995; Chaapveld et al, 1998; Chilton & Stoker 2000). In the mouse, PTP σ and its various isoforms have been shown to promote axon outgrowth and growth cone guidance (Ledig et al, 1999; Rashid-Doubell, 2002).

Ligands for PTP σ have been described in the chick, namely Heparan Sulphate Proteoglycans within the retinotectal system (Haj et al, 1999; Aricesu et al 2002; Sajani-Perez, 2003). These molecules have been shown to be required for motor neuron development and have been ascribed a role in the midline guidance of axons (Uetani et al, 2006; Inatani et al, 2003; Stepanek et al, 2005). A further ligand for PTP σ has also been described, Nucleolin, which is expressed in developing muscle tissue (Alete et al 2005).

The PTP σ knock out in the mouse has highlighted its role during the proliferation and adhesiveness of neuronal cell types (Elchebly et al, 1999). These mice presented defects in pituitary gland development, reduced brain size and retarded growth patterns (Wallace et al, 1999).

7.1.1 PTP σ expression and RNAi

PTP σ has a striking expression pattern in the early spinal cord, with areas of strong expression in the ventricular zone and mantle zone, where the various neuronal subtypes are generated, and in the lateral motor columns by E4 (Chilton & Stoker, 2000). A lower level of expression is observed throughout the remainder of the cord. PTP σ expression remains within in the ventricular zone to E6 (Chilton & Stoker, 2000).

A recent study using dsRNAi in ovo to knock down the expression of PTP σ and other phosphatases during neurogenesis in the lumbar region has shown defects in the dorsal anterior iliotibialis nerve despite apparently normal development of the limbs (Stepanek et al, 2005). Combined RNAi targeting of two or more PTPs has shown less severe phenotypes than the silencing of single PTP implying a dose dependant function of PTPs during axonal outgrowth or a degree of functional redundancy. This also suggest that PTPs may work through mutual antagonism as is seen in drosophila studies (Desai et al, 1996).

7.1.2 Aims.

The expression and function of this gene in the chick has not been studied in the early spinal cord prior to HH18. In order to elucidate its function during neurogenesis, RNAi was used to transiently reduce PTP σ expression levels in this domain. In this section, I aimed to collect preliminary data on PTP σ function and generation of motor neurons from mitotically active radial glia, coincidentally the site of early PTP σ expression.

7.2 PTP σ loss-of-function constructs and in ovo electroporation.

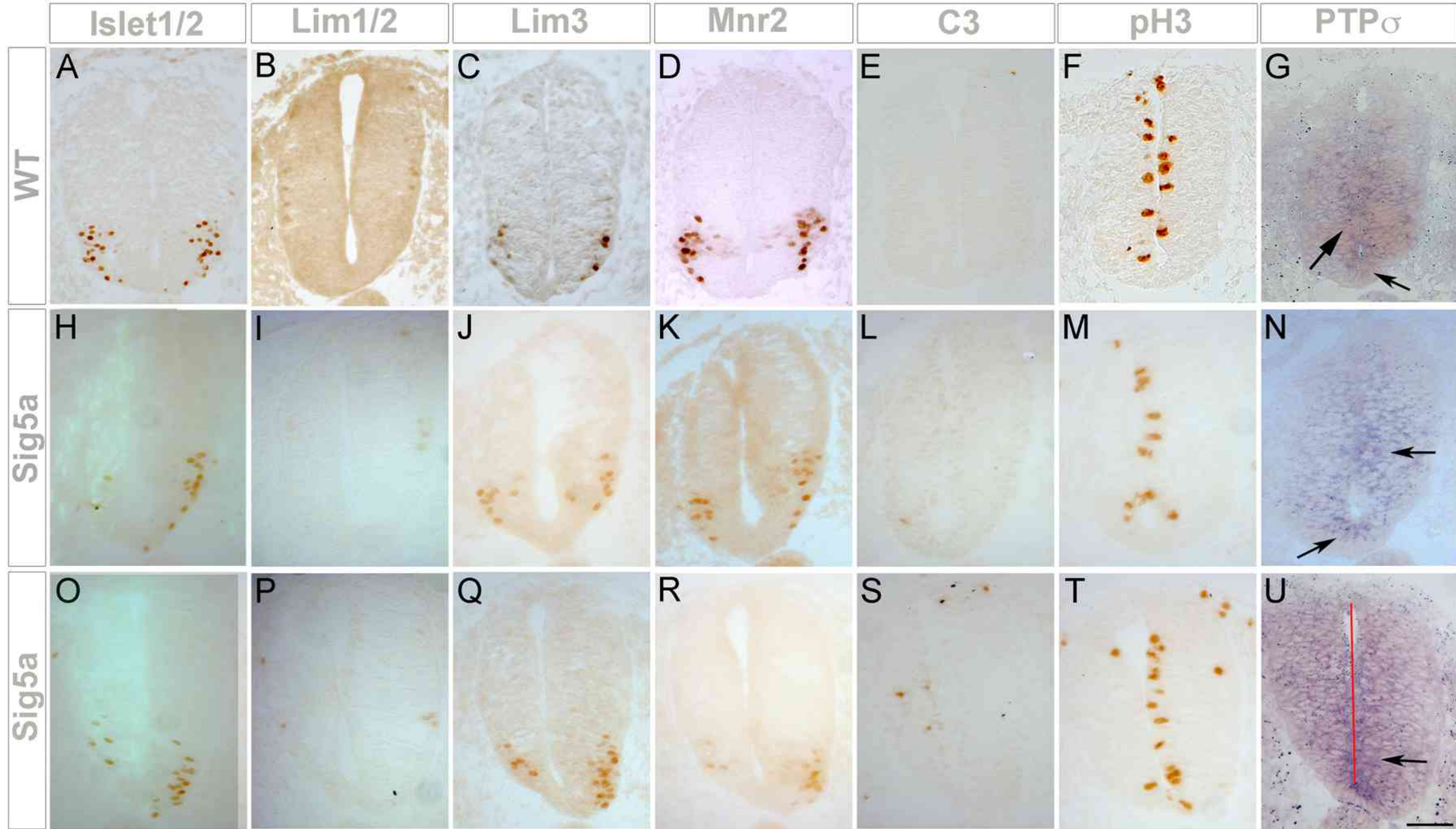
Six loss-of-function constructs were generated against PTP σ (Chapter 3.2.1). Based on in vitro experiments, the vector Sig5a was found to induce very effective PTP σ loss-of-function due to its strong knock down in HEK 293T cells (Figure 3.5). This construct was injected into the neural tube at the brachial level to a final concentration of 1-2 μ g/ μ l at HH10 according to the same protocol as the PTP γ silencing experiments. A control set of embryos treated with a control hairpin-encoding vector were harvested at HH18 following the onset of PTP σ expression, and treated in a similar way to PTP σ silenced embryos.

7.3 PTP σ silencing has a general effect on LIM-HD expressing cells.

Using in situ detection, PTP σ mRNA revealed a diffuse expression pattern within the ventricular and intermediate zones, with higher patterns of staining associated closely with the ventricular layer of mitotic cells (Figure 7.1 Panel G, N, U Arrows). Strong levels of expression were also detected amongst the floor plate cells (Figure 7.1 Panel G, arrow).

Embryos electroporated with control vector showed a normal pattern of development as previous cell counts demonstrate (see Chapter 5). As the same control vectors were used for PTP γ and PTP σ loss-of-function studies, these control experiments were not repeated here. No significant apoptotic activity was observed and both the frequency and the distribution of mitotic cells appeared normal (Figure 7.1 Panels E & F).

Figure 7.1 Immunocytochemical and DIG-labelled mRNA in situ hybridisation in transverse serial sections of HH18 chick brachial spinal cord wild type (A-G), and two Sig5 treated embryos (H-N) & (O-U) to (A) Islet 1/2 (B) Lim 1/2, (C) Lim 3; (D) Mnr2; (E) Caspase3; (F) pHistone3 showing a reduced number of mitotic cells; (G) PTP σ arrows indicate stronger areas of expression in the ventricular zone and floor plate; (H) Islet 1/2 (I) Lim 1/2, (J) Lim 3; (K) Mnr2; (L) Caspase3; (M) pHistone3; (N) In situ to PTP σ , arrow shows area of stronger PTP σ staining; (O) Islet 1/2 (P) Lim 1/2, (Q) Lim 3; (R) Mnr2; (S) Caspase3; (T) pHistone3; (U) In situ to PTP σ , red line represent neural tube midline, arrows show areas of strong PTP σ staining. Scale bar is 0.5mm.



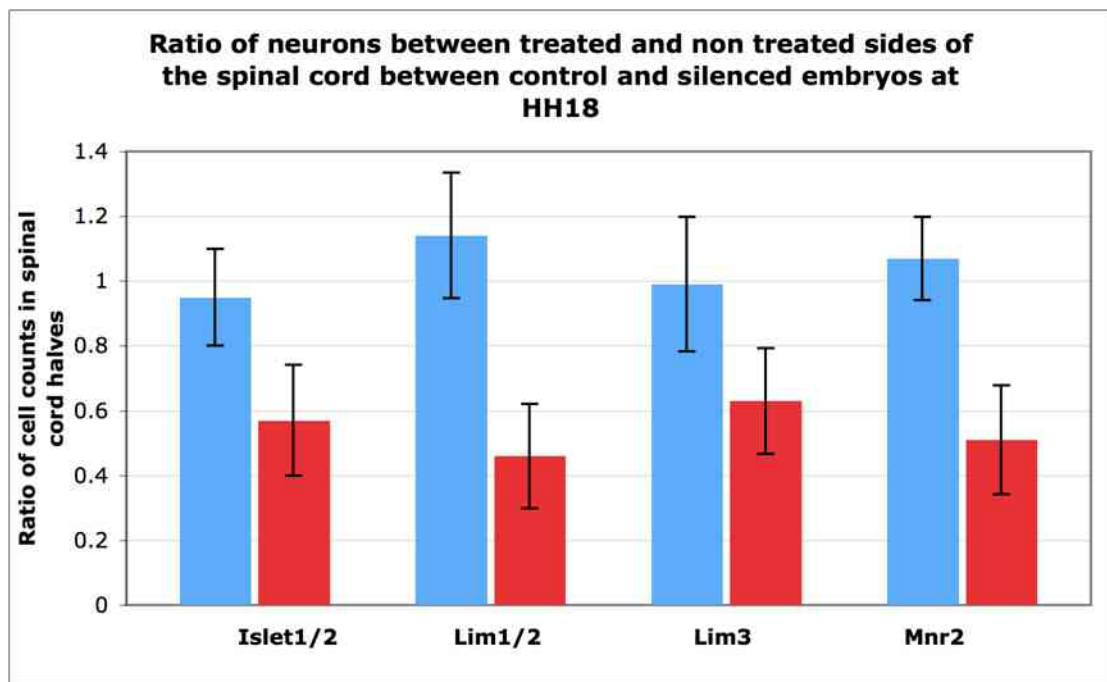
Amongst 12 embryos treated with Sig5a, a consistent and significant reduction in the number of LIM-HD expressing cells was evident in 9 out of 12 embryos (Figure 7.1 Panels H-K and O-R, two examples shown). By in situ hybridisation, there was little evidence of a reduced RNA signal, however the PTP σ probe did not give as clean a signal as the PTP γ probe. The shRNA could, however be reducing RNA translation of PTP σ (see Discussion) (Figure 7.1 Panels N & U).

Cells counts were carried out on these cell populations as previously described and amongst a set of 9 PTP σ loss-of-function embryos, the ratio of Islet1/2 cells on the treated and non-treated sides of the spinal cord between control and PTP σ silenced sets reduced from 0.95 to 0.57 respectively (Figure 7.2). Lim1/2 demonstrated a similar trend, with a significant reduction in the ratios between embryos of 0.99 to 0.46 (Figure 7.2). Lim3 cell numbers were down on average from a ratio of 0.95 to 0.63 and finally Mnr2 positive cells were reduced in number amongst silenced embryos by of 0.97 to 0.51 (Figure 7.2). This demonstrates a broad reduction in the total number of LIM HD expressing cells by PTP σ loss-of-function at stage HH18.

7.4 PTP σ loss-of-function triggers apoptosis of LIM HD fated progenitor motor neurons in the spinal cord.

Observing the apoptotic activity of cells within the spinal cord amongst controls and PTP σ silenced embryos by Caspase-3 activity, a significant up-regulation of the apoptosis programme within the neural tube was seen.

Figure 7.2. Chart of LIM-HD positive cell numbers. Ratio of neurons compared between treated (Blue Bars) and non treated (Red Bars) sides of the spinal cord between control and PTP σ loss-of-function embryo sets at HH18. All four markers studied, Islet 1/2 (n=8)(P<0.001; Student T Test), Lim 1/2 (n=8)(P<0.0001; Student T test), Lim 3 (n=9)(P<0.001; Student T Test) and Mnr 2 (n=8)(P<0.0001; Student T Test) showed a significant reduction in their cell numbers in PTP σ loss-of-function groups (Error bars show SD).



Key: **Blue Bars** denote ratio of cells between treated and non-treated sides of the spinal cord among control shRNA samples. **Red Bars** denote ratio of cells between treated and non-treated sides of the spinal cord among PTPσ loss of function samples.

This was less than 1 apoptotic cell on each section amongst controls to 3.4 cells on average on the treated side of PTP σ silenced embryos (Figure 7.3). These cells appear to be at different dorsoventral locations in the spinal cord and amongst our sample set of 9 embryos they appeared not to be restricted to any particular progenitor domain (Figure 7.1, Panels 7.1 L & S). We can conclude from these findings that neural tube cells at different locations undergo apoptosis after PTP σ loss-of-function, correlating with a ‘narrowing’ of the spinal cord area on the treated side of silenced embryos.

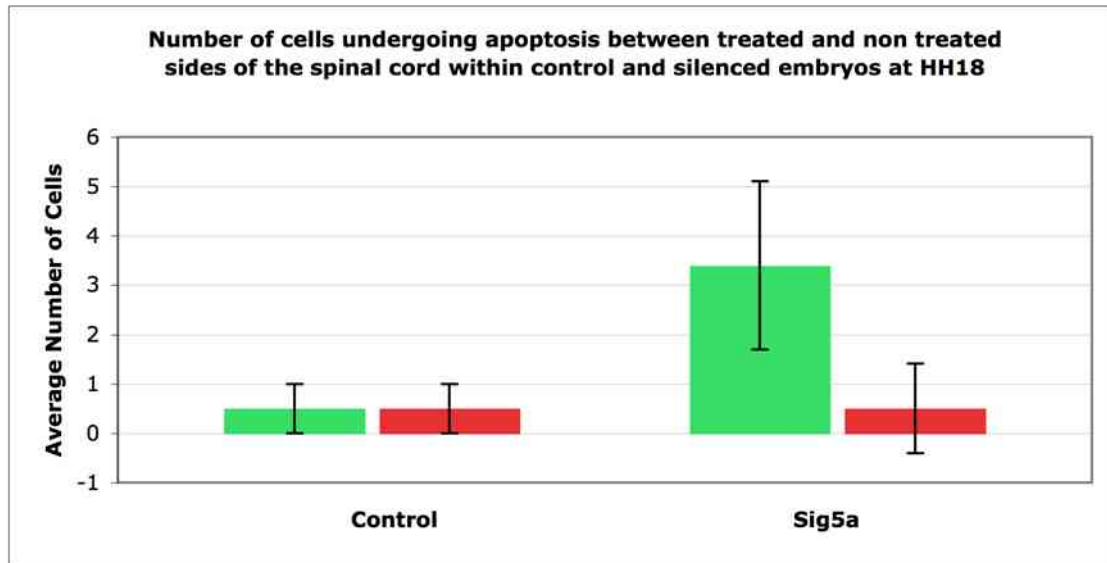
7.5 PTP σ gain-of-function induces a reduction in the number of mitotically active radial glia.

Further studies recording the mitotic activity of ventricular zone reveals a highly significant reduction in the number of proliferating cells along the ventricular zone associated with the lumen. Amongst 8 PTP σ loss-of-function embryos, the number of phosphorylated Histone 3 positive cells when compared to controls was reduced in number on average from a ratio of 0.93 to 0.60 (Figure 7.4) (Figure 7.1 Panels M & T). Amongst PTP σ loss-of-function embryos PTP σ mRNA expression appears slightly reduced, when compared to the control side, yet this maybe a result of the loss of neural tube tissue observed (Figure 7.1 N & U).

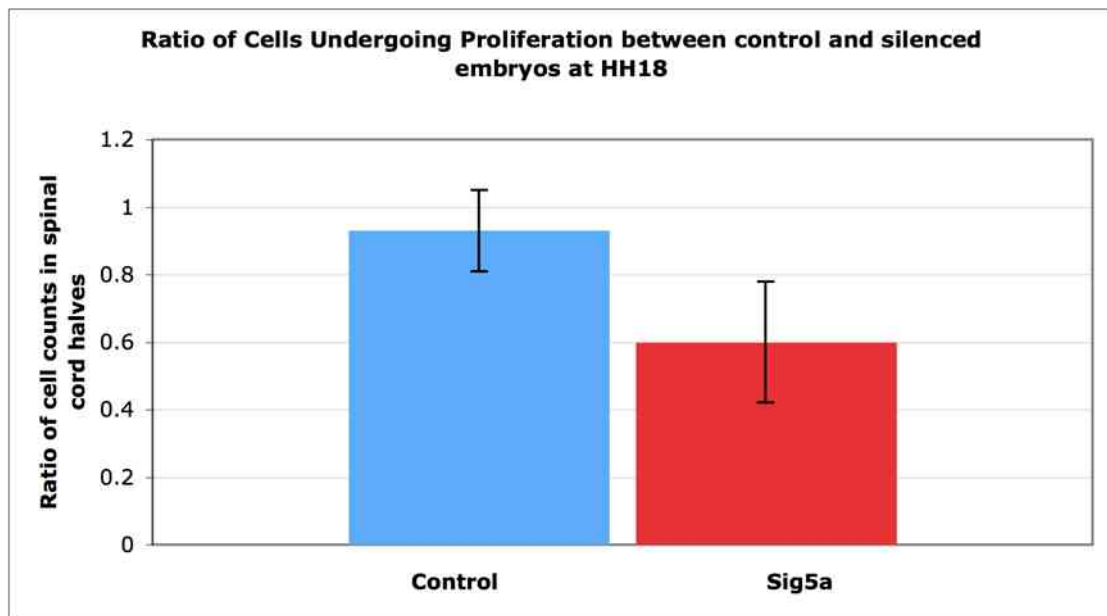
These results show that a plausible explanation for the reduction of LIM HD expressing cells within treated samples, is that their progenitor populations are being depleted or are stalling at some stage of the cell cycle preventing normal entry to M-Phase. The reduction in cell number can also be partly attributed to a triggering of the apoptosis programme evident from the caspase-3 staining within the spinal cord.

Figure 7.3 Chart of Caspase 3 positive cell numbers. Number of cells undergoing apoptosis between treated (Green Bars) and non treated (Red Bars) sides of the spinal cord between control and PTP σ loss-of-function embryo sets at HH18. The control embryos showed no significant change in the number of dying cells (n=6)(P<0.01; Student T Test) however this was significantly increased in PTP σ loss-of-function groups, observing 3 cells on average on the treated half of the neural tube (n=8)(P<0.001; Student T Test) (Error bars show SD).

Figure 7.4 Chart of proliferating cell numbers. Ratio of cells undergoing proliferation between treated (Blue Bars) and non treated sides (Red Bars) of the spinal cord between control and PTP σ loss-of-function embryo sets at HH18 (n=8)(P<0.01; Student T Test) (Error bars show SD).



Key : **Green Bars** denote the average number of cells on the treated sides of the spinal cord among control shRNA & Sig5a sample groups. **Red Bars** denote the average number of cells on the non-treated sides of the spinal cord among control shRNA & Sig5a sample groups.



Key: **Blue Bars** denote ratio of cells between treated and non-treated sides of the spinal cord among control shRNA samples. **Red Bars** denote ratio of cells between treated and non-treated sides of the spinal cord among Sig5a shRNA PTP σ loss of function samples.

7.6 Discussion.

The data reveals a pattern of PTP σ gene expression within the sub-ventricular zone, mantle layer, floor plate and stronger expression proximal to the ventricular lumen, the site of mitotically active precursor cells. Reducing this activity along the dorsoventral aspect of the spinal cord leads at HH18 to a reduction in the number of cells fated with LIM-HD expression profiles. Further analysis using markers of apoptosis and proliferation show that the reduction in cell numbers is brought about by both cell death within the ventricular zone, and a reduction the proliferative capacity of radial glia at the ventricular surface.

In comparison, no obvious defects were detected at HH18 amongst the PTP γ loss-of-function embryos attributable to the onset of this gene's expression at around HH18. PTP σ is however expressed clearly by HH18 in the spinal cord, unlike PTP γ . This may explain why at stage HH18 Sig5a demonstrated an effect on the spinal cord whereas Si3 at this stage did not yield any phenotypes. Furthermore, amongst the Sig5 treated samples studied at HH18, none displayed evidence of mislocated cells through their expression of LIM-HD expression factors. This is unlike the heterotopic phenotype observed with PTP γ at later stages.

Recent studies on the functions of PTP σ and PTP δ in mice using double knockouts carrying a combination of alleles reveal a loss of motor neurons in the spinal cord and muscle dysgenesis. The single gene knockouts were, however, viable suggesting these genes may complement each other's function. Moreover, these double mutants appeared normal at E13 when analysed using Islet-1. However, at E18.5 in the mouse

(approximately HH44 in the chick) a motor neuron deficit was detected and a single gene dose of PTP σ was sufficient for the survival of these motor neurons during axon extension (Uetani et al, 2006). PTP σ therefore makes an essential contribution to motor neuron survival at later stages of development in mammals. Our experiments further support a role for PTP σ in LIM-HD motor neuron development in the spinal cord from the mouse to the chick, however as PTP σ loss of function mutants in the mouse were viable (possibly due to functional redundancy with other RPTPs) in the chick this the loss of PTP σ may not be compensated.

It would be interesting to determine the effects of double silencing directed against PTP σ and PTP γ and moreover if PTP γ overexpression is able to either enhance or rescue the early defects seen at HH18 amongst PTP σ loss-of-function embryos. The PTP σ loss-of-function experiments show that shRNAi can be used for another RPTP expressed in the spinal cord, and that PTP γ and PTP σ may be involved in motor neuron proliferation during the early stages of neurogenesis.

Chapter 8: Discussion

The balance of phosphorylation states of proteins in cells during neuronal development gives rise to intricate patterns of neuronal connectivity, as previous studies into the function of the Ephrin and PTP receptors have demonstrated. Phosphorylation enables receptors to communicate, and is involved in the guidance of axons to their target sites. The function of numerous signalling pathways are dependent upon this very balance with PTKs and PTPs working to phosphorylate and dephosphorylate key protein interactors involved in cell proliferation and neuronal migration (den Hertog et al, 2008; Larsen et al, 2003). In this thesis I have shown for the first time that a receptor tyrosine phosphatase, PTP γ , can control proliferation and survival of neural tube progenitors. My data also suggests that PTP γ influences the localisation of neural precursors mediolaterally in the cord.

PTP's and PTK's have been shown to be associated with adhesive sites that bind to the cell matrix. The neural tube following closure consists of exclusively radial glial cells attached to the ventricular surface at one end and to the pial surface through pial end feet at the other (Fujita 2003). The nuclei of these self-renewing cells shuttle back and forth through INM driven by microtubules and actin fibres, as the cell progresses through the cell cycle during growth and synthesis stages in the outer half of the ventricular zone. It is at the ventricular surface that cells undergo mitosis where they acquire information from their environment that specifies their fate. During mitosis the integrity of the adhesive junctions are temporarily compromised, allowing the radial glial progenitor cells at the midline to undergo division and proliferation, after

which time these junctions are re-established (Jacobson, 1991; Hartsock & Nelson, 2007). Adherens junctions have Cadherins and Catenins both of which are controlled by tyrosine phosphorylation (Nelson et al, 2004; Lilien & Balsamo, 2005).

At the end of mitosis, cells either decide to differentiate and migrate towards the pial surface, losing their connections at both ends, or re-enter the cell cycle and form adherens junctions and pial end feet. These events are governed by a complex series of phosphorylation and dephosphorylation controlled by cell-cell interactions and diffusible factors within the neural tube. (Fujita, 2003; McDermott, 2005; Orford & Scadden, 2008).

Wnt signalling through the β -catenin pathway has been shown to regulate cell cycle progression, controlling the entry and exit of progenitor cells through this cycle. The transcriptional regulation of the Cyclin genes and balance of phosphorylation states have served as 'start' and 'stop' cues. Moreover β -catenin itself undergoes tyrosine phosphorylation (Brault et al, 2001; Megason & McMahon, 2002). The influences of the β HHLH and LIM-HD genes then guide differentiated neurons to domain specific locations in the periphery guided along the radial glia parent cell (Lumsden, 1995; Hollyday, 2001; Wilcock et al, 2007). Tyrosine phosphorylation of proteins is therefore a post translational modification that regulates the signal propagation of receptors leading to proliferation, differentiation and communication with the neighbouring cells, cell matrix components and their associated adhesive properties (Burridge et al, 2006; Sallee et al, 2006).

The expression profiles of members of the RPTP family in the neural tube suggested they might have a specific function in the development of this tissue. A few studies to date have highlighted the role of members of the RPTP family in the spinal cord, but only during axon growth and guidance and motor neuron targeting and survival (Stepanek et al, 2005; Uetani et al, 2006). The aims of our study were to address the role of these receptors during earlier neurogenesis and spinal cord development, initially looking principally at PTP γ , but also PTP σ function (Chilton & Stoker, 2000; Gustafson & Mason, 2000).

In the mouse, knock out studies of PTP γ have not shed light on its potential function within the nervous system (Lamprianou et al 2006). A recent study has described the crystal structures of the carbonic anhydrase-like domains of PTP γ and demonstrated their interaction directly with immunoglobulin subunits of members of the contactin family. These molecules are GPI anchored membrane proteins that can interact with extra cellular cues. They are involved in the construction of neural networks and this was the first report of potential ligands for PTP γ (Bouyain & Watkins, 2010).

To address the function of RPTPs *in vivo*, RNAi was considered an appropriate approach to silence RPTP genes. It could be used flexibly, both temporally and spatially, in order to analyse gene function, although few studies had used it *in ovo* when I started this project. I confirmed the efficiency of the loss-of-function shRNA constructs in culture, and showed these genes could be specifically targeted through RNAi. From the six silencing constructs generated for PTP γ , three provided a knock down of over 80% in *in vitro* studies using human carcinoma cell cultures. Using these vectors, the results of perturbing PTP γ function *in ovo* demonstrated an effect

on cell cycle progression, differentiation and lateral positioning of LIM-HD motor neurons and dorsal interneurons.

8.1 PTP γ loss-of-function function disrupts neurogenesis in the chick.

Knocking down PTP γ *in ovo* initially gave us a range of phenotypes histologically. In severe cases, we observed heterotopia with a disruption of the ependymal cell layer and luminal ingrowths of neurons. When immunohistochemically stained with various antibodies, the cells within the ingrowths stained positive for Nkx2.2 and Islet1/2 and were therefore differentiating cells residing in ectopic locations.

Milder phenotypic cases displayed a truncation of the spinal cord, in particular a dorsoventral shortening and mediolateral narrowing of the neural tube. There appeared to be no significant changes in the numbers of Islet1/2 positive cells between control and loss-of-function embryos at E5. However, a significant finding was that a large reduction was seen in the number of Lim1/2 positive cells on the electroporated side of the neural tube.

The PTP γ knockout mouse has been generated and presents no motor or interneuron specific spinal cord defects, yet it is worthy to note that the expression patterns of this gene are very different between species (Lamprianou et al 2006). In stark contrast to the chick, it was shown that PTP γ is not expressed widely in the early mouse spinal cord (Chilton & Stoker, unpublished data). Furthermore, Lamprianou and colleagues identified murine PTP γ expression at low levels among oligodendrocytes and microglia within glial cultures. Murine PTP γ expression was also seen in all the

sensory organs such as the eyes, ears and tongue suggesting a role for PTP γ in sensory neurons.

The murine expression profile of PTP γ may thus suggest that the function of PTP γ in the chick spinal cord may be replaced by another RPTP in the mouse, suggesting redundancy amongst the phosphatases across species. Future experiments may consider crossing two transgenic mouse lines to generate double knockouts with PTP γ , particularly RPTPs with similar expression patterns in order to address possible redundancy issues, namely double loss of function of PTP γ with PTP σ , PTP δ and PTPZ/ β both in the mouse and chick (Chilton & Stoker, 2000).

8.2 PTP γ function and Lim HD transcription factors

A significant phenotype observed in the majority of successfully electroporated cases was a deficit in LIM HD expressing motor and interneurons, especially those expressing Lim1/2 in the LMC and more dorsal interneurons. Embryos observed prior to PTP γ expression around HH18 appeared normal, and cellular deficits were only observed after HH20. The lateral aspect of the LMC appeared most affected as neurons only begin to populate this branch of the motor column at around HH18 (Tsuchida et al, 1994). This suggests that Lim1/2-positive cells in the LMCI may be a specific target of PTP γ . The effects on Lim1/2 may be due to a specific functional requirement for PTP γ during the development of these neural cell groups. Another more mundane possibility for the effect of PTP γ loss-of-function on Lim1/2 cells, may be largely the temporal coincidence of PTP γ expression and function with the birthdates of LMCI neurons.

The loss of neurons coincides with the onset of PTP γ expression within the neural tube as it extends from its dorsal and lateral origins to more ventral locations. The smaller dorsal loss of Lim1/2 cells may suggest that other PTPs operate a certain level of functional redundancy that could compensate for the dorsal function of PTP γ . PTP γ function may also be dose-dependent, where loss-of-function may not remove 100% of PTP γ function and thus have more of an effect on low level expression within the pMN domain.

The pMN domain was most sensitive to the mislocation of neurons seen and therefore appeared most readily affected, due to its lower PTP γ expression compared to dorsal or lateral cells. It is also worthy to note that the effects of the shNRA vectors delivered by electroporation is likely to be transient and a certain level of recovery may ensue past HH20, as the shRNA expression becomes diluted away.

Future experimental strategies may involve using either a retroviral or a lentiviral vector to deliver more stable RNA interference in order to circumvent the transiency of the RNAi effect. Here, the lentiviral system would ensure efficient, stable transduction of targeted cells. In addition, with the right type of vector, their RNAi dose can be modulated through doxycycline and the infected cells also traced through a bicistronic GFP-shRNA transcript (Amy Chen et al, 1999; Stegmeier et al, 2005; Snove & Rossi, 2006). Morpholinos could also be used in ovo, but these are likely to be diluted even faster than shRNA vectors

8.3 Ventricular zone activity and neural differentiation.

Within the neural tube, one could assume that the loss of LIM HD expressing cells after knockdown of PTP γ , arises from the reduction in the motor and interneuron precursors that ultimately give rise to neurons occupying distinct levels of the dorsoventral spinal cord. The lateral motor columns appear to be particularly sensitive to these deficits. In the pMN domain where most motor neurons are generated, a loss of progenitor tissue was observed in PTP γ silenced embryos, along with ectopically located motor neurons, some of which actually sat within the lumen of the spinal cord.

Within this pMN region, Olig2 causes repression of Irx3 and other genes to regulate the expression of neuronal markers MNR2/Hb9, Lim3, Isl1/2, Lim1/2 and pan neural transcription factors Ngn2, NeuroM. Following PTP γ loss of function, levels of NeuroM were largely unaffected (Figure 5.14, Panel N and Figure 5.16 Panel N). It would be interesting to check the levels of Neurogenin2 to see if this was affected. With PTP γ loss-of-function, levels of Olig2 also remain unaffected as do levels of En1, indicating early actors upstream of Olig2 and En1 progenitors are unaltered, i.e. LIM HD expression as β HHLH genes remain active in radial glial cells (Figure 1.4). Perturbation of PTP γ did not appear to affect these early progenitor markers.

An increase in the level of apoptosis seen in this region during PTP γ shRNA treatment, suggests that cells were dying as they were moving away from the ventricular zone. However, cell death was observed dorsally and ventrally in the neural tube and was not specific to the pMN domain. The loss or exhaustion of

progenitor tissue may therefore result from premature differentiation of the precursor cells either directly or indirectly, rather than loss by cell death.

The loss of tissue in the ventral neural tube and the ectopically located cells may point to a cell autonomous effect, or the migration of these cells may be directly influenced by PTP γ through a contact mediated process. In order to delineate further which populations of neurons were effected by PTP γ loss of function, future experiments should consider using markers that highlight, in the ventral neural tube, Evx1/2 for V0 neurons. Furthermore, no real change in neuronal numbers were observed with En1 for V1 neurons in PTP γ loss of function neural tubes. The markers of V2 neurons Chx10 and Gata2/3 should be used in future experiments as well as Sim1 for V3 neurons. It would also be worthwhile considering post mitotic markers of dorsal neuronal populations (dI6 to dI1) such as Lbx1 for dI4 to dI6, Islet1/2 for dI3, Foxd3 for dI2 and finally Lhx2/9 for the dorsal-most neuronal dI1 population (Zechner et al, 2007). This would give an accurate indication of which neuronal populations dorsoventrally, were specifically affected by PTP γ modulation.

One further possibility for the loss of tissue may arise from a negative progenitor feedback system where motor neurons feedback to their progenitors once they have differentiated and migrated laterally to their pool specific domains. PTP γ may play a role in such feedback, directly or indirectly, whereby if PTP γ acts non-autonomously, then the signals from the lateral glial cells bodies or neuroblasts could still be received medially. Although we have no evidence for this, such a potential negative feedback of motor neurons has been described in Islet1 deficient mice (Chitnis et al, 1995; Pfaff et al, 1996).

There is some controversy as to the extent that the RNAi technique itself can contribute non-specifically to the rate of apoptosis, and the contribution of normal cell death programmes within the chick (Li et al, 1998; Homma et al, 1994). Another group has demonstrated that RNAi hairpins may increase the apoptotic activity within tissues (Wakamatsu et al, 2007). Nevertheless, our controls did not reveal any significant increase in apoptosis. Our data reveals that some of the apoptotic cells in PTP γ shRNA-treated embryos were located in distal locations away from the ventricular lumen suggesting that the cell death might be occurring either in differentiating neurons, or in progenitors outside of M-Phase.

In the PTP γ loss-of-function experiments, a reduction in the mitotic activity of cells was observed. The role that PTP γ plays in the cell cycle is of particular interest and this has been touched on in a few studies from the proliferation of cancerous cells to the progression of the cell cycle where PTP γ was found to act as a potential tumour suppressor gene (Liu et al, 2004; Cheung et al, 2008). When considering the functions of other RPTPs it is worthy to note that PTP λ has been implicated in the proliferation of midline tissue and PTP σ has been shown to play a role in stem cell differentiation and function during neurogenesis (Badde & Schulte, 2008; Kirkham et al, 2006; Meathrel et al, 2002). PTP γ could therefore be involved in controlling the cell cycle directly, or the balance between cycling cells and their post-mitotic, differentiating offspring. Of note also is a study in PC12 cells, where PTP γ was shown to block morphological differentiation of these neuronal cells (Shintani et al, 2001) although an effect on the cell cycle was not determined.

8.4 PTP γ gain-of-function.

Within the spinal cord, PTP γ gain-of-function resulted in gross dorsal and ventral retardation, unlike PTP γ loss-of-function where the greatest effect was ventral. In order to gain more insight into which populations of neurons were affected by PTP γ over expression, we studied the expression profiles of motor neuron markers and the states of proliferative activity and cell death from stage HH20. At this stage, of the 4 neuronal markers observed, *Islet1/2*, *Lim1/2*, *Lim3* and *Mnr2*, all consistently demonstrated a reduction in the total number of cells marked along with a significant shortening and narrowing of the spinal cord in many cases. These findings led us to ask a further question to account for the loss of spinal cord tissue and LIM HD positive neurons in tissue over-expressing PTP γ . If no cell death programme has been initiated one could either assume that a minority of LIM HD fated cells were not being born, or that the radial glial cells giving rise to such neurons were blocked at some stage of the cell cycle, whereby they were not able to self renew or proliferate.

During PTP γ over-expression, a significant reduction of cells undergoing mitosis were again observed, whilst the luminal length was not significantly affected by this gain-of-function. This may favour a hypothesis that a number of radial glial progenitors are either arrested in the cell cycle or in fact are slowed down during the G1 phase or another phase of the cell cycle by high levels of PTP γ . This would not favour the generation of neurons, nor the capacity for self-renewal, thus ultimately reducing the total pool of radial glial progenitors, resulting in a reduction in size and proliferative capacity of the spinal cord.

8.5 Knocking down PTP σ

Further preliminary experiments used the RNAi approach to knock down the function of another member of the RPTP family, PTP σ , within the spinal cord. In situ hybridisation data on the expression profile of this gene at HH18 reveals a pattern of PTP σ gene expression within the sub-ventricular zone, floor plate and stronger expression proximal to the ventricular lumen, the site of mitotically active progenitor cells.

PTP σ and PTP δ loss of function mice reveal no neural tube defects nor any axon targeting defects indicating these genes maybe functionally redundant as they are both highly expressed in the spinal cord and more widely in the CNS. Double PTP σ and PTP δ loss of function mice mutants however generate embryos that are paralysed with severe muscle dysgenesis along with a severe loss of motor neurons during motor axon extension within the spinal cord (Uetani et al, 2006).

At earlier stages, however, E13 in the mouse, the populations of Islet1/2 positive motor neurons within the motor columns appeared largely normal in double PTP σ ^{-/-} and PTP δ ^{-/-} mutants, with a single gene dose of PTP σ (PTP σ ^{+/-} / PTP δ ^{-/-}) being sufficient to retain motor neuron survival similar to control levels. Further defects of the phrenic nerves were found along with targeting defects and stalling of motor neuron axons from the cervical spinal cord. This study concluded that PTP σ and PTP δ complement each others function during normal development and this function was essential for the correct targeting of motor neuron axons and axonogenesis (Uetani et al, 2006).

Reducing the activity of PTP σ in the chick along the dorsoventral aspect of the spinal cord again leads to a reduction in the number of cells fated with LIM HD expression profiles. Further analysis using markers of apoptosis and proliferation, show that the reduction in cell numbers is brought about by both cell death within the ventricular zone and a reduction in the proliferative capacity of radial glia at the ventricular surface.

Furthermore, amongst the PTP σ loss-of-function samples studied at HH18, none displayed evidence of mislocated cells through their expression of LIM HD expression factors. However, this stage may be too early to physically see such events due to the small size of the cord and limited numbers of neurons born at this stage. This preliminary study on PTP σ therefore indicates that other RPTPs may also be playing important roles in early neurogenesis. This justifies future research to investigate this in more detail.

8.6 The role of PTPs during the development of the neural tube.

Recent studies have implicated PTP γ in gastric and colonic cancers suggesting a potential role as a candidate tumour suppressor gene, supporting its activity in proliferating cells (Wang et al, 2005; Wu et al 2006). PTP γ has been used to identify myeloid dendritic cells and macrophages whereby its expression is absent from infectious macrophages. However increased levels of PTP γ are associated with a decreased ability to induce proliferation and interferon- γ secretion of T-cells in the haematopoietic systems of cancer patients. Earlier studies have also shown PTP γ to provide an inhibitory signal for neuronal outgrowth through modulation of the

p13suc1 complex where in PTP γ expressing cell lines, MAP kinases and PKC were inactivated (Shintani et al 2001). PTP γ may therefore have an impact on motor neuron proliferation as the results from perturbing the function of this gene indicate. This previous work indicates that PTP γ influences proliferation and differentiation in other systems. My data indicates that knockdown and over expression both suppressed proliferation within the neural tube.

8.7 Cadherins, adhesion and migration.

When considering the potential functions of PTP γ within the neural tube, one possibility is that PTP γ influences the molecular components and function of adhesive junctions in the neuroepithelium. These junctions are an important site for cellular signalling, and many phosphatases have been implicated in binding E, N and VE Cadherin family members and β -catenin. These binding partners also act as substrates to the RPTPs, which in turn bind either homophilically, or heterophilically (reviewed in Salle, 2006). It can be noted that the local concentration of PTPs at adhesive sites may be important when establishing a low level of phosphorylation at these crucial adhesive junctions, to maintain their integrity. Reducing the levels of PTP activity will increase the tyrosine phosphorylation of cadherins and catenins, thus breaking down the epithelial barrier function.

Therefore, the effect of RPTPs on β -catenin signalling and the effect of tyrosine phosphorylation (either directly or indirectly by PTP γ or PTP σ) on adherens and tight epithelial junction must be looked at in more detail. This may ultimately have an effect on the radial glial population and the tightly associated daughter cells that give

rise to differentiated neurons. Furthermore there may also be an effect on the migration of neuronal precursors through cadherins (Lilien et al, 2002; Nelson & Nusse, 2004). Our group also has evidence that PTP γ gain-of-function does support β -catenin driven TCF signalling (Hashemi et al, 2011).

Tyrosine phosphorylation of cadherins affect the stability of adherens junctions within epithelial cells (Lampugnani et al 1997). Treatment with a PTP inhibitor pervandate caused raised phosphorylation levels in adherens junctions and their consequent disassembly (Michalides et al 1994). This implicates PTP function early on in cell-cell adhesion, later supported by studies with PTP μ and its role in the maintenance of junctional integrity (Sui et al, 2005). There may also exist functional redundancies or multiple isoforms of PTP γ that are specific to different subtypes of ligand, which could rescue function later in development (Xiong et al 1996).

A structurally similar phosphatase to PTP γ , PTP ζ/β , has been shown to bind Pleiotropin, a heparin binding protein that promotes the migration of neurons in the cortex, thereby inhibiting PTP ζ/β activity (Meng et al 2000). PTP ζ/β has been shown to interact directly with β -catenin, whose tyrosine phosphorylation regulates cell-cell adhesion via disassociation of cadherins from the actin cytoskeleton (Meng et al, 2000; Stoker et al, 2005).

Our studies show that not only did motor neurons mislocate to the progenitor zone, they effectively replaced this tissue in some cases. The most likely explanation for this is that the progenitor cells were depleted or pushed aside, leaving the motor precursors to differentiate *in situ*. Alternatively it is possible that adhesive defects in

these cells meant that they migrated medially rather than laterally, although I feel this is unlikely. The ingrowth of Isl1-expressing cells in some embryos looks almost neoplastic. However, we saw no evidence of increased mitoses in these regions and so it is more likely that they have arisen through the local generation of motor precursors that have failed to move away. Their failure to move laterally may thus have arisen through defective cadherin interactions, or other cell-autonomous defects in cell movement.

8.8 PTP γ , β -Catenin and Wnt proliferation control.

What role does PTP γ play in the development of the spinal cord, and how could it cause a disruption in the LIM HD profile? If PTP γ interacts with β -catenin, then this could explain some of the progenitor cell behaviours that have been observed, since β -catenin is closely involved in cell cycle control and adherens junctions (Kijiguchi et al 2007; Badde & Schulte, 2008). Our data indicates that PTP γ may have a direct effect on motor neuron production or indirectly in the maintenance of progenitor pools. As we have suggested, a plausible role for PTP γ interaction in the neural tube may be through Cadherins and β -catenin signalling (Price et al, 2002; Salle et al, 2006). Here, β -catenin function has been attributed to phosphotyrosine signalling.

It may be an interesting possibility as β -catenin is a transcription factor that controls neuronal proliferation through a Wnt gradient, and plays a role in the cell adhesive processes of epithelial cells through Cadherin modulation as previous studies suggest (Megason & McMahon, 2002; Lilien & Balsamo, 2005). In these β -catenin knock out studies in mice, a ventral loss of cell was observed in the spinal cord, not dissimilar to

the phenotypes observed with PTP γ and PTP σ . A number of phosphatases have been implicated in β -Catenin dephosphorylation interacting directly with other RPTPs and PTKs (Lilien & Balsamo, 2005; Nelson et al, 2004; Stoker, 2005.) β -catenin activity onset by Wnt signalling regulates the proliferation and terminal differentiation of progenitor cells via phosphorylation. (Megason & McMahon, 2002).

As a regulator of proliferation and differentiation in the neural tube, the canonical Wnt/ β -catenin signalling pathway is a plausible target of PTP γ . This pathway is activated by graded Wnt signals whereby β -catenin regulated cell-cell adhesion through cadherins at adherens junctions and further drives the transcriptional regulation of targets through complexes with TCF/LEF proteins. β -catenin itself has been shown to be regulated by tyrosine phosphorylation both at the nuclear and cell surface levels (Lilien & Balsamo, 2005).

Previous studies in the chick neural tube blocking TCF/LEF function demonstrated similar phenotypes to our PTP γ loss-of-function results (Megason & McMahon, 2002). Recent studies in our laboratory examined the effect of PTP γ perturbation on the Wnt pathway through assessing TCF activity using a pTOPGFP and pTOPRFP reporter where GFP/RFP expression indicates binding of activated β -catenin-TCF/LEF complex to consensus TCF/LEF binding sites in the GFP (or RFP) promoter. This vector demonstrated a steep dorsoventral gradient of GFP expression, which was unaffected in PTP γ loss-of-function neural tubes. PTP γ gain-of-function embryos however suppressed pTOPRFP expression by more than 80% across the entire neural tube (Hashemi et al, 2011).

β -catenin may serve as a possible target for PTP γ as its tyrosine phosphorylation influences its transcriptional activity and adhesion to cadherins. *In vitro* experiments where the phosphorylation state of β -catenin at one of its regulatory tyrosine residues, Y654 would affect β -catenin complexes at its active site, nucleus and adherens junctions were carried out in our laboratory. The results indicated that spinal cord cells expressing β -catenin-GFP fusion proteins with Y654-F mutations that mimic a dephosphorylated state, such complexes localised at adherens junctions mainly, compared to WT β -catenin-GFP (Hashemi et al, 2011).

However, β -catenin-GFP fusion proteins with Y654-E mutations that mimic a phosphorylated state resulted in the protein complex to localise in the nucleus and cytoplasm. This indicated that the tyrosine residue at Y654 of β -catenin could regulate its function, however this may not be sufficient to alter signalling as our group found that the Y654-E mutation should have a dominant-active phenotype that should induce tissue hypertrophy yet this failed to transpire. Further, PTP γ was able to efficiently dephosphorylate β -catenin *in vitro* with tyrosine-phosphorylated β -catenin treated with purified catalytic domains of human PTP γ (Hashemi et al, 2011).

PTP γ may therefore be participating in a signalling cascade that involves β -catenin. Indeed our lab had recently shown that PTP γ interacts with β -catenin (Hashemi et al, 2011). A recent study has also implicated another RPTP, PTP λ , within the MHB as a negative modulator of Wnt1 expression in this region, and as an inhibitor of the canonical Wnt signalling pathway through sequestration of β -catenin (Badde & Schulte, 2008). In this study, PTP λ over expression, PTP λ being normally expressed

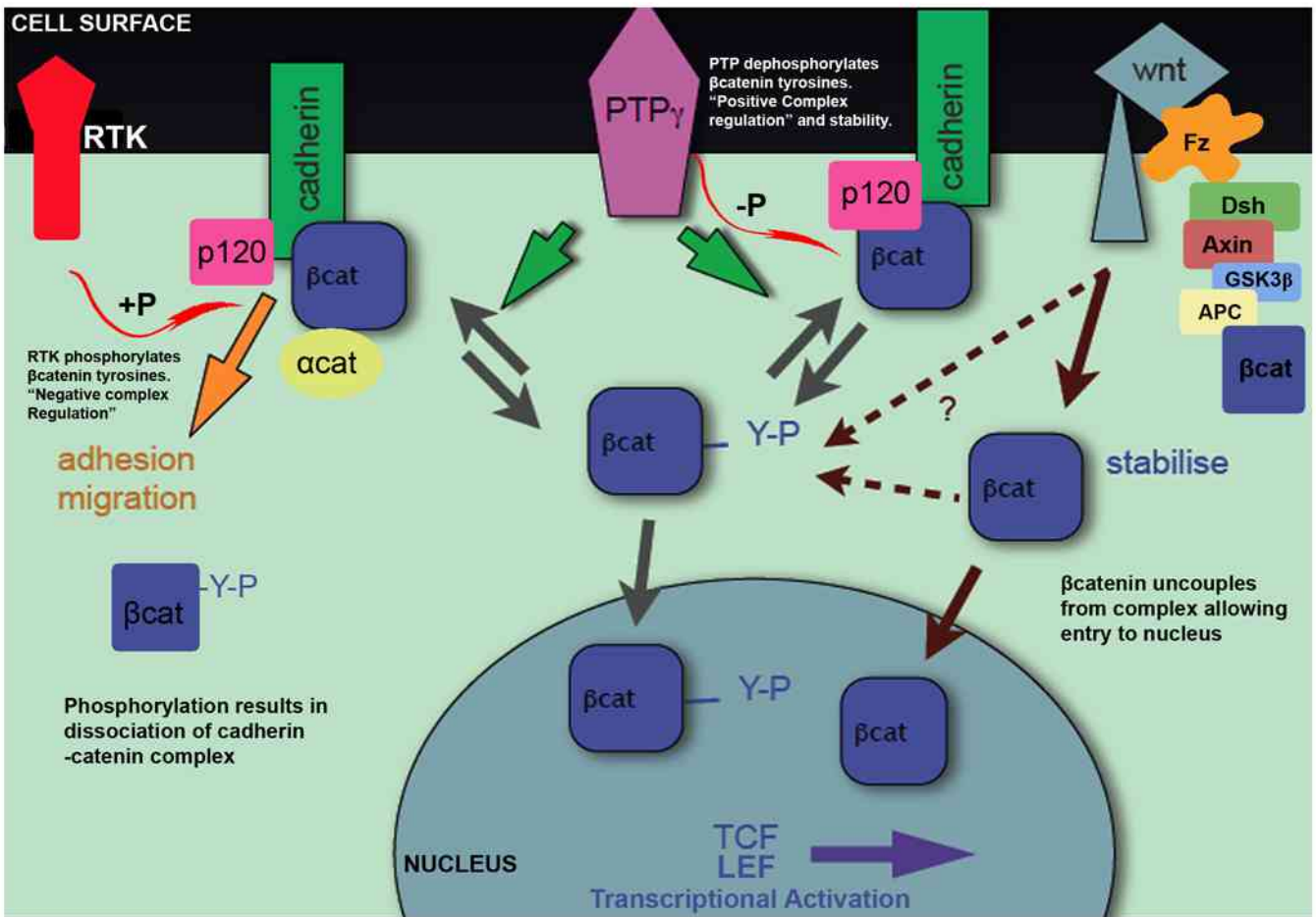
in a ring of cells anterior to the Wnt1 domain of expression at the MHB, inhibits Wnt1 expression here.

Furthermore dose dependent Fgf8 signals from the MHB are required for the transcription of PTP λ and Wnt1. The inhibition of Wnt1 by PTP λ overexpression was specific to this gene within the MHB without affecting other markers in this region. Over expression of PTP λ at the MHB a failure of Wnt1 upregulation was observed following further stimulation by Fgf8, however the MHB cells expressed En1, Pax2 and Pax5. The group concluded that Wnt1 and PTP λ border in expression domains rostrally where PTP λ at the MHB may serve to act as a Ras-MAP Kinase feedback inhibitor restricting anterior expansion of the Wnt1 domain (Badde & Schulte, 2008).

β -catenin has been previously shown to be dephosphorylated by PTP λ in vitro, and over expression of PTP λ in the MHB disrupted the canonical Wnt pathway whereby neuroepithelial proliferation was reduced along with a reduction in the activation of β -catenin responsive promoters. The group found further receptor tyrosine phosphatases expressed in the MHB, namely PTP ζ/β was expressed at the same time as PTP λ and has been found to interact with the diffusion of Wnt/Fgf signals (Badde & Schulte, 2008). PTP γ may therefore function in a similar way to PTP λ and this could be investigated in future studies. A similar scheme for PTP γ is proposed in Figure 8.1.

Here, PTP γ causes desphosphorylation of specific tyrosine residues on β -catenin, namely position Y654 (Kajiguchi et al, 2011) bound to p120, causing positive cadherin/catenin complex stability and integrity.

Figure 8.1 Scheme of possible PTP γ interaction with the Catenin/Cadherin pathway. PTP γ causes desphosphorylation of tyrosine residues on β -catenin, bound to p120, causing positive cadherin/catenin complex stability. Wnt signalling and RTK action negatively regulates the cadherin/catenin complex, through phosphorylation of β -catenin tyrosine residues and allows β -catenin to enter the nucleus and activate transcription of target genes via the TCF/LEF pathway. β -cat - β -catenin; Fz - frizzled receptor; RTK - Receptor Tyrosine Kinase; Y-P, phosphorylated tyrosine of β -catenin. Adapted from A. Stoker (Personal Communication).



RTK action negatively regulates the cadherin/catenin complex, through phosphorylation of β -catenin tyrosine residues and allows β -catenin to enter the nucleus and activate transcription of target genes via the TCF/LEF pathway (Rhee et al, 2007). Furthermore, the migration of motor neuron precursors is controlled in part by cadherin regulated adhesive contacts and ultimately dependent on PTK and PTP regulation of β -catenin (Price et al, 2002). Our proposed model suggests that PTP γ regulates β -catenin tyrosine phosphorylation in balance with PTKs allowing some β -catenin to translocate into the nucleus, both phosphorylated and non-phosphorylated forms (Kim & Lee, 2001). During overexpression of PTP γ , more β -catenin is dephosphorylated and associated with cadherin complexes. This is also a plausible adhesion effect of PTP γ yet there may be redundancy issues among the PTPs and along the cadherin/catenin pathway.

8.9 PTP γ and neural tube patterning

In what ways does PTP γ interact with protein complexes to bring about a loss of Lim1/2 cells? Transcriptional complexes control specific generation of motor neuron pools and clues could be provided in the E-box regulatory regions or enhancer regions of the Lim1/2 gene. Interestingly Islet1 itself is tyrosine phosphorylated when considering the role of cell-cell interactions as a potential mode of PTP γ interaction (Hobert & Westphal, 2000).

This is interesting as Islet1 is nuclear and PTP γ is thought to be membrane-associated, it may be possible that PTP γ is also cleaved and then travels to the nucleus for a possible interaction with Lim1/2 (Anders et al, 2006). However, it is more likely that

progenitor populations are affected through either cell death or disruption in the cell cycle through up and down regulation of PTP γ activity.

Further studies in our laboratory addressing whether PTP γ function was upstream or downstream of Notch signalling demonstrated normal patterns of Hes5-1, Pax 6 and Nkx6.1 among PTP γ loss-of-function embryos. This indicates that PTP γ functions occur downstream of Notch signalling independently of this signalling pathway. Our PTP γ gain of function studies showed a reduction in motor neuron and interneuron numbers along, along with increased apoptosis, without affecting the expression of Pax3 or Nkx6.1 (Hashemi et al 2011). The loss of tissue arises partly from the reduction in mitosis without activating apoptosis. The reduction of mitosis and proliferative activity appears to be cell-autonomous through PTP γ gain of function.

Further experiments in our group also showed no difference in mitotic spindle angle distributions through perturbing PTP γ activity, indicating self-renewal processes and determination of neurogenic fate were possibly unaffected, although the relation between spindle orientation and neurogenesis has recently been called into doubt (Vilas-Boas et al, 2011; Das & Storey, 2012) . Loss of PTP γ function also perturbs cell-cell adhesion in the neuroepithelial cells whose nuclei are normally well aligned increased the spread of angles and an increase in nuclei without random polarities and orientation (Hashemi et al, 2011). These findings point towards a cell autonomous effect of PTP γ loss-of-function, where loss of progenitors occurs through apoptosis, along with a further defect causing displacement of motor neurons that fail to migrate laterally. Therefore PTP γ function is needed for cell survival and correct cell-cell adhesion and migration of neuronal precursor cells (Hashemi et al, 2011).

PTP γ loss of function resulted in a particular loss of pMN progenitor tissue and mislocation of motor neurons not observed with neurons in other ventricular zones. As they mature, motor neurons could provide feedback to progenitor cells deterring them from a motor neuron fate. Such a model has been suggested to *Isl1* (Lee & Pfaff 2003). The loss of *Islet1* or *Lim-1*-expressing neurons here after PTP γ loss, may affect motor neuron survival as the feedback system is lost, causing compensatory motor neuron production and progenitor exhaustion. The particular sensitivity at the pMN may be caused by the extinguishing of the already low levels of PTP γ through its loss of function. Alternatively, it is possible that a specific cadherin-based function of PTP γ is disrupted in this pMN region, or another regionalised substrate of PTP γ is expressed in this region, causing the more extreme defects in tissue structure (Hashemi et al, 2011).

8.10 Future Studies

Future studies should look more closely at further analysing the effects of PTP γ on neuronal populations within the neural tube at HH20, focussing on cell expressing *Neurogenin2*, *Pax6*, *Olig2* and *Nkx6.1* for example. This may provide insight into whether specific neuronal populations were being affected by PTP perturbation. Moreover, genes expressed within the LMC should be looked at further amongst the PTP γ perturbed embryos to determine if the effects seen may be non-cell autonomous, in order to delineate the potential mechanisms for PTP γ function during neurogenesis. Maintaining shRNA levels for longer, using viral delivery, may also reinforce the phenotypes observed and clarify their basis.

Examining the role of Catenins/Wnts and especially β -catenin as an interactor with PTP γ should also be a high priority. As a potential candidate for PTP γ interaction, β -catenin loss of function (as with PTP γ gain of function) both in the chick and the mouse results in a loss of ventral progenitor cells. Furthermore PTP γ is able to suppress Wnt/ β -catenin signalling via TCF and is able to dephosphorylate β -catenin in vitro. PTP λ has also been shown to interact with β -catenin directly and affect CNS development. My preliminary study of PTPs also demonstrates a role in neurogenesis in the neural tube. These studies raise the critical issue of functional redundancy between RPTPs, making interpretation of gain of function studies and loss of function studies more difficult, since changes in PTP γ may be compensated by other phosphatases under some but not all circumstances.

Furthermore, other components of the Wnt/TCF pathway should be considered as interactors of PTP γ here, as β -catenin phosphorylation may not be sufficient to drive TCF signalling. Namely the cadherin family, whose cell-cell adhesive functions are regulated by tyrosine phosphorylation (Price et al, 2002; Sallee et al, 2006). Thus these further experiments should address whether the function of PTP γ is specifically directed through particular signalling pathways with its own specific substrates, or whether it acts upstream of the cadherin/catenin pathways with consequent, broad downstream consequences.

My study has demonstrated for the first time that RPTPs control neurogenesis, neuronal patterning and positioning in the early chick spinal cord. It is likely that several further RPTP family members could also prove to be functionally relevant within this region, playing unique and overlapping roles.

References

Adams CL, Nelson WJ. *Curr Opin Cell Biol.* Cytomechanics of cadherin-mediated cell-cell adhesion. 1998 Oct;10(5):572-7.

Alete DE, Weeks ME, Hovanessian AG, Hawadle M, Stoker AW. Cell surface nucleolin on developing muscle is a potential ligand for the axonal receptor protein tyrosine phosphatase-sigma. *FEBS J.* 2006 Oct;273(20):4668-81.

Alexandre P, Reugels AM, Barker D, Blanc E, Clarke JD. Neurons derive from the more apical daughter in asymmetric divisions in the zebrafish neural tube. *Nat Neurosci.* 2010 Jun;13(6):673-9.

Alonso, A., Sasin, J., Bottini, N., Friedberg, I., Osterman, A., Godzik, A., Hunter, T., Dixon, J., Mustelin, T. Protein tyrosine phosphatases in the human genome. *Cell.* 2004; 117, 699-711.

Altman J, Bayer SA. Embryonic development of the rat cerebellum. *J Comp Neurol.* 1985 Jan 1;231(1):1-65.

Ambros V. The functions of animal microRNAs. *Nature.* 2004 Sep 16;431(7006):350-5.

Amy Chen CM, Smith DM, Peters MA, Samson ME, Zitz J, Tabin CJ, Cepko CL. Production and design of more effective avian replication-incompetent retroviral vectors. *Dev Biol.* 1999 Oct 15;214(2):370-84.

Anastasiadis PZ, Reynolds AB. The p120 catenin family: complex roles in adhesion, signaling and cancer. *J Cell Sci.* 2000 Apr;113 (Pt 8):1319-34.

Anders L, Mertins P, Lammich S, Murgia M, Hartmann D, Saftig P, Haass C, Ullrich A. Furin-, ADAM 10-, and gamma-secretase-mediated cleavage of a receptor tyrosine phosphatase and regulation of beta-catenin's transcriptional activity. *Mol Cell Biol.* 2006 May;26(10):3917-34.

Anthony TE, Klein C, Fishell G, Heintz N. Radial glia serve as neuronal progenitors in all regions of the central nervous system. *Neuron.* 2004 Mar 25;41(6):881-90.

Arber S, Han B, Mendelsohn M, Smith M, Jessell TM, Sockanathan S. Requirement for the homeobox gene Hb9 in the consolidation of motor neuron identity. *Neuron.* 1999 Aug;23(4):659-74.

Aricescu AR, McKinnell IW, Halfter W, Stoker AW. Heparan sulfate proteoglycans are ligands for receptor protein tyrosine phosphatase sigma. *Mol Cell Biol.* 2002 Mar;22(6):1881-92.

Badde, A., Schulte, D. A role for receptor protein tyrosine phosphatase lambda in midbrain development. *J Neurosci.* 2008; 28, 6152-6164.

Bai CB, Auerbach W, Lee JS, Stephen D, Joyner AL. Gli2, but not Gli1, is required for initial Shh signaling and ectopic activation of the Shh pathway. *Development*. 2002 Oct;129(20):4753-61.

Bai CB, Stephen D, Joyner AL. All mouse ventral spinal cord patterning by hedgehog is Gli dependent and involves an activator function of Gli3. *Dev Cell*. 2004 Jan;6(1):103-15.

Baye LM, Link BA. Interkinetic nuclear migration and the selection of neurogenic cell divisions during vertebrate retinogenesis. *J Neurosci*. 2007 Sep 19;27(38):10143-52.

Bel-Vialar S, Itasaki N, Krumlauf R. Initiating Hox gene expression: in the early chick neural tube differential sensitivity to FGF and RA signaling subdivides the HoxB genes in two distinct groups. *Development*. 2002 Nov;129(22):5103-15.

Berns K, Hijmans EM, Mullenders J, Brummelkamp TR, Velds A, Heimerikx M, Kerkhoven RM, Madiredjo M, Nijkamp W, Weigelt B, Agami R, Ge W, Cavet G, Linsley PS, Beijersbergen RL, Bernards R. A large-scale RNAi screen in human cells identifies new components of the p53 pathway. *Nature*. 2004 Mar 25;428(6981):431-7.

Bernstein E, Caudy AA, Hammond SM, Hannon GJ. Role for a bidentate ribonuclease in the initiation step of RNA interference. *Nature*. 2001 Jan 18;409(6818):363-6.

Bertrand N, Castro DS, Guillemot F. Proneural genes and the specification of neural cell types. *Nat Rev Neurosci*. 2002 Jul;3(7):517-30.

Bertrand V, Hudson C, Caillol D, Popovici C, Lemaire P. Neural tissue in ascidian embryos is induced by FGF9/16/20, acting via a combination of maternal GATA and Ets transcription factors. *Cell*. 2003 Nov 26;115(5):615-27.

Bonni A, Sun Y, Nadal-Vicens M, Bhatt A, Frank DA, Rozovsky I, Stahl N, Yancopoulos GD, Greenberg ME. Regulation of gliogenesis in the central nervous system by the JAK-STAT signaling pathway. *Science*. 1997 Oct 17;278(5337):477-83.

Bourikas D, Stoeckli ET. New tools for gene manipulation in chicken embryos. *Oligonucleotides*. 2003;13(5):411-9.

Bourikas D, Pekarik V, Baeriswyl T, Grunditz A, Sadhu R, Nardó M, Stoeckli ET. Sonic hedgehog guides commissural axons along the longitudinal axis of the spinal cord. *Nat Neurosci*. 2005 Mar;8(3):297-304.

Bouyain S, Watkins DJ. The protein tyrosine phosphatases PTPRZ and PTPRG bind to distinct members of the contactin family of neural recognition molecules. *Proc Natl Acad Sci U S A*. 2010 Feb 9;107(6):2443-8.

Brady-Kalnay SM, Rimm DL, Tonks NK. Receptor protein tyrosine phosphatase PTPmu associates with cadherins and catenins in vivo. *J Cell Biol*. 1995 Aug;130(4):977-86.

Brady-Kalnay SM, Mourton T, Nixon JP, Pietz GE, Kinch M, Chen H, Brackenbury R, Rimm DL, Del Vecchio RL, Tonks NK. Dynamic interaction of PTPmu with multiple cadherins in vivo. *J Cell Biol.* 1998 Apr 6;141(1):287-96.

Braut V, Moore R, Kutsch S, Ishibashi M, Rowitch DH, McMahon AP, Sommer L, Boussadia O, Kemler R. Inactivation of the beta-catenin gene by Wnt1-Cre-mediated deletion results in dramatic brain malformation and failure of craniofacial development. *Development.* 2001 Apr;128(8):1253-64.

Brigidi GS, Bamji SX. Cadherin-catenin adhesion complexes at the synapse. *Curr Opin Neurobiol.* 2011 Apr;21(2):208-14.

Briscoe J, Novitsch BG. Regulatory pathways linking progenitor patterning, cell fates and neurogenesis in the ventral neural tube. *Philos Trans R Soc Lond B Biol Sci.* 2008 Jan 12;363(1489):57-70.

Briscoe J, Sussel L, Serup P, Hartigan-O'Connor D, Jessell TM, Rubenstein JL, Ericson J. Homeobox gene Nkx2.2 and specification of neuronal identity by graded Sonic hedgehog signalling. *Nature.* 1999 Apr 15;398(6728):622-7.

Briscoe J, Pierani A, Jessell TM, Ericson J. A homeodomain protein code specifies progenitor cell identity and neuronal fate in the ventral neural tube. *Cell.* 2000 May 12;101(4):435-45.

Briscoe J, Ericson J. Specification of neuronal fates in the ventral neural tube. *Curr Opin Neurobiol.* 2001 Feb;11(1):43-9.

Briscoe J, Wilkinson DG. Establishing neuronal circuitry: Hox genes make the connection. *Genes Dev.* 2004 Jul 15;18(14):1643-8.

Briscoe J, Ericson J. The specification of neuronal identity by graded Sonic Hedgehog signalling. *Semin Cell Dev Biol.* 1999 Jun;10(3):353-62.

Bron R, Eickholt BJ, Vermeren M, Fragale N, Cohen J. Functional knockdown of neuropilin-1 in the developing chick nervous system by siRNA hairpins phenocopies genetic ablation in the mouse. *Dev Dyn.* 2004 Jun;230(2):299-308.

Brummelkamp TR, Bernards R, Agami R. "A system for stable expression of short interfering RNAs in mammalian cells." *Science.* 2002 Apr 19;296(5567):550-3.

Burrige K, Sastry SK, Sallee JL. Regulation of cell adhesion by protein-tyrosine phosphatases. I. Cell-matrix adhesion. *J Biol Chem.* 2006 Jun 9;281(23):15593-6.

Burrill JD, Moran L, Goulding MD, Saueressig H. PAX2 is expressed in multiple spinal cord interneurons, including a population of EN1+ interneurons that require PAX6 for their development. *Development.* 1997 Nov;124(22):4493-503.

- Cadigan KM, Nusse R. Wnt signaling: a common theme in animal development. *Genes Dev.* 1997 Dec 15;11(24):3286-305.
- Calegari F, Haubensak W, Haffner C, Huttner WB. Selective lengthening of the cell cycle in the neurogenic subpopulation of neural progenitor cells during mouse brain development. *J Neurosci.* 2005 Jul 13;25(28):6533-8.
- Canatella PJ, Karr JF, Petros JA, Prausnitz MR, Schaapveld RQ, Schepens JT, Bächner D, Attema J, Wieringa B, Jap PH, Hendriks WJ. Quantitative study of electroporation-mediated molecular uptake and cell viability. *Biophys J.* 2001 Feb;80(2):755-64.
- Catala M, Teillet MA, De Robertis EM, Le Douarin ML. A spinal cord fate map in the avian embryo: while regressing, Hensen's node lays down the notochord and floor plate thus joining the spinal cord lateral walls. *Development.* 1996 Sep;122(9):2599-610.
- Cepko C, Ryder EF, Austin CP, Walsh C, Fekete DM. Lineage analysis using retrovirus vectors. *Methods Enzymol.* 1995;254:387-419.
- Castro B, Barolo S, Bailey AM, Posakony JW. Lateral inhibition in proneural clusters: cis-regulatory logic and default repression by Suppressor of Hairless. *Development.* 2005 Aug;132(15):3333-44.
- Chagnon MJ, Uetani N, Tremblay ML. Functional significance of the LAR receptor protein tyrosine phosphatase family in development and diseases. *Biochem Cell Biol.* 2004 Dec;82(6):664-75.
- Chamberlain CE, Jeong J, Guo C, Allen BL, McMahon AP. Notochord-derived Shh concentrates in close association with the apically positioned basal body in neural target cells and forms a dynamic gradient during neural patterning. *Development.* 2008 Mar;135(6):1097-106.
- Schaapveld RQ, Schepens JT, Bächner D, Attema J, Wieringa B, Jap PH, Hendriks WJ. Developmental expression of the cell adhesion molecule-like protein tyrosine phosphatases LAR, RPTPdelta and RPTPsigma in the mouse. *Mech Dev.* 1998 Sep;77(1):59-62.
- Chen Y, Low TY, Choong LY, Ray RS, Tan YL, Toy W, Lin Q, Ang BK, Wong CH, Lim S, Li B, Hew CL, Sze NS, Druker BJ, Lim YP. Phosphoproteomics identified Endofin, DCBLD2, and KIAA0582 as novel tyrosine phosphorylation targets of EGF signaling and Iressa in human cancer cells. *Proteomics.* 2007 Jul;7(14):2384-97.
- Chen WL, Lin CT, Lo HF, Lee JW, Tu IH, Hu FR. The role of protein tyrosine phosphorylation in the cell-cell interactions, junctional permeability and cell cycle control in post-confluent bovine corneal endothelial cells. *Exp Eye Res.* 2007 Aug;85(2):259-69.
- Chen MH, Li YJ, Kawakami T, Xu SM, Chuang PT. Palmitoylation is required for the production of a soluble multimeric Hedgehog protein complex and long-range signaling in vertebrates. *Genes Dev.* 2004 Mar 15;18(6):641-59.

Chen JK, Taipale J, Cooper MK, Beachy PA. Inhibition of Hedgehog signaling by direct binding of cyclopamine to Smoothened. *Genes Dev.* 2002 Nov 1;16(21):2743-8.

Cheng J, Wu K, Armanini M, O'Rourke N, Dowbenko D, Lasky LA. A novel protein-tyrosine phosphatase related to the homotypically adhering kappa and mu receptors. *J Biol Chem.* 1997 Mar 14;272(11):7264-77.

Chenn A, McConnell SK. Cleavage orientation and the asymmetric inheritance of Notch1 immunoreactivity in mammalian neurogenesis. *Cell.* 1995 Aug 25;82(4):631-41.

Chenn A, Zhang YA, Chang BT, McConnell SK. Intrinsic polarity of mammalian neuroepithelial cells. *Mol Cell Neurosci.* 1998 Jul;11(4):183-93.

Chesnutt C, Niswander L. Plasmid-based short-hairpin RNA interference in the chicken embryo. *Genesis.* 2004 Jun;39(2):73-8.

Chesnutt C, Burrus LW, Brown AM, Niswander L. Coordinate regulation of neural tube patterning and proliferation by TGFbeta and WNT activity. *Dev Biol.* 2004 Oct 15;274(2):334-47.

Cheung AK, Lung HL, Hung SC, Law EW, Cheng Y, Yau WL, Bangarusamy DK, Miller LD, Liu ET, Shao JY, Kou CW, Chua D, Zabarovsky ER, Tsao SW, Stanbridge EJ, Lung ML. Functional analysis of a cell cycle-associated, tumor-suppressive gene, protein tyrosine phosphatase receptor type G, in nasopharyngeal carcinoma. *Cancer Res.* 2008 Oct 1;68(19):8137-45.

Chiang C, Litingtung Y, Lee E, Young KE, Corden JL, Westphal H, Beachy PA. Cyclopia and defective axial patterning in mice lacking Sonic hedgehog gene function. *Nature.* 1996 Oct 3;383(6599):407-13.

Chilton JK, Stoker AW. Expression of receptor protein tyrosine phosphatases in embryonic chick spinal cord. *Mol Cell Neurosci.* 2000 Oct;16(4):470-80.

Chitnis, A., Henrique, D., Lewis, J., Ish-Horowicz, D., Kintner, C. Primary neurogenesis in *Xenopus* embryos regulated by a homologue of the *Drosophila* neurogenic gene Delta. *Nature.* 1995; 375, 761-766.

Clandinin TR, Lee CH, Herman T, Lee RC, Yang AY, Ovasapyan S, Zipursky SL. *Drosophila* LAR regulates R1-R6 and R7 target specificity in the visual system. *Neuron.* 2001 Oct 25;32(2):237-48.

Coles CH, Shen Y, Tenney AP, Siebold C, Sutton GC, Lu W, Gallagher JT, Jones EY, Flanagan JG, Aricescu AR. Proteoglycan-specific molecular switch for RPTP α clustering and neuronal extension. *Science.* 2011 Apr 22;332(6028):484-8.

Dai P, Akimaru H, Tanaka Y, Maekawa T, Nakafuku M, Ishii S. Sonic Hedgehog-induced activation of the Gli1 promoter is mediated by GLI3. *J Biol Chem*. 1999 Mar 19;274(12):8143-52.

Das RM, Storey KG. Mitotic spindle orientation can direct cell fate and bias Notch activity in chick neural tube. *EMBO Rep*. 2012 Nov 6;13(11).

Dasen JS, De Camilli A, Wang B, Tucker PW, Jessell TM. Hox repertoires for motor neuron diversity and connectivity gated by a single accessory factor, FoxP1. *Cell*. 2008 Jul 25;134(2):304-16.

Dasen JS, Tice BC, Brenner-Morton S, Jessell TM. A Hox regulatory network establishes motor neuron pool identity and target-muscle connectivity. *Cell*. 2005 Nov 4;123(3):477-91.

Dasen JS, Liu JP, Jessell TM. Motor neuron columnar fate imposed by sequential phases of Hox-c activity. *Nature*. 2003 Oct 30;425(6961):926-33.

Das RM, Van Hateren NJ, Howell GR, Farrell ER, Bangs FK, Porteous VC, Manning EM, McGrew MJ, Ohyama K, Sacco MA, Halley PA, Sang HM, Storey KG, Placzek M, Tickle C, Nair VK, Wilson SA. A robust system for RNA interference in the chicken using a modified microRNA operon. *Dev Biol*. 2006 Jun 15;294(2):554-63.

De Felipe J, Conti F, Van Eyck SL, Manzoni T. Demonstration of glutamate-positive axon terminals forming asymmetric synapses in cat neocortex. *Brain Res*. 1988 Jul 5;455(1):162-5.

Delaune E, Lemaire P, Kodjabachian L. Neural induction in *Xenopus* requires early FGF signalling in addition to BMP inhibition. *Development*. 2005 Jan;132(2):299-310.

Del Bene F, Wehman AM, Link BA, Baier H. Regulation of neurogenesis by interkinetic nuclear migration through an apical-basal notch gradient. *Cell*. 2008 Sep 19;134(6):1055-65.

Deneen B, Ho R, Lukaszewicz A, Hochstim CJ, Gronostajski RM, Anderson DJ. The transcription factor NFIA controls the onset of gliogenesis in the developing spinal cord. *Neuron*. 2006 Dec 21;52(6):953-68.

De Robertis EM, Sasai Y. A common plan for dorsoventral patterning in Bilateria. *Nature*. 1996 Mar 7;380(6569):37-40.

Desai CJ, Krueger NX, Saito H, Zinn K. Competition and cooperation among receptor tyrosine phosphatases control motoneuron growth cone guidance in *Drosophila*. *Development*. 1997 May;124(10):1941-52.

Desai CJ, Gindhart JG Jr, Goldstein LS, Zinn K. Receptor tyrosine phosphatases are required for motor axon guidance in the *Drosophila* embryo. *Cell*. 1996 Feb 23;84(4):599-609.

Dessaud E, Yang LL, Hill K, Cox B, Ulloa F, Ribeiro A, Mynett A, Novitsch BG, Briscoe J. Interpretation of the sonic hedgehog morphogen gradient by a temporal adaptation mechanism. *Nature*. 2007 Nov 29;450(7170):717-20.

Dessaud E, McMahon AP, Briscoe J. Pattern formation in the vertebrate neural tube: a sonic hedgehog morphogen-regulated transcriptional network. *Development*. 2008 Aug;135(15):2489-503.

Dickinson ME, Krumlauf R, McMahon AP. Evidence for a mitogenic effect of Wnt-1 in the developing mammalian central nervous system. *Development*. 1994 Jun;120(6):1453-71.

Donovan SL, Dyer MA. Regulation of proliferation during central nervous system development. *Semin Cell Dev Biol*. 2005 Jun;16(3):407-21.

Driever W, Nüsslein-Volhard C. The bicoid protein is a positive regulator of hunchback transcription in the early *Drosophila* embryo. *Nature*. 1989 Jan 12;337(6203):138-43.

Dunah AW, Hueske E, Wyszynski M, Hoogenraad CC, Jaworski J, Pak DT, Simonetta A, Liu G, Sheng M. LAR receptor protein tyrosine phosphatases in the development and maintenance of excitatory synapses. *Nat Neurosci*. 2005 Apr;8(4):458-67.

Durstion AJ, Timmermans JP, Hage WJ, Hendriks HF, de Vries NJ, Heideveld M, Nieuwkoop PD. Retinoic acid causes an anteroposterior transformation in the developing central nervous system. *Nature*. 1989 Jul 13;340(6229):140-4.

Elbashir SM, Harborth J, Lendeckel W, Yalcin A, Weber K, Tuschl T. Duplexes of 21-nucleotide RNAs mediate RNA interference in cultured mammalian cells. *Nature*. 2001 May 24;411(6836):494-8.

Elchebly M, Wagner J, Kennedy TE, Lanctôt C, Michaliszyn E, Itié A, Drouin J, Tremblay ML. Neuroendocrine dysplasia in mice lacking protein tyrosine phosphatase sigma. *Nat Genet*. 1999 Mar;21(3):330-3.

Ensini M, Tsuchida TN, Belting HG, Jessell TM. The control of rostrocaudal pattern in the developing spinal cord: specification of motor neuron subtype identity is initiated by signals from paraxial mesoderm. *Development*. 1998 Mar;125(6):969-82.

Ensslen-Craig SE, Brady-Kalnay SM. Receptor protein tyrosine phosphatases regulate neural development and axon guidance. *Dev Biol*. 2004 Nov 1;275(1):12-22.

Ensslen-Craig SE, Brady-Kalnay SM. PTP mu expression and catalytic activity are required for PTP mu-mediated neurite outgrowth and repulsion. *Mol Cell Neurosci.* 2005 Jan;28(1):177-88.

Ericson J, Rashbass P, Schedl A, Brenner-Morton S, Kawakami A, van Heyningen V, Jessell TM, Briscoe J. Pax6 controls progenitor cell identity and neuronal fate in response to graded Shh signaling. *Cell.* 1997 Jul 11;90(1):169-80.

Ericson J, Morton S, Kawakami A, Roelink H, Jessell TM. Two critical periods of Sonic Hedgehog signaling required for the specification of motor neuron identity. *Cell.* 1996 Nov 15;87(4):661-73.

Ericson J, Thor S, Edlund T, Jessell TM, Yamada T. Early stages of motor neuron differentiation revealed by expression of homeobox gene *Islet-1*. *Science.* 1992 Jun 12;256(5063):1555-60.

Erskine L, Patel K, Clarke JD. Progenitor dispersal and the origin of early neuronal phenotypes in the chick embryo spinal cord. *Dev Biol.* 1998 Jul 1;199(1):26-41.

Fan G, Martinowich K, Chin MH, He F, Fouse SD, Hutnick L, Hattori D, Ge W, Shen Y, Wu H, ten Hoeve J, Shuai K, Sun YE. DNA methylation controls the timing of astrogliogenesis through regulation of JAK-STAT signaling. *Development.* 2005 Aug;132(15):3345-56.

Faux C, Hawadle M, Nixon J, Wallace A, Lee S, Murray S, Stoker A. PTPsigma binds and dephosphorylates neurotrophin receptors and can suppress NGF-dependent neurite outgrowth from sensory neurons. *Biochim Biophys Acta.* 2007 Nov;1773(11):1689-700.

Ferreri DM, Minnear FL, Yin T, Kowalczyk AP, Vincent PA. N-cadherin levels in endothelial cells are regulated by monolayer maturity and p120 availability. *Cell Commun Adhes.* 2008 Nov;15(4):333-49.

Ferrier V. Genetics still moving forward. *Nat Cell Biol.* 2001 Oct;3(10):E231

Fire A, Xu S, Montgomery MK, Kostas SA, Driver SE, Mello CC. Potent and specific genetic interference by double-stranded RNA in *Caenorhabditis elegans*. *Nature.* 1998 Feb 19;391(6669):806-11.

Fortini ME. Notch signaling: the core pathway and its posttranslational regulation. *Dev Cell.* 2009 May;16(5):633-47.

Frade JM. Interkinetic nuclear movement in the vertebrate neuroepithelium: encounters with an old acquaintance. *Prog Brain Res.* 2002;136:67-71. Review.

Fry EJ, Chagnon MJ, López-Vales R, Tremblay ML, David S. Corticospinal tract regeneration after spinal cord injury in receptor protein tyrosine phosphatase sigma deficient mice. *Glia.* 2010 Mar;58(4):423-33.

- Fuchs M, Müller T, Lerch MM, Ullrich A. Association of human protein-tyrosine phosphatase kappa with members of the armadillo family. *J Biol Chem*. 1996 Jul 12;271(28):16712-9.
- Fujita S. Analysis of neuron differentiation in the central nervous system by titrated thymidine autoradiography. *J Comp Neurol*. 1964 Jun;122:311-27.
- Fujita S. The discovery of the matrix cell, the identification of the multipotent neural stem cell and the development of the central nervous system. *Cell Struct Funct*. 2003 Aug;28(4):205-28.
- Garrity PA, Lee CH, Salecker I, Robertson HC, Desai CJ, Zinn K, Zipursky SL. Retinal axon target selection in *Drosophila* is regulated by a receptor protein tyrosine phosphatase. *Neuron*. 1999 Apr;22(4):707-17.
- Goodman CS. Mechanisms and molecules that control growth cone guidance. *Annu Rev Neurosci*. 1996;19:341-77.
- Götz M, Huttner WB. The cell biology of neurogenesis. *Nat Rev Mol Cell Biol*. 2005 Oct;6(10):777-88.
- Goulding MD, Lumsden A, Gruss P. Signals from the notochord and floor plate regulate the region-specific expression of two Pax genes in the developing spinal cord. *Development*. 1993 Mar;117(3):1001-16.
- Guidato S, Prin F, Guthrie S. Somatic motoneurone specification in the hindbrain: the influence of somite-derived signals, retinoic acid and Hoxa3. *Development*. 2003 Jul;130(13):2981-96.
- Gupta S, Schoer RA, Egan JE, Hannon GJ, Mittal V. Inducible, reversible, and stable RNA interference in mammalian cells. *Proc Natl Acad Sci U S A*. 2004 Feb 17;101(7):1927-32.
- Gustafson AL, Mason I. Expression of receptor tyrosine phosphatase gamma during early development of the chick embryo. *Mech Dev*. 2000 Nov;98(1-2):183-6.
- Guthrie S, Butcher M, Lumsden A. Patterns of cell division and interkinetic nuclear migration in the chick embryo hindbrain. *J Neurobiol*. 1991 Oct;22(7):742-54.
- Haj F, McKinnell I, Stoker A. Retinotectal ligands for the receptor tyrosine phosphatase CRYPalpha. *Mol Cell Neurosci*. 1999 Sep;14(3):225-40.
- Halbleib JM, Nelson WJ. Cadherins in development: cell adhesion, sorting, and tissue morphogenesis. *Genes Dev*. 2006 Dec 1;20(23):3199-214.
- Halfter W, Dong S, Yip YP, Willem M, Mayer U. A critical function of the pial basement membrane in cortical histogenesis. *J Neurosci*. 2002 Jul 15;22(14):6029-40.

Hamburger, V., Hamilton, H.L., 1951. A series of normal stages in the development of the chick embryo. 1992; *Dev Dyn* 195, 231-272.

Hammond SM, Bernstein E, Beach D, Hannon GJ. An RNA-directed nuclease mediates post-transcriptional gene silencing in *Drosophila* cells. *Nature*. 2000 Mar 16;404(6775):293-6.

Hammond SM, Boettcher S, Caudy AA, Kobayashi R, Hannon GJ. Argonaute2, a link between genetic and biochemical analyses of RNAi. *Science*. 2001 Aug 10;293(5532):1146-50.

Hannon GJ. RNA interference. *Nature*. 2002 Jul 11;418(6894):244-51.

Harpavat S, Cepko CL. RCAS-RNAi: a loss-of-function method for the developing chick retina. *BMC Dev Biol*. 2006 Jan 22;6:2.

Hartsock A, Nelson WJ. Adherens and tight junctions: structure, function and connections to the actin cytoskeleton. *Biochim Biophys Acta*. 2008 Mar;1778(3):660-9.

Hashemi H, Hurley M, Gibson A, Panova V, Tchetchelnitski V, Barr A, Stoker AW. Receptor tyrosine phosphatase PTPy is a regulator of spinal cord neurogenesis. *Mol Cell Neurosci*. 2011 Feb;46(2):469-82.

Hemmati-Brivanlou A, Melton DA. Inhibition of activin receptor signaling promotes neuralization in *Xenopus*. *Cell*. 1994 Apr 22;77(2):273-81.

Hendriks WJ, Elson A, Harroch S, Pulido R, Stoker A, den Hertog J. Protein tyrosine phosphatases in health and disease. *FEBS J*. 2012 Sep 1. doi: 10.1111/febs.12000. [Epub ahead of print]

den Hertog J, Ostman A, Böhmer FD. Protein tyrosine phosphatases: regulatory mechanisms. *FEBS J*. 2008 Mar;275(5):831-47.

Hofmeyer K, Treisman JE. The receptor protein tyrosine phosphatase LAR promotes R7 photoreceptor axon targeting by a phosphatase-independent signaling mechanism. *Proc Natl Acad Sci U S A*. 2009 Nov 17;106(46):19399-404.

Holliday, M., Hamburger, V., 1977. An autoradiographic study of the formation of the lateral motor column in the chick embryo. *Br. Res.* 321, 197-208.

Hollyday M. Neurogenesis in the vertebrate neural tube. *Int J Dev Neurosci*. 2001 Apr;19(2):161-73.

Hollyday, M., 1980. Organization of motor pools in the chick lumbar lateral motor column. *J Comp Neurol* 194, 143-170.

Homma, S., Yaginuma, H., Oppenheim, R.W., 1994. Programmed cell death during the earliest stages of spinal cord development in the chick embryo: a possible means of early phenotypic selection. *J Comp Neurol* 345, 377-395.

Hobert O, Westphal H. Functions of LIM-homeobox genes. *Trends Genet.* 2000 Feb;16(2):75-83.

Ikeya M, Lee SM, Johnson JE, McMahon AP, Takada S. Wnt signalling required for expansion of neural crest and CNS progenitors. *Nature.* 1997 Oct 30;389(6654):966-70.

Inatani M, Irie F, Plump AS, Tessier-Lavigne M, Yamaguchi Y. Mammalian brain morphogenesis and midline axon guidance require heparan sulfate. *Science.* 2003 Nov 7;302(5647):1044-6.

Ivanova, A., Agochiya, M., Amoyel, M., Richardson, W.D., 2004. Receptor tyrosine phosphatase zeta/beta in astrocyte progenitors in the developing chick spinal cord. *Gene Expr Patterns* 4, 161-166.

Jacob J, Briscoe J. Gli proteins and the control of spinal-cord patterning. *EMBO Rep.* 2003 Aug;4(8):761-5.

Jacobson M. Clonal analysis and cell lineages of the vertebrate central nervous system. *Annu Rev Neurosci.* 1985;8:71-102.

Jamora C, Fuchs E. Intercellular adhesion, signalling and the cytoskeleton. *Nat Cell Biol.* 2002 Apr;4(4):E101-8.

Jeong J, McMahon AP. Growth and pattern of the mammalian neural tube are governed by partially overlapping feedback activities of the hedgehog antagonists patched 1 and Hhip1. *Development.* 2005 Jan;132(1):143-54.

Jessell TM. Neuronal specification in the spinal cord: inductive signals and transcriptional codes. *Nat Rev Genet.* 2000 Oct;1(1):20-9.

Johe KK, Hazel TG, Muller T, Dugich-Djordjevic MM, McKay RD. Single factors direct the differentiation of stem cells from the fetal and adult central nervous system. *Genes Dev.* 1996 Dec 15;10(24):3129-40.

Johnson KG, Holt CE. Expression of CRYP-alpha, LAR, PTP-delta, and PTP-rho in the developing *Xenopus* visual system. *Mech Dev.* 2000 Apr;92(2):291-4.

Johnson KG, McKinnell IW, Stoker AW, Holt CE. Receptor protein tyrosine phosphatases regulate retinal ganglion cell axon outgrowth in the developing *Xenopus* visual system. *J Neurobiol.* 2001 Nov 5;49(2):99-117.

Johnson KG, Van Vactor D. Receptor protein tyrosine phosphatases in nervous system development. *Physiol Rev.* 2003 Jan;83(1):1-24.

Jungbluth S, Bell E, Lumsden A. Specification of distinct motor neuron identities by the singular activities of individual Hox genes. *Development.* 1999 Jun;126(12):2751-8.

Kageyama R, Ohtsuka T, Kobayashi T. Roles of Hes genes in neural development. *Dev Growth Differ*. 2008 Jun;50 Suppl 1:S97-103.

Kajiguchi T, Chung EJ, Lee S, Stine A, Kiyoi H, Naoe T, Levis MJ, Neckers L, Trepel JB. FLT3 regulates beta-catenin tyrosine phosphorylation, nuclear localization, and transcriptional activity in acute myeloid leukemia cells. *Leukemia*. 2007 Dec;21(12):2476-84.

Kajiguchi T, Katsumi A, Tanizaki R, Kiyoi H, Naoe T. Y654 of β -catenin is essential for FLT3/ITD-related tyrosine phosphorylation and nuclear localization of β -catenin. *Eur J Haematol*. 2012 Apr;88(4):314-20.

Karlsson O, Thor S, Norberg T, Ohlsson H, Edlund T. Insulin gene enhancer binding protein Isl-1 is a member of a novel class of proteins containing both a homeo- and a Cys-His domain. *Nature*. 1990 Apr 26;344(6269):879-82.

Katahira T, Nakamura H. Gene silencing in chick embryos with a vector-based small interfering RNA system. *Dev Growth Differ*. 2003 Aug;45(4):361-7.

Kaufmann N, DeProto J, Ranjan R, Wan H, Van Vactor D. Drosophila liprin-alpha and the receptor phosphatase Dlar control synapse morphogenesis. *Neuron*. 2002 Mar 28;34(1):27-38.

Kessaris N, Pringle N, Richardson WD. Ventral neurogenesis and the neuron-glia switch. *Neuron*. 2001 Sep 13;31(5):677-80.

Kiecker C, Niehrs C. A morphogen gradient of Wnt/beta-catenin signalling regulates anteroposterior neural patterning in *Xenopus*. *Development*. 2001 Nov;128(21):4189-201.

Kim, K., Lee, K.Y., 2001. Tyrosine phosphorylation translocates beta-catenin from cell-cell interface to the cytoplasm, but does not significantly enhance the LEF-1-dependent transactivating function. *Cell Biol Int* 25, 421-427.

Kirkham, D.L., Pacey, L.K., Axford, M.M., Siu, R., Rotin, D., Doering, L.C., 2006. Neural stem cells from protein tyrosine phosphatase sigma knockout mice generate an altered neuronal phenotype in culture. *BMC Neurosci* 7, 50.

Konno D, Shioi G, Shitamukai A, Mori A, Kiyonari H, Miyata T, Matsuzaki F. Neuroepithelial progenitors undergo LGN-dependent planar divisions to maintain self-renewability during mammalian neurogenesis. *Nat Cell Biol*. 2008 Jan;10(1):93-101.

Kopan R, Ilagan MX. The canonical Notch signaling pathway: unfolding the activation mechanism. *Cell*. 2009 Apr 17;137(2):216-33.

Krueger NX, Van Vactor D, Wan HI, Gelbart WM, Goodman CS, Saito H. The transmembrane tyrosine phosphatase DLAR controls motor axon guidance in *Drosophila*. *Cell*. 1996 Feb 23;84(4):611-22.

Kypta RM, Su H, Reichardt LF. Association between a transmembrane protein tyrosine phosphatase and the cadherin-catenin complex. *J Cell Biol.* 1996 Sep;134(6):1519-29.

Lamb TM, Knecht AK, Smith WC, Stachel SE, Economides AN, Stahl N, Yancopoulos GD, Harland RM. Neural induction by the secreted polypeptide noggin. *Science.* 1993 Oct 29;262(5134):713-8.

Lamprianou, S., Vacaresse, N., Suzuki, Y., Meziane, H., Buxbaum, J.D., Schlessinger, J., Harroch, S., 2006. Receptor protein tyrosine phosphatase gamma is a marker for pyramidal cells and sensory neurons in the nervous system and is not necessary for normal development. *Mol Cell Biol* 26, 5106-5119.

Lamprianou S, Chatzopoulou E, Thomas JL, Bouyain S, Harroch S. A complex between contactin-1 and the protein tyrosine phosphatase PTPRZ controls the development of oligodendrocyte precursor cells. *Proc Natl Acad Sci U S A.* 2011 Oct 18;108(42):17498-503.

Lampugnani MG, Corada M, Andriopoulou P, Esser S, Risau W, Dejana E. Cell confluence regulates tyrosine phosphorylation of adherens junction components in endothelial cells. *J Cell Sci.* 1997 Sep;110 (Pt 17):2065-77.

Landmesser, L. The distribution of motoneurons supplying chick hind limb muscles. *J Physiol.* 1978; 284, 371-389.

Landmesser LT. The acquisition of motoneuron subtype identity and motor circuit formation. *Int J Dev Neurosci.* 2001 Apr;19(2):175-82.

Larsen M, Hoffman MP, Sakai T, Neibaur JC, Mitchell JM, Yamada KM. Role of PI 3-kinase and PIP3 in submandibular gland branching morphogenesis. *Dev Biol.* 2003 Mar 1;255(1):178-91.

Larsen M, Tremblay ML, Yamada KM. Phosphatases in cell-matrix adhesion and migration. *Nat Rev Mol Cell Biol.* 2003 Sep;4(9):700-11. Review.

Leber SM, Sanes JR. Migratory paths of neurons and glia in the embryonic chick spinal cord. *J Neurosci.* 1995 Feb;15(2):1236-48.

Ledig MM, McKinnell IW, Mrcic-Flogel T, Wang J, Alvares C, Mason I, Bixby JL, Mueller BK, Stoker AW. Expression of receptor tyrosine phosphatases during development of the retinotectal projection of the chick. *J Neurobiol.* 1999 Apr;39(1):81-96.

Ledig MM, Haj F, Bixby JL, Stoker AW, Mueller BK. The receptor tyrosine phosphatase CRYPalpha promotes intraretinal axon growth. *J Cell Biol.* 1999 Oct 18;147(2):375-88.

Lee SK, Pfaff SL. Synchronization of neurogenesis and motor neuron specification by direct coupling of bHLH and homeodomain transcription factors. *Neuron.* 2003 Jun 5;38(5):731-45.

Lee SH, Peng IF, Ng YG, Yanagisawa M, Bamji SX, Elia LP, Balsamo J, Lilien J, Anastasiadis PZ, Ullian EM, Reichardt LF. Synapses are regulated by the cytoplasmic tyrosine kinase Fer in a pathway mediated by p120catenin, Fer, SHP-2, and beta-catenin. *J Cell Biol.* 2008 Dec 1;183(5):893-908.

Lee SK, Jurata LW, Funahashi J, Ruiz EC, Pfaff SL. Analysis of embryonic motoneuron gene regulation: derepression of general activators function in concert with enhancer factors. *Development.* 2004 Jul;131(14):3295-306.

Lee KJ, Mendelsohn M, Jessell TM. Neuronal patterning by BMPs: a requirement for GDF7 in the generation of a discrete class of commissural interneurons in the mouse spinal cord. *Genes Dev.* 1998 Nov 1;12(21):3394-407.

Lee KF, Chan JY, Lau KF, Lee WC, Miller CC, Anderton BH, Shaw PC. Molecular cloning and expression analysis of human glycogen synthase kinase-3 alpha promoter. *Brain Res Mol Brain Res.* 2000 Dec 8;84(1-2):150-7.

Li, L., Prevette, D., Oppenheim, R.W., Milligan, C.E. Involvement of specific caspases in motoneuron cell death in vivo and in vitro following trophic factor deprivation. *Mol Cell Neurosci.* 1998; 12, 157-167.

Liem KF Jr, Tremml G, Roelink H, Jessell TM. Dorsal differentiation of neural plate cells induced by BMP-mediated signals from epidermal ectoderm. *Cell.* 1995 Sep 22;82(6):969-79.

Lilien, J., Balsamo, J. The regulation of cadherin-mediated adhesion by tyrosine phosphorylation/dephosphorylation of beta-catenin. *Curr Opin Cell Biol.* 2005; 17, 459-465.

Lilien J, Balsamo J, Arregui C, Xu G. Turn-off, drop-out: functional state switching of cadherins. *Dev Dyn.* 2002 May;224(1):18-29. Review.

Liu, S., Sugimoto, Y., Sorio, C., Tecchio, C., Lin, Y.C. Function analysis of estrogenically regulated protein tyrosine phosphatase gamma (PTPgamma) in human breast cancer cell line MCF-7. *Oncogene* 2004;23, 1256-1262.

Liu CZ, Yang JT, Yoon JW, Villavicencio E, Pfendler K, Walterhouse D, Iannaccone P. Characterization of the promoter region and genomic organization of GLI, a member of the Sonic hedgehog-Patched signaling pathway. *Gene.* 1998 Mar 16;209(1-2):1-11.

Liu X, Yue J, Frey RS, Zhu Q, Mulder KM. Transforming growth factor beta signaling through Smad1 in human breast cancer cells. *Cancer Res.* 1998 Oct 15;58(20):4752-7.

Liu JP, Laufer E, Jessell TM. Assigning the positional identity of spinal motor neurons: rostrocaudal patterning of Hox-c expression by FGFs, Gdf11, and retinoids. *Neuron.* 2001 Dec 20;32(6):997-1012.

- Lumsden A. Neural development. A 'LIM code' for motor neurons? *Curr Biol.* 1995 May 1;5(5):491-5.
- Lumsden A, Krumlauf R. Patterning the vertebrate neuraxis. *Science.* 1996 Nov 15;274(5290):1109-15.
- Louvi A, Artavanis-Tsakonas S. Notch signalling in vertebrate neural development. *Nat Rev Neurosci.* 2006 Feb;7(2):93-102.
- Ma YC, Song MR, Park JP, Henry Ho HY, Hu L, Kurtev MV, Zieg J, Ma Q, Pfaff SL, Greenberg ME. Regulation of motor neuron specification by phosphorylation of neurogenin 2. *Neuron.* 2008 Apr 10;58(1):65-77.
- Maden M. Retinoids and spinal cord development. *J Neurobiol.* 2006 Jun;66(7):726-38.
- Marchal L, Luxardi G, Thomé V, Kodjabachian L. BMP inhibition initiates neural induction via FGF signaling and *Zic* genes. *Proc Natl Acad Sci U S A.* 2009 Oct 13;106(41):17437-42.
- Marquardt T, Pfaff SL. Cracking the transcriptional code for cell specification in the neural tube. *Cell.* 2001 Sep 21;106(6):651-4.
- Matise MP, Epstein DJ, Park HL, Platt KA, Joyner AL. *Gli2* is required for induction of floor plate and adjacent cells, but not most ventral neurons in the mouse central nervous system. *Development.* 1998 Aug;125(15):2759-70.
- Maurel-Zaffran C, Suzuki T, Gahmon G, Treisman JE, Dickson BJ. Cell-autonomous and -nonautonomous functions of *LAR* in R7 photoreceptor axon targeting. *Neuron.* 2001 Oct 25;32(2):225-35.
- McDermott KW, Barry DS, McMahon SS. Role of radial glia in cytogenesis, patterning and boundary formation in the developing spinal cord. *J Anat.* 2005 Sep;207(3):241-50. Review.
- McLachlan RW, Yap AS. Not so simple: the complexity of phosphotyrosine signaling at cadherin adhesive contacts. *J Mol Med.* 2007 Jun;85(6):545-54.
- McLean J, Batt J, Doering LC, Rotin D, Bain JR. Enhanced rate of nerve regeneration and directional errors after sciatic nerve injury in receptor protein tyrosine phosphatase sigma knock-out mice. *J Neurosci.* 2002 Jul 1;22(13):5481-91.
- McMahon AP, Bradley A. The *Wnt-1* (*int-1*) proto-oncogene is required for development of a large region of the mouse brain. *Cell.* 1990 Sep 21;62(6):1073-85.
- McMahon JA, Takada S, Zimmerman LB, Fan CM, Harland RM, McMahon AP. *Noggin*-mediated antagonism of BMP signaling is required for growth and patterning of the neural tube and somite. *Genes Dev.* 1998 May 15;12(10):1438-52.

Meathrel, K., Adamek, T., Batt, J., Rotin, D., Doering, L.C., 2002. Protein tyrosine phosphatase sigma-deficient mice show aberrant cytoarchitecture and structural abnormalities in the central nervous system. *J Neurosci Res* 70, 24-35.

Megason, S.G., McMahon, A.P. A mitogen gradient of dorsal midline Wnts organizes growth in the CNS. *Development*. 2002; 129, 2087-2098.

Meng K, Rodriguez-Peña A, Dimitrov T, Chen W, Yamin M, Noda M, Deuel TF. Pleiotrophin signals increased tyrosine phosphorylation of beta beta-catenin through inactivation of the intrinsic catalytic activity of the receptor-type protein tyrosine phosphatase beta/zeta. *Proc Natl Acad Sci U S A*. 2000 Mar 14;97(6):2603-8.

Mette MF, Aufsatz W, van der Winden J, Matzke MA, Matzke AJ. Transcriptional silencing and promoter methylation triggered by double-stranded RNA. *EMBO J*. 2000 Oct 2;19(19):5194-201.

Michalides R, Volberg T, Geiger B. Augmentation of adherens junction formation in mesenchymal cells by co-expression of N-CAM or short-term stimulation of tyrosine-phosphorylation. *Cell Adhes Commun*. 1994 Dec;2(6):481-90.

Miner JH, Yurchenco PD. Laminin functions in tissue morphogenesis. *Annu Rev Cell Dev Biol*. 2004;20:255-84. Review.

Mohebiany AN, Nikolaienko RM, Bouyain S, Harroch S. Receptor-type tyrosine phosphatase ligands: looking for the needle in the haystack. *FEBS J*. 2012 Jun 11. doi: 10.1111/j.1742-4658.2012.08653.x. [Epub ahead of print]

Moreels M, Vandenabeele F, Deryck L, Lambrichts I. Radial glial cells derived from the neonatal rat spinal cord: morphological and immunocytochemical characterization. *Arch Histol Cytol*. 2005 Dec;68(5):361-9.

Muhr J, Andersson E, Persson M, Jessell TM, Ericson J. Groucho-mediated transcriptional repression establishes progenitor cell pattern and neuronal fate in the ventral neural tube. *Cell*. 2001 Mar 23;104(6):861-73.

Müller T, Choidas A, Reichmann E, Ullrich A. Phosphorylation and free pool of beta-catenin are regulated by tyrosine kinases and tyrosine phosphatases during epithelial cell migration. *J Biol Chem*. 1999 Apr 9;274(15):10173-83.

Müller T, Brohmann H, Pierani A, Heppenstall PA, Lewin GR, Jessell TM, Birchmeier C. The homeodomain factor *lhx1* distinguishes two major programs of neuronal differentiation in the dorsal spinal cord. *Neuron*. 2002 May 16;34(4):551-62.

Mullor JL, Dahmane N, Sun T, Ruiz i Altaba A. Wnt signals are targets and mediators of Gli function. *Curr Biol*. 2001 May 15;11(10):769-73.

Muroyama Y, Fujihara M, Ikeya M, Kondoh H, Takada S. Wnt signaling plays an essential role in neuronal specification of the dorsal spinal cord. *Genes Dev.* 2002 Mar 1;16(5):548-53.

Myat A, Henrique D, Ish-Horowicz D, Lewis J. A chick homologue of Serrate and its relationship with Notch and Delta homologues during central neurogenesis. *Dev Biol.* 1996 Mar 15;174(2):233-47.

Namihira M, Kohyama J, Semi K, Sanosaka T, Deneen B, Taga T, Nakashima K. Committed neuronal precursors confer astrocytic potential on residual neural precursor cells. *Dev Cell.* 2009 Feb;16(2):245-55.

Nelson WJ, Nusse R. Convergence of Wnt, beta-catenin, and cadherin pathways. *Science.* 2004 Mar 5;303(5663):1483-7.

Nelson CM, Pirone DM, Tan JL, Chen CS. Vascular endothelial-cadherin regulates cytoskeletal tension, cell spreading, and focal adhesions by stimulating RhoA. *Mol Biol Cell.* 2004 Jun;15(6):2943-53. Epub 2004 Apr 9.

Nelson BR, Hartman BH, Georgi SA, Lan MS, Reh TA. Transient inactivation of Notch signaling synchronizes differentiation of neural progenitor cells. *Dev Biol.* 2007 Apr 15;304(2):479-98.

Newsome TP, Asling B, Dickson BJ. Analysis of *Drosophila* photoreceptor axon guidance in eye-specific mosaics. *Development.* 2000 Feb;127(4):851-60.

Norden C, Young S, Link BA, Harris WA. Actomyosin is the main driver of interkinetic nuclear migration in the retina. *Cell.* 2009 Sep 18;138(6):1195-208.

Nordström U, Maier E, Jessell TM, Edlund T. An early role for WNT signaling in specifying neural patterns of Cdx and Hox gene expression and motor neuron subtype identity. *PLoS Biol.* 2006 Jul;4(8):e252.

Novitsch BG, Chen AI, Jessell TM. Coordinate regulation of motor neuron subtype identity and pan-neuronal properties by the bHLH repressor Olig2. *Neuron.* 2001 Sep 13;31(5):773-89.

Nurse P. A long twentieth century of the cell cycle and beyond. *Cell.* 2000 Jan 7;100(1):71-8. Review.

Nurse PM. Nobel Lecture. Cyclin dependent kinases and cell cycle control. *Biosci Rep.* 2002 Oct-Dec;22(5-6):487-99.

Nusse R. Developmental biology. Making head or tail of Dickkopf. *Nature.* 2001 May 17;411(6835):255-6.

Oblander SA, Ensslen-Craig SE, Longo FM, Brady-Kalnay SM. E-cadherin promotes retinal ganglion cell neurite outgrowth in a protein tyrosine phosphatase-mu-

dependent manner. *Mol Cell Neurosci.* 2007 Mar;34(3):481-92.

Oblander SA, Brady-Kalnay SM. Distinct PTPmu-associated signaling molecules differentially regulate neurite outgrowth on E-, N-, and R-cadherin. *Mol Cell Neurosci.* 2010 May;44(1):78-93.

Ohkawa J, Taira K. Control of the functional activity of an antisense RNA by a tetracycline-responsive derivative of the human U6 snRNA promoter. *Hum Gene Ther.* 2000 Mar 1;11(4):577-85.

Ohnuma S, Harris WA. Neurogenesis and the cell cycle. *Neuron.* 2003 Oct 9;40(2):199-208. Review.

Orford KW, Scadden DT. Deconstructing stem cell self-renewal: genetic insights into cell-cycle regulation. *Nat Rev Genet.* 2008 Feb;9(2):115-28.

Park HL, Bai C, Platt KA, Matisse MP, Beeghly A, Hui CC, Nakashima M, Joyner AL. Mouse *Gli1* mutants are viable but have defects in SHH signaling in combination with a *Gli2* mutation. *Development.* 2000 Apr;127(8):1593-605.

Pekarik, V., Bourikas, D., Miglino, N., Joset, P., Preiswerk, S., Stoeckli, E.T., 2003. Screening for gene function in chicken embryo using RNAi and electroporation. *Nat Biotechnol* 21, 93-96.

Pera EM, Ikeda A, Eivers E, De Robertis EM. Integration of IGF, FGF, and anti-BMP signals via *Smad1* phosphorylation in neural induction. *Genes Dev.* 2003 Dec 15;17(24):3023-8.

Persson M, Stamatakis D, te Welscher P, Andersson E, Böse J, Rütger U, Ericson J, Briscoe J. Dorsal-ventral patterning of the spinal cord requires *Gli3* transcriptional repressor activity. *Genes Dev.* 2002 Nov 15;16(22):2865-78.

Pfaff, S.L., Mendelsohn, M., Stewart, C.L., Edlund, T., Jessell, T.M., 1996. Requirement for LIM homeobox gene *Isl1* in motor neuron generation reveals a motor neuron-dependent step in interneuron differentiation. *Cell* 84, 309-320.

Piccolo S, Sasai Y, Lu B, De Robertis EM. Dorsoventral patterning in *Xenopus*: inhibition of ventral signals by direct binding of chordin to BMP-4. *Cell.* 1996 Aug 23;86(4):589-98.

Pierani A, Moran-Rivard L, Sunshine MJ, Littman DR, Goulding M, Jessell TM. Control of interneuron fate in the developing spinal cord by the progenitor homeodomain protein *Dbx1*. *Neuron.* 2001 Feb;29(2):367-84.

Pierfelice T, Alberi L, Gaiano N. Notch in the vertebrate nervous system: an old dog with new tricks. *Neuron.* 2011 Mar 10;69(5):840-55

Poh, A., Karunaratne, A., Kolle, G., Huang, N., Smith, E., Starkey, J., Wen, D., Wilson, I., Yamada, T., Hargrave, M., 2002. Patterning of the vertebrate ventral spinal

cord. *Int J Dev Biol* 46, 597-608.

Polakis P. Casein kinase 1: a Wnt'er of disconnect. *Curr Biol*. 2002 Jul 23;12(14):R499-R501.

Price, S.R., De Marco Garcia, N.V., Ranscht, B., Jessell, T.M. Regulation of motor neuron pool sorting by differential expression of type II cadherins. *Cell*. 2002; 109, 205-216.

Price SR, Briscoe J. The generation and diversification of spinal motor neurons: signals and responses. *Mech Dev*. 2004 Sep;121(9):1103-15.

Pringle, N.P., Yu, W.P., Howell, M., Colvin, J.S., Ornitz, D.M., Richardson, W.D. Fgfr3 expression by astrocytes and their precursors: evidence that astrocytes and oligodendrocytes originate in distinct neuroepithelial domains. *Development*. 2003; 130, 93-102.

Raff MC, Lillien LE, Richardson WD, Burne JF, Noble MD. Platelet-derived growth factor from astrocytes drives the clock that times oligodendrocyte development in culture. *Nature*. 1988 Jun 9;333(6173):562-5.

Ravin R, Hoepfner DJ, Munno DM, Carmel L, Sullivan J, Levitt DL, Miller JL, Athaide C, Panchision DM, McKay RD. Potency and fate specification in CNS stem cell populations in vitro. *Cell Stem Cell*. 2008 Dec 4;3(6):670-80.

Rakic P. Mode of cell migration to the superficial layers of fetal monkey neocortex. *J Comp Neurol*. 1972 May;145(1):61-83.

Rashid-Doubell F, McKinnell I, Aricescu AR, Sajjani G, Stoker A. Chick PTPsigma regulates the targeting of retinal axons within the optic tectum. *J Neurosci*. 2002 Jun 15;22(12):5024-33.

Rhee J, Buchan T, Zukerberg L, Lilien J, Balsamo J. Cables links Robo-bound Abl kinase to N-cadherin-bound beta-catenin to mediate Slit-induced modulation of adhesion and transcription. *Nat Cell Biol*. 2007 Aug;9(8):883-92.

Robertson CP, Braun MM, Roelink H. Sonic hedgehog patterning in chick neural plate is antagonized by a Wnt3-like signal. *Dev Dyn*. 2004 Mar;229(3):510-9.

Roelink H, Porter JA, Chiang C, Tanabe Y, Chang DT, Beachy PA, Jessell TM. Floor plate and motor neuron induction by different concentrations of the amino-terminal cleavage product of sonic hedgehog autoproteolysis. *Cell*. 1995 May 5;81(3):445-55.

Roztocil T, Matter-Sadzinski L, Alliod C, Ballivet M, Matter JM. NeuroM, a neural helix-loop-helix transcription factor, defines a new transition stage in neurogenesis. *Development*. 1997 Sep;124(17):3263-72.

Rubin JB, Choi Y, Segal RA. Cerebellar proteoglycans regulate sonic hedgehog responses during development. *Development*. 2002 May;129(9):2223-32.

- Ruiz i Altaba A. Catching a Gli-mpse of Hedgehog. *Cell*. 1997 Jul 25;90(2):193-6
- Saha MS, Miles RR, Grainger RM. Dorsal-ventral patterning during neural induction in *Xenopus*: assessment of spinal cord regionalization with xHB9, a marker for the motor neuron region. *Dev Biol*. 1997 Jul 15;187(2):209-23.
- Sakaguchi, N., Muramatsu, H., Ichihara-Tanaka, K., Maeda, N., Noda, M., Yamamoto, T., Michikawa, M., Ikematsu, S., Sakuma, S., Muramatsu, T. Receptor-type protein tyrosine phosphatase zeta as a component of the signaling receptor complex for midkine-dependent survival of embryonic neurons. *Neurosci Res*. 2003; 45, 219-224.
- Sallee, J.L., Wittchen, E.S., Burrige, K. Regulation of cell adhesion by protein tyrosine phosphatases 2. Cell-cell adhesion. *J Biol Chem*. 2006 Jun 16;281(24):16189-92.
- Sajnani-Perez G, Chilton JK, Aricescu AR, Haj F, Stoker AW. Isoform-specific binding of the tyrosine phosphatase PTPsigma to a ligand in developing muscle. *Mol Cell Neurosci*. 2003 Jan;22(1):37-48.
- Sasai Y. Roles of Sox factors in neural determination: conserved signaling in evolution? *Int J Dev Biol*. 2001;45(1):321-6
- Schaapveld RQ, Schepens JT, Bächner D, Attema J, Wieringa B, Jap PH, Hendriks WJ. Developmental expression of the cell adhesion molecule-like protein tyrosine phosphatases LAR, RPTPdelta and RPTPsigma in the mouse. *Mech Dev*. 1998 Sep;77(1):59-62.
- Schoenwolf GC, Folsom D, Moe A. A reexamination of the role of microfilaments in neurulation in the chick embryo. *Anat Rec*. 1988 Jan;220(1):87-102.
- Schoenwolf GC, Alvarez IS. Role of cell rearrangement in axial morphogenesis. *Curr Top Dev Biol*. 1992;27:129-73. Review.
- Schneeberger EE, Lynch RD. The tight junction: a multifunctional complex. *Am J Physiol Cell Physiol*. 2004 Jun;286(6):C1213-28. Review.
- Sechrist J, Bronner-Fraser M. Birth and differentiation of reticular neurons in the chick hindbrain: ontogeny of the first neuronal population. *Neuron*. 1991 Dec;7(6):947-63
- Seibler J, Kleinridders A, Küter-Luks B, Niehaves S, Brüning JC, Schwenk F. Reversible gene knockdown in mice using a tight, inducible shRNA expression system. *Nucleic Acids Res*. 2007;35(7):e54.
- Shapiro L, Colman DR. Structural biology of cadherins in the nervous system. *Curr Opin Neurobiol*. 1998 Oct;8(5):593-9. Review
- Sharma K, Leonard AE, Lettieri K, Pfaff SL. Genetic and epigenetic mechanisms contribute to motor neuron pathfinding. *Nature*. 2000 Aug 3;406(6795):515-9.

Shen Y, Tenney AP, Busch SA, Horn KP, Cuascut FX, Liu K, He Z, Silver J, Flanagan JG. PTPsigma is a receptor for chondroitin sulfate proteoglycan, an inhibitor of neural regeneration. *Science*. 2009 Oct 23;326(5952):592-6.

Shimojo H, Ohtsuka T, Kageyama R. Oscillations in notch signaling regulate maintenance of neural progenitors. *Neuron*. 2008 Apr 10;58(1):52-64.

Shintani T, Maeda N, Nishiwaki T, Noda M. Characterization of rat receptor-like protein tyrosine phosphatase gamma isoforms. *Biochem Biophys Res Commun*. 1997 Jan 13;230(2):419-25.

Shintani T, Maeda N, Noda M. Receptor-like protein tyrosine phosphatase gamma (RPTPgamma), but not PTPzeta/RPTPbeta, inhibits nerve-growth-factor-induced neurite outgrowth in PC12D cells. *Dev Neurosci*. 2001;23(1):55-69.

Shintani, T., Ihara, M., Sakuta, H., Takahashi, H., Watakabe, I., Noda, M. Eph receptors are negatively controlled by protein tyrosine phosphatase receptor type O. *Nat Neurosci*. 2006; 9, 761-769.

Shirasaki, R., Pfaff, S.L. Transcriptional codes and the control of neuronal identity. *Annu Rev Neurosci*. 2002; 25, 251-281.

Shukla V, Coumoul X, Deng CX. RNAi-based conditional gene knockdown in mice using a U6 promoter driven vector. *Int J Biol Sci*. 2007 Jan 5;3(2):91-9.

Silva JM, Hammond SM, Hannon GJ. RNA interference: a promising approach to antiviral therapy? *Trends Mol Med*. 2002 Nov;8(11):505-8.

Simeone A, Acampora D, Nigro V, Faiella A, D'Esposito M, Stornaiuolo A, Mavilio F, Boncinelli E. Differential regulation by retinoic acid of the homeobox genes of the four HOX loci in human embryonal carcinoma cells. *Mech Dev*. 1991 Mar;33(3):215-27.

Smith JC. Dorso-ventral patterning in the neural tube. *Curr Biol*. 1993 Sep 1;3(9):582-5.

Smith JL, Schoenwolf GC. Neurulation: coming to closure. *Trends Neurosci*. 1997 Nov;20(11):510-7.

Snøve O Jr, Rossi JJ. Expressing short hairpin RNAs in vivo. *Nat Methods*. 2006 Sep;3(9):689-95.

Sockanathan, S., Jessell, T.M. Motor neuron-derived retinoid signaling specifies the subtype identity of spinal motor neurons. *Cell*. 1998; 94, 503-514.

Sockanathan S, Perlmann T, Jessell TM. Retinoid receptor signaling in postmitotic motor neurons regulates rostrocaudal positional identity and axonal projection pattern. *Neuron*. 2003 Sep 25;40(1):97-111.

- Sockanathan S. Towards cracking the code: LIM protein complexes in the spinal cord. *Trends Neurosci.* 2003 Feb;26(2):57-9.
- Sommer, L., Rao, M., Anderson, D.J., 1997. RPTP delta and the novel protein tyrosine phosphatase RPTP psi are expressed in restricted regions of the developing central nervous system. *Dev Dyn* 208, 48-61.
- Sorio C, Melotti P, D'Arcangelo D, Mendrola J, Calabretta B, Croce CM, Huebner K. Receptor protein tyrosine phosphatase gamma, Ptp gamma, regulates hematopoietic differentiation. *Blood.* 1997 Jul 1;90(1):49-57.
- Soula C, Danesin C, Kan P, Grob M, Poncet C, Cochard P. Distinct sites of origin of oligodendrocytes and somatic motoneurons in the chick spinal cord: oligodendrocytes arise from Nkx2.2-expressing progenitors by a Shh-dependent mechanism. *Development.* 2001 Apr;128(8):1369-79.
- Spemann, H. *Embryonic Development and Induction.* New Haven, Yale University Press, 1938.
- Stamatakis D, Ulloa F, Tsoni SV, Mynett A, Briscoe J. A gradient of Gli activity mediates graded Sonic Hedgehog signaling in the neural tube. *Genes Dev.* 2005 Mar 1;19(5):626-41.
- Stegmeier F, Hu G, Rickles RJ, Hannon GJ, Elledge SJ. A lentiviral microRNA-based system for single-copy polymerase II-regulated RNA interference in mammalian cells. *Proc Natl Acad Sci U S A.* 2005 Sep 13;102(37):13212-7.
- Stepanek, L., Stoker, A.W., Stoeckli, E., Bixby, J.L. Receptor tyrosine phosphatases guide vertebrate motor axons during development. *J Neurosci.* 2005; 25, 3813-3823.
- Stoker AW. Isoforms of a novel cell adhesion molecule-like protein tyrosine phosphatase are implicated in neural development. *Mech Dev.* 1994 Jun;46(3):201-17.
- Stoker AW, Gehrig B, Haj F, Bay BH. Axonal localisation of the CAM-like tyrosine phosphatase CRYP alpha: a signalling molecule of embryonic growth cones. *Development.* 1995 Jun;121(6):1833-44.
- Stoker AW. Receptor tyrosine phosphatases in axon growth and guidance. *Curr Opin Neurobiol.* 2001 Feb;11(1):95-102.
- Stoker AW. Protein tyrosine phosphatases and signalling. *J Endocrinol.* 2005 Apr;185(1):19-33.
- Streit A, Berliner AJ, Papanayotou C, Sirulnik A, Stern CD. Initiation of neural induction by FGF signalling before gastrulation. *Nature.* 2000 Jul 6;406(6791):74-8.
- Sui G, Soohoo C, Affar el B, Gay F, Shi Y, Forrester WC, Shi Y. A DNA vector-based RNAi technology to suppress gene expression in mammalian cells. *Proc Natl Acad Sci U S A.* 2002 Apr 16;99(8):5515-20.

Sui XF, Kiser TD, Hyun SW, Angelini DJ, Del Vecchio RL, Young BA, Hasday JD, Romer LH, Passaniti A, Tonks NK, Goldblum SE. Receptor protein tyrosine phosphatase micro regulates the paracellular pathway in human lung microvascular endothelia. *Am J Pathol.* 2005 Apr;166(4):1247-58.

Sun QL, Wang J, Bookman RJ, Bixby JL. Growth cone steering by receptor tyrosine phosphatase delta defines a distinct class of guidance cue. *Mol Cell Neurosci.* 2000 Nov;16(5):686-95.

Sun Q, Schindelholz B, Knirr M, Schmid A, Zinn K. Complex genetic interactions among four receptor tyrosine phosphatases regulate axon guidance in *Drosophila*. *Mol Cell Neurosci.* 2001 Feb;17(2):274-91.

Taira M, Jamrich M, Good PJ, Dawid IB. The LIM domain-containing homeo box gene *Xlim-1* is expressed specifically in the organizer region of *Xenopus* gastrula embryos. *Genes Dev.* 1992 Mar;6(3):356-66.

Taira M, Hayes WP, Otani H, Dawid IB. Expression of LIM class homeobox gene *Xlim-3* in *Xenopus* development is limited to neural and neuroendocrine tissues. *Dev Biol.* 1993 Sep;159(1):245-56.

Takahashi T, Nowakowski RS, Caviness VS Jr. Mode of cell proliferation in the developing mouse neocortex. *Proc Natl Acad Sci U S A.* 1994 Jan 4;91(1):375-9.

Takahashi H, Arstikaitis P, Prasad T, Bartlett TE, Wang YT, Murphy TH, Craig AM. Postsynaptic TrkC and presynaptic PTP σ function as a bidirectional excitatory synaptic organizing complex. *Neuron.* 2011 Jan 27;69(2):287-303.

Takebayashi H, Yoshida S, Sugimori M, Kosako H, Kominami R, Nakafuku M, Nabeshima Y. Dynamic expression of basic helix-loop-helix Olig family members: implication of *Olig2* in neuron and oligodendrocyte differentiation and identification of a new member, *Olig3*. *Mech Dev.* 2000 Dec;99(1-2):143-8.

Tanabe Y, Jessell TM. Diversity and pattern in the developing spinal cord. *Science.* 1996 Nov 15;274(5290):1115-23.

Tanabe Y, William C, Jessell TM. Specification of motor neuron identity by the MNR2 homeodomain protein. *Cell.* 1998 Oct 2;95(1):67-80.

Tessier-Lavigne M, Goodman CS. The molecular biology of axon guidance. *Science.* 1996 Nov 15;274(5290):1123-33.

Thaler J, Harrison K, Sharma K, Lettieri K, Kehrl J, Pfaff SL. Active suppression of interneuron programs within developing motor neurons revealed by analysis of homeodomain factor HB9. *Neuron.* 1999 Aug;23(4):675-87.

Timmer JR, Wang C, Niswander L. BMP signaling patterns the dorsal and intermediate neural tube via regulation of homeobox and helix-loop-helix transcription factors. *Development.* 2002 May;129(10):2459-72.

Tonks NK. Protein tyrosine phosphatases: from genes, to function, to disease. *Nat Rev Mol Cell Biol.* 2006 Nov;7(11):833-46.

Tonks NK, Neel BG. Combinatorial control of the specificity of protein tyrosine phosphatases. *Curr Opin Cell Biol.* 2001 Apr;13(2):182-95.

Tosney KW, Hotary KB, Lance-Jones C. Specifying the target identity of motoneurons. *Bioessays.* 1995 May;17(5):379-82.

Tsuda S, Kitagawa T, Takashima S, Asakawa S, Shimizu N, Mitani H, Shima A, Tsutsumi M, Hori H, Naruse K, Ishikawa Y, Takeda H. FAK-mediated extracellular signals are essential for interkinetic nuclear migration and planar divisions in the neuroepithelium. *J Cell Sci.* 2010 Feb 1;123(Pt 3):484-96.

Tsuchida T, Ensini M, Morton SB, Baldassare M, Edlund T, Jessell TM, Pfaff SL. Topographic organization of embryonic motor neurons defined by expression of LIM homeobox genes. *Cell.* 1994 Dec 16;79(6):957-70.

Uetani, N., Chagnon, M.J., Kennedy, T.E., Iwakura, Y., Tremblay, M.L. Mammalian motoneuron axon targeting requires receptor protein tyrosine phosphatases sigma and delta. *J Neurosci.* 2006; 26, 5872-5880.

Van der Zee CE, Man TY, Van Lieshout EM, Van der Heijden I, Van Bree M, Hendriks WJ. Delayed peripheral nerve regeneration and central nervous system collateral sprouting in leucocyte common antigen-related protein tyrosine phosphatase-deficient mice. *Eur J Neurosci.* 2003 Mar;17(5):991-1005.

Vilas-Boas F, Fior R, Swedlow JR, Storey KG, Henrique D. A novel reporter of notch signalling indicates regulated and random Notch activation during vertebrate neurogenesis. *BMC Biol.* 2011 Aug 31;9:58. doi: 10.1186/1741-7007-9-58.

Waddington CH, Waterman AJ. The Development in vitro of Young Rabbit Embryos. *J Anat.* 1933 Apr;67(Pt 3):355-70.

Wakamatsu, Y., Nakamura, N., Lee, J.A., Cole, G.J., Osumi, N. Translin, a nestin-like intermediate filament protein, mediates cortical localization and the lateral transport of Numb in mitotic avian neuroepithelial cells. *Development.* 2007; 134, 2425-2433.

Wallace MJ, Batt J, Fladd CA, Henderson JT, Skarnes W, Rotin D. Neuronal defects and posterior pituitary hypoplasia in mice lacking the receptor tyrosine phosphatase PTPsigma. *Nat Genet.* 1999 Mar;21(3):334-8.

Wang Y, Johnson P. Expression of CD45 lacking the catalytic protein tyrosine phosphatase domain modulates Lck phosphorylation and T cell activation. *J Biol Chem.* 2005 Apr 8;280(14):14318-24.

Wang J, Bixby JL. Receptor tyrosine phosphatase-delta is a homophilic, neurite-promoting cell adhesion molecular for CNS neurons. *Mol Cell Neurosci.* 1999 Oct-Nov;14(4-5):370-84.

- Wang B, Fallon JF, Beachy PA. Hedgehog-regulated processing of Gli3 produces an anterior/posterior repressor gradient in the developing vertebrate limb. *Cell*. 2000 Feb 18;100(4):423-34.
- Wilcock AC, Swedlow JR, Storey KG. Mitotic spindle orientation distinguishes stem cell and terminal modes of neuron production in the early spinal cord. *Development*. 2007 May;134(10):1943-54.
- Willert K, Brown JD, Danenberg E, Duncan AW, Weissman IL, Reya T, Yates JR 3rd, Nusse R. Wnt proteins are lipid-modified and can act as stem cell growth factors. *Nature*. 2003 May 22;423(6938):448-52.
- William CM, Tanabe Y, Jessell TM. Regulation of motor neuron subtype identity by repressor activity of Mnx class homeodomain proteins. *Development*. 2003 Apr;130(8):1523-36.
- Wills Z, Bateman J, Korey CA, Comer A, Van Vactor D. The tyrosine kinase Abl and its substrate enabled collaborate with the receptor phosphatase Dlar to control motor axon guidance. *Neuron*. 1999 Feb;22(2):301-12.
- Wilson PA, Hemmati-Brivanlou A. Induction of epidermis and inhibition of neural fate by Bmp-4. *Nature*. 1995 Jul 27;376(6538):331-3.
- Wine-Lee L, Ahn KJ, Richardson RD, Mishina Y, Lyons KM, Crenshaw EB 3rd. Signaling through BMP type 1 receptors is required for development of interneuron cell types in the dorsal spinal cord. *Development*. 2004 Nov;131(21):5393-403
- Wilson SI, Rydström A, Trimborn T, Willert K, Nusse R, Jessell TM, Edlund T. The status of Wnt signalling regulates neural and epidermal fates in the chick embryo. *Nature*. 2001 May 17;411(6835):325-30.
- Wu CW, Kao HL, Li AF, Chi CW, Lin WC. Protein tyrosine-phosphatase expression profiling in gastric cancer tissues. *Cancer Lett*. 2006 Oct 8;242(1):95-103.
- Wyszynski M, Kim E, Dunah AW, Passafaro M, Valtschanoff JG, Serra-Pagès C, Streuli M, Weinberg RJ, Sheng M. Interaction between GRIP and liprin-alpha/SYD2 is required for AMPA receptor targeting. *Neuron*. 2002 Mar 28;34(1):39-52.
- Xiong Q, Guo X, Zong CS, Jong Sm, Jiang Y, Chan J, Wang LH. Cloning and Expression of Chicken Protein Tyrosine Phosphatase Gamma. *J Biomed Sci*. 1996 Jul-Aug;3(4):266-274.
- Yamada S, Pokutta S, Drees F, Weis WI, Nelson WJ. Deconstructing the cadherin-catenin-actin complex. *Cell*. 2005 Dec 2;123(5):889-901.
- Yan Q, Liu WB, Qin J, Liu J, Chen HG, Huang X, Chen L, Sun S, Deng M, Gong L, Li Y, Zhang L, Liu Y, Feng H, Xiao Y, Liu Y, Li DW. Protein phosphatase-1 modulates the function of Pax-6, a transcription factor controlling brain and eye

development. *J Biol Chem.* 2007 May 11;282(19):13954-65.

Yang, X., Tomita, T., Wines-Samuelson, M., Beglopoulos, V., Tansey, M.G., Kopan, R., Shen, J. Notch1 signaling influences v2 interneuron and motor neuron development in the spinal cord. *Dev Neurosci.* 2006; 28, 102-117.

Yasuda Y, Fujita S. Distribution of MAP1A, MAP1B, and MAP2A&B during layer formation in the optic tectum of developing chick embryos. *Cell Tissue Res.* 2003 Dec;314(3):315-24.

Yurchenco PD, Wadsworth WG. Assembly and tissue functions of early embryonic laminins and netrins. *Curr Opin Cell Biol.* 2004 Oct;16(5):572-9.

Zamore PD, Tuschl T, Sharp PA, Bartel DP. RNAi: double-stranded RNA directs the ATP-dependent cleavage of mRNA at 21 to 23 nucleotide intervals. *Cell.* 2000 Mar 31;101(1):25-33.

Zechner, D., Fujita, Y., Hulsken, J., Muller, T., Walther, I., Taketo, M.M., Crenshaw, E.B., 3rd, Birchmeier, W., Birchmeier, C. beta-Catenin signals regulate cell growth and the balance between progenitor cell expansion and differentiation in the nervous system. *Dev Biol.* 2003; 258, 406-418.

Zechner D, Müller T, Wende H, Walther I, Taketo MM, Crenshaw EB 3rd, Treier M, Birchmeier W, Birchmeier C. Bmp and Wnt/beta-catenin signals control expression of the transcription factor Olig3 and the specification of spinal cord neurons. *Dev Biol.* 2007 Mar 1;303(1):181-90.

Zhong, W., Chia, W. Neurogenesis and asymmetric cell division. *Curr Opin Neurobiol.* 2008; 18, 4-11.

Zhou Q, Choi G, Anderson DJ. The bHLH transcription factor Olig2 promotes oligodendrocyte differentiation in collaboration with Nkx2.2. *Neuron.* 2001 Sep 13;31(5):791-807.

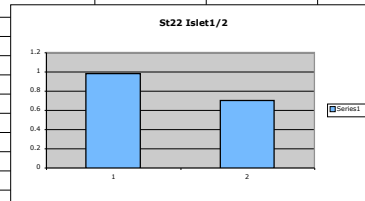
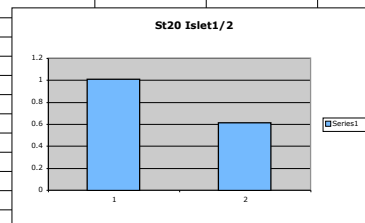
Zhuang B, Sockanathan S. Dorsal-ventral patterning: a view from the top. *Curr Opin Neurobiol.* 2006 Feb;16(1):20-4.

Zondag GC, Reynolds AB, Moolenaar WH. Receptor protein-tyrosine phosphatase RPTPmu binds to and dephosphorylates the catenin p120(ctn). *J Biol Chem.* 2000 Apr 14;275(15):11264-9.

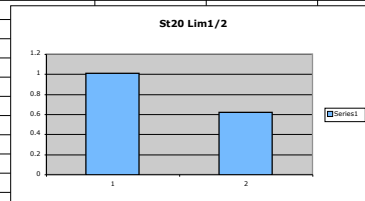
APPENDIX A

Neuronal Counts

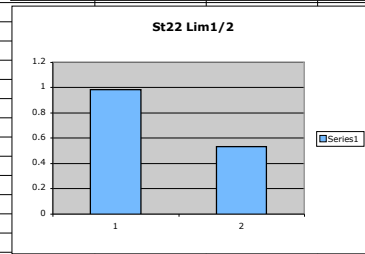
St20-Islet1/2	Si3	Con	Ratio	Negcon	Con	Ratio
Av 2 per Emb	8.57814E-05	Ttest 2T UEV	0.13837426	SD		0.105261579
a	19	29	0.66	28	27	1.03
b	12	26	0.46	30	31	0.97
c	9	21	0.43	29	30	0.97
d	12	22	0.55	26	29	0.9
e	12	20	0.6	22	19	1.16
f	18	26	0.69	23	20	1.15
g	21	28	0.75	26.33333333	26	1.03
h	26	29	0.9			
I	8	14	0.57			
j	16	27	0.59			
k	10	21	0.48			
l	12	21	0.57	1.01	0.61	
m	8	20	0.4	n=6	n=13	
	14.07692308	23.38461538	0.588461538			



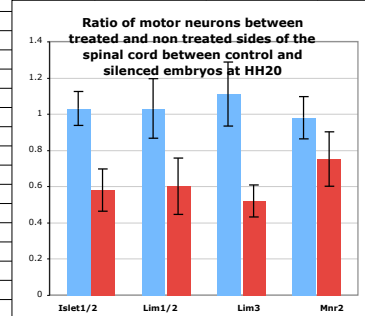
St22-Islet1/2	Si3	Con	Ratio	Negcon	Con	Ratio
Av 2 per Emb	6.68772E-05	Ttest 2T UEV	0.104690019	SD		0.104578519
a	34	43	0.79	40	46	0.87
b	34	44	0.77	41	36	1.14
c	22	41	0.54	38	42	0.9
d	27	41	0.66	44	45	0.98
e	17.5	35	0.5	46	43	1.07
f	20	30.5	0.66	39	42	0.93
g	32	44	0.73	41.33333333	42.33333333	0.981666667
h	31.5	40	0.79			
I	33	42	0.79	0.98	0.7	
j	29	41	0.71	n=6	n=10	
	28	40.15	0.694			



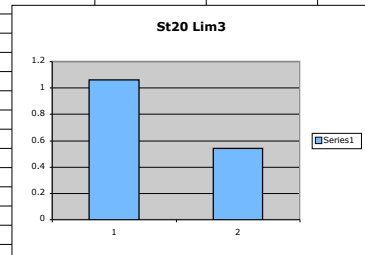
St20-Lim1/2	Si3	Con	Ratio	Negcon	Con	Ratio
Av 2 per Emb	0.000353167	Ttest 2T UEV	0.161993266			0.185013513
a	7	15	0.47	15	15	1
b	4	10	0.4	14	16	0.88
c	7	11	0.64	13	10	1.3
d	8	16	0.5	18	15	1.2
e	8	13	0.62	13.5	16	0.84
f	10	17	0.59	14	15	0.93
g	12	15	0.8	14.58333333	14.5	1.025
h	12.5	16	0.78			
I	11	14	0.79	1.01	0.62	
j	3	9	0.33	n=6	n=11	
k	10	14	0.71			
	8.409090909	13.63636364	0.602727273			



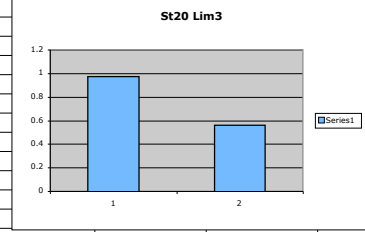
St22-Lim1/2	Si3	Con	Ratio	Negcon	Con	Ratio
Av 2 per Emb	5.66545E-08	Ttest 2T UEV	0.145693743			0.102111051
a	19	26	0.73	29	26	1.12
b	11	27	0.41	28	27	1.04
c	10	28	0.36	22	26	0.85
d	10.5	22	0.48	24	25	0.96
e	9	24	0.38	25	28	0.89
f	18	26	0.69	26	25	1.04
g	11	27	0.41	25.66666667	26.16666667	0.983333333
h	13	23.5	0.55			
I	14	23	0.61	0.98	0.53	
j	18	25	0.72	n=6	n=10	
	13.35	25.15	0.534			



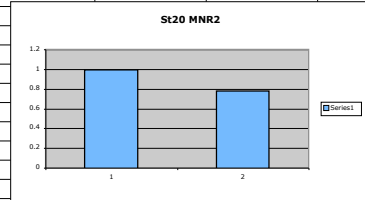
St20-Lim3	Si3	Con	Ratio	Negcon	Con	Ratio
Av 2 per Emb	0.000897405	Ttest 2T UEV	0.093464464			0.18622567
a	4.5	9.5	0.47	7	6	1.17
b	7.5	15	0.5	7.5	9.5	0.8
c	15	23.5	0.51	5	4	1.25
d	10	14	0.71	10.5	9.5	1.11
e	4.5	7.5	0.6	5	4	1.25
f	9.5	13.5	0.48	7	6.6	1.116
g	3.5	6	0.58			
h	2	4.5	0.44	1.06	0.54	
I	4	6.5	0.62	n=6	n=12	
j	7.5	19	0.39			
k	6.5	12.5	0.52			
l	13	32	0.41			
	7.291666667	13.625	0.519166667			



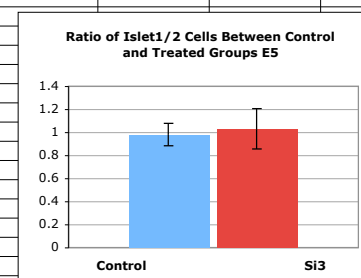
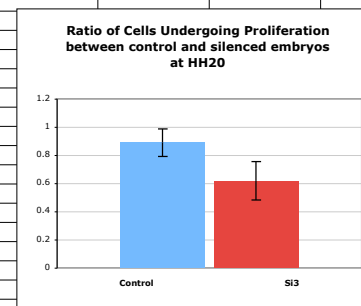
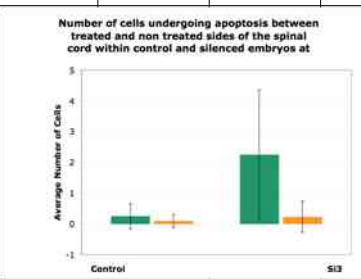
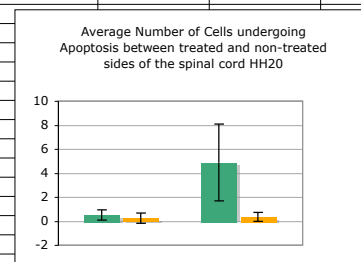
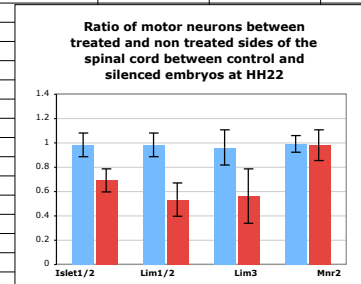
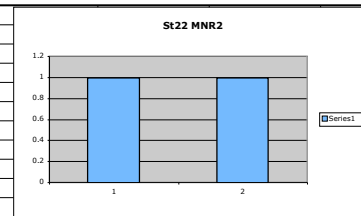
St22-Lim3	Si3	Con	Ratio	Negcon	Con	Ratio
Av 2 per Emb	0.000854047	Ttest 2T UEV	0.261298042			0.157056253
a	0	5	0	6	5	1.2
b	2	3	0.67	5	5	1
c	4	6	0.67	4	4	1
d	3	4	0.75	3	4	0.75
e	3	6	0.5	5	6	0.83
f	3	4	0.75	5	5	1
g	1	5	0.2	4.666666667	4.833333333	0.963333333
h	4	5	0.8			
I	2	3	0.67	0.97	0.56	
j	3	5	0.6	n=6	n=10	
	2.5	4.6	0.561			



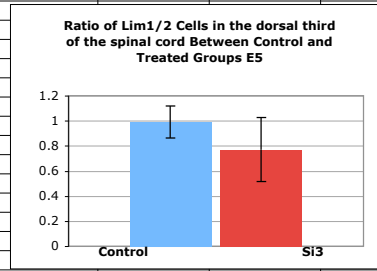
St20-MNR2	Si3	Con	Ratio	Negcon	Con	Ratio
Av 2 per Emb	0.003543041	Ttest 2T UEV	0.162095651			0.127226832
a	31	33	0.94	14	16.5	0.85
b	12.5	24.5	0.51	39	36	1.09
c	13	16	0.81	18.7	16.7	1.12
d	5	10.5	0.48	18.5	22.5	0.82
e	10.5	13	0.81	24	25	0.96
f	8	11	0.73	19	18	1.06



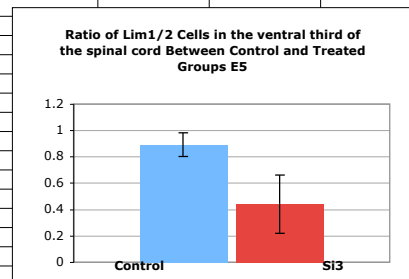
g	18.5	20	0.93	22.2	22.45	0.983333333
h	13	17	0.76			
I	25	31	0.81	0.99	0.78	
	15.1666667	19.5555556	0.753333333	n=7	n=9	
St22-MNR2	Si3	Con	Ratio	Negcon	Con	Ratio
Av 2 per Emb	0.769875	Ttest 2T UEV	0.14399074			0.067354782
a	9	9	1	26	28	0.93
b	12	12	1	25	23	1.09
c	22	22	1	22	24	0.92
d	30	31	0.97	28	27	1.04
e	7	11	0.64	20	21	0.95
f	18	19	0.95	24	24	1
g	28	29	0.96	24.1666667	24.5	0.988333333
h	19	17	1.12			
I	24	20	1.2	0.99	0.99	
j	22	23	0.96	n=6	n=10	
	19.1	19.3	0.98			
St20-C3	Si3	Con	Ratio	Negcon	Con	Ratio
Av 2 per Emb	3.21117193	0.369072765	SD	0.447213595	0.418330013	
a	5.5	0		0	1	
b	3	0		1	0	
c	3.25	0.5		0.5	0.5	
d	6.5	1		1	0	
e	6.5	0		0.5	0	
f	7	0.5		0	0	
g	9	1		0.5	0.25	
h	6.67	0				
I	3.67	0				
j	4	1				
k	0	0.33				
l	1	0	6.6648E-06	Ttest 1T EqV		
m	0	0.33				
n	12	0.25				
o	9	0.25				
p	3.5	0				
q	3	0.5				
r	4	0.67				
	4.866111111	0.351666667		0.5	0.25	
		n=18			n=6	
St22-C3	Si3	Con	Ratio	Negcon	Con	Ratio
Av 2 per Emb	2.108475537	0.51877478		0.418330013	0.204124145	
a	5	1.75		0	0.5	
b	4.5	0.25		0	0	
c	0	0		1	0	
d	5.25	0.25		0	0	
e	0	0		0	0	
f	2	0		0.5	0	
g	1.33	0		0.25	0.083333333	
h	1.33	0				
I	1	0	0.00284847	Ttest 1T EqV		
j	0	0.33				
k	4.33	0				
	2.249090909	0.234545455		0.25	0.083333333	
		n=11			n=6	
St20 -H3	Si3	Con	Ratio	Negcon	Con	Ratio
Av 2 per Emb	0.001019906	Ttest 2T UEV	0.141562707			0.096626428
a	6	10	0.6	13	14	0.93
b	8	12	0.67	12	15	0.8
c	10	15	0.67	18	17	1.06
d	11	22	0.5	15	17	0.88
e	5	12	0.42	13	16	0.81
f	7	10	0.7	11	13	0.85
g	11	12	0.92	13.6666667	15.33333333	0.888333333
h	7	14	0.5			
I	9	13	0.69			
j	6	11	0.55			
	8	13.1	0.622	13.66667	15.3333333	
		n=10			n=6	
E5 Islet1/2	Si3	Con	Ratio	Negcon	Con	Ratio
Av 2 per Emb	0.780083106	Ttest 2T UEV	0.183612228			0.102502033
a	163	185	0.88	133	137	0.97
b	118	124	0.95	101	92	1.1
c	110	137	0.8	114	125	0.91
d	101	110	0.92	164	186	0.88
e	131	136	0.96	122	109	1.12
f	145	194	0.75	141	153	0.92
g	265	183	1.45	129.1666667	133.6666667	0.983333333
h	227	213	1.07			
I	178	130	1.37			
j	186	149	1.25			
k	92	97	0.95	0.97	1.03	
l	104	86	1.21	n=6	n=19	
m	75	88	0.85			
n	92	93	0.99			
o	87	91	0.96			
p	145	147	0.99			
q	126	123	1.02			
r	145	129	1.12			
s	124	123	1.01			
	137.5789474	133.5789474	1.026315789			
E5 Lim1/2 UP	Si3	Con	Ratio	Negcon	Con	Ratio
Av 2 per Emb	0.006787394	Ttest 2T UEV	0.274705076			0.133028819
a	31	41	0.76	39	44	0.89



b	29	40	0.73	38	40	0.95
c	51	34	1.5	45	41	1.1
d	20	47	0.43	43	47	0.91
e	28	41	0.68	40	45	0.89
f	30	32	0.94	47	39	1.21
g	19	40	0.48	42	42.6666667	0.991666667
h	29	41	0.71			
I	29	33	0.88			
j	35	40	0.88	0.99	0.75	
k	39	54	0.72	n=6	n=12	
l	38	63	0.6			
	31.5	42.1666667	0.775833333			

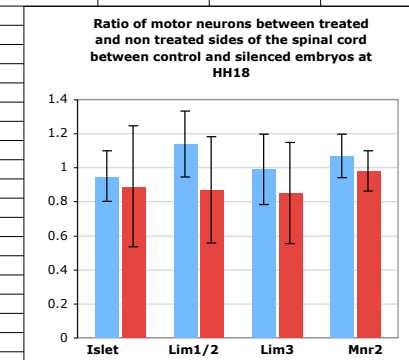


E5 Lim1/2 LO	Si3	Con	Ratio	Negcon	Con	Ratio
Av 2 per Emb	0.000451441	Ttest 2T UEV	0.257478261			0.096626428
a	19	52	0.37	43	57	0.75
b	36	59	0.61	51	57	0.89
c	16	51	0.31	48	46	1.04
d	46	56	0.82	55	60	0.92
e	4	17	0.24	38	46	0.83
f	2	12	0.17	44	49	0.9
g	5	11	0.45	46.5	52.5	0.888333333
h	2	14	0.14			
I	1	2	0.5			
j	14	34	0.41	0.89	0.51	
k	11	39	0.28	n=6	n=14	
l	19	72	0.26			
m	33	58	0.57			
n	73	69	1.06			
AV	20.07142857	39	0.442142857			



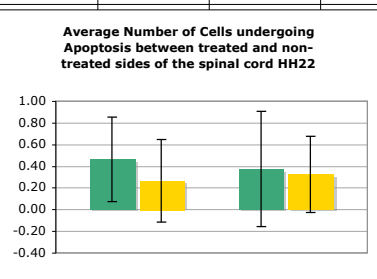
St18-Islet1/2	Si3	Con	Ratio	Negcon	Con	Ratio
Av 2 per Emb	0.819588581	Ttest 2T UEV	0.379598786			0.150166574
a	1	3.5	0.29	7	8	0.88
b	5	4	1.25	6.5	8	0.81
c	15.5	15.5	1	8	9.5	0.84
d	3.5	2.5	1.4	4	4	1
e	6.5	7.5	0.87	5.5	4.5	1.22
f	2	3.5	0.57	6	6.5	0.92
g	11	12.5	0.88	6.16666667	6.75	0.945
AV	6.357142857	7	0.894285714	n=6		

St18-Lim1/2	Si3	Con	Ratio	Negcon	Con	Ratio
Av 2 per Emb	0.53258489	Ttest 2T UEV	0.324338154			0.197433533
a	2.5	2.5	1	3	3.5	0.86
b	7	5.5	1.27	5	5	1
c	3.5	6.5	0.54	5.5	4	1.38
d	1.5	2.5	0.6	3	2.5	1.2
e	2.5	4.5	0.56	4.5	4	1.13
f	4.5	3.5	1.29	4.2	3.8	1.114
g	3	3.5	0.86			
AV	3.5	4.071428571	0.874285714	n=5		

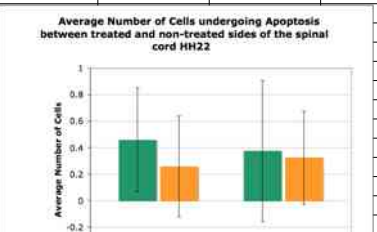


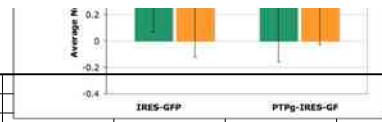
St18-Lim3	Si3	Con	Ratio	Negcon	Con	Ratio
Av 2 per Emb	0.314023769	Ttest 2T UEV	0.303342491			0.211021326
a	5	7.5	0.67	5	4	1.25
b	6	9.5	0.63	4.5	5.5	0.82
c	3	4.5	0.67	5	6	0.83
d	4	3.5	1.14	3.5	4	0.88
e	6	4.5	1.33	6	5	1.2
f	3	4.5	0.67	4.8	4.9	0.996
AV	4.5	5.66666667	0.851666667	n=5		

St18-MNr2	Si3	Con	Ratio	Negcon	Con	Ratio
Av 2 per Emb	0.813267093	Ttest 2T UEV	0.120733867			0.133678719
a	5.5	6	0.92	6	5.5	1.1
b	4.5	5	0.9	5	5	1
c	5	6	0.83	5.5	5	1.1
d	3	3	1	4	4.5	0.89
e	4	3.5	1.14	5	4	1.25
f	6	5.5	1.1	5.1	4.8	1.068
AV	4.66666667	4.833333333	0.981666667			

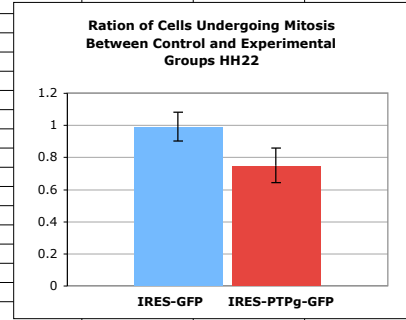


St22 c3	ires	Con	Ratio	Negcon	Con	Ratio
Av 2 per Emb	0.33913249	Ttest 1T EqV				
a	0	0.5		0.66	0	
b	0	0		1	1	
c	0.33	0.33		0	0.33	
d	1.33	0		0.66	0	
e	0	0		0	0	
f	1	0		0.464	0.266	
g	0	1				
h	0.33	0.66		IRES-GFP		
I	0	0				
j	2	0.33		treated		0.464
k	0	0		non treated		0.266
l	0	0				
m	0	0.33				
n	0.66	0.33		IRES-PTPg-GFP		
o	0.33	0.66				
p	0	0		treated		0.375
q	0	0		Non teated		0.324
r	0.66	0.66				
s	1	1				

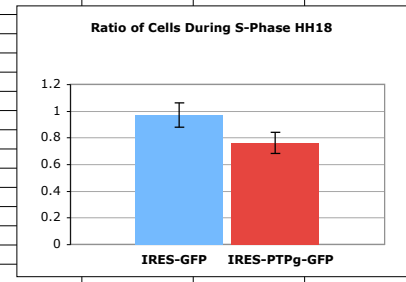




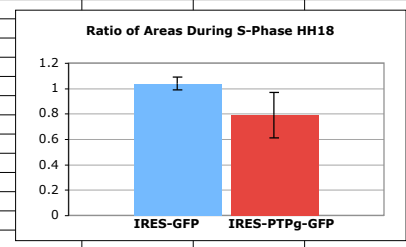
t	0.33	0.33				
u	0	0				
v	0	0.33				
w	0.66	1				
	0.375217391	0.324347826				
SD	0.533989016	0.356151476		0.398677815	0.388618064	



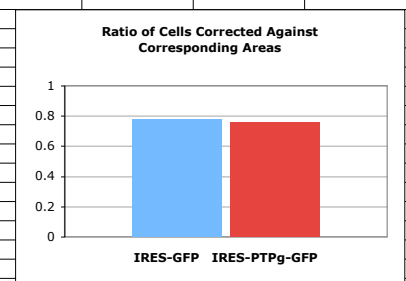
St22 h3	ires	Con	Ratio	Negcon	Con	Ratio
	6.92058E-05	Ttest 2T UEV	0.107135873			0.091800178
	13	9	0.69	17	15	1.13
	12.5	9	0.72	15.5	15	1.03
	13.5	7	0.52	14.5	15	0.97
	11.5	8	0.7	12.5	13.5	0.93
	10.5	10	0.95	14	12.5	1.12
	12.5	9	0.72	11.5	11	1.05
	14	10	0.71	13.5	16	0.84
	14	10.5	0.75	16	17	0.94
	18	14.5	0.81	15	17	0.88
	15	12.5	0.83	16.5	16.5	1
	10	8	0.8	10	10.5	0.95
	14	9	0.64	14.18181818	14.45454545	0.985454545
	12.5	9	0.72			
	13.5	12.5	0.93	Ires-gfp		0.99
	13	10	0.77	sd		0.092
	13.16666667	9.866666667	0.750666667			
				Ires-PTPg-gfp		0.75
				sd		0.107



St18 brdu	ires	Con	Ratio	Area ires	Area con	Ratio
	0.024647283	Ttest 2T UEV	0.080062476			0.182211721
	69	81.7	0.84	1.1632	1.5261	0.76
	45	54	0.83	1.3329	1.7404	0.76
	46	73.5	0.63	0.8124	1.3491	0.6
	49	69	0.71	0.8051	1.4561	0.55
	79.5	103.5	0.77	2.371	2.3873	0.99
	67.5	105.5	0.64	1.3173	2.507	0.53
	69	90	0.76	2.2264	2.7732	0.81
	97	128	0.76	1.9686	2.0123	0.98
	62	71	0.87	1.3727	1.5814	0.87
	61	78	0.78	1.7121	1.6759	1.02
av	64.5	85.42	0.759	1.50817	1.90088	0.787

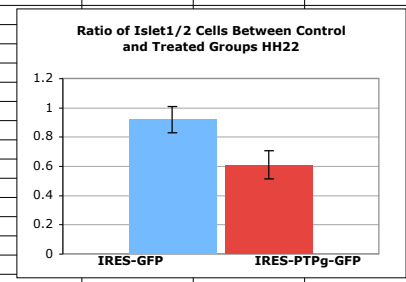


			0.090719347			0.048166378
control	78	93	0.96	3.1465	2.856	1.1
	107	112	0.84	2.4104	2.4586	0.98
	95	94	1.01	1.5853	1.5203	1.05
	83	76	1.09	1.7956	1.6987	1.06
	68	70	0.97	2.3722	2.3719	1
av	86.2	89	0.974	2.262	2.1811	1.038

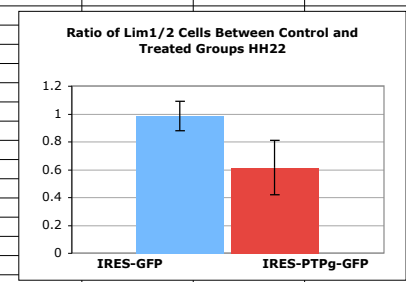


ratio of cells			Ratio of areas			
ires-gfp		0.97	ires-gfp		1.04	
sd		0.09	sd		0.05	
ires-gamma		0.76	ires-gamma		0.79	
sd		0.08	sd		0.18	
CORRECTED VALUES						
cells		0.78				
area		0.76				

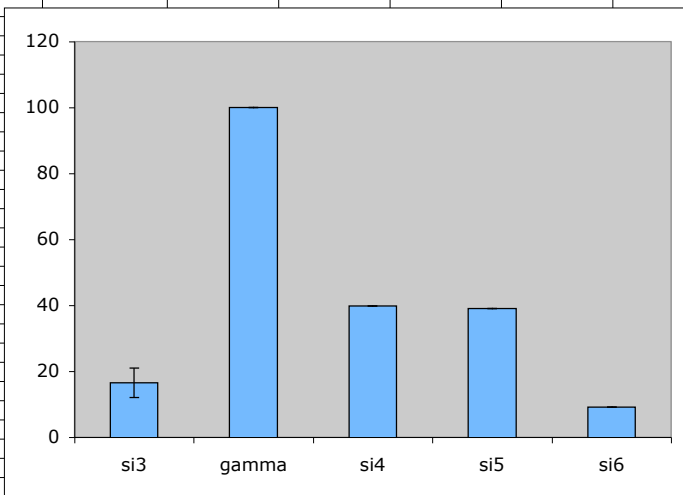
St22 islet	ires	Con	Ratio	Negcon	Con	Ratio
	0.000707109	Ttest 2T UEV	0.096947565			0.088185411
	8.5	13.5	0.63	18	22	0.82
	10	19	0.53	33	36	0.92
	16	24	0.67	13	14	0.93
	8.5	11.5	0.74	28	32	0.88
	11.3	18	0.63	43	49	0.88
	6.5	11	0.59	42	39	1.08
	16	22.5	0.71	29.5	32	0.918333333
	40.5	81.5	0.5			
	5	9.5	0.53			
	4.5	9	0.5	islet1/2		
	17.5	24	0.73			
	6.5	13	0.5	IRES-GFP		0.918
	7	14	0.5	sd		0.0881
	5.5	10.5	0.52			
	9	13.5	0.67	IRES-PTPg-GFP		0.6089
	89	115.5	0.77	sd		0.0969
	5.5	11	0.5			
	7.5	12	0.63			
	83	116	0.72			
av	18.80526316	28.89473684	0.608947368			



St22 Lim1/2	ires	Con	Ratio	Negcon	Con	Ratio
	0.001635473	Ttest 2T UEV	0.203171286			
	2.5	7	0.36	33	37	0.89
	11	29	0.38	46	44	1.05
	36	54.5	0.66	24	28	0.86
	36	43.5	0.83	58	53	1.09
	26	33.5	0.78	47	51	0.92
	33	51.5	0.64	35	32	1.09
	32.5	38.5	0.84	40.5	40.83333333	0.983333333
	16.5	40.5	0.41			
av	24.1875	37.25	0.6125	Lim1/2		
				IRES-GFP		0.98333
				sd		0.105



Western Blot Raw Data - PTPgamma							
exp 1	od	luciferase	od/luciferase	E / y14	average	av si3	
si3/y14	0.15	327302	4.58292E-07	0.103633647	0.128571418		
	0.05					0.164139494	
si3/gfp	0	200665					
gfp/y14	1.2	271356	4.42223E-06	1		1	
	0.27						
si3/y14	0.21	309345	6.78854E-07	0.153509189			
	0.06						
exp 2							
si3/gfp	0	132108					
si3/y14	0.17	79832	2.12947E-06	0.104237649			
	0.07						
gfp/y14	1.28	62656	2.0429E-05	1			
	0.2						
si4/y14	1	122898	8.13683E-06	0.398297775			
	0.27						
si5/y14	0.74	92583	7.99283E-06	0.391248933			
	0.14						
exp3							
si3/y14	0.41	327302	1.25267E-06	0.298174003			
	0.38						
si3/gfp	0	200665					
	0.64						
gfp/y14	1.14	271356	4.20112E-06	1			
	0.62						
si3/y14	0.39	309345	1.26073E-06	0.300093151			
	0.61						
exp4							
gfp/y14	2.06	85036	2.4225E-05	1			
	1.09						
si3/y14	0.2	65745	3.04206E-06	0.125574908			
	0.1						
si6/y14	0.15	68571	2.18751E-06	0.090299715			
	0.03						
si3/gfp	0	79082					
degly exp							
gfp/si3 w-enz	0	79082					
gfp/y14 w-enz	0.11	85037	1.29355E-06				
	0.07						
gfp/si3 w/o-enz	0	79082					
gfp/y14 w/o-enz	0.19	85037	2.23432E-06				
	0.09						
Western							
			average				
si3	0.12857142	si3	0.164481995	16.4481995	4.5		
	0.10423765	gamma	1	100	0		
	0.299544	si4	0.39829778	39.829778	0		
	0.12557491	si5	0.39124893	39.124893	0		
	0.090690788	si6	0.09029971	9.029971	0		
gamma	1		1				
	1						
	1						
	1						
si4	0.39829778						
si5	0.39124893						
si6	0.09029971						
si3							
gamma							
si4							
si5							
si6							



APPENDIX B

Publication